

Forschungszentrum Karlsruhe
Technik und Umwelt

Wissenschaftliche Berichte
FZKA 5582

**Measurements of
Turbulent Velocity and
Temperature in a
Wall Channel of a
Heated Rod Bundle**

T. Krauss, L. Meyer

Institut für Neutronenphysik und Reaktortechnik

Mai 1995

Forschungszentrum Karlsruhe

Technik und Umwelt

Wissenschaftliche Berichte

FZKA 5582

**Measurements of Turbulent
Velocity and Temperature in a
Wall Channel of a Heated
Rod Bundle**

T. Krauss, L. Meyer

Institut für Neutronenphysik und Reaktortechnik

Forschungszentrum Karlsruhe GmbH, Karlsruhe

1995

Als Manuskript gedruckt
Für diesen Bericht behalten wir uns alle Rechte vor

Forschungszentrum Karlsruhe GmbH
Postfach 3640, 76021 Karlsruhe

ISSN 0947-8620

Measurements of Turbulent Velocity and Temperature in a Wall Channel of a Heated Rod Bundle

Abstract

Turbulent air flow in a wall sub-channel of a heated 37-rod bundle ($P/D=1.12$, $W/D=1.06$) was investigated. Measurements were performed with a hot-wire probe with x-wires and a temperature wire. The mean velocity, the mean fluid temperature, the wall shear stress and wall temperature, the turbulent quantities such as the turbulent kinetic energy, the Reynolds-stresses and the turbulent heat fluxes were measured and are discussed with respect to data from isothermal flow in a wall channel and heated flow in a central channel of the same rod bundle. Also, data on the power spectral densities of the velocity and temperature fluctuations are presented. These data show the existence of large scale periodic fluctuations of velocity and temperature in the gap region of two adjacent rods or between rods and the wall. These fluctuations are responsible for the high intersubchannel heat and momentum exchange.

Messungen der turbulenten Geschwindigkeit und Temperatur in einem Wandkanal eines beheizten Stabbündels

Zusammenfassung

Turbulente Strömung durch einen Wandkanal eines beheizten 37-Stabbündels ($P/D=1.12$, $W/D=1.06$) wurde untersucht. Die Messungen wurden mit einer Hitzdrahtsonde mit x-Drähten und einem Temperaturdraht durchgeführt. Die mittleren Strömungsgeschwindigkeiten und -temperaturen, Wandschubspannungen und Wandtemperaturen, Turbulenzgrößen wie die turbulente kinetische Energie, die Reynoldschen Schubspannungen und die turbulenten Wärmeströme wurden gemessen und werden mit den Ergebnissen bei isothermer Strömung in einem Wandkanal und bei beheizter Strömung in einem Zentralkanal dieses Stabbündels verglichen. Spektrale Leistungsdichten der Geschwindigkeits- und Temperaturschwankungen werden ebenfalls dargestellt. Sie weisen auf die Existenz von periodischen großskaligen Schwankungen der Geschwindigkeit und Temperatur im Spalt zwischen zwei benachbarten Stäben oder zwischen Stäben und der Wand hin. Diese Schwankungen sind für den großen Wärme- und Impulsaustausch zwischen den Unterkanälen verantwortlich.

CONTENTS

1. INTRODUCTION	1
2. EXPERIMENTAL APPARATUS AND PROCEDURE.....	2
3. RESULT	5
3.1. Wall shear stress and wall temperature distribution	5
3.2. Mean velocity and temperature distribution	6
3.3. Turbulent intensities and kinetic energy.....	7
3.4. Reynolds shear stress.....	8
3.5. Turbulent heat flux	9
3.6. Eddy diffusivities of heat and momentum.....	10
3.7. Triple correlations	12
3.8. Skewness and flatness.....	13
3.9. Frequency analysis	14
4. CONCLUSION.....	15
5. NOMENCLATURE	16
6. REFERENCES	18

1. INTRODUCTION

The prediction of the temperature distribution within the rod bundle of a nuclear reactor is of major importance in nuclear reactor design. The thermal-hydraulic analysis is performed by solution of the conservation equation for mass, momentum and energy. Recently developed codes [1] applying a distributed parameter analysis need empirical information on turbulent transport properties of both momentum and energy transport.

A large number of experiments has been performed in various rod bundle geometries with isothermal flow (for a review see Ref. 2). It has been found that distributions of the turbulence intensities in rod bundles are unusual and different from those in tubes and parallel plates [3,4,5]. The highest turbulence intensities were observed at positions of greatest distance from the walls in the gap region. The eddy viscosities parallel to walls are considerably higher than those normal to walls and depend strongly on the pitch to diameter ratio of the rod bundle. The high mixing rates between subchannels of rod bundles have been explained by the effects of secondary flow for a long time, although Rowe [6,7] in 1973 had noticed that a non-gradient macroscopic flow process, possibly flow pulsation, affects the mixing between subchannels. Detailed turbulence measurements of the axial flow through closely-spaced rod bundles have confirmed the observations of Rowe and have shown that an energetic and almost periodic flow pulsation exists through the gaps between the rods and between rods and channel walls, respectively [8,9]. It was demonstrated that these flow pulsations are the reason for the high mixing rates between the subchannels of rod bundles [10,11] and secondary flows in subchannels do not contribute significantly to the mixing rates. In a recent investigation on turbulent flow through compound rectangular channels [12] it was shown that these large scale flow pulsations or vortices are a general phenomenon existing in any longitudinal slot or groove in a wall or a connecting gap between two flow channels, provided its depth is more than approximately twice its width. Thus, the momentum- and heat transfer processes in the rod-gap area for turbulent flow through closely spaced rod arrays are governed by a low frequency quasi-periodic fluctuation of the velocity component directed through the gap.

To model correctly the heated flow it is necessary to know the turbulent quantities of the velocity and those of the temperature such as the eddy diffusivity of heat in all directions. No such data were available for flow through rod bundles. In carrying on the 15 years of research on turbulent flow through rod bundles at Kernforschungszentrum Karlsruhe (KfK) the investigations were continued at a heated 37-rod bundle. The results of the measurements in a central channel have been published earlier [13]. Here we present the main results of the measurements in a wall subchannel and discuss them with respect to those results in the central channel and with isothermal flow in the wall channel [14].

2. EXPERIMENTAL APPARATUS AND PROCEDURE

A rod bundle of 37 parallel rods (O.D. $D = 140$ mm) arranged in triangular array in a hexagonal symmetric channel was built (Fig.1). The position of the channel is horizontal. The total length of the working section is $L = 11.50$ m with an unheated entrance length of $L_{iso} = 4.60$ m and a heated length of $L_{heat} = 6.90$ m. The pitch to diameter ratio of the rods is $P/D = 1.12$ ($W/D = 1.06$), which gives a length to hydraulic diameter of central channel ratio for the heated part of $L_{heat}/D_{h,c} = 128$. The rods are made of epoxy reinforced with fiberglas, sheathed with a $50 \mu\text{m}$ foil of monel metal, which serves as resistance heating element. It is heated by low voltage, high direct current to temperatures in the range of 60° to 100°C . Since the metal foil has a very accurate thickness the heat flux is uniform around the perimeter of the rods. The heat conduction is very small due to the small thickness of the metal foil and the low conductivity of the rod material. Thus, the circumferential temperature variations due to different heat transfer will not be eliminated by conduction. The wall heat flux was determined from the measurements of the current and the voltage drop along the rods with an estimated error of $\pm 1.5\%$.

The channel walls are made of aluminum covered with a thick insulation at the outside to minimize the heat losses. The whole bundle is made up from five sections, each 2.30 m long. The rod gap spacers were made of 4 mm thick and 15 mm wide

(in axial direction) steel with rounded edges. Due to extremely small manufacturing tolerances the deviations from the nominal bundle geometry are less than 0.2 mm, including the bending of the rods. The fluid is air at atmospheric pressure and room temperature at the entrance. The air is driven by a centrifugal blower. Before entering the working section it passes through a filter to remove particles greater than 1 μm and an entrance section of 5 m length with a honeycomb grid and a number of fine grid screens.

The measurements are performed at a position 20 mm upstream of the outlet. The time-mean values of the axial velocity and the wall shear stresses are measured by Pitot and Preston tubes (O.D. $d=0.6$ mm), respectively, the mean temperatures are measured by sheathed thermocouples (O.D. $d=0.25$ mm). The wall temperatures are measured by an infrared pyrometer (Heimann KT 4), which has a range of 0°C-100°C and a target area of 5 mm diameter at 1 m distance. Mainly due to difficulties with calibration the uncertainty is ± 1 K.

The turbulent quantities are measured by hot wire anemometry using a three-wire probe. This probe consists of an x-wire probe with an additional cold wire perpendicular to the x-wire plane for simultaneous measurement of two components of instantaneous velocity and temperature. The x-wires have a length of 1.1 mm, a diameter of 2.5 μm and a spacing of 0.35 mm. The cold wire has a diameter of 1 μm , a length of 0.9 mm and is positioned 0.1 mm upstream of the x-wire prong tips. The measuring volume is approximately 1 mm³. The probe was fabricated in our laboratory. The calibration and evaluation method uses look-up tables as described by Lueptow et al. [15], extended by the temperature dimension [16]. Since the cold wire is run in the Constant Current Anemometer-mode (CCA) the frequency response is not as good as that of the x-wires, which are run in the Constant Temperature Anemometer-mode (CTA). The attenuation and phase shift of the temperature signal leads to errors in all correlations of u , v and θ . A rough estimate for a 1 μm wire gives the following maximum errors: $\overline{\theta^2}$ is 2%, $\overline{u\theta}$ is 4% and $\overline{v\theta}$ is 6% too small; $\overline{u^2}$ and \overline{uv} are 4% too large and there is a negligible error in $\overline{v^2}$.

Apart from these errors there are several errors typical for x-probes, such as the error due to the velocity component normal to the x-plane and the errors due to the finite length of the wires and the distance between them. The velocity component normal to the x-plane will result in the evaluation of too high axial components \bar{u}^2 , while the finite length of and the distance between the wires leads to errors in \bar{v}^2 , \bar{w}^2 and in the correlations such as \bar{uv} . Those latter errors depend on the velocity and temperature gradient [16].

The performance of the measurements is fully automated; the mass flow rate, the heating power and the traversing of the measuring probe are controlled by a 486-PC. The triple wire probe is run by two CTA- and one CCA-bridge of an AN-1003 anemometer system. The signals were digitized at sample rates of 7 kHz per channel by a DT2829-card, which provided sample and hold digitization with 16-bit resolution. The total number of samples taken in a continuous stream were 49152 per channel, with a measuring time of 7 seconds. The raw data were loaded into extended memory of the computer by DMA. The evaluation of all correlations takes approximately 20 seconds. At each measuring point the probe is turned into eight positions to measure all six Reynolds stresses, three turbulent heat fluxes and ten triple products [17]. To evaluate the above correlations it is necessary to roll the probe about its axis to the positions 0° , 45° , 90° and 135° with respect to the start. The positions 180° , 225° , 270° and 315° are used to compute the average between two corresponding positions, 0° and 180° for example, in order to minimize possible errors in the radial or azimuthal components.

In a wall channel measurements at 636 positions (Fig. 2) were taken under non-isothermal conditions, which took approximately forty hours. The data of the heated experiment were: Reynolds number in the wall channel $Re = 6.5 \times 10^4$, hydraulic diameter $D_{h,w} = 0.0488$ m with a bulk velocity $U_b = 19.4$ m/s and a bulk temperature $T_b = 29.1$ °C. The wall heat flux in the present experiment was 1.39 kW/m².

3. RESULTS

3.1. Wall shear stress and wall temperature distribution

Fig.3 shows the measured wall shear stress distribution of the 37-rod bundle in comparison to the results of a 4-rod bundle. The shear stress was calculated by Preston's method. The properties of air were evaluated at the fluid temperature at $y=0.3$ mm, which is the radius of the Preston tube.

The wall shear stress reduced by the average wall shear stress of the wall and the rod ($\tau_{w,av} = 1.21$ N/m²) shows no relevant difference between the heated and isothermal data in a wall subchannel of the 37-rod bundle. Even the shear stress distribution in the 4-rod bundle shows good agreement with these results, which confirms the similarity of flow through wall channels of 4-rod- and 37-rod bundles. Compared to the data obtained in a heated central channel of the 37-rod bundle, the wall shear stress in the wall channel of the bundle is about 13% larger. The minimum value of τ_w occurs in the rod-to-wall gap region and the maximum value at the position of maximum channel width.

In Fig.4 local wall temperatures of the heated and unheated wall bounding the wall channel are plotted versus mean temperatures of each boundary. As expected, the temperature gradient along the unheated wall is very small due to excellent thermal conductance of the wall material. The values of this unheated wall show a maximum in the rod-to-wall gap and decrease gradually with increasing distance from the gap. In contrast to this the temperature distribution of the heated rod varies over a wider range with the minimum appearing at the position of maximum wall shear stress. The highest temperatures are reached in the rod-to-rod gap region.

3.2. Mean velocity and mean temperature distribution

Isoline and x-y-plots of the time mean velocity are shown in Figs. 5 and 6. Time mean velocities are related to the bulk velocity of the wall channel $U_b = 19.4 \text{ m/s}$. The distribution of time mean temperature is shown in Figs. 7 and 8. The bulk temperature in the wall subchannel was $T_b = 29.1^\circ\text{C}$ and the difference $(T_w - T_b)$ was 19.55°C . There is no relevant difference in the velocity data between the isothermal and the heated case. The temperature differences in the wall channel are very large compared to a central channel, due to the proximity of an unheated wall. As expected, the temperature reaches its maximum value in the rod-to-rod gap region.

The logarithmic plots of the radial velocity distribution, computed with local friction velocities (Figs. 9 and 10) follow the law of the wall $u^+ = 2.5 \ln y^+ + 5$ with reasonable agreement at most azimuthal positions. The logarithmic temperature profiles are shown in Figs. 11 and 12, together with the lines $T^+ = 2.5 \ln y^+$, displaced by 1 K every second angular position. Fig. 11 shows the logarithmic temperature profiles calculated with local friction velocities in accordance with the calculation of u^+ . Previous measurements in a heated central channel of our 37-rod-bundle have shown that the logarithmic temperature profiles at different azimuthal positions would not collapse if local friction velocities were used. Therefore temperature profiles computed with the friction velocity averaged over the perimeter of the heated rod are presented in Fig. 12. The logarithmic profiles in Fig. 12 are slightly higher compared to Fig. 11, but the tendency to change its slope at different angular positions remains the same. The slope of the profiles is higher in the rod-to-wall gap and lower in the gap between two heated rods, the latter also being found in central channels. The temperature profiles, calculated with local friction velocities can be fitted by logarithmic laws that gradually change from $3.69 \ln y^+ - 6.21$ in the rod-to-wall gap to $2.32 \ln y^+ - 0.25$ in the gap between two heated rods. The reason for the deviation of these temperature profiles from a single logarithmic law is the extremely asymmetric temperature distribution in the wall channel.

3.3. Turbulent intensities and kinetic energy

All quantities displayed in isoline plots were scaled by values of the friction velocity and temperature that are averaged over the perimeter of the rod and along the wall. All data are shown for the heated case. The differences between the unheated case and the heated case were negligible. Compared to the data from measurements in central channels the variation of all three velocity components in azimuthal direction is larger. All turbulent intensities except for the radial velocity component are higher in the wall channel.

The turbulent intensities in axial direction $\sqrt{u^2} / u_{t,av}$, shown in Figs. 13 and 14, are much higher than in a central channel, where the maximum value of 1.9 was reached close to the wall. Here it reaches its maximum value of 2.6 near the line of maximum wall distance in the gap rod-to-wall at an angular position between 30° and 35°. The distribution of the turbulent intensities in radial direction (Figs. 15 and 16) close to the walls and at 0° and 90° is similar to that in central channels with $\sqrt{v^2} / u_{t,av} = 0.9$ near the wall and 0.6 at the symmetry line. With increasing distance from the gap region the radial distribution becomes flatter. The turbulent intensities in azimuthal direction $\sqrt{w^2} / u_{t,av}$, shown in Figs. 17 and 18, are very high in the narrow rod-to-wall gap at the line of maximum wall distance (=1.9) and somewhat lower near the wall. This is due to the existence of large scale quasi-periodic velocity fluctuations in the rod gap regions. In the rest of the wall channel the wall-parallel turbulent intensities are highest near the wall. Because the rod-to-rod gap is twice as wide as the rod-to-wall gap, the large scale velocity fluctuations are less pronounced between the rods. The relative kinetic energy

$$k^+ = \frac{1}{2} (\bar{u}^2 + \bar{v}^2 + \bar{w}^2) / u_{t,av}^2 \quad (1)$$

in Figs. 19 and 20 is mainly governed by the intensity in axial direction, being the largest contributor in all positions except for the rod-to-wall gap region, where the azimuthal intensities are largest. The intensities of the temperature fluctuation

$\sqrt{\theta} / T_{\tau,av}$ (Figs. 21 and 22) are larger than those of the central channel because of the asymmetric distribution of the temperature in wall channels. The maximum values are reached in the gap between two heated rods, independent of the wall distance. In this region the temperature gradient in azimuthal direction and the intensity of the azimuthal velocity component both are large, which leads to an intensive exchange of fluid of different temperature. In contrast to this, the smallest values of the temperature fluctuation are measured near the unheated wall. The variation of the temperature fluctuation in azimuthal direction is negligible near the unheated wall and becomes most significant close to the heated rod at an angular position between 35° and 75°, with its minimum value near 50°.

3.4. Reynolds shear stress

The scaled turbulent shear stresses normal to the wall $\overline{-uv} / u_{\tau,av}^2$ (Figs. 23 and 24) and in azimuthal direction $\overline{uw} / u_{\tau,av}^2$ show exactly the same distribution as for isothermal flow in wall channels. Near the wall $\overline{-uv} / u_{\tau,av}^2$ reaches the same values as in central channels and decreases linearly with increasing distance from the wall. The turbulent shear stress normal to the wall tends to zero at the line of maximum wall distance, where also the gradient of mean velocity in radial direction $\partial U / \partial y$ is equal to zero (Figs. 29 and 30).

The scaled azimuthal shear stress $\overline{uw} / u_{\tau,av}^2$, shown in Figs. 25 and 26, is close to zero near the symmetry line at 0° in the rod-to-wall gap region and between 60° and 90° in the rod-to-rod gap region, where the azimuthal gradient of mean velocity $\partial U / \partial \phi$ vanishes (Figs. 31 and 32). The maximum values are reached at an angular position between 20° and 30° at the line of maximum wall distance, exactly in the region, where the highest values of the axial intensity $\sqrt{u^2} / u_{\tau,av}$ have been obtained. Compared to the results from measurements in central channels of this rod bundle the maximum values found in this wall channel are higher by a factor of about eight.

Values of the planar shear stress $\overline{vw} / u_{\tau,av}^2$ have rarely been measured in the past. With an X-wire probe aligned with the mean flow direction the planar shear stress cannot be measured directly because the heat transfer from a given wire of the probe is dependent only on the component of velocity normal to the wire. If the probe is rolled about its axis to the position 45° and 135° with respect to the start, \overline{vw} can be determined as a difference between the obtained intensities normal to the probe axis [17]. As $\overline{vw} / u_{\tau,av}^2$ is very small and is determined as a difference between two quantities, it may be expected to have considerable scatter. Nevertheless the planar shear stress measured by Hooper [18] in a six-rod bundle and our present results (Figs. 27 and 28) show some similarity in magnitude and distribution. In the wall region values of about 0.2 are obtained for $\overline{vw} / u_{\tau,av}^2$, which decrease rapidly with increasing wall distance. At the line of maximum velocity, high values are reached at angular positions where $\overline{uw} / u_{\tau,av}^2$ is high, due to the influence of this component on the magnitude of $\overline{vw} / u_{\tau,av}^2$. The unsteadiness of the data at the line of maximum velocity is due to the choice of the coordinate system, which is not continual there.

3.5. Turbulent heat flux

The distribution of the turbulent heat flux in azimuthal direction $\overline{w\theta} / u_{\tau,av} T_{\tau,av}$, shown in Figs. 33 and 34, has some similarity to the measured azimuthal shear stress. At the position of maximum azimuthal shear stress ($\phi = 20^\circ$ - 30°) $\overline{w\theta} / u_{\tau,av} T_{\tau,av}$ reaches its highest negative values of -1.2. The maximum positive values of 1.2 have been measured in the gap between two heated rods, where the intensity of the temperature fluctuation also has a maximum. At an angular position of 45° , $\overline{w\theta} / u_{\tau,av} T_{\tau,av}$ is equal to zero, due to a vanishing azimuthal gradient of mean temperature $\partial T / \partial \phi$ (Figs. 41 and 42). In contrast to the data obtained in a heated central channel, the variation along the perimeter of the heated rod is very large, the maximum values of the azimuthal heat flux being about 3.5 times higher.

The scaled turbulent heat flux in axial direction, $\bar{u}\theta / u_{t,av} T_{t,av}$, shown in Figs. 35 and 36, has its absolute maximum close to the wall at an angular position of 25°-30°, where both the intensity of the temperature and the axial velocity fluctuation reach high values. Additionally there is a local maximum near 75°-80° in the region of highest temperature fluctuations. On approaching the unheated wall the axial heat flux decreases to zero at the symmetry line. Compared to the results of a heated central channel $\bar{u}\theta / u_{t,av} T_{t,av}$ is higher by a factor of about 1.7.

At the heated wall the scaled turbulent heat flux in radial direction $\bar{v}\theta / u_{t,av} T_{t,av}$ (Figs. 37 and 38) is of the same magnitude as in central channels. It has its maximum at $\phi = 30^\circ$ - 50° near the heated rod. From the line of maximum velocity towards the unheated wall $\bar{v}\theta / u_{t,av} T_{t,av}$ decreases almost linearly. The variation of the radial turbulent heat flux along the perimeter of the rod is small. Figs. 39 and 40 show the radial gradient of mean temperature $\partial T / \partial y$ that has its maximum values directly at the heated wall as expected. With increasing distance from the heated wall $\partial T / \partial y$ decreases continually.

3.6. Eddy diffusivities of heat and momentum

The eddy diffusivity of momentum or eddy viscosity normal to the wall is defined by

$$\varepsilon_{mr} = \frac{-\bar{uv}}{\partial U / \partial y} \quad (2)$$

Shown in Fig. 43 is the non-dimensional eddy viscosity

$$\varepsilon_{mr}^+ = \varepsilon_{mr} / (\hat{y}_{max} u_{t,av}), \quad (3)$$

i.e. it is scaled by the average value of the friction velocity and the maximum profile length \hat{y}_{max} at $\phi=55^\circ$. The non-dimensional eddy viscosity in azimuthal direction and the non-dimensional eddy diffusivities of heat are derived in the same way. As for

central channels the eddy viscosities normal to the wall are slightly higher than the pipe data and are only a weak function of the azimuthal position. The non-dimensional eddy diffusivities of heat in radial direction

$$\varepsilon_{hr}^+ = \frac{-\bar{v}\theta}{\frac{\partial T}{\partial y} \hat{y} u_{r,av}} \quad (4)$$

presented in Fig. 44 are smaller than those of momentum, especially in the region next to the heated rod. In a region near the unheated wall the uncertainty of the radial eddy diffusivity of heat is high since both, the turbulent radial heat flux $\bar{v}\theta$ and the radial gradient of mean temperature $\partial T / \partial y$ tend to zero there. Nevertheless these data are published here for completeness. The radial turbulent Prandtl number Pr_{tr} , which is defined as the ratio between the eddy diffusivity of momentum and the eddy diffusivity of heat in radial direction takes values between 2 and 2.5 next to the heated rod. At longer distances from this wall Pr_{tr} is close to unity, which is generally assumed for pipe flow.

The non-dimensional eddy viscosity in azimuthal direction (Fig. 45) is defined by

$$\varepsilon_{ma}^+ = \frac{-\bar{u}w}{\frac{1}{y} \frac{\partial U}{\partial \phi} \hat{y}_{max} u_{r,av}} \quad (5)$$

Because the gradient of mean velocity in azimuthal direction $\partial U / \partial \phi$ is very small, reasonable values of ε_{ma}^+ are available only at few positions and the scatter is quite large. The eddy viscosities in azimuthal direction are considerably higher than those normal to the walls, especially in the rod-to-wall gap region. The anisotropy, that is the ratio of the eddy diffusivities of momentum in azimuthal and radial direction is very high. Maximum values of about 100 are reached in the gap between rod and wall due to strong pulsations parallel to the wall.

The non-dimensional eddy diffusivity of heat in azimuthal direction

$$\varepsilon_{ha}^+ = \frac{-\overline{w\theta}}{\frac{1}{y} \frac{\partial T}{\partial \phi} \hat{y}_{max} u_{r,av}}, \quad (6)$$

is plotted in Fig. 46. There are serious problems in evaluating ε_{ha}^+ due to small gradients of mean temperature in azimuthal direction (see Figs. 41 and 42), especially in the rod-to-wall gap region and near the unheated wall and the scatter of the computed data is expected to be quite large. In regions where the azimuthal gradient of mean temperature is significant the turbulent Prandtl number parallel to the wall takes values between 1 and 2, like the radial turbulent Prandtl number. It is not indicated to determine an azimuthal turbulent Prandtl number in the rod-to-wall gap region and near the unheated wall, where $\partial T / \partial \phi$ is close to zero.

3.7. Triple correlations

Triple correlations are a part of the diffusion term of the transport equations that are the basis of recent approaches to solve the closure problem of turbulence. All ten triple correlations that can be computed from the three velocity components were measured. For the solution of the transport equation of the Reynolds stresses the correlation $\overline{u^3}$ is not necessary because it only appears as a derivation of the axial direction which is zero by definition in hydrodynamically developed flow. The correlations $\overline{v^3}$ and $\overline{w^3}$ can be computed from each skewness $S_v = \overline{v^3} / (\sqrt{\overline{v^2}})^3$ and $S_w = \overline{w^3} / (\sqrt{\overline{w^2}})^3$. The remaining seven triple correlations are discussed in the following. The correlation $\overline{u^2v}$ is shown in Fig. 47. The minimum value of $\overline{u^2w}$, shown in Figs. 48 and 49 is reached at an angular position of 40° at the line of maximum velocity. The variation of this correlation along the perimeter of the rod is very small. The highest positive values of $\overline{uv^2}$ are reached at a position where the axial intensity also has its maximum. The correlation $\overline{uw^2}$ is very small in the whole wall channel, together with $\overline{vw^2}$, $\overline{v^2w}$ and \overline{uvw} (Figs. 50-54). The correlation $\overline{uw^2}$ (Fig. 55 and 56)

has its minimum value of -1.5 at the line of maximum velocity between 30° and 40°. Directly in the rod-to-wall gap region the highest positive values of $\overline{uw^2}$ are reached. The variation along the perimeter of the rod again is very small.

3.8. Skewness and flatness

The skewness of u , defined by $S_u = \overline{u^3} / \sigma_u^3$ with $\sigma_u = \sqrt{\overline{u^2}}$ is shown in Figs. 57 and 58. The high negative values of the skewness of u near the center of the wall channel indicate the existence of high negative values of the axial velocity component. In the rod-to-rod and rod-to-wall gap the skewness of u is positive, which indicates the preference of high positive fluctuations of u in this region. The skewness of v has its highest positive values at the rod and the highest negative values at the unheated wall (Figs. 59 and 60). This denotes the presence of high values of the radial component that are oriented away from the walls. The variation of the skewness along the perimeter of the rod and along the wall is very small. The skewness of the azimuthal velocity component, shown in Figs. 61 and 62 has negative values almost in the entire wall channel. Consequently in the rod-to-wall gap region high values of the azimuthal fluctuation are oriented away from the gap in the direction of the wall channel and in the region between two rods these high values of w are directed from the wall channel into the gap. The skewness of θ (Figs. 63 and 64) reaches its highest negative values of -1.0 in the rod-to-rod gap region where the fluctuation of temperature $\sqrt{\overline{\theta^2}}$ has its maximum. In Fig. 75 the maximum of the probability density function of the temperature fluctuations at position 3 is shifted to positive values, which corresponds to the negative skewness at this point. Negative values of the skewness signify the presence of temperature fluctuations that are often far below the time average $\sqrt{\overline{\theta^2}}$. At maximum wall distance near the symmetry line the skewness of the temperature fluctuation has maximum values of about 1.5.

The flatness or kurtosis of u , shown in Figs. 65 and 66 is defined by $K_u = \overline{u^4} / \sigma_u^4$. The highest values of K_u are reached near the center of the wall channel, where the skewness of u has its minimum. High values of the flatness of u imply large devia-

tions of the axial component from its time average. The minimum value of 2.2 is reached at an angular position between 25° and 35° where the axial intensity has its maximum. The probability density function at this point (position 2 in Fig. 73) is nearly symmetric with maxima at ± 2.5 m/s, which is characteristic for a sine wave with random noise. In the rod-to-wall gap region and the gap between two rods the flatness of v (Figs. 67 and 68) reaches its maximum values of 4.1-4.4. In the remaining wall channel K_v takes values between 3.2 and 3.6 which characterizes a turbulent motion that's nearly random. Directly in the rod-to-wall gap the flatness of w (Figs. 69 and 70) has its minimum value of 2.4. This is due to the existence of quasi-periodic pulsations through the gap that are responsible for the somewhat periodic character of the azimuthal component (see also Fig. 74). In Figs. 71 and 72 the flatness of the temperature fluctuation has its minimum values of 2.2-2.4 at the angular positions between 25° and 30° and between 75° and 85° where the turbulent transport of this scalar quantity is somewhat periodic. Maximum values of K_θ are reached at the symmetry line of the wall channel near the unheated wall which indicates peaky time traces of the temperature fluctuation.

3.9. Frequency analysis

Auto- and cross-spectral power density functions of velocity and temperature fluctuations were measured at selected positions to characterize the large scale eddies. The auto-spectral power density functions of both, the velocity and temperature fluctuations (Fig. 76) show characteristic frequencies of quasi-periodic pulsations in the narrow rod-to-wall gap. The maxima of these, which are a function of the mean velocity and the dimensions of the gap, occur at frequencies of about 50 to 60 Hz. In the wider gap between two rods, the auto-spectral power density function of the azimuthal velocity component has its peak at a lower frequency of 30-40 Hz. Similar frequencies are also reflected by all cross-spectral power density functions. The appearance of similar frequencies in the spectra of both, velocity and temperature fluctuations, indicates the relationship between the involved transport processes.

4. CONCLUSION

Measurements of turbulence in a wall subchannel of a heated rod bundle were performed. The results compared to flow in heated central channels and isothermal wall channels of the same bundle indicate that:

- (1) The wall shear stress, mean velocity and all velocity fluctuations show the same distribution previously measured in a wall channel in isothermal flow.
- (2) The distribution of wall temperature at the heated rod varies over a wider range compared to a central channel. The highest temperatures are reached in the gap region between two heated rods.
- (3) The intensities of the axial and azimuthal velocity fluctuations reach higher values and are more dependent on the angular position than in comparable central channels.
- (4) The intensities of turbulent temperature fluctuations are larger than those measured in central channels. The maximum values are reached in the gap region between two heated rods.
- (5) Values of the planar shear stress, measured for the first time in a 37-rod bundle, are very small compared to the other components of the Reynolds stress tensor.
- (6) The turbulent heat fluxes in axial and in azimuthal direction are higher than in a central channel. The variation of the azimuthal heat flux along the perimeter of the wall is very large.
- (7) The anisotropy, that is the difference between the eddy diffusivities in radial and in azimuthal direction is very large.
- (8) The power-spectra of turbulent velocity and temperature fluctuations show characteristic frequencies of quasi-periodic pulsations through the gaps.

5. NOMENCLATURE

$D_{h,c}$	hydraulic diameter of the central channel [m],
$D_{h,w}$	hydraulic diameter of the wall channel [m],
D	rod diameter [m],
P	rod pitch, distance between rod centers [m],
W	distance between wall and rod plus D [m],
L	length of rod bundle [m],
k^+	relative kinetic energy of turbulence [-],
q_w	wall heat flux [W/m^2],
Re	Reynolds number [-],
T	time mean fluid temperature [$^\circ\text{C}$],
T^+	dimensionless temperature, $(T_w - T)/T_{\tau,\text{av}}$ [-],
$T_{\tau,\text{av}}$	average friction temperature, $q_w/\rho c_p u_{\tau,\text{av}}$ [$^\circ\text{C}$],
T_w	local wall temperature [$^\circ\text{C}$],
$T_{w,\text{av}}$	average wall temperature [$^\circ\text{C}$],
U	time mean velocity in axial direction [ms^{-1}],
u^+	dimensionless velocity, U/u_τ [-],
u_τ	local friction velocity, $\sqrt{\tau_w / \rho}$ [ms^{-1}],
$u_{\tau,\text{av}}$	average friction velocity [ms^{-1}],
u	fluctuating velocity in axial direction [ms^{-1}],
v	fluctuating velocity in radial direction [ms^{-1}],
w	fluctuating velocity in azimuthal direction [ms^{-1}],
u', v', w'	$\sqrt{\bar{u}^2}, \sqrt{\bar{v}^2}, \sqrt{\bar{w}^2}$ [ms^{-1}],
y	distance normal to the wall [m],
\hat{y}	distance between wall and line of maximum velocity [m],
\hat{y}_{\max}	maximum distance between wall and centerline [m],
y^+	dimensionless distance from the wall, $y u_\tau / v$ [-],
ε_m	eddy diffusivity of momentum, Eq. (2) [m^2s^{-1}],
ε_h	eddy diffusivity of heat, Eq. (5) [m^2s^{-1}],
ε^+	dimensionless eddy diffusivity, Eq. (3) [-],

θ	temperature fluctuation [K],
θ'	$\sqrt{\overline{\theta^2}}$ [K],
ν	kinematic viscosity [m^2s^{-1}],
ρ	density of fluid (air) [kgm^{-3}],
τ_w	local wall shear stress [Nm^{-2}],
$\tau_{w,\text{av}}$	average wall shear stress [Nm^{-2}],
ϕ	angular coordinate with origin at the rod-to-wall gap [$^\circ$],
z	azimuthal coordinate with origin at the rod-to-wall gap [m],
Φ_u, Φ_w	auto-spectral power density functions of velocity fluctuations [m^2s^{-1}],
Φ_θ	auto-spectral power density function of temperature fluctuations [K^2s],
Φ_{uw}	cross-spectral power density function of velocity fluctuations [m^2s^{-1}],
$\Phi_{w\theta}$	cross-spectral power density function of velocity and temperature fluctuations [Km].

5.1. Subscripts and superscripts

a	azimuthal,
b	bulk,
h	heat,
m	momentum,
r	radial,
w	wall,
-	time averaged quantities.

6. REFERENCES

1. W. Zeggel and N. Neelen, Validation of a wall parallel eddy viscosity formulation, IAHR 5th Int. Meeting on Liquid Metal Thermal Hydraulics, Grenoble (1986).
2. K. Rehme, The structure of turbulent flow through rod bundles, Nuclear Engineering and Design 99, 141-154 (1987).
3. K. Rehme, Experimental Observations of Turbulent Flow Through Subchannels of Rod Bundles, Exp. Thermal and Fluid Sci., 2, 341 - 349, 1989.
4. J. Hejna, and F. Mantlik, The Structure of Turbulent Flow in Finite Rod Bundles, Proc. 1st World Conf. Exp. Heat Transfer, Fluid Mech., and Thermodynamics, Edts. R.K. Shah, E.N. Ganic & K.T. Yang, Elsevier, 1712 - 1719, 1988.
5. X. Wu, and A.C. Trupp, Experimental Study on the Unusual Turbulence Intensity Distributions in Rod-to-Wall Gap Regions, Exp. Thermal and Fluid Sci., 6(4), 360-370, 1993.
6. D.S. Rowe, Measurement of Turbulent Velocity, Intensity and Scale in Rod Bundle Flow Channels, BNWL-1736, Battelle Pacific Northwest Laboratories, Richland, Washington, 1973.
7. D.S. Rowe, B.M. Johnson and J.G. Knudsen, Implications Concerning Rod Bundle Crossflow Mixing Based on Measurements of Turbulent Flow Structure, Int. J. Heat Mass Transfer, 17, 407-419, (1974)
8. J.D. Hooper and K. Rehme, Large-scale Structural Effects in Developed Turbulent Flow Through closely-spaced Rod Arrays, J. Fluid Mech., 145, 305 - 337, 1984.
9. S.V. Möller, On Phenomena of Turbulent Flow Through Rod Bundles, Exp. Thermal and Fluid Sci., 4, 25 - 35, 1991.
10. S.V. Möller, Single-phase Turbulent Mixing in Rod Bundles, Exp. Thermal and Fluid Science, 5, 26-33, 1992.
11. K. Rehme, The Structure of Turbulence in Rod Bundles and the Implications on Natural Mixing Between the Subchannels, Int. J. Heat Mass Transfer, 35(2), 567-581, 1992.
12. L. Meyer and K. Rehme, Large Scale Turbulence Phenomena in Compound Rectangular Channels, Exp. Thermal Fluid Science, 8, 286-304 (1994), and KfK-Rep. 4818 (1991).

13. L. Meyer, Measurements of Turbulent Velocity and Temperature in a Central Channel of a Heated Rod Bundle, Nucl. Engrg. Des. 146, 71-82 (1994)
14. L. Meyer and K. Rehme, Turbulente Strömung durch Wandkanäle von Stab-bündeln ($P/D = 1.12$, $W/D = 1.06$), KfK-Rep. 5007 (1992). Kernforschungs-zentrum Karlsruhe, FRG.
15. R.M. Lueptow, K.S.Breuer and J.H.Haritonidis, Computer Aided Calibration of X-probes Using a Look-up Table, Exp. in Fluids 6, 115-118 (1988).
16. L. Meyer, Calibration of a Three-Wire-Probe for Measurements in Nonisothermal Flow, Exp.Thermal Fluid Sci. 5, 260-267 (1992)
17. A.D. Cutler, P. Bradshaw, A crossed hot-wire technique for complex turbulent flows, Exp. in Fluids 12, 17-22 (1991).
18. J.D. Hooper, Fully developed turbulent flow through a rod cluster, Ph.D. Thesis, School of Nuclear Engineering, University of New South Wales (1980).

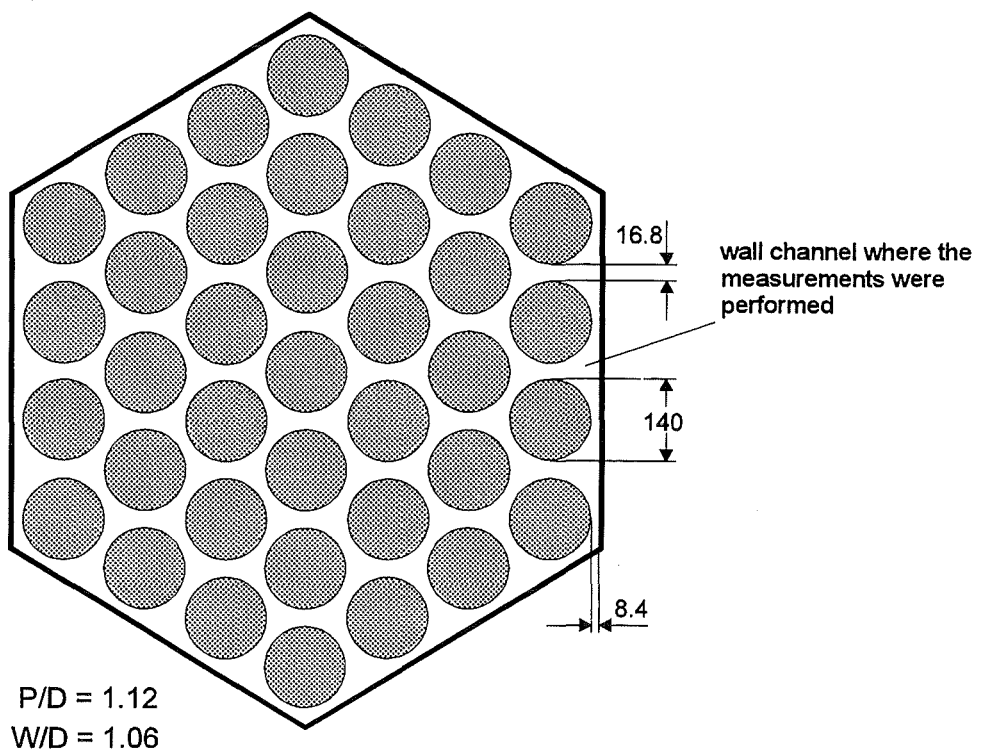


Fig. 1. Cross section of 37-rod bundle.

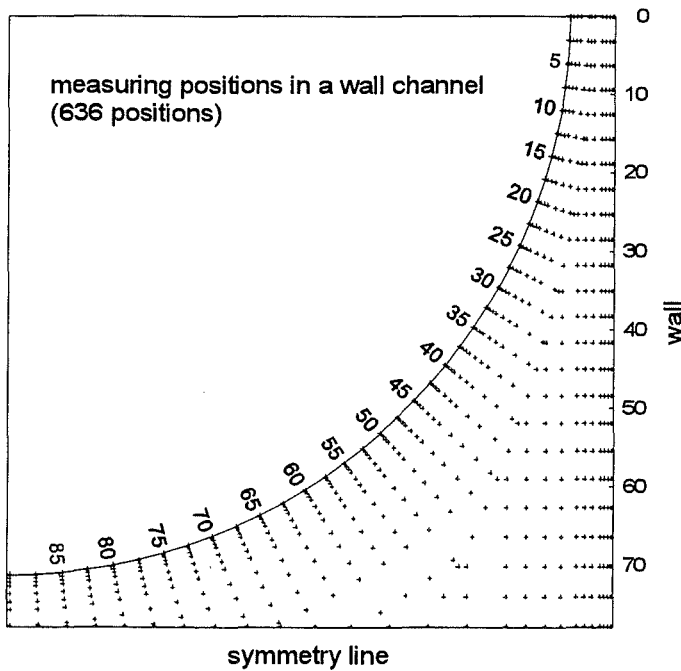


Fig. 2. Measuring positions in a wall channel.

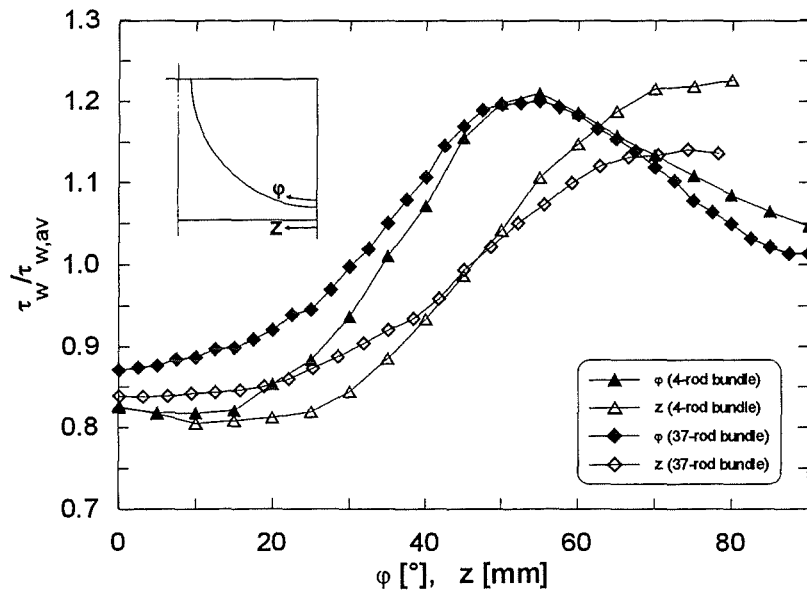


Fig. 3. Wall shear stress distribution.

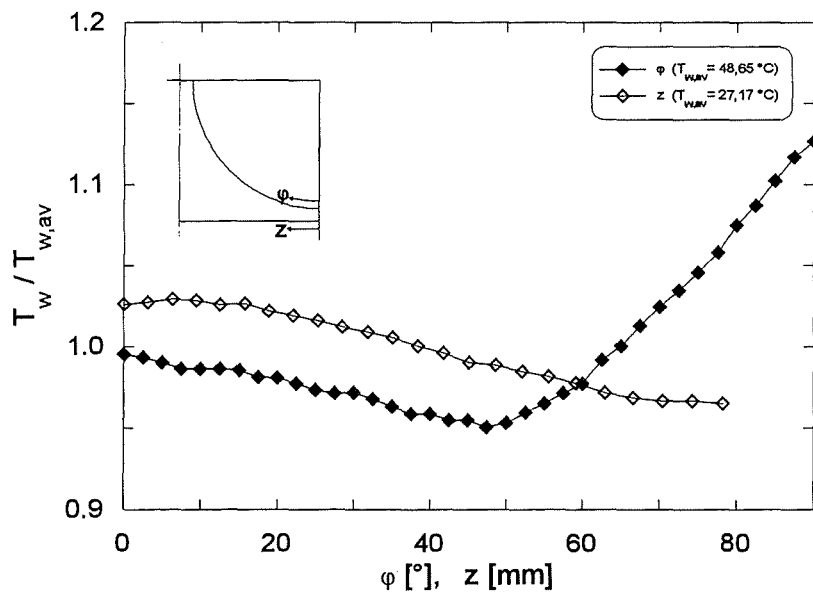


Fig. 4. Wall temperature distribution.

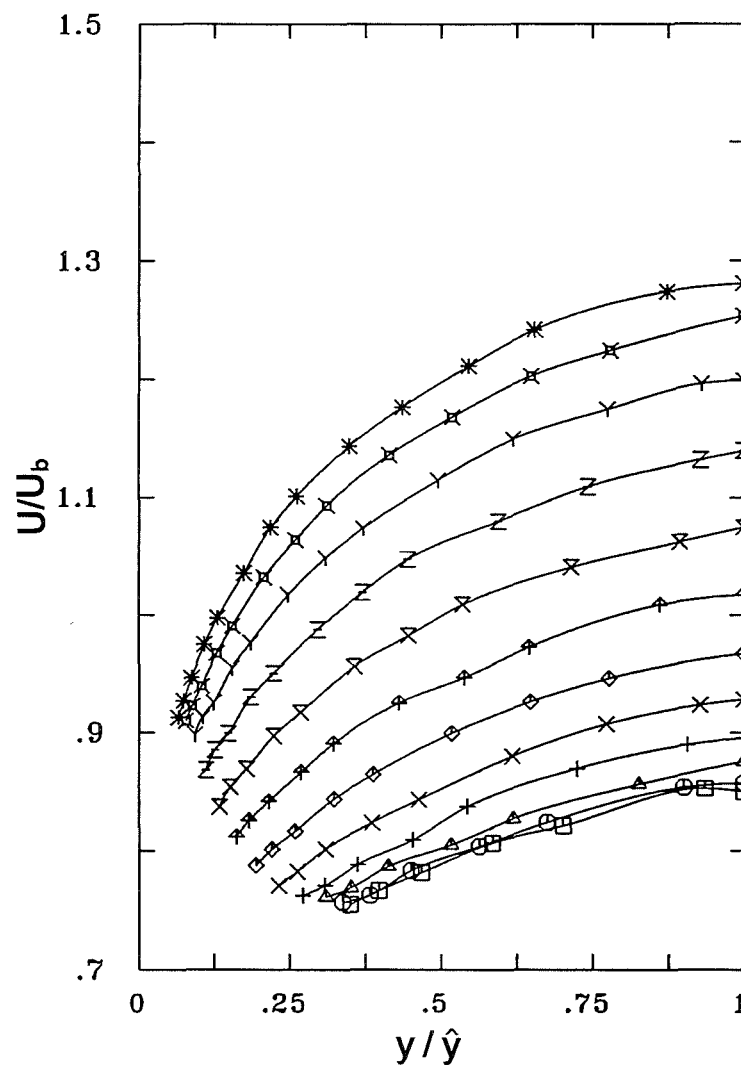
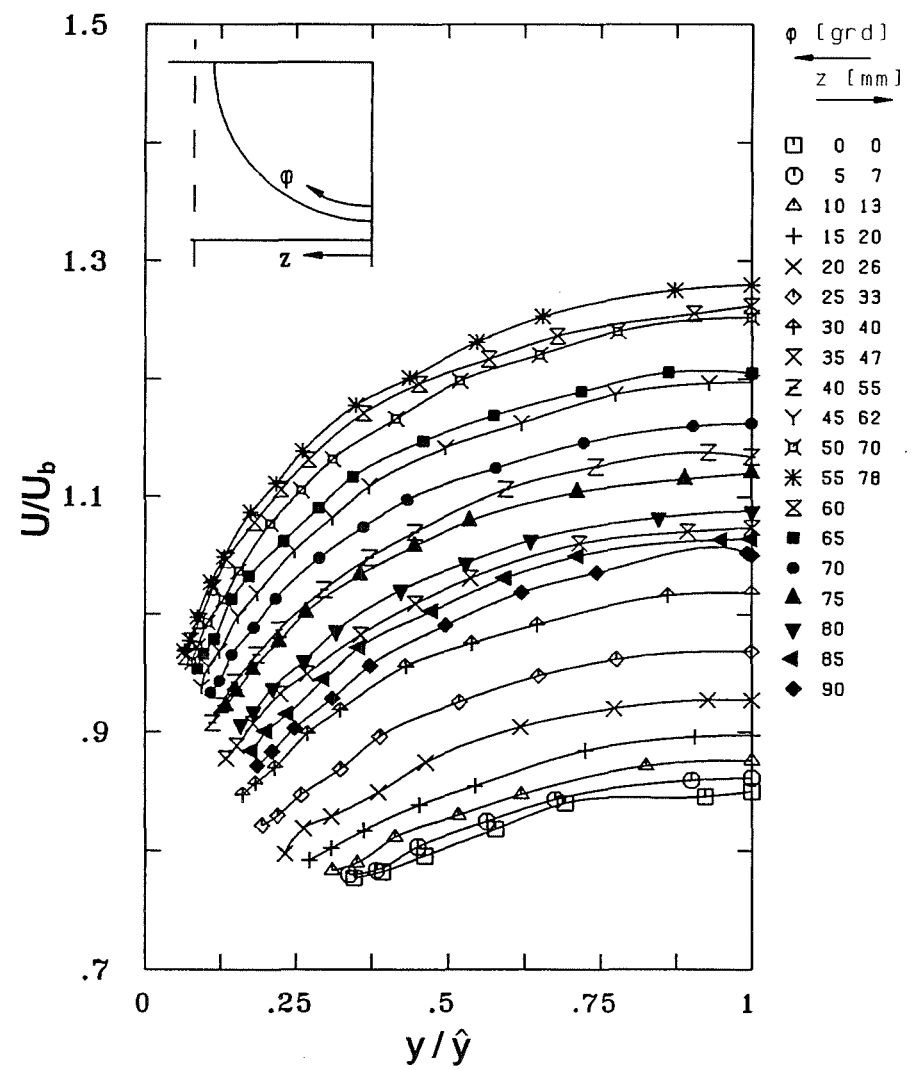


Fig. 5 Distribution of relative time mean velocity

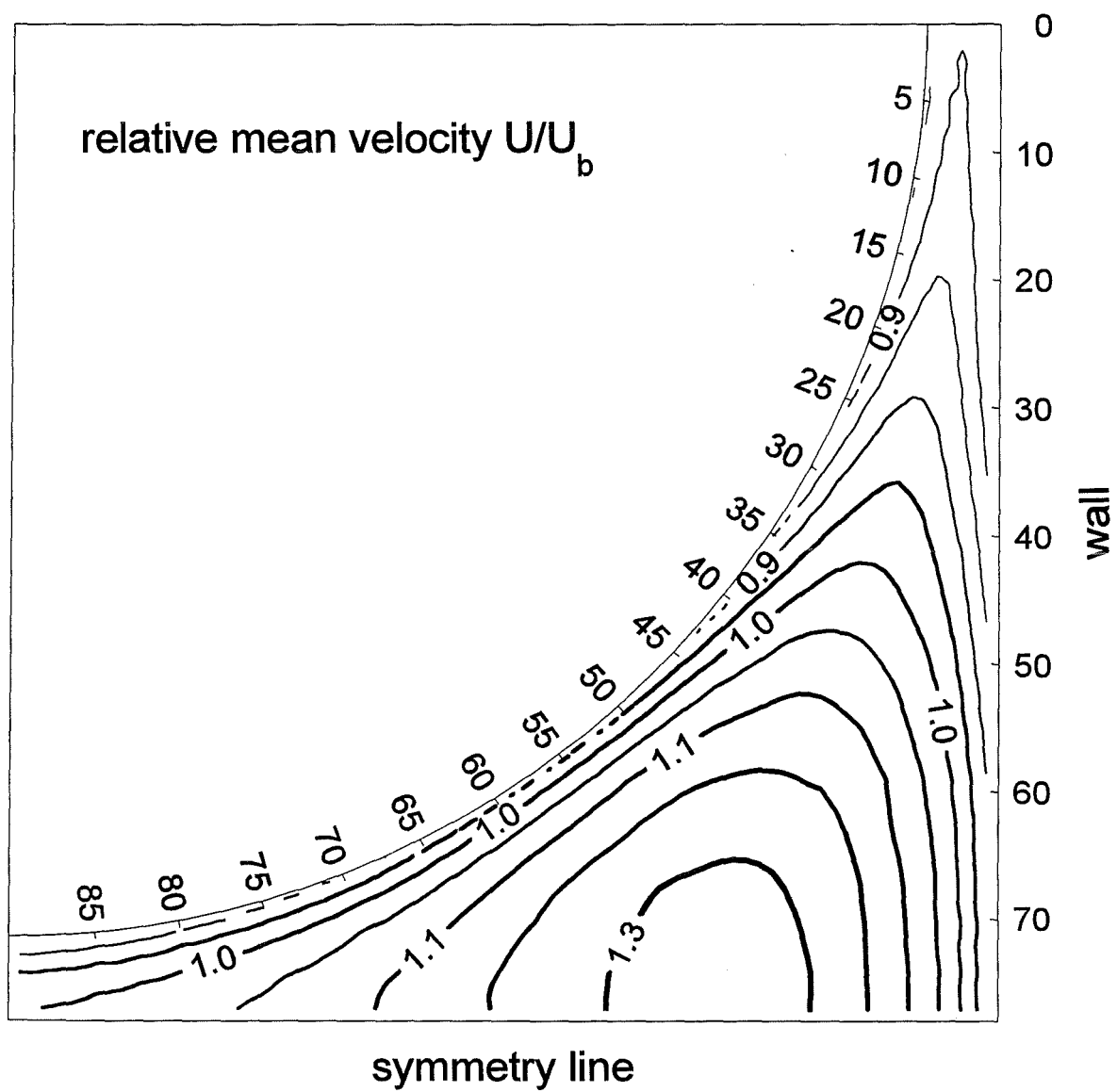


Fig. 6 Contour plot of relative time mean velocity

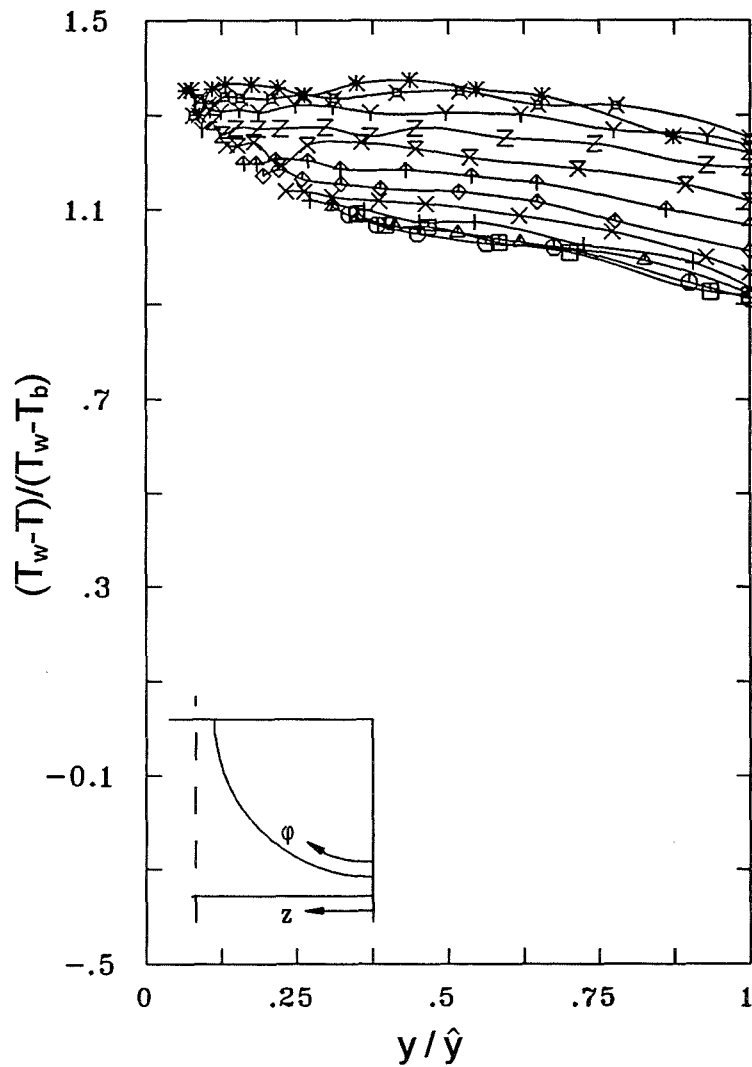
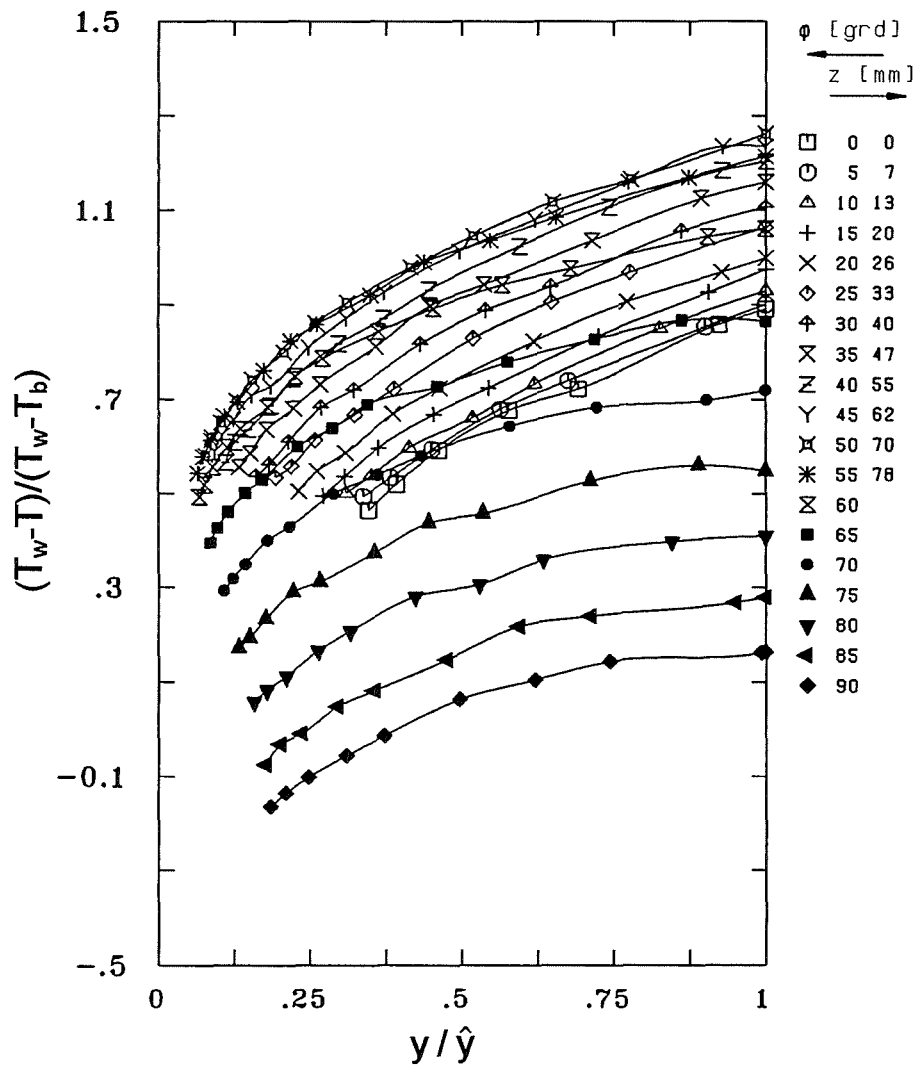


Fig. 7 Distribution of relative time mean temperature

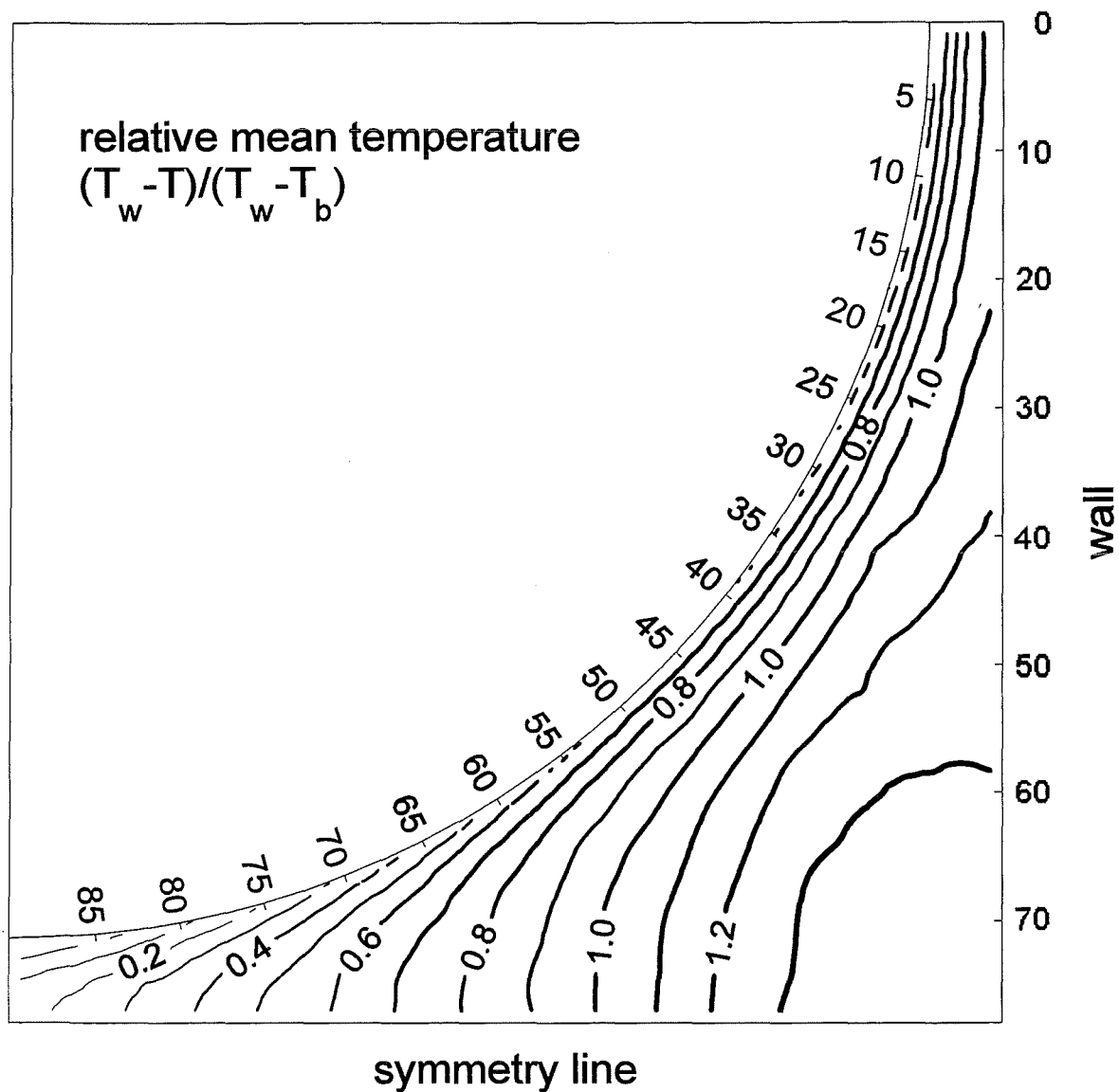


Fig. 8 Contour plot of relative time mean temperature

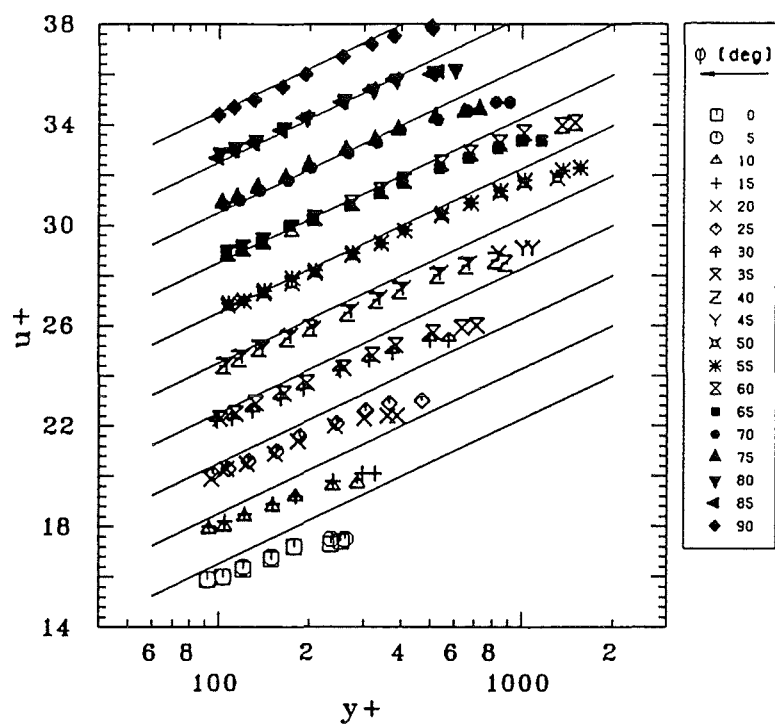


Fig. 9. Logarithmic profiles of the dimensionless velocity (rod).

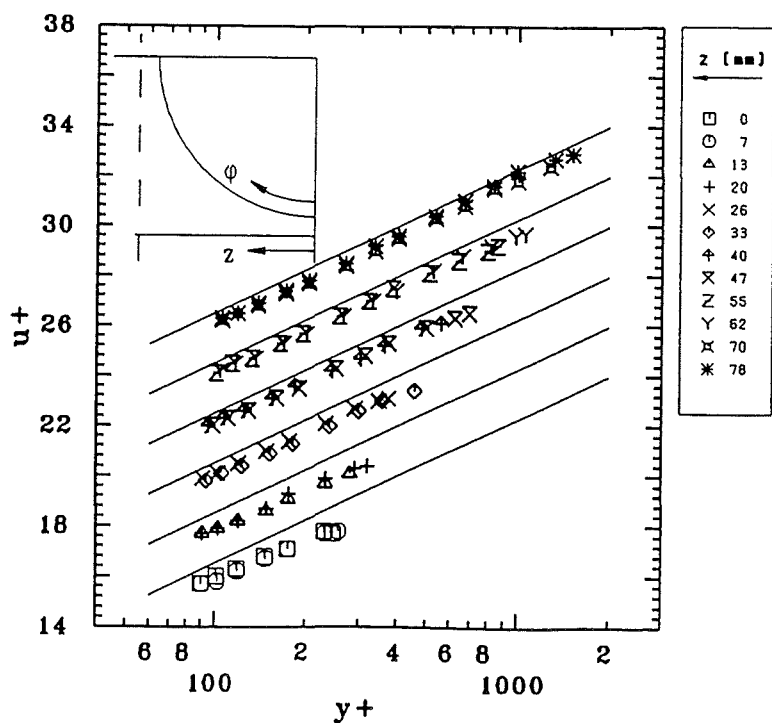


Fig. 10. Logarithmic profiles of the dimensionless velocity (wall).

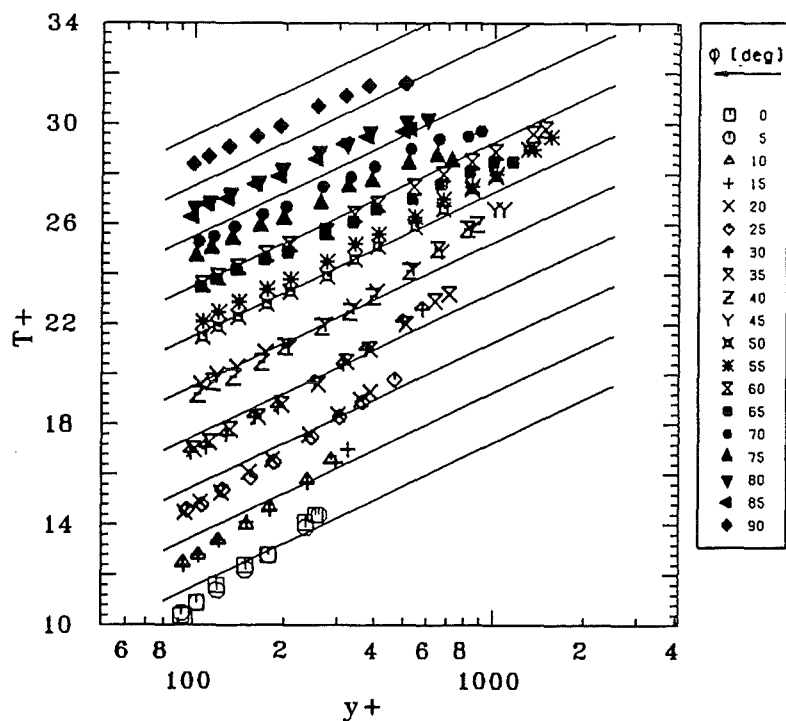


Fig. 11. Logarithmic profiles of the dimensionless temperature (local).

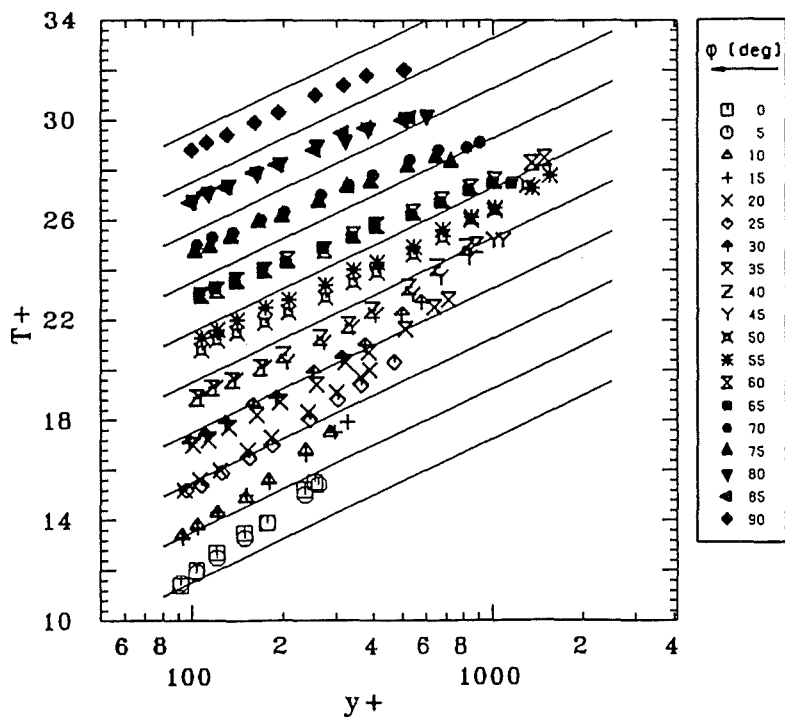


Fig. 12. Logarithmic profiles of the dimensionless temperature (average).

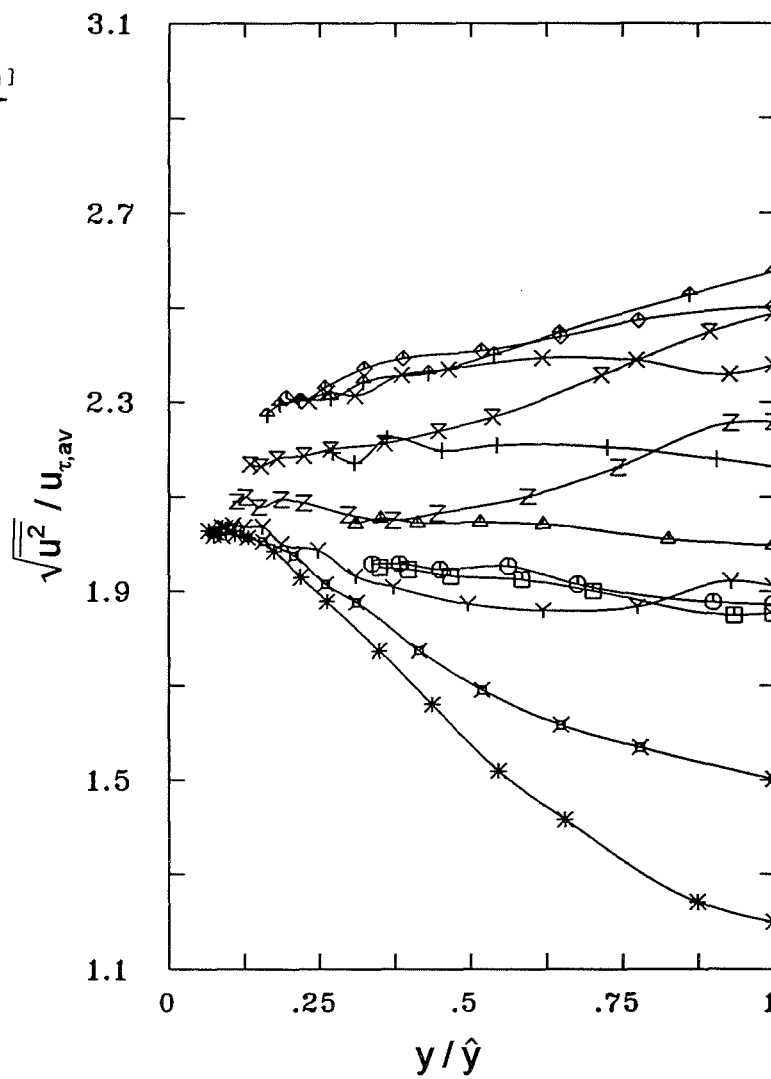
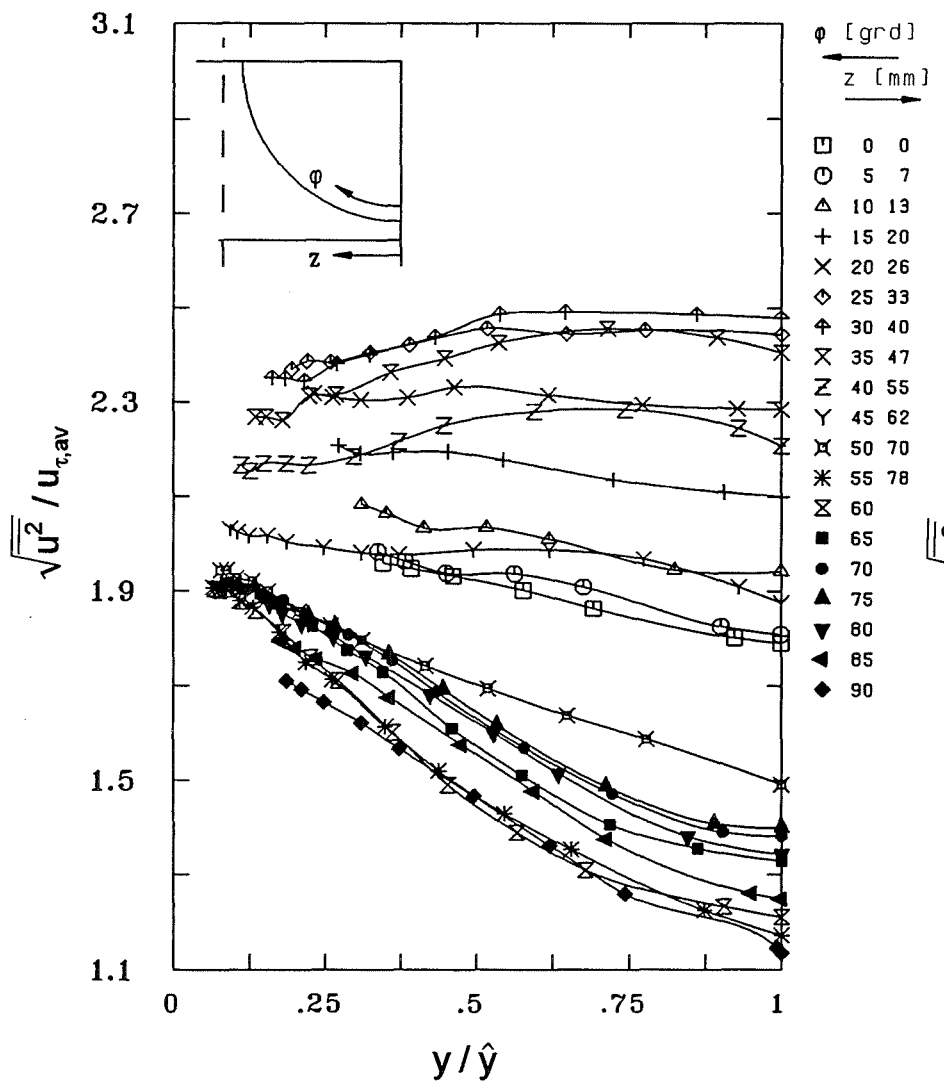


Fig. 13 Turbulent intensity of the axial velocity component

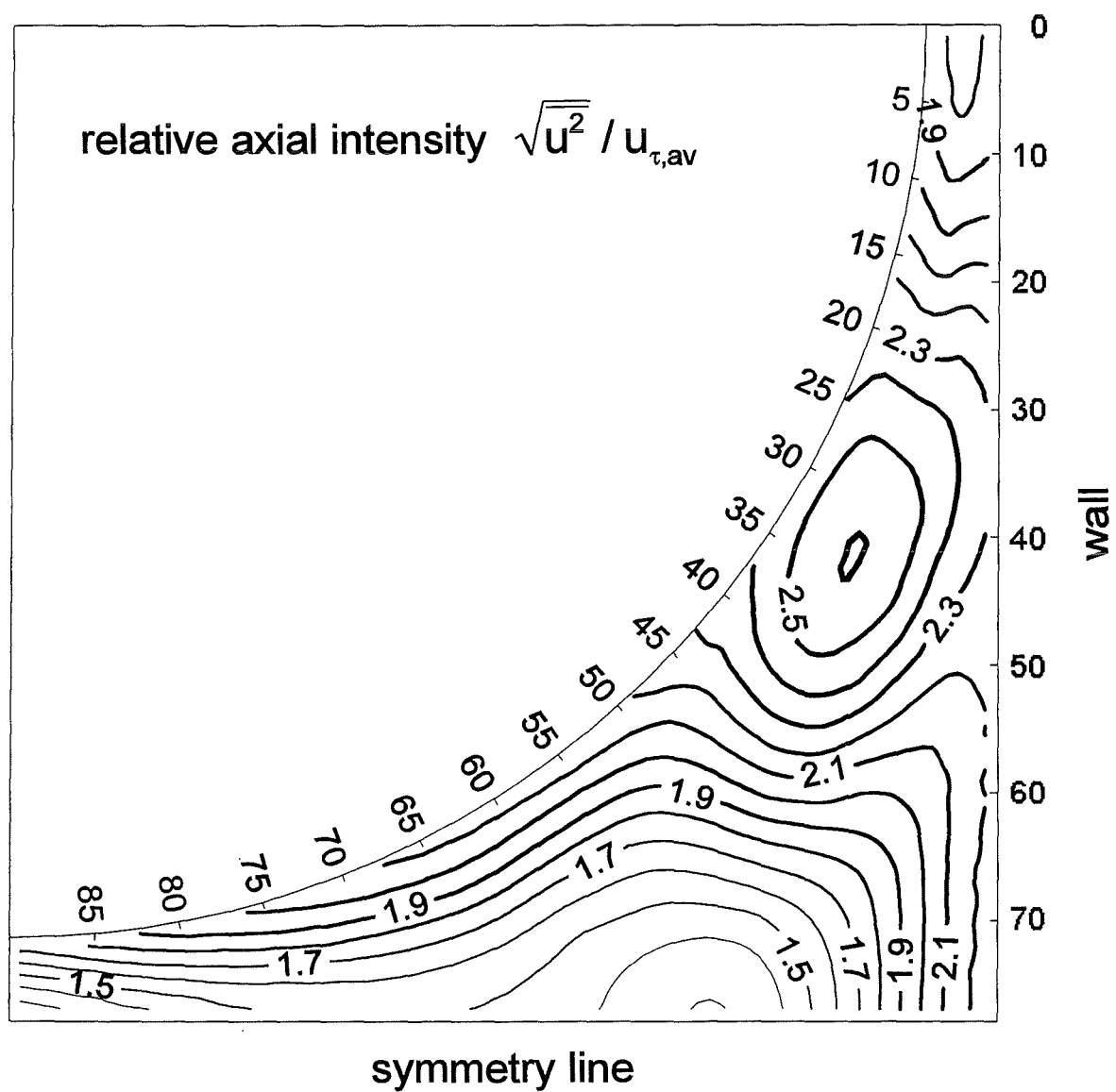


Fig. 14 Contour plot of relative axial intensity

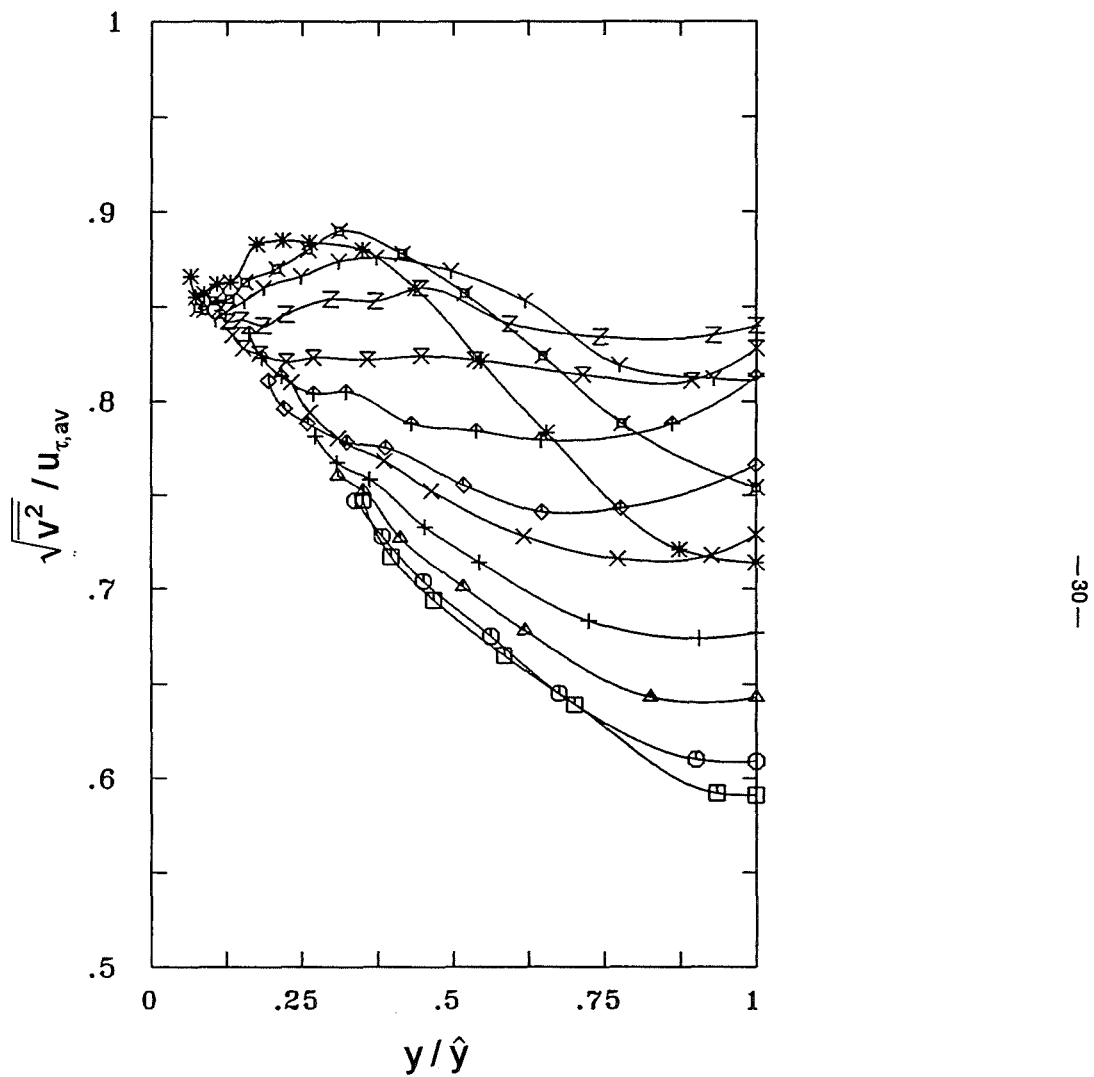
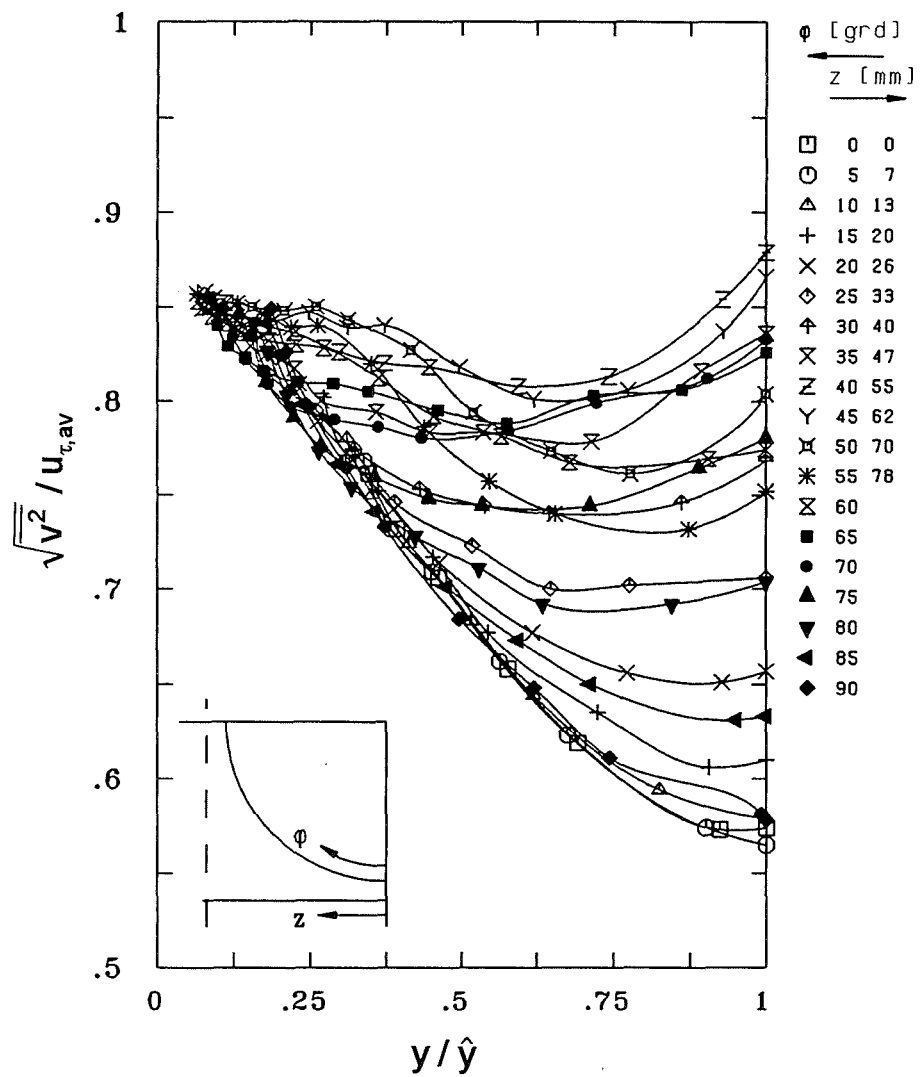


Fig. 15 Turbulent intensity of the radial velocity component

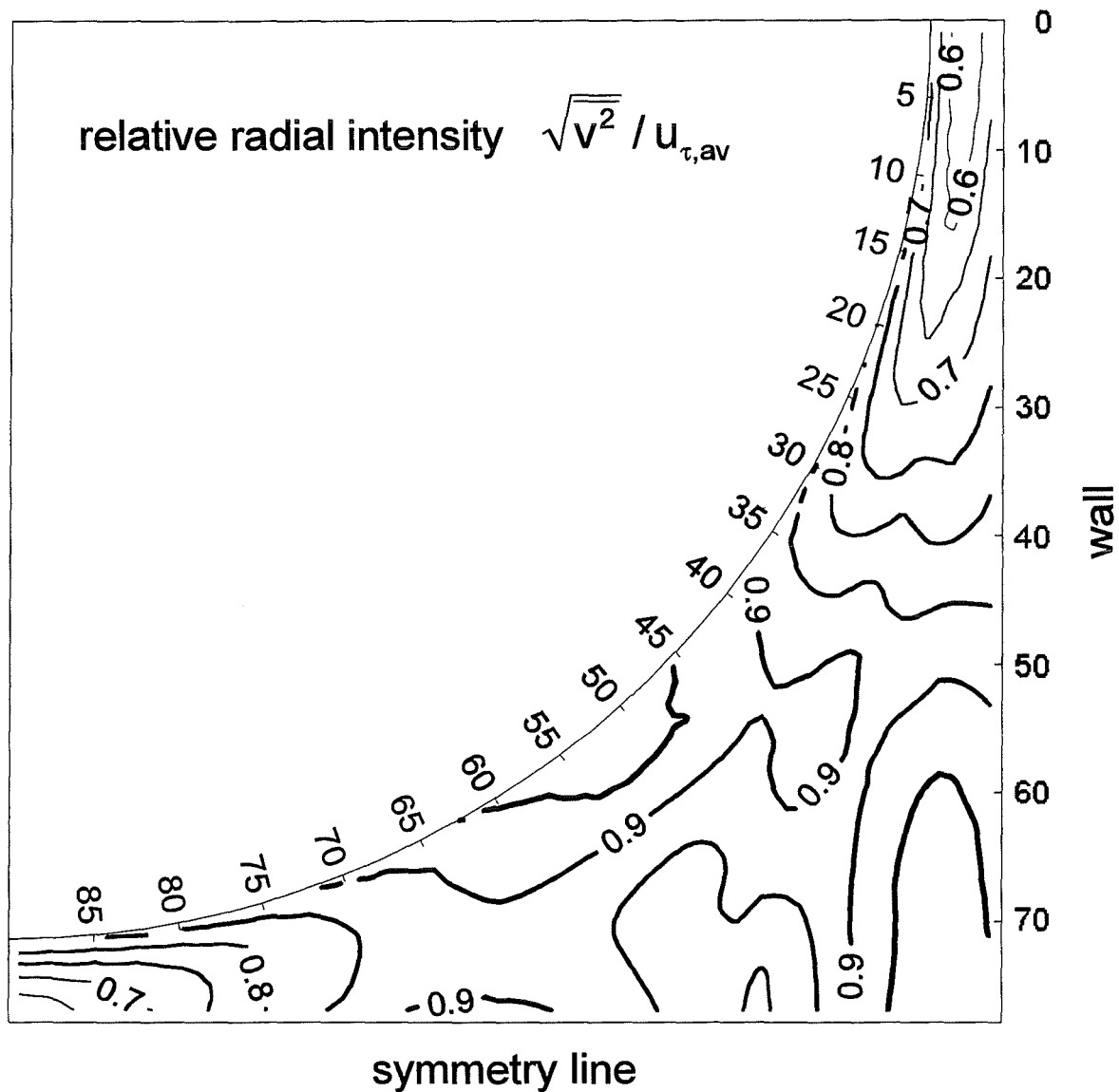


Fig. 16 Contour plot of relative radial intensity

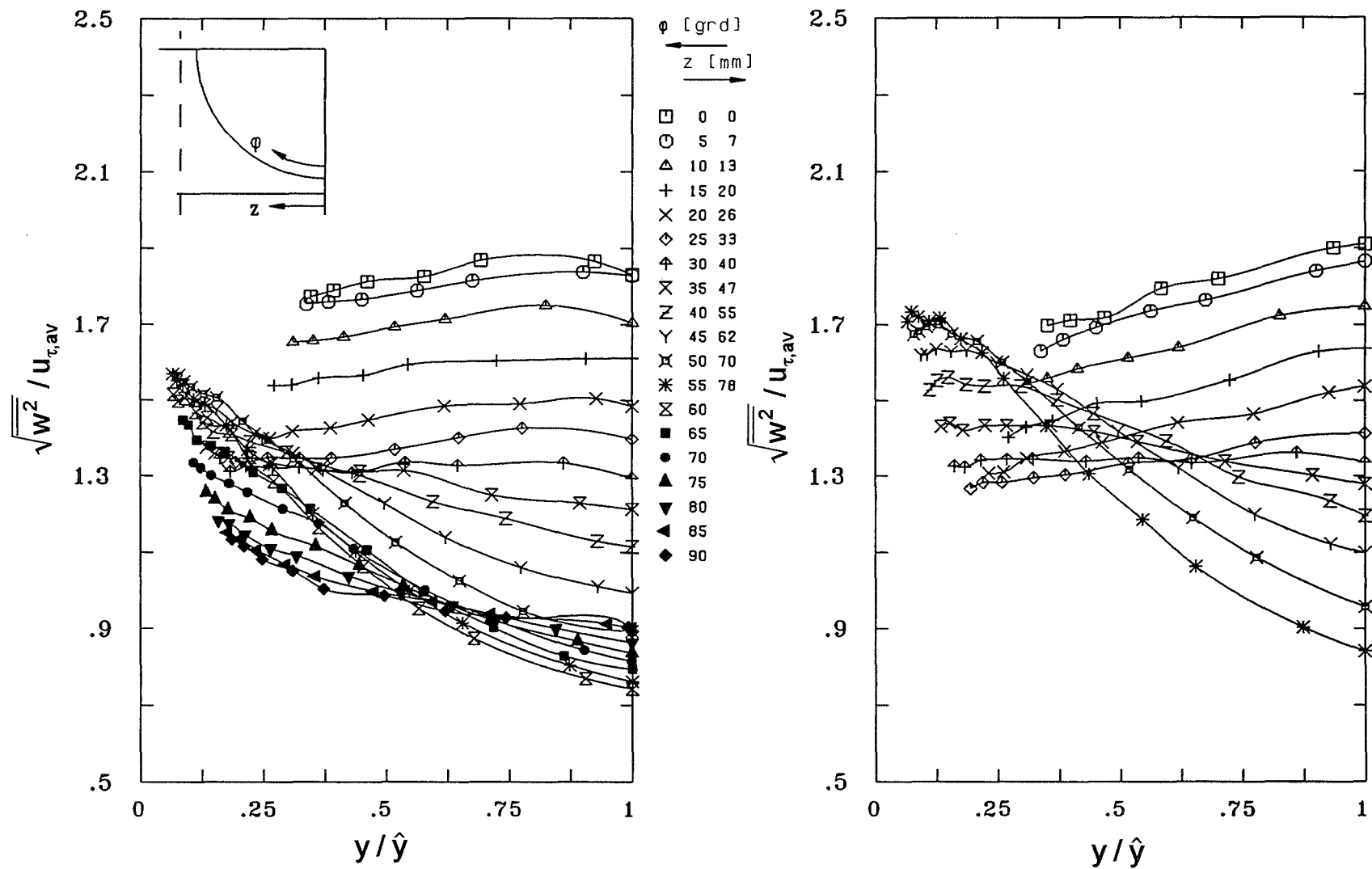


Fig. 17 Turbulent intensity of the azimuthal velocity component

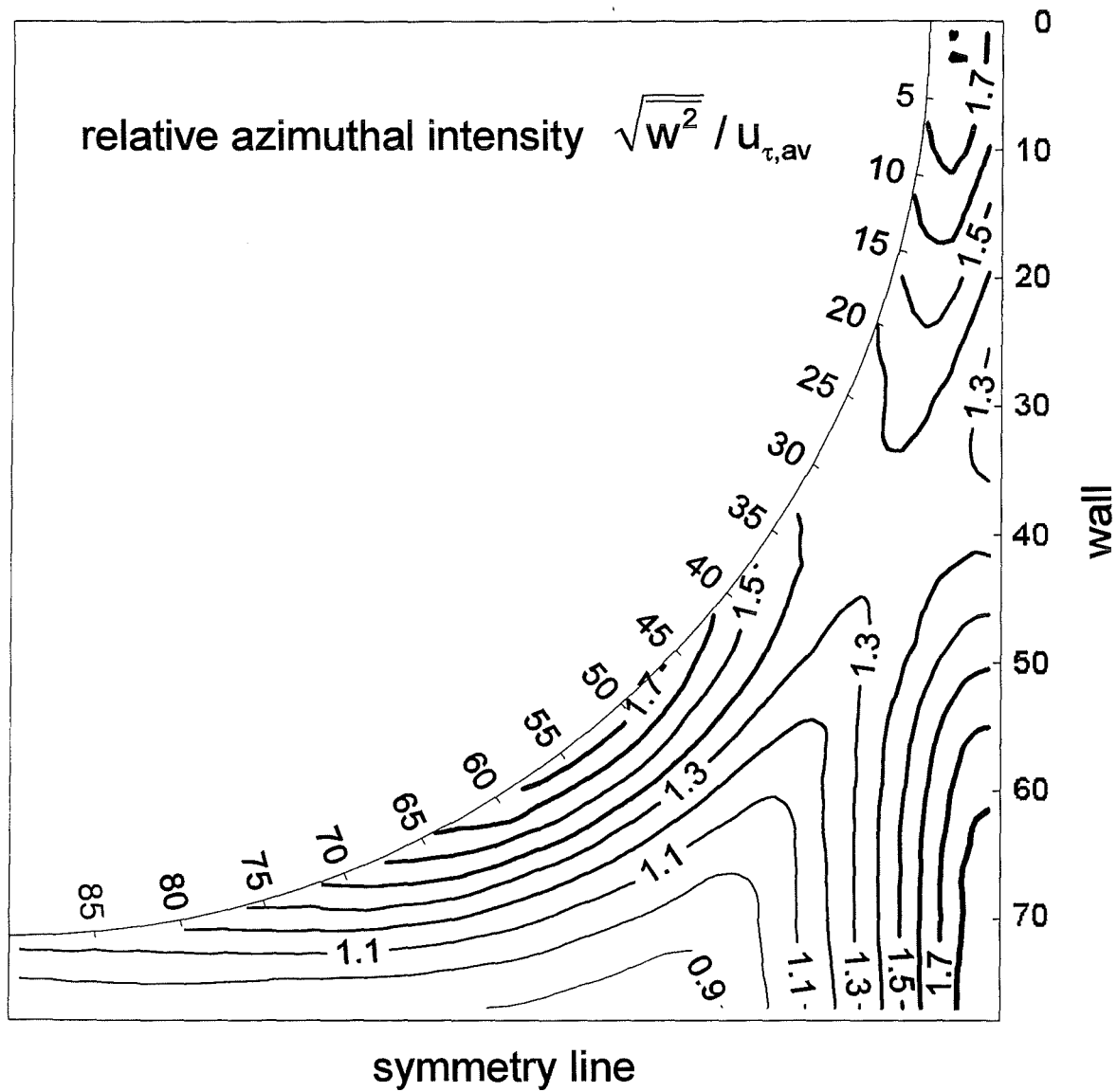


Fig. 18 Contour plot of relative azimuthal intensity

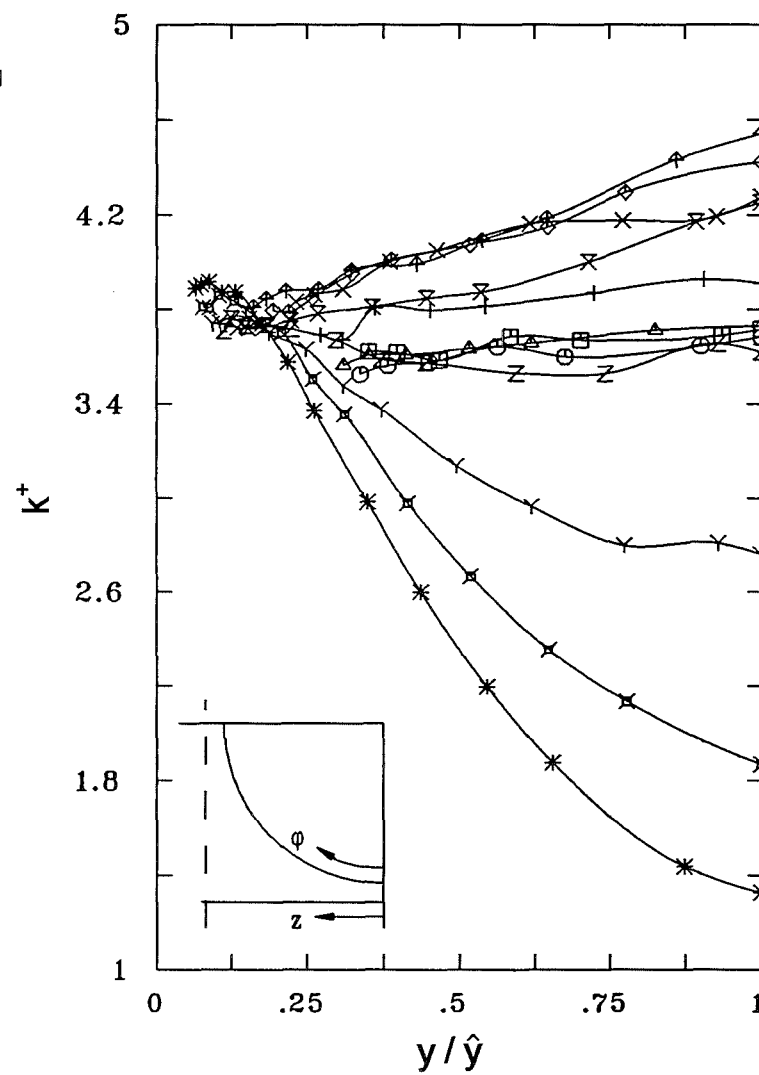
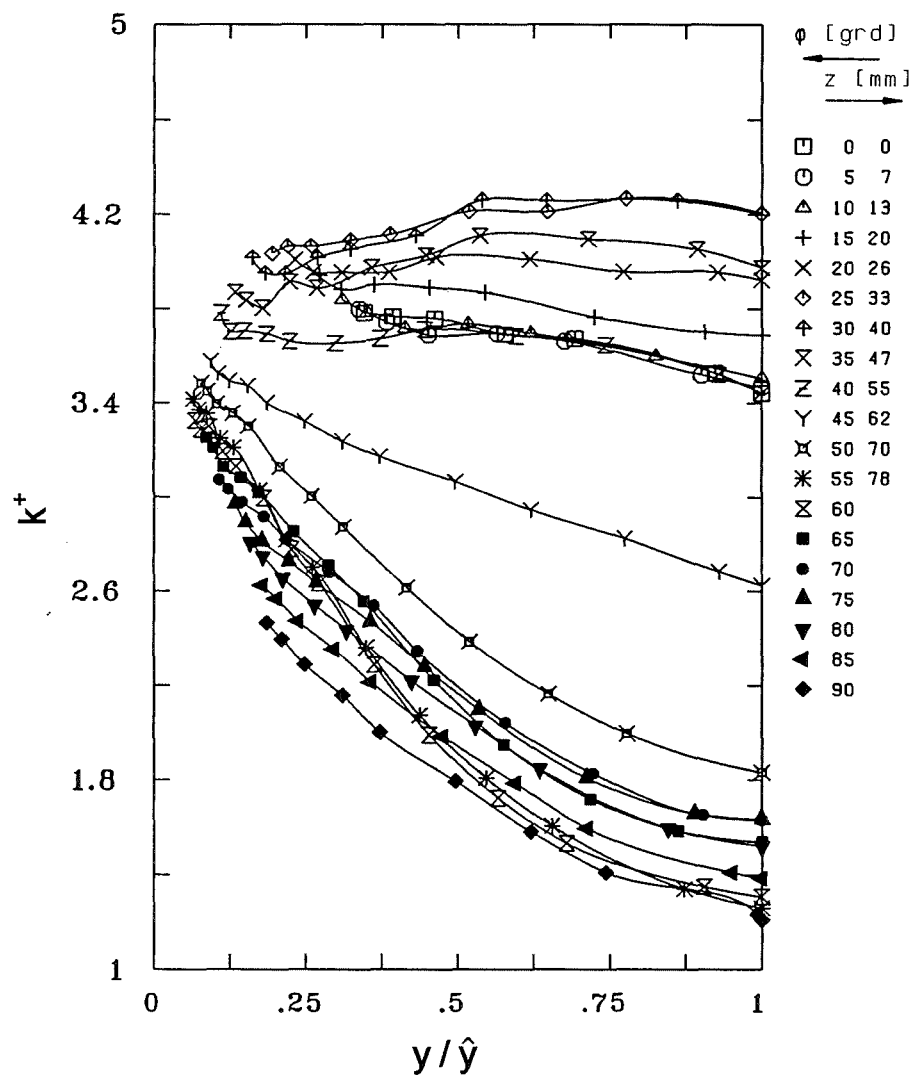


Fig. 19 Turbulent kinetic energy

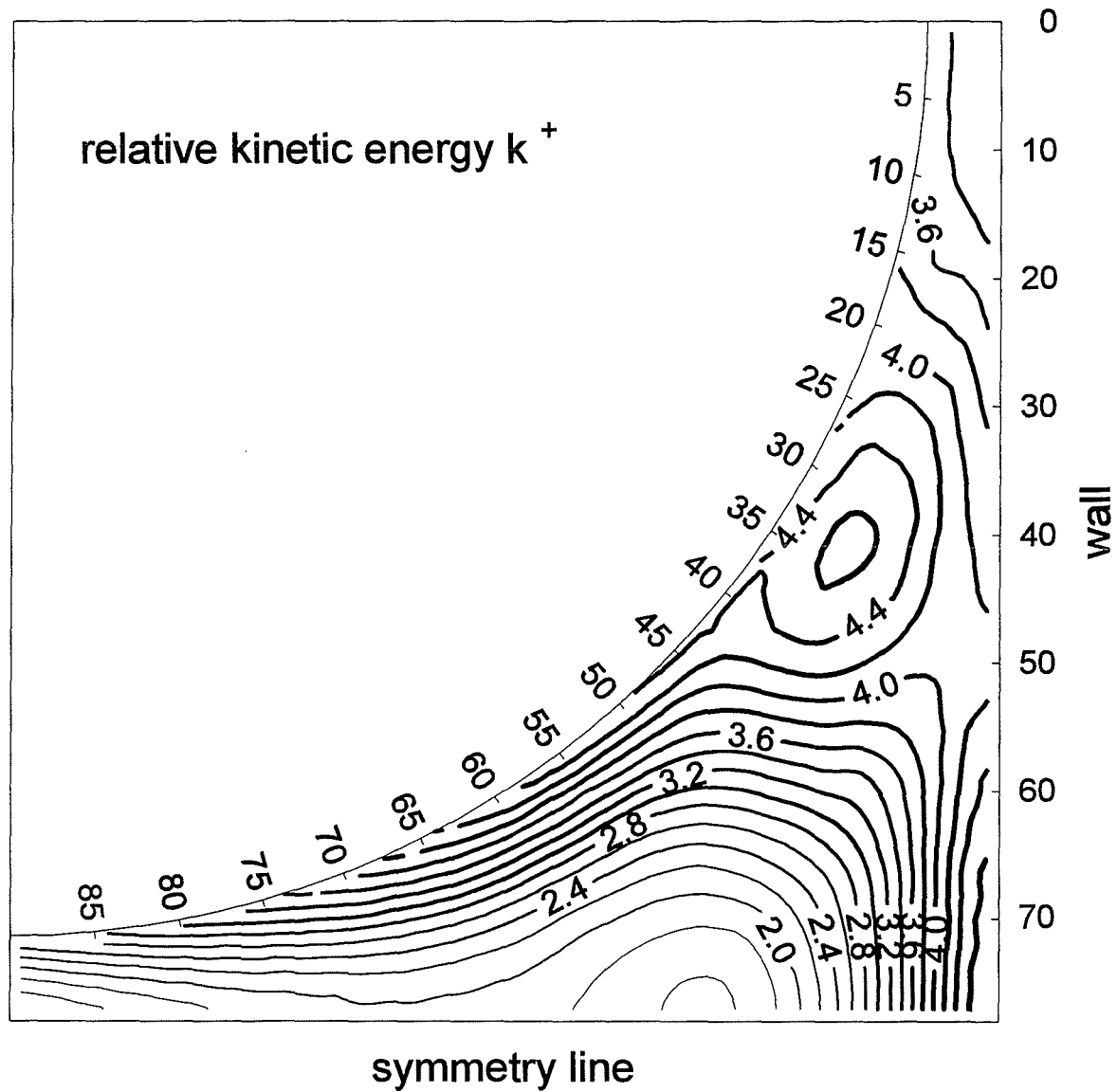


Fig. 20 Contour plot of relative kinetic energy

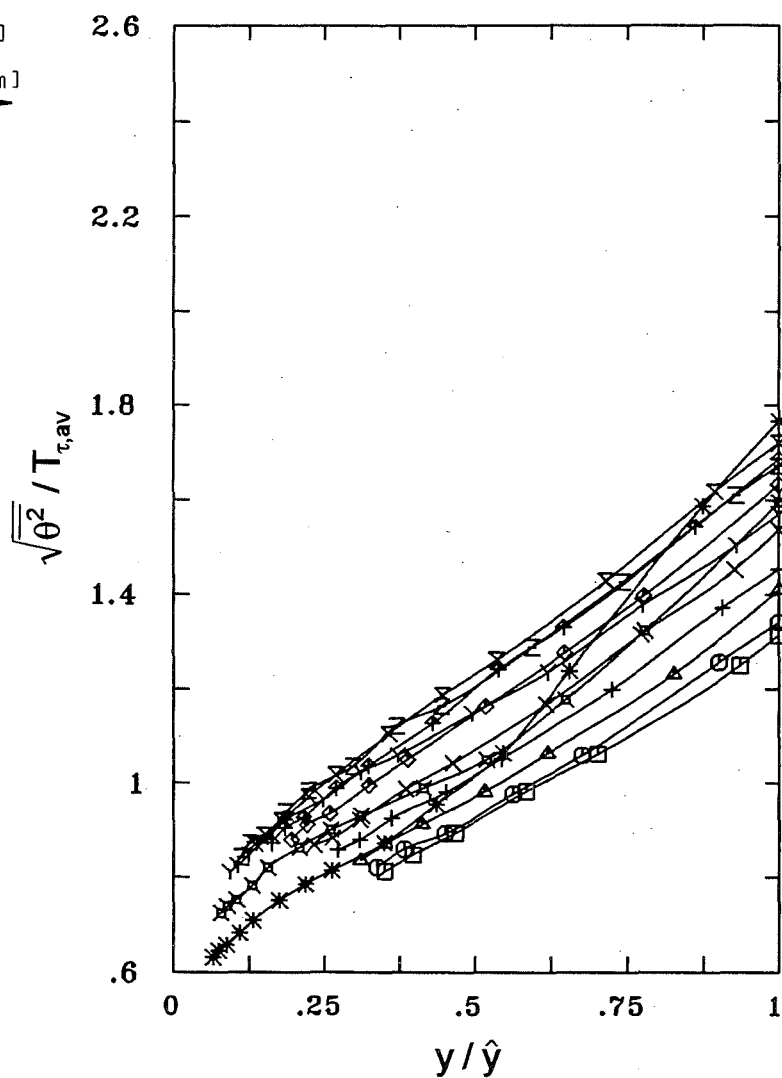
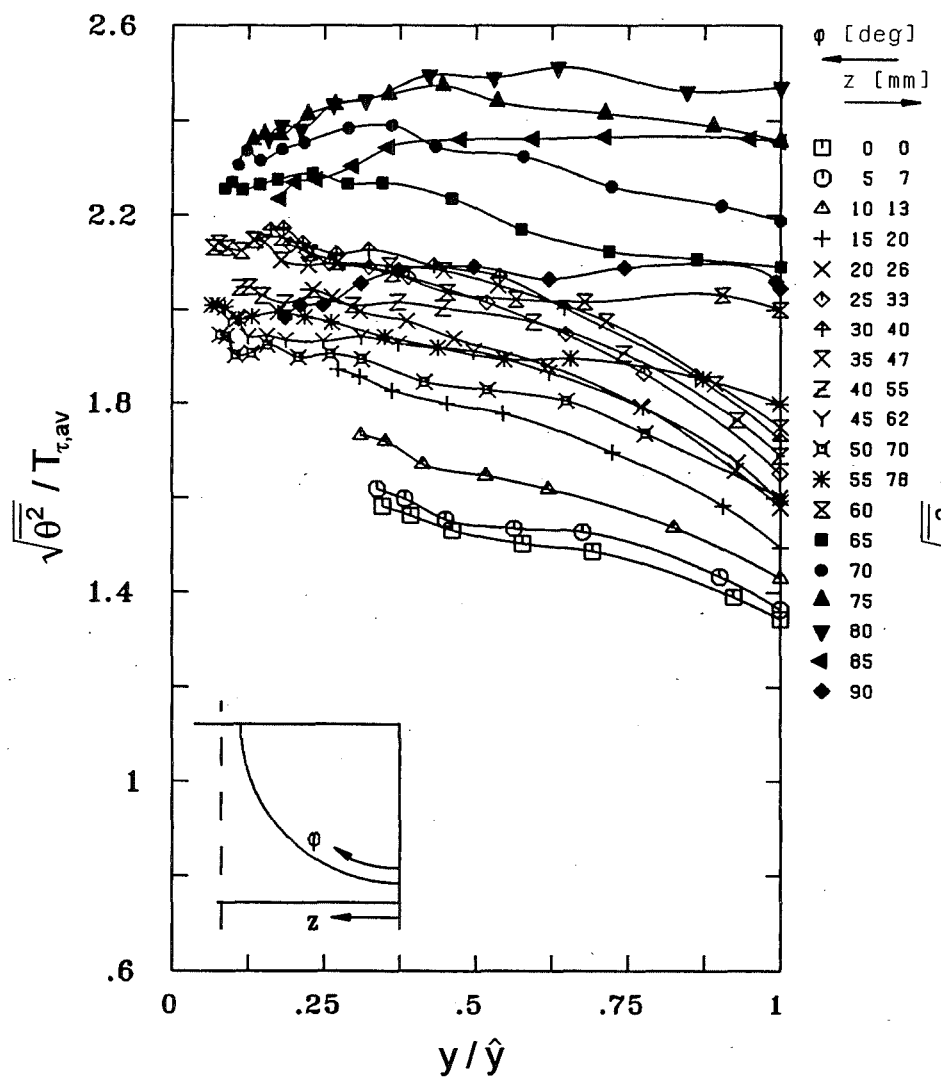


Fig. 21 Turbulent intensity of temperature

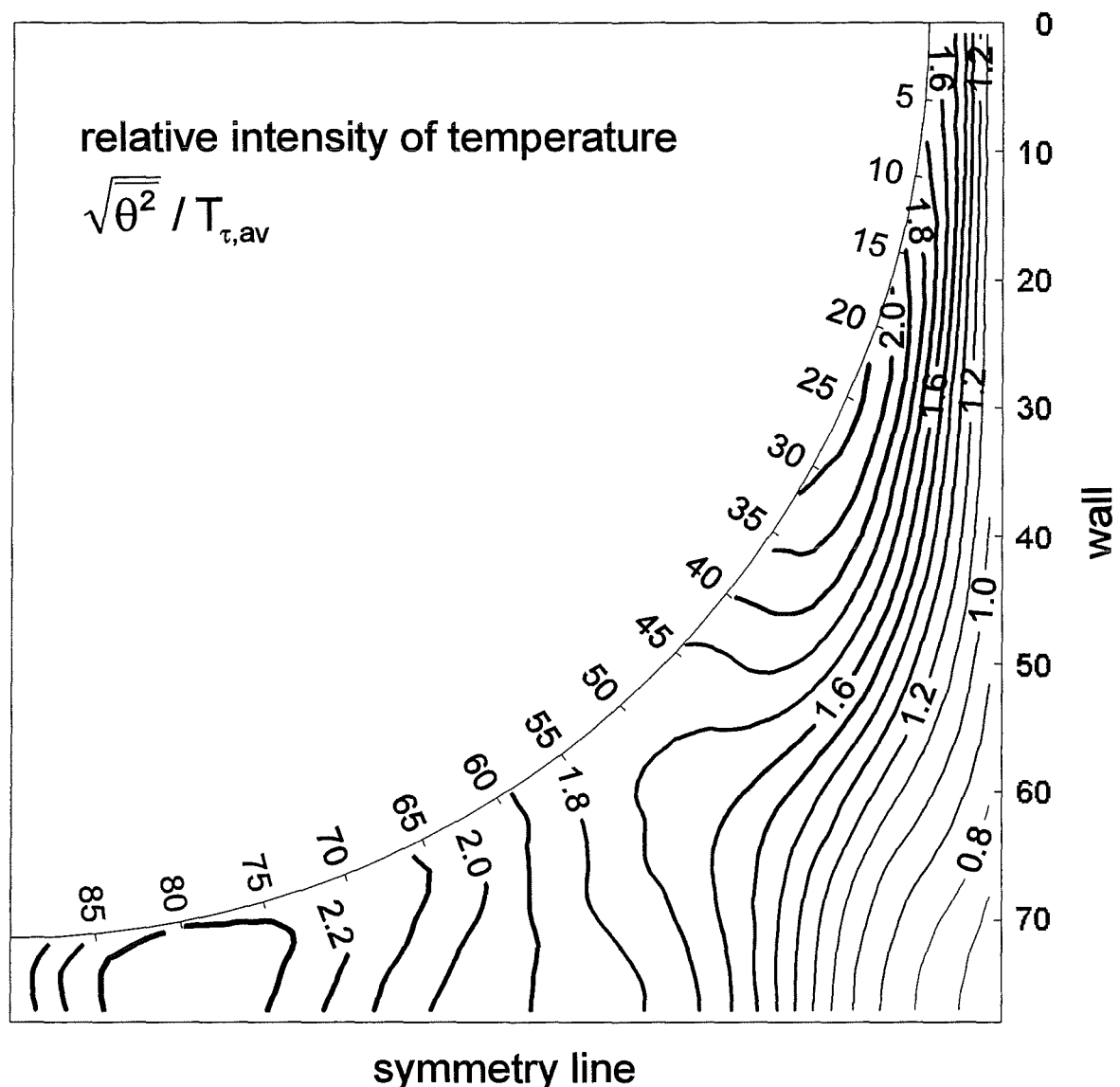


Fig. 22 Contour plot of relative intensity of temperature

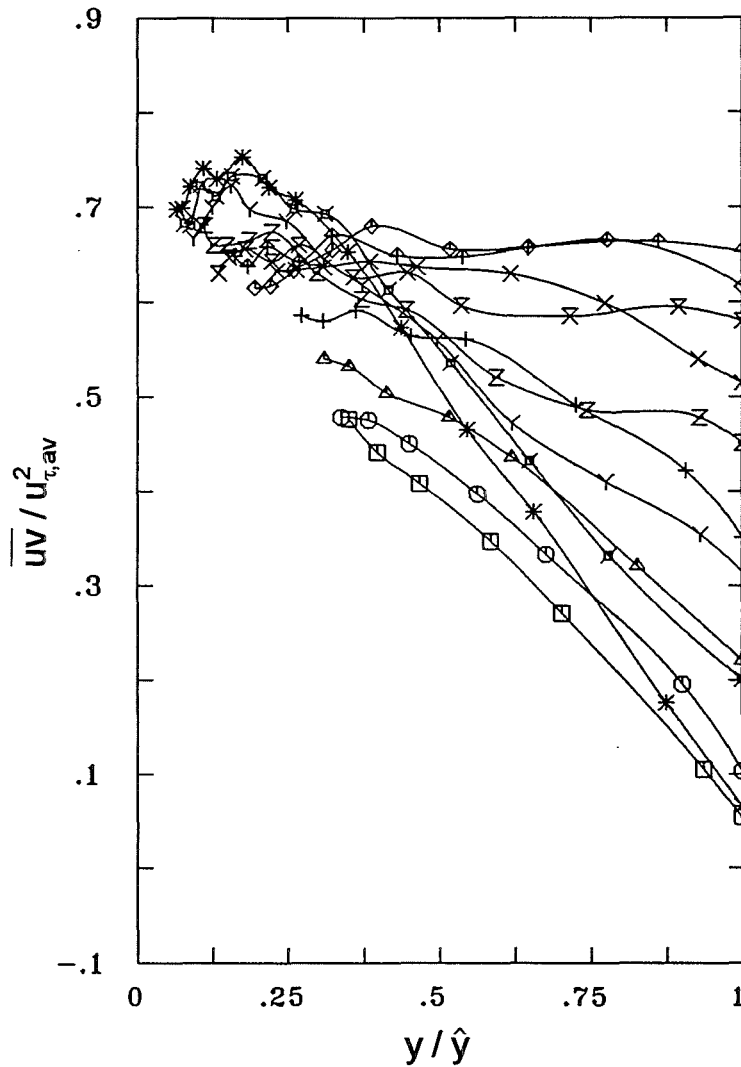
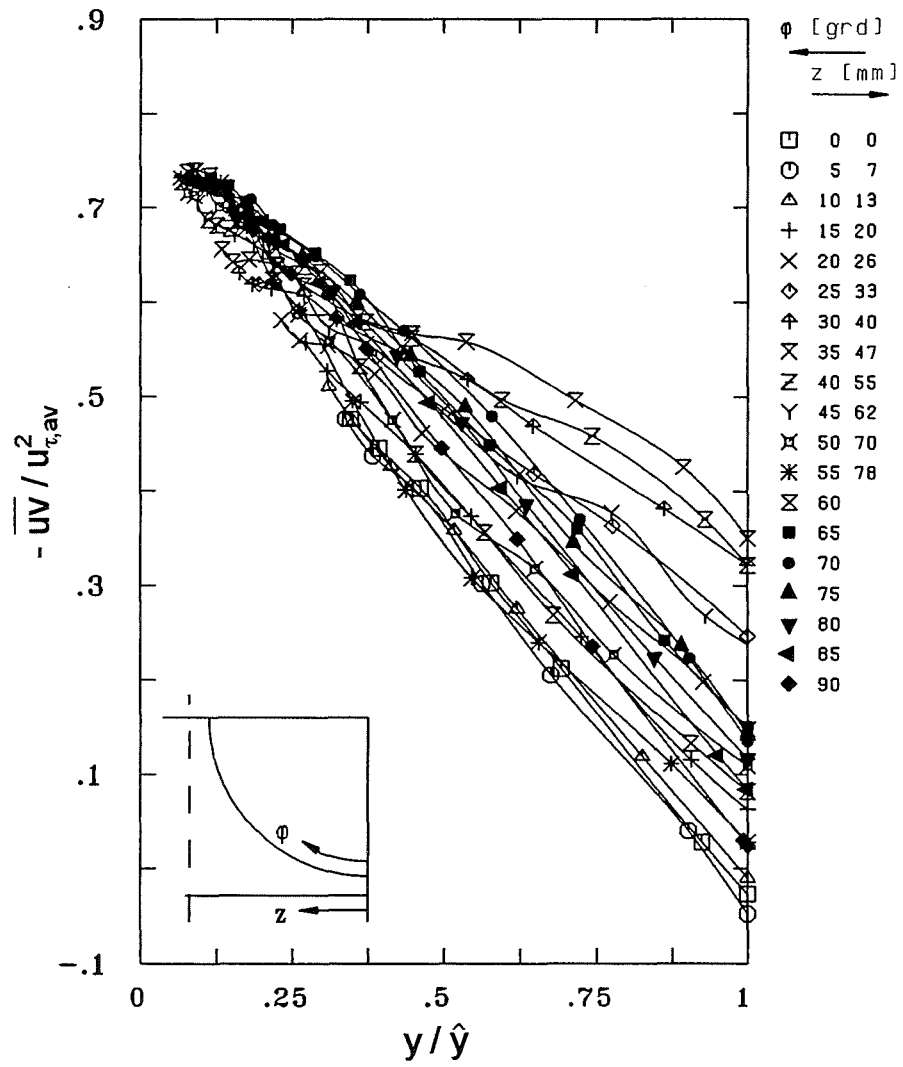


Fig. 23 Relative turbulent shear stress normal to the wall

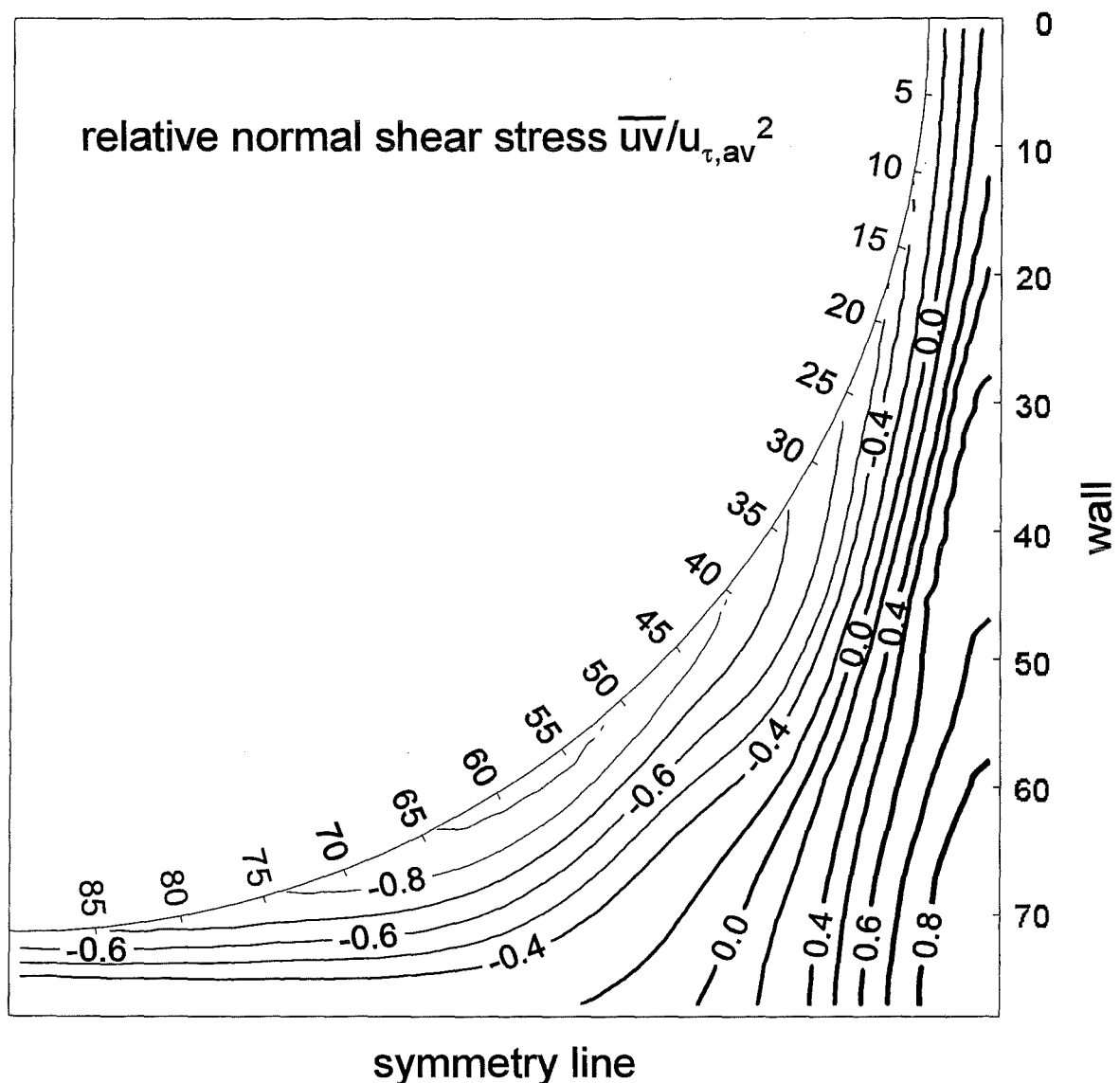


Fig. 24 Contour plot of relative normal shear stress

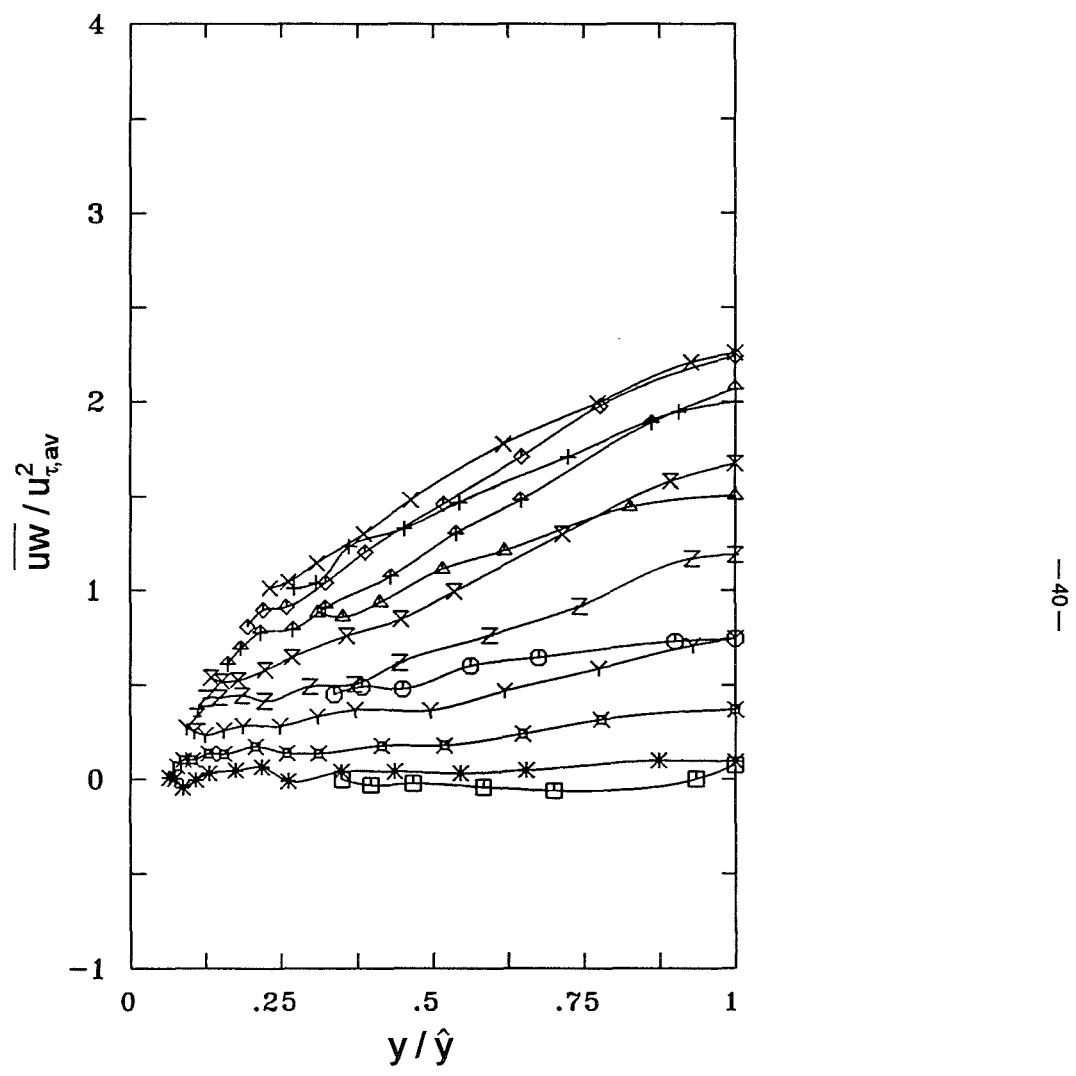
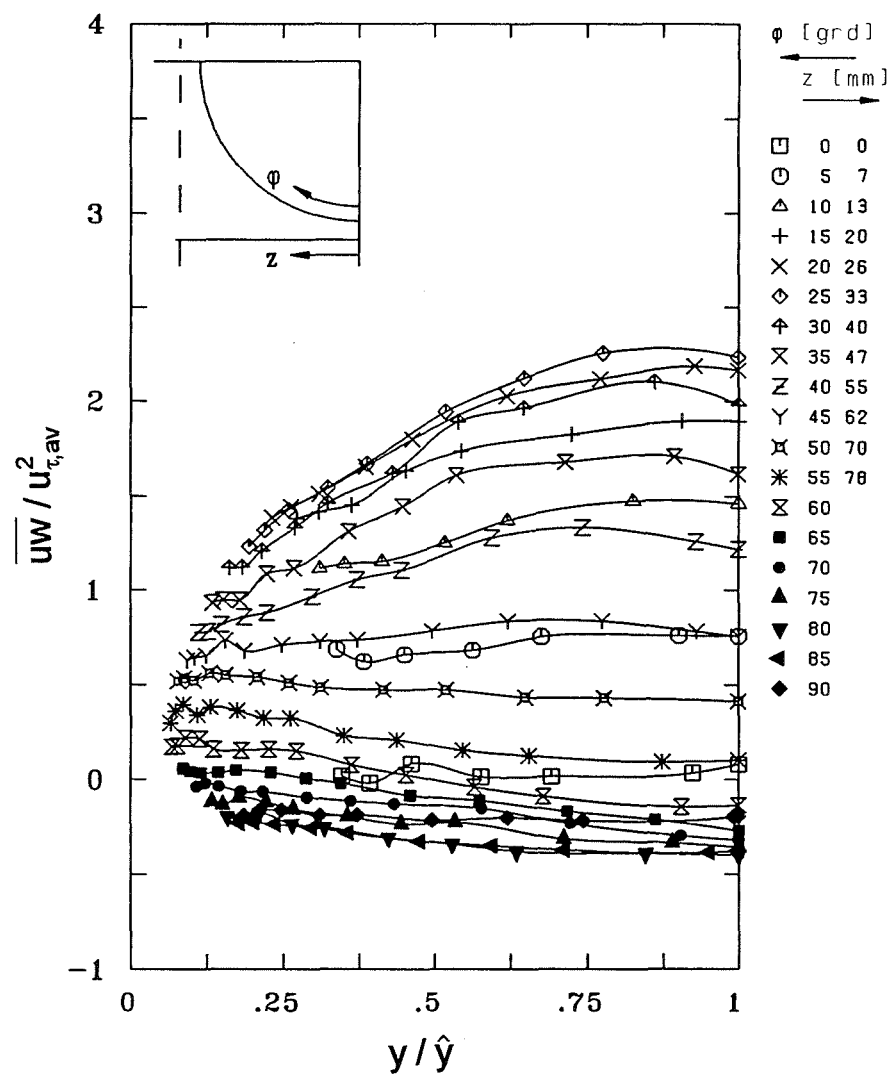


Fig. 25 Relative turbulent shear stress in azimuthal direction

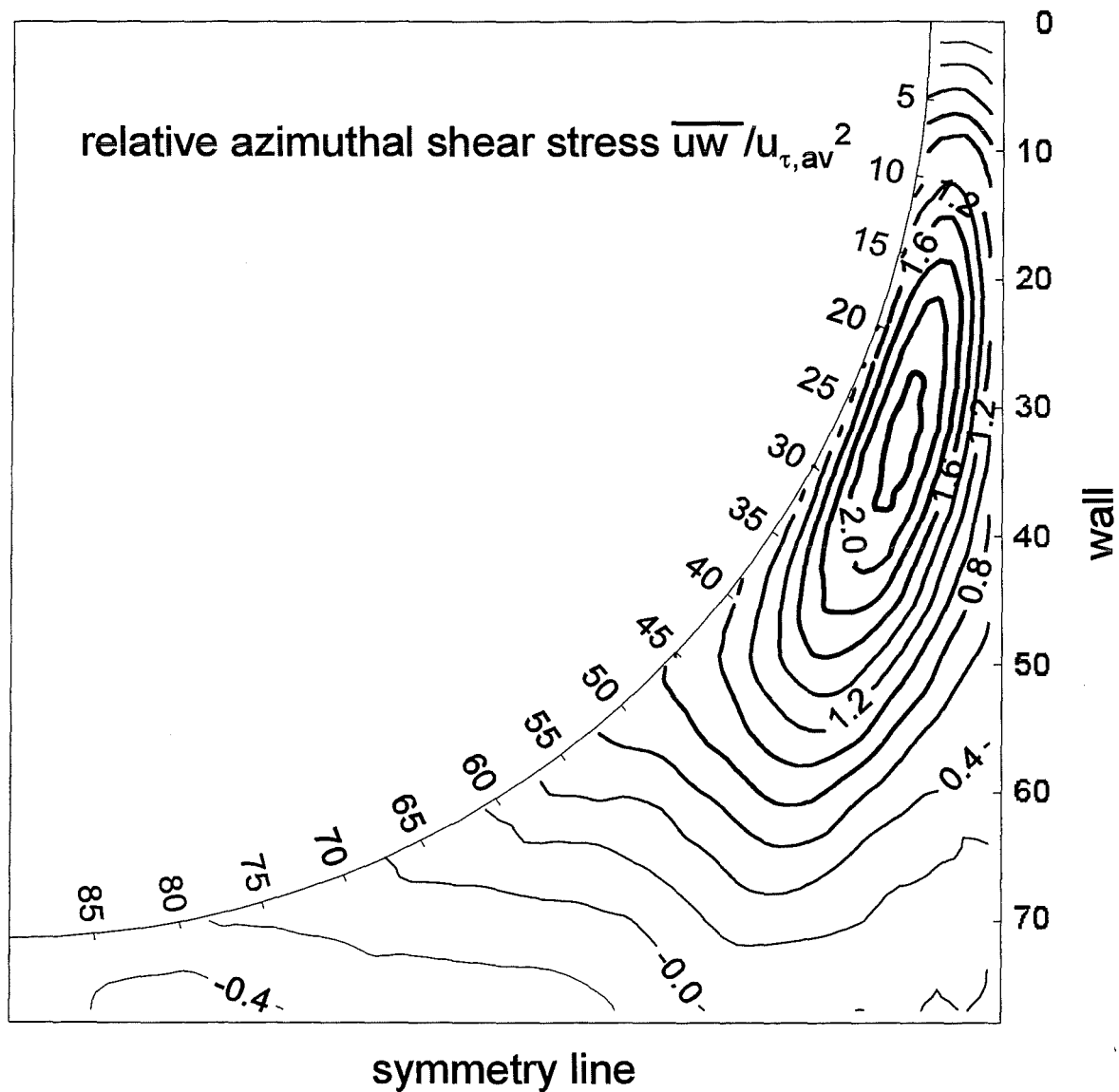


Fig. 26 Contour plot of relative azimuthal shear stress

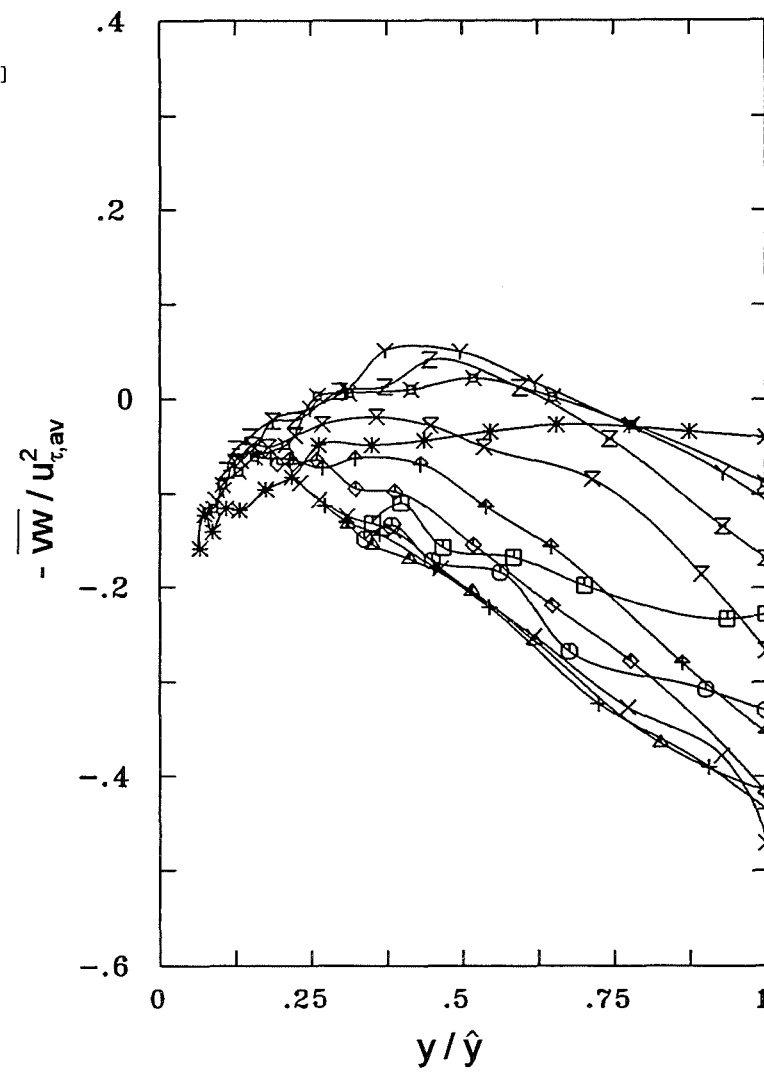
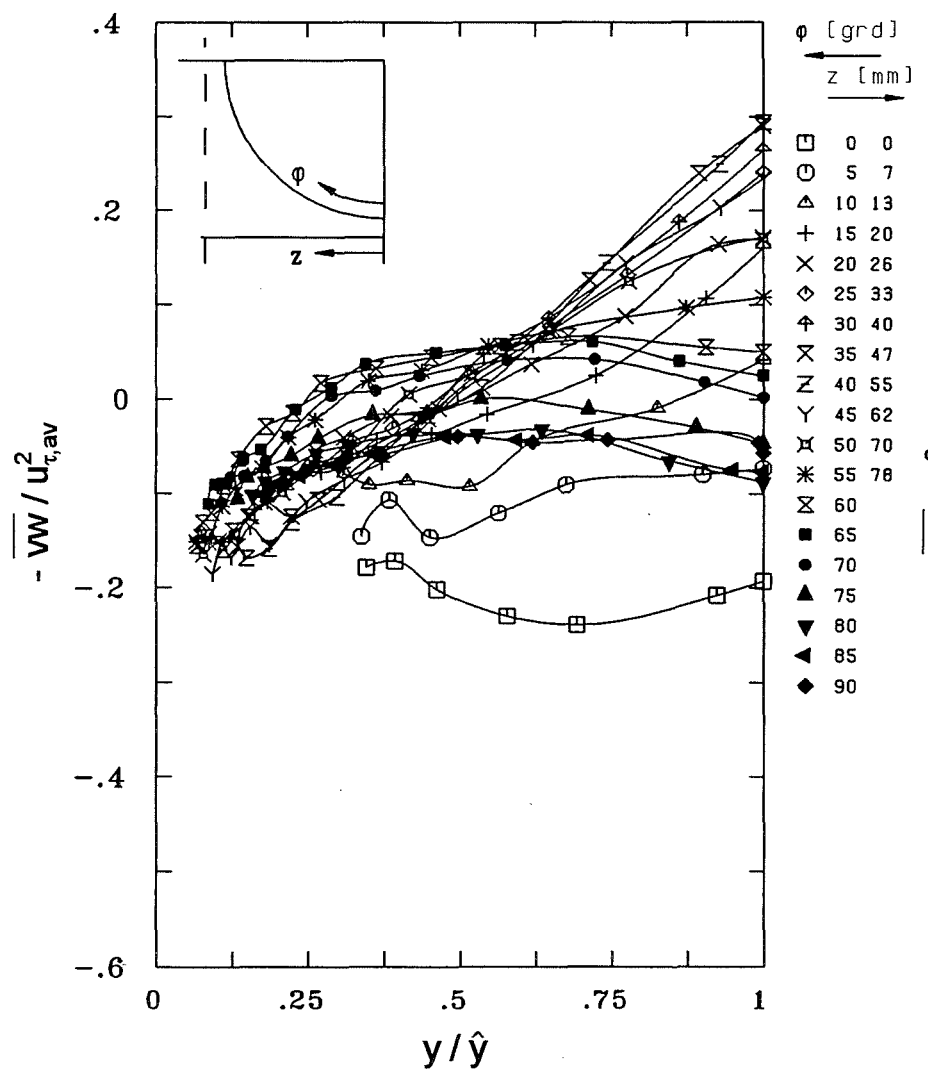


Fig. 27 Relative turbulent planar shear stress

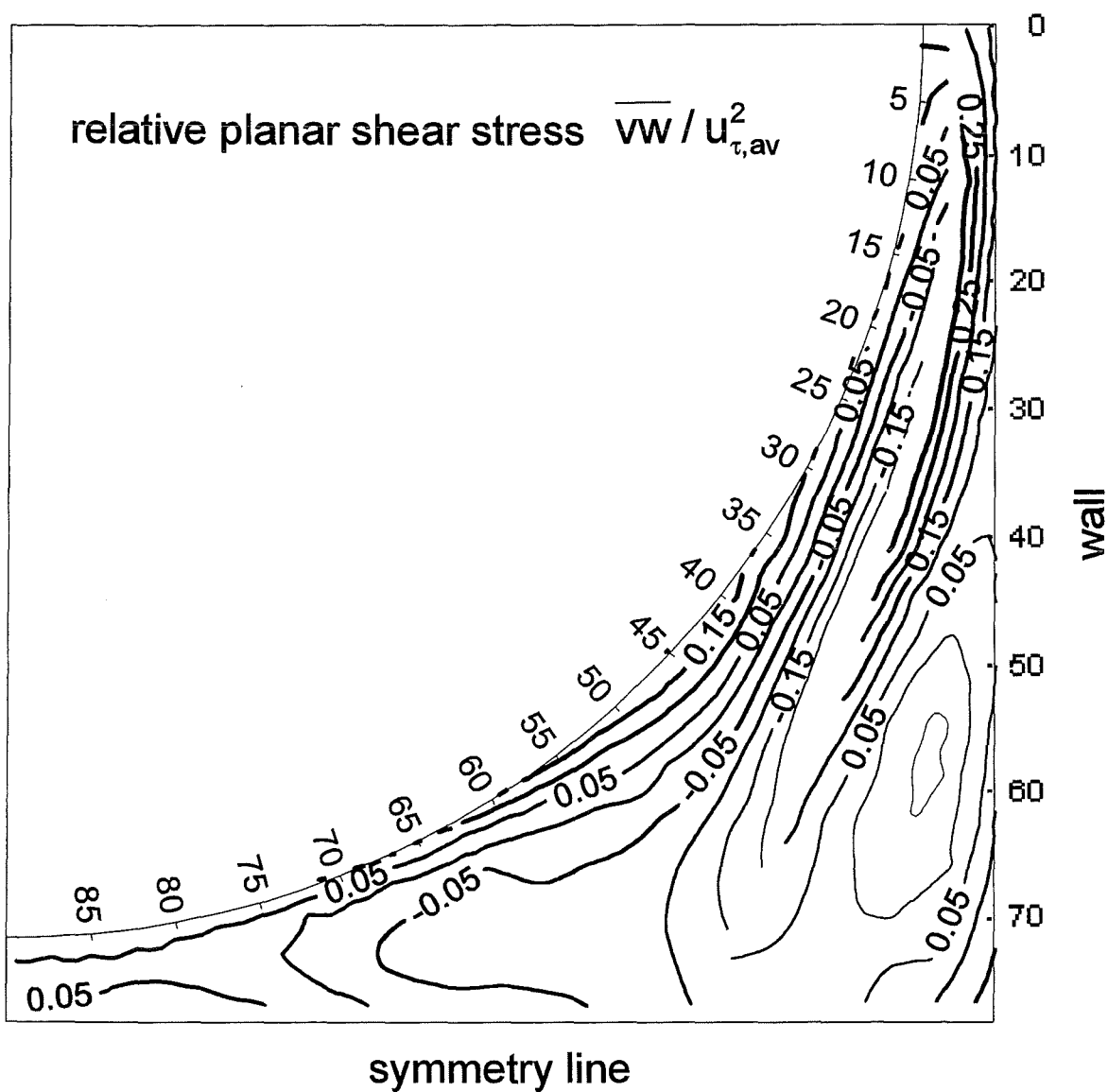


Fig. 28 Contour plot of relative planar shear stress

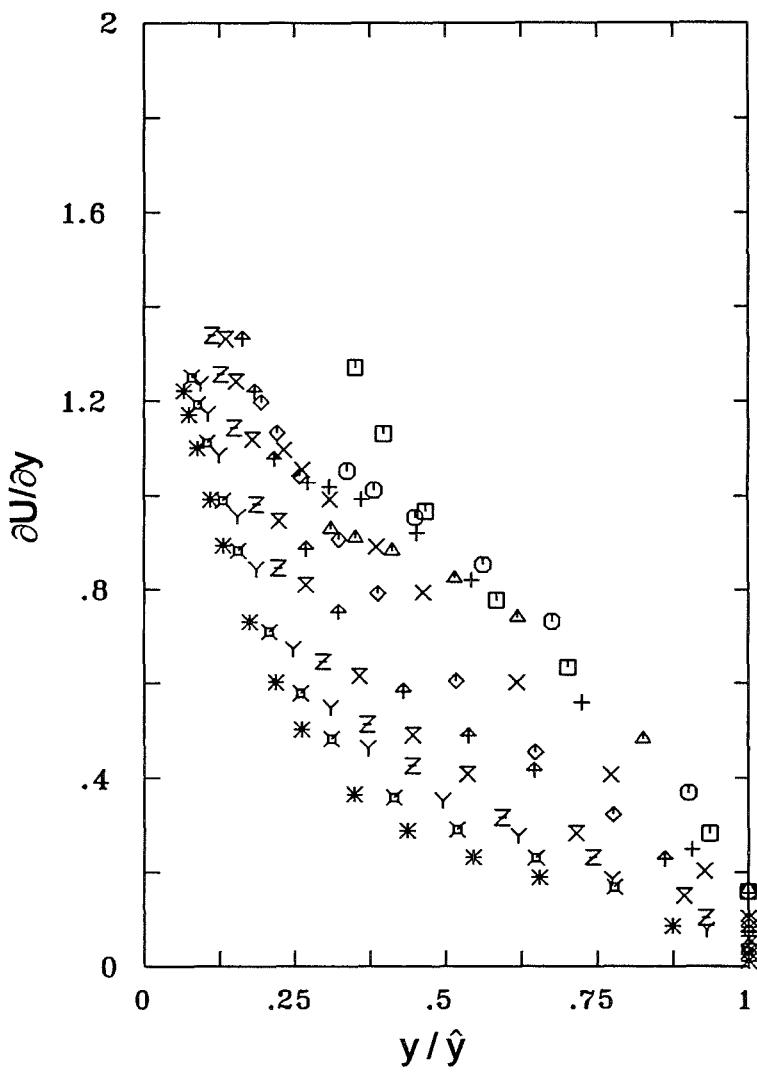
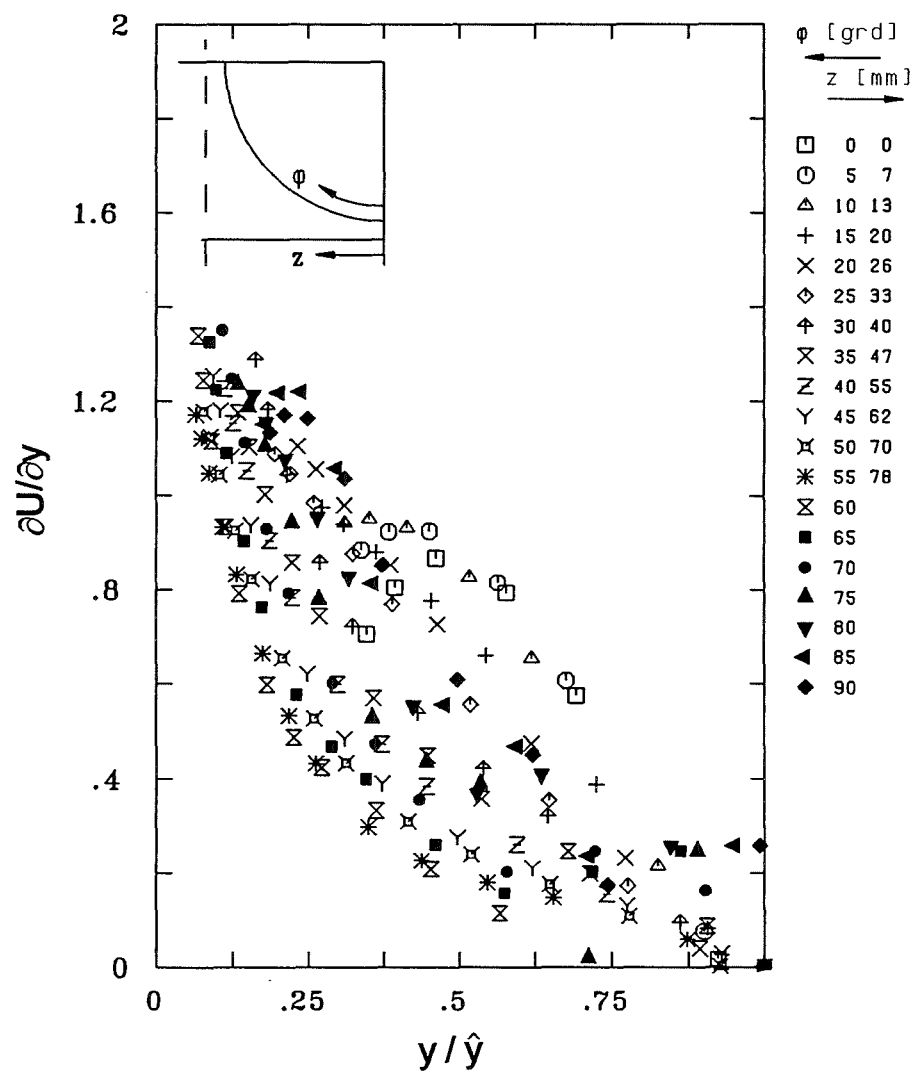


Fig. 29 Radial gradient of time mean velocity

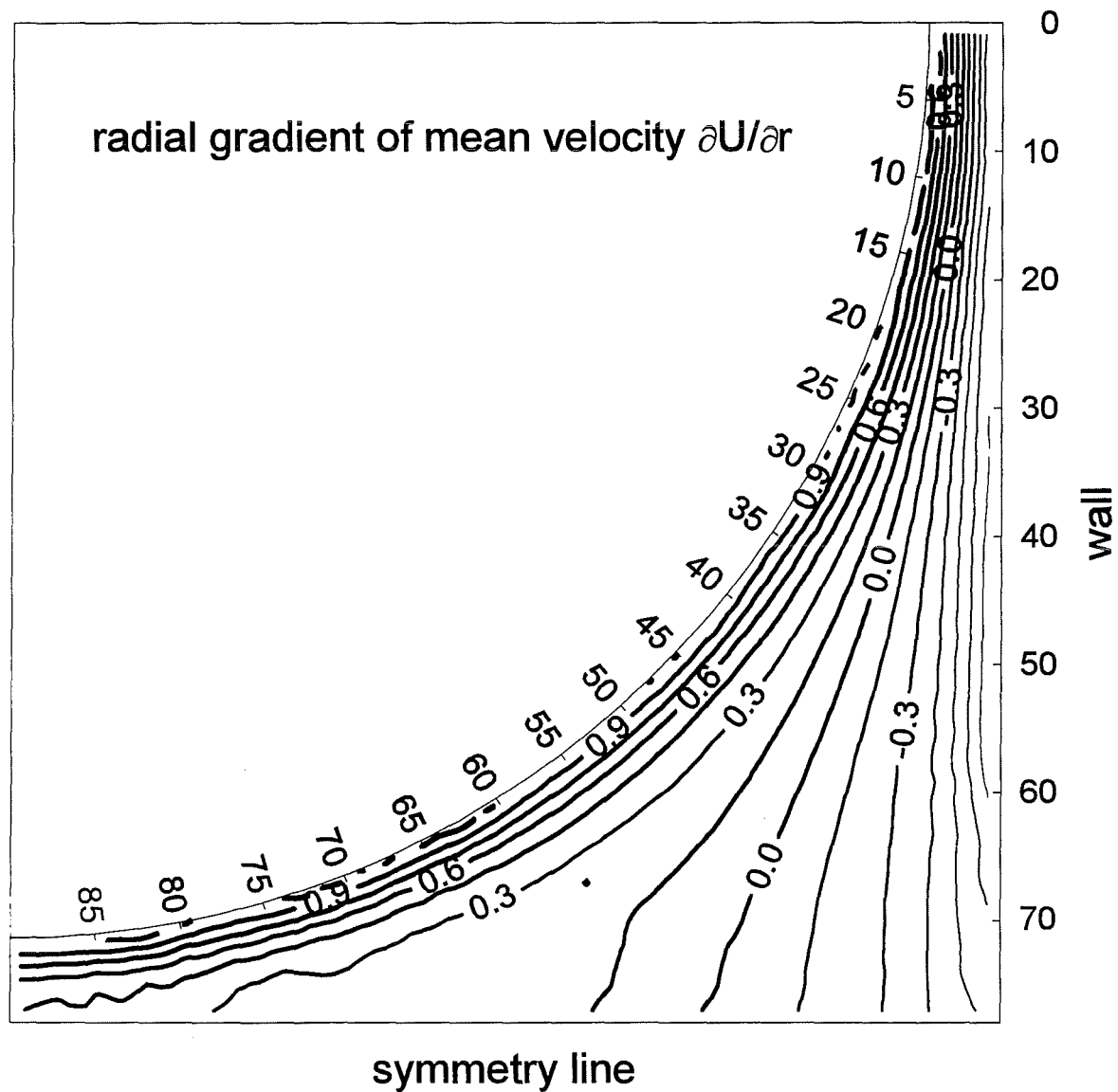


Fig. 30 Contour plot of the radial gradient of time mean velocity

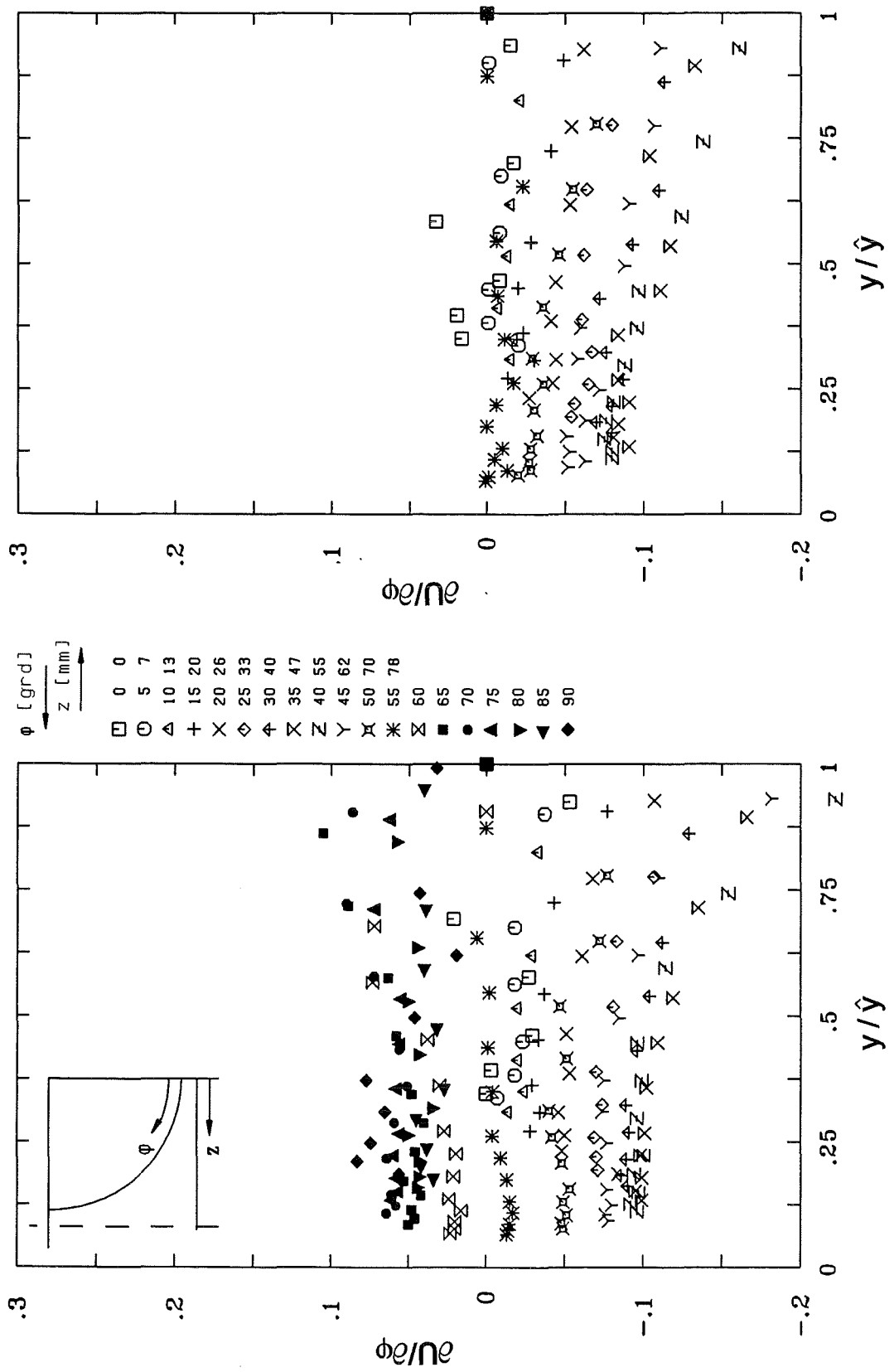


Fig. 31 Azimuthal gradient of time mean velocity

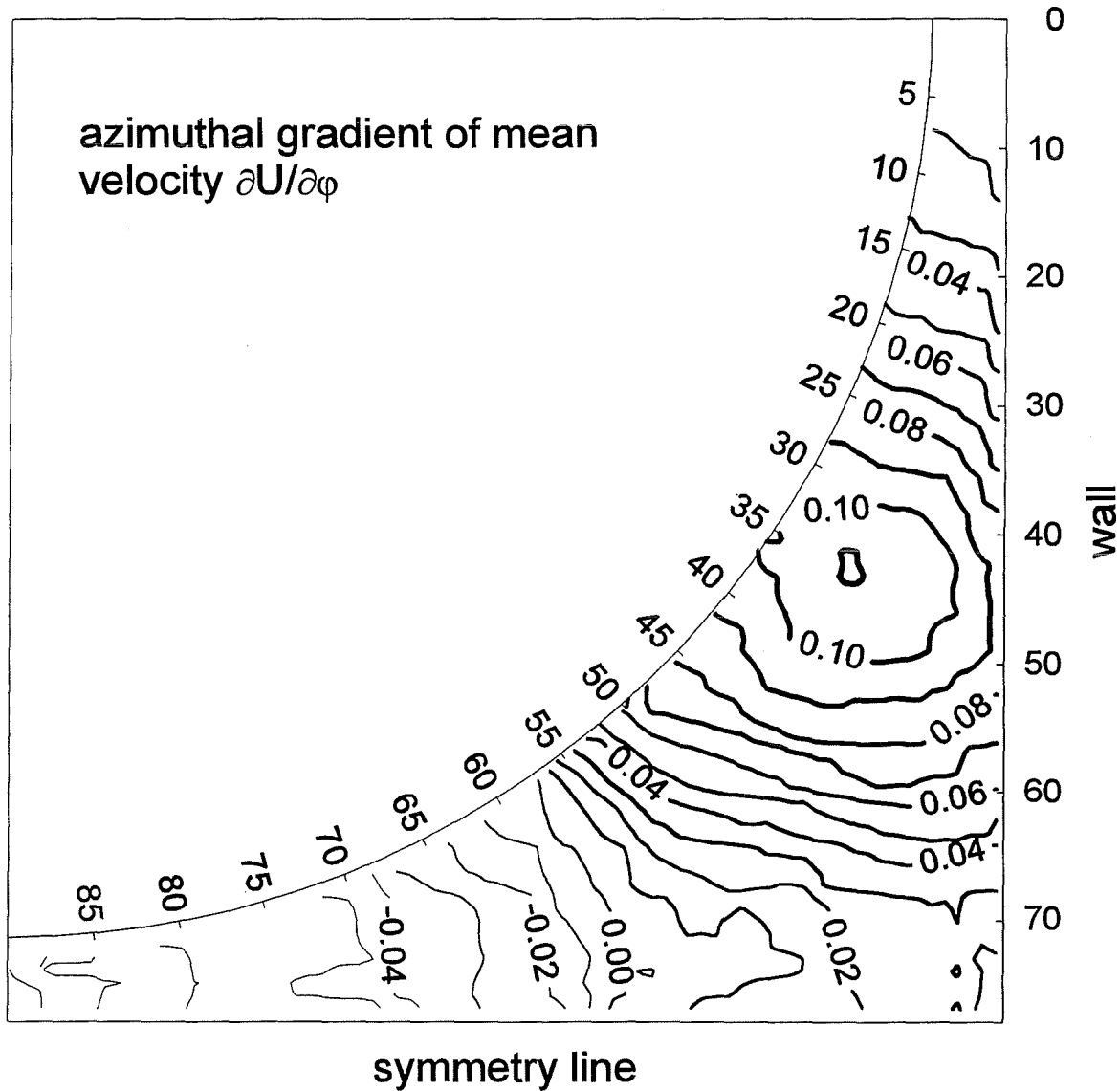


Fig. 32 Contour plot of the azimuthal gradient of time mean velocity

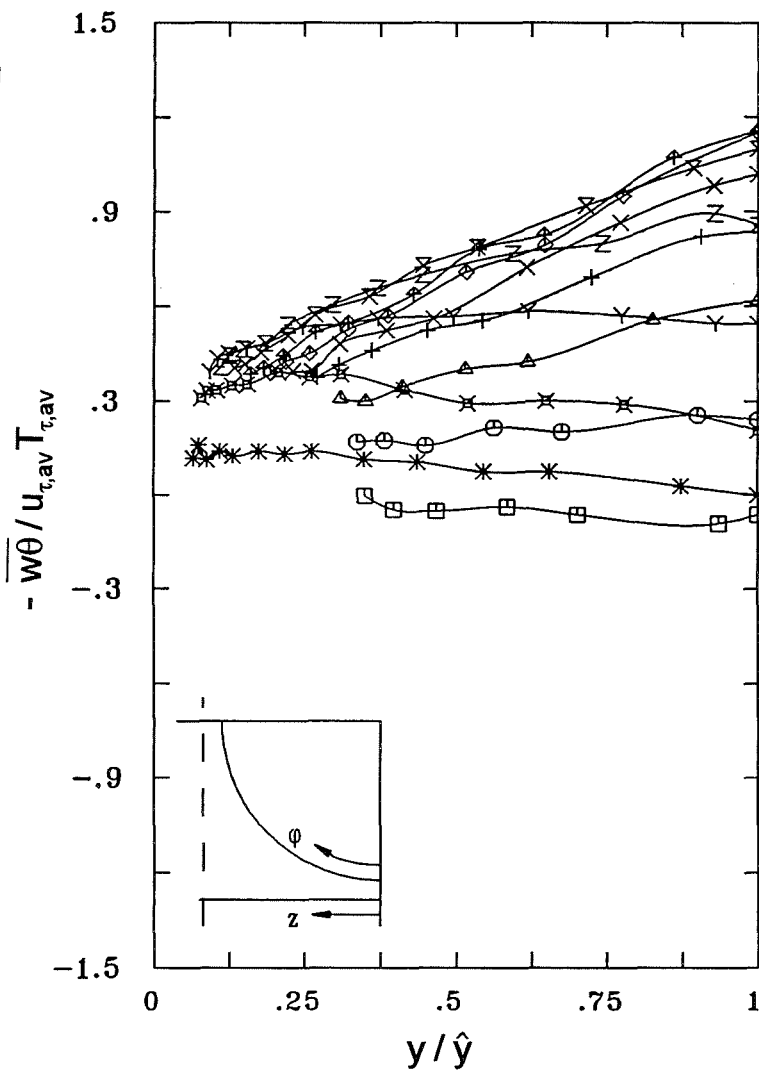
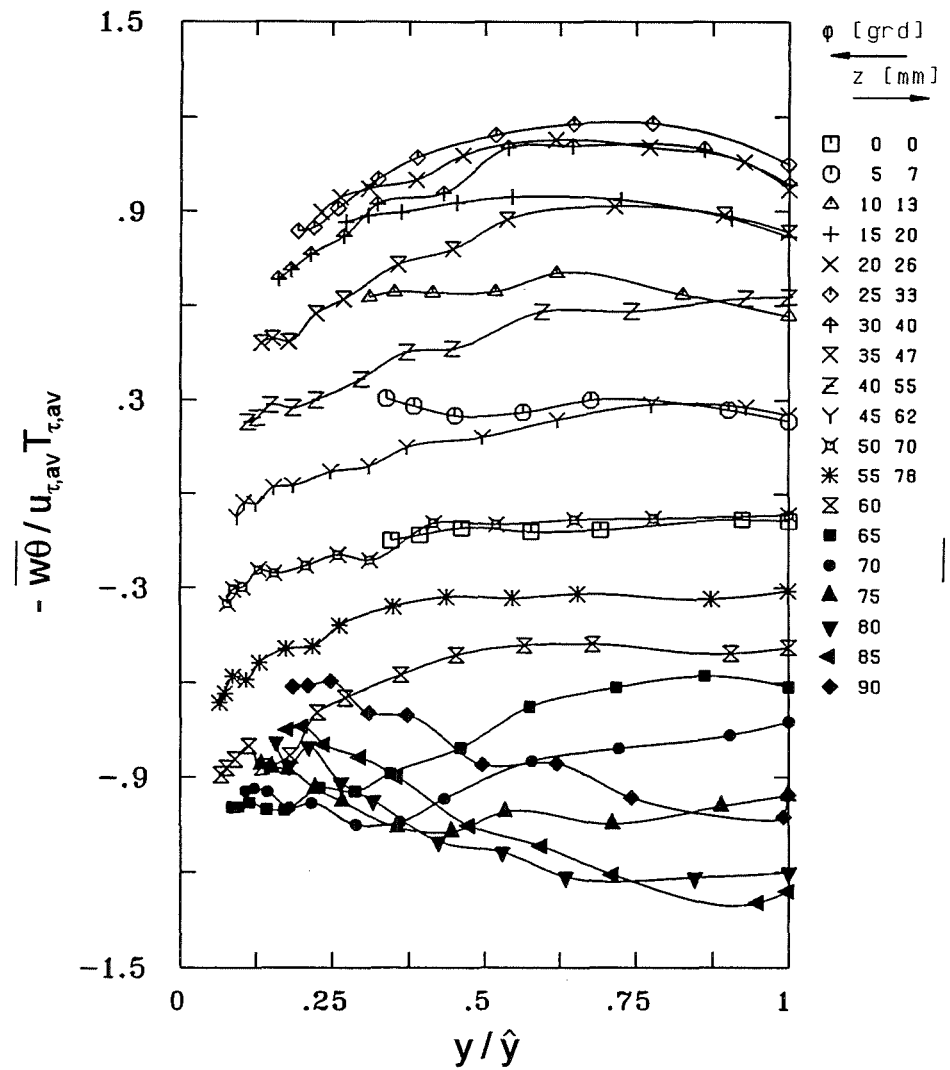


Fig. 33 Relative turbulent heat flux in azimuthal direction

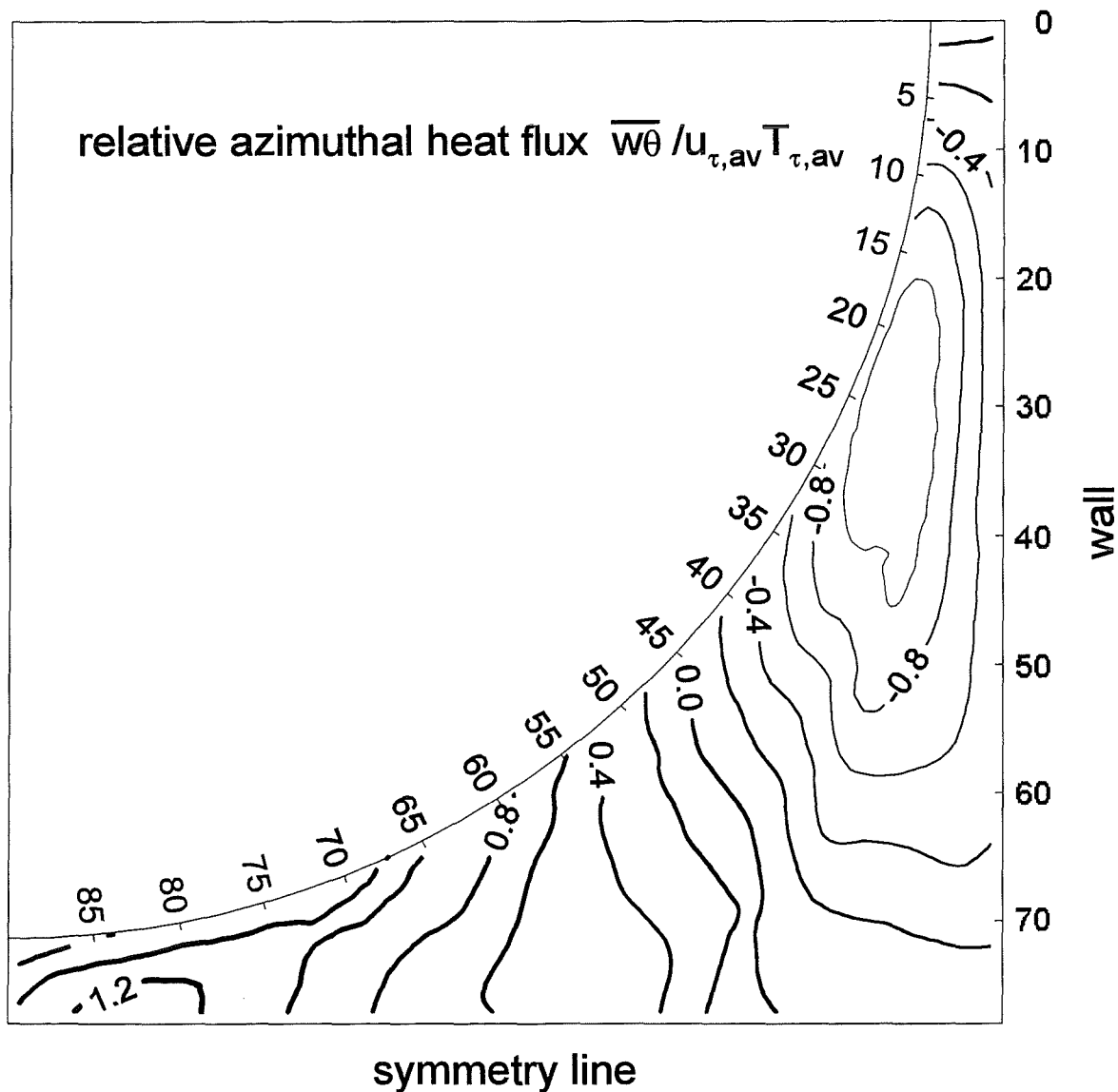


Fig. 34 Contour plot of relative azimuthal heat flux

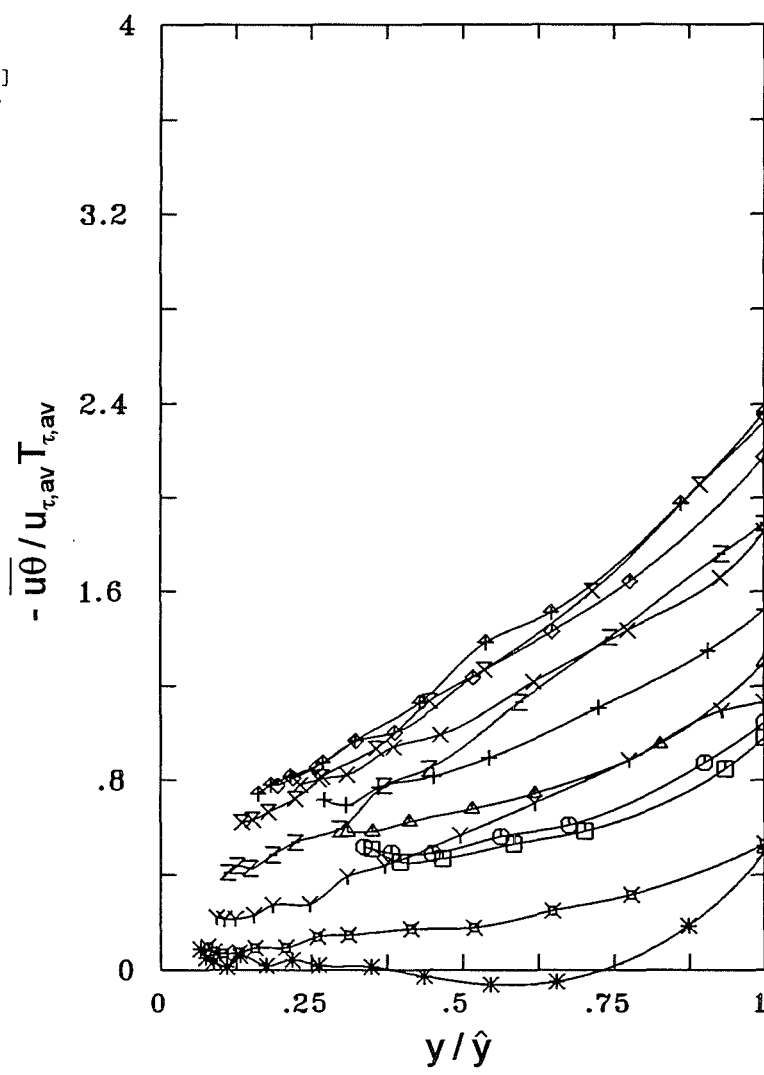
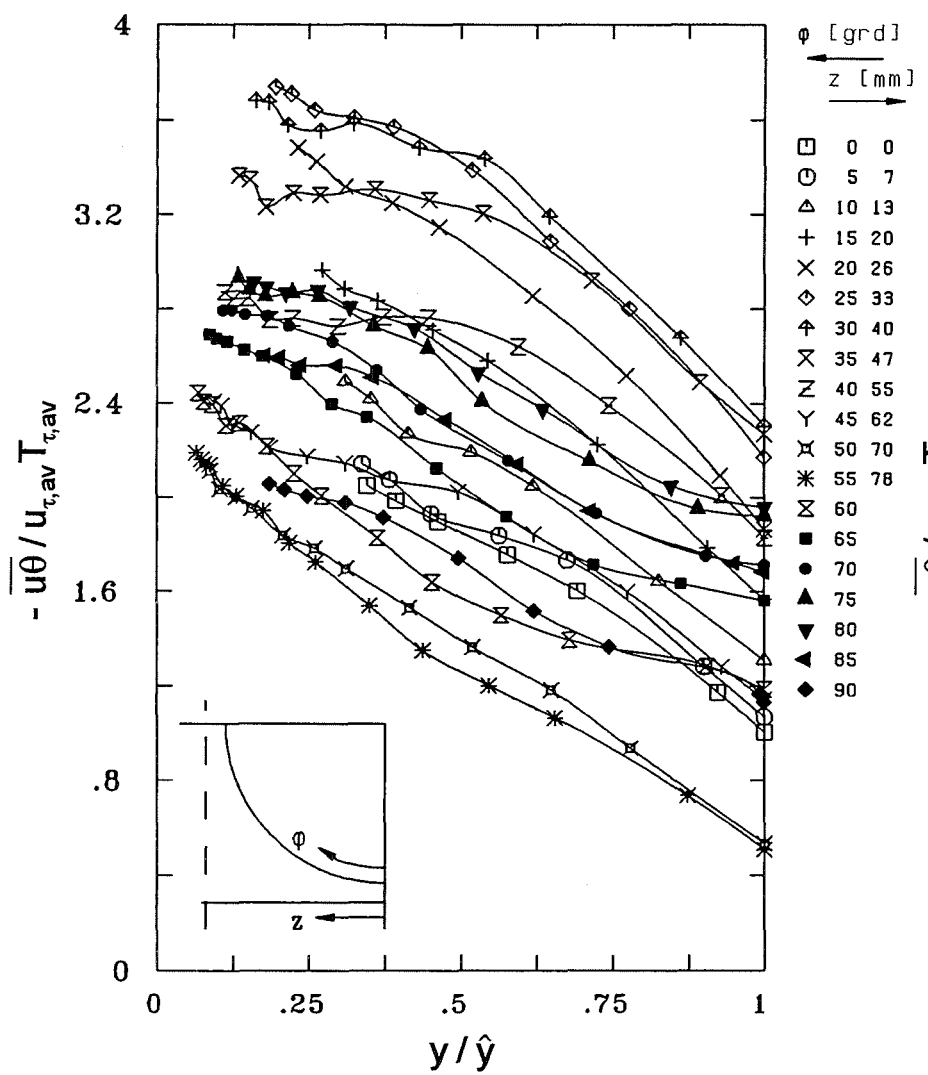


Fig. 35 Relative turbulent heat flux in axial direction

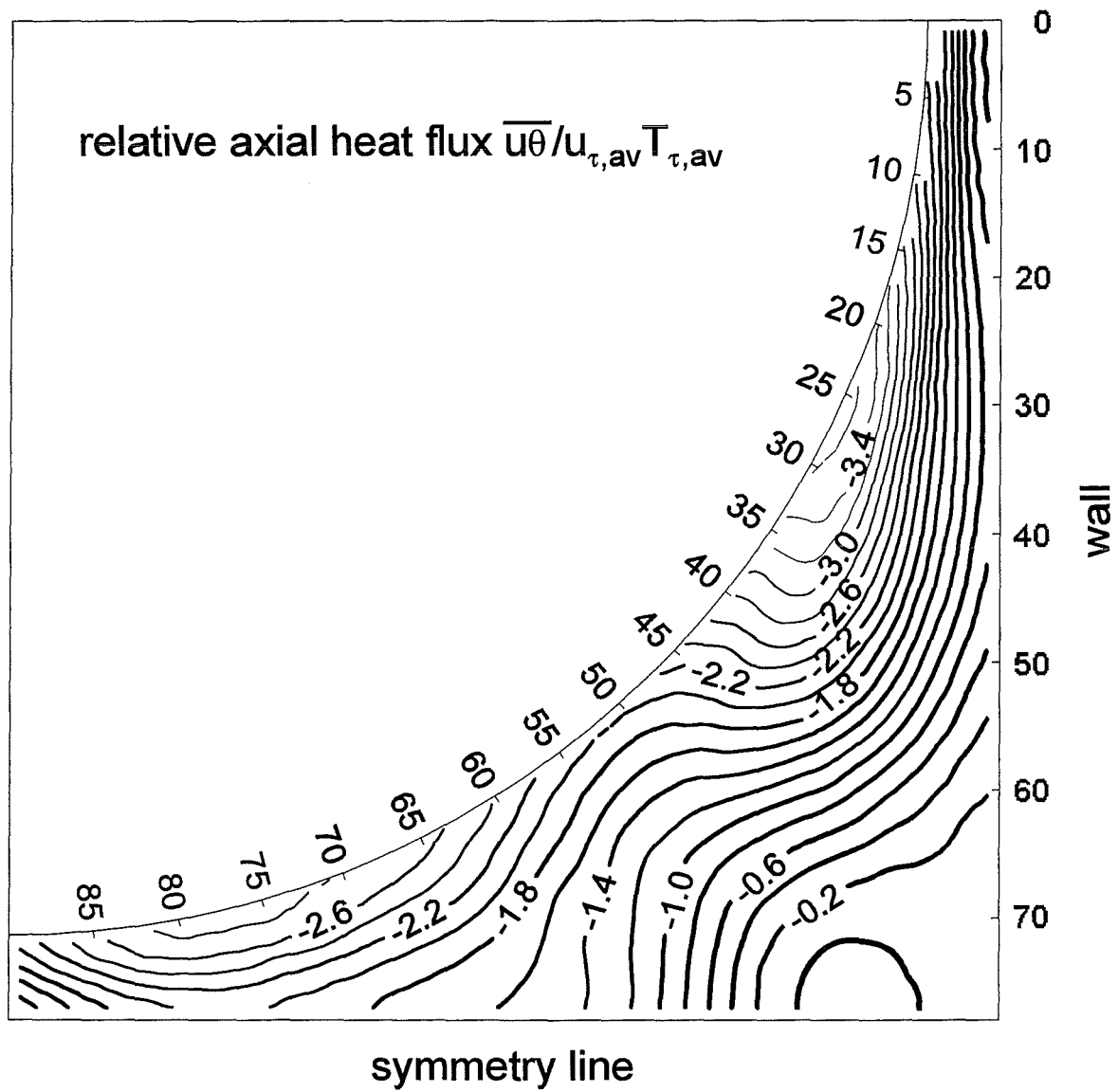


Fig. 36 Contour plot of relative axial heat flux

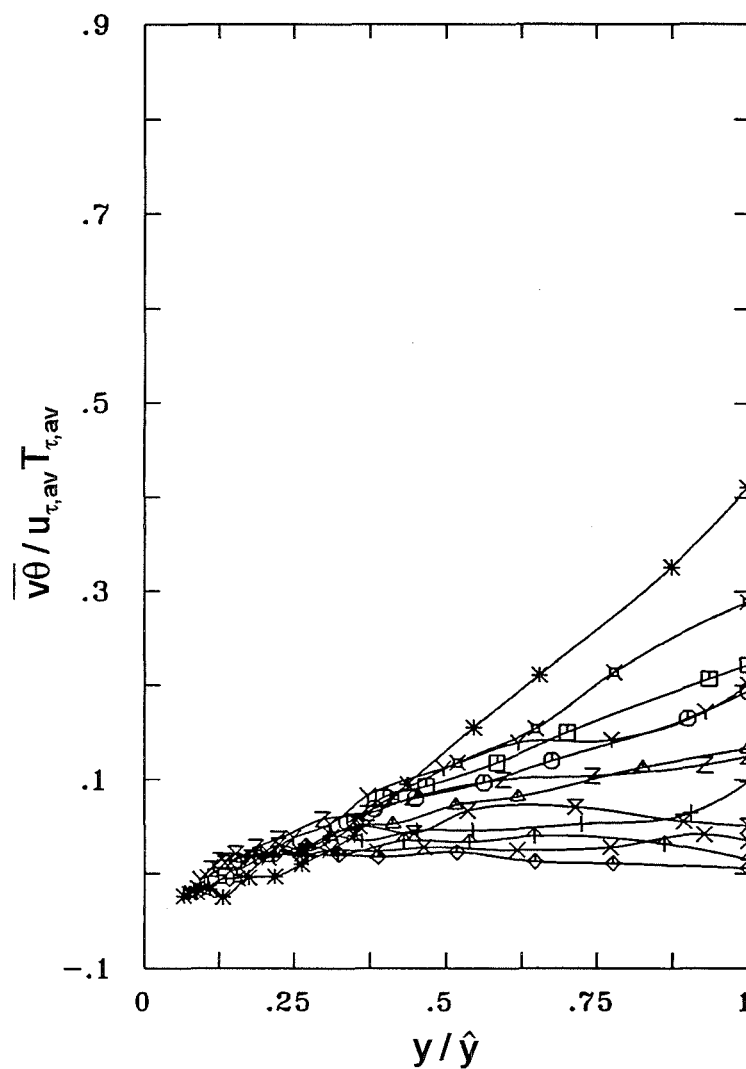
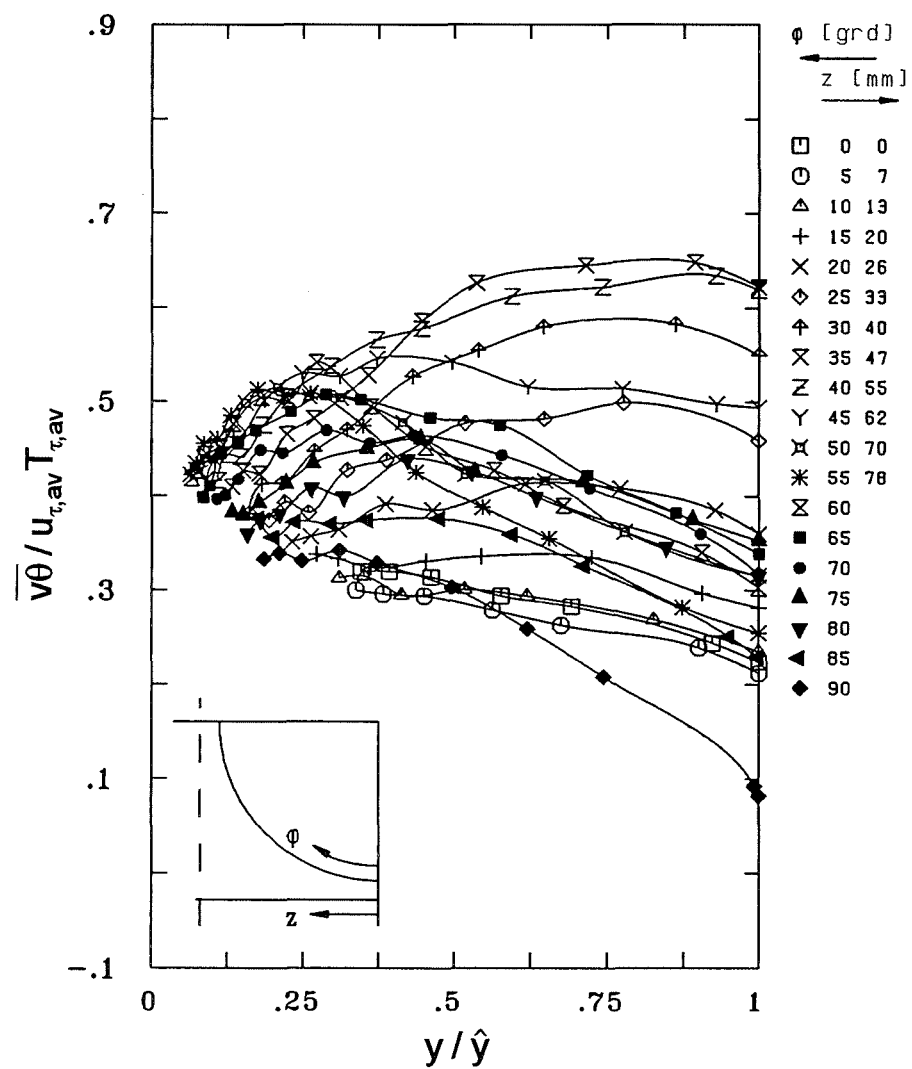


Fig. 37 Relative turbulent heat flux in radial direction

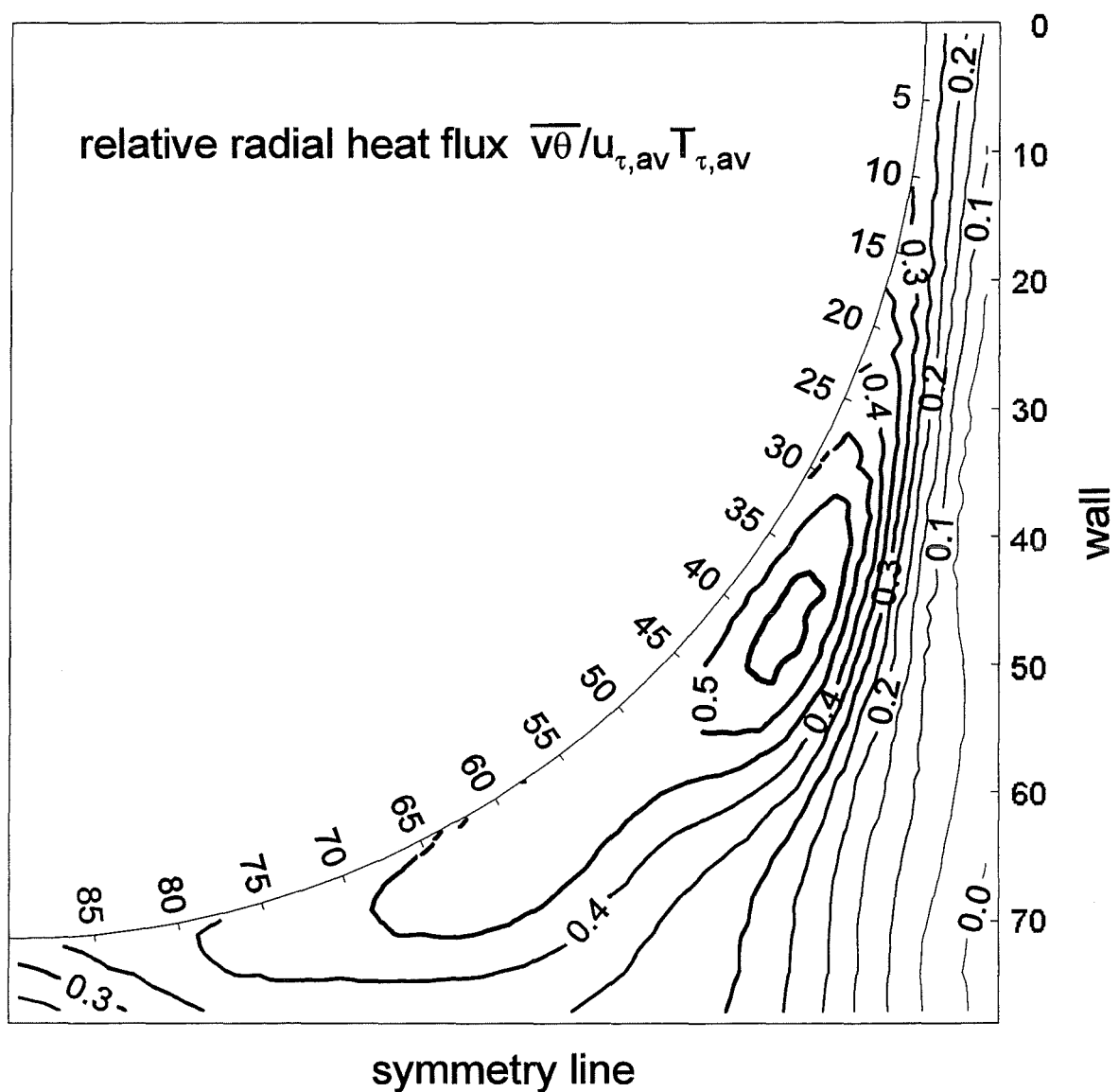


Fig. 38 Contour plot of relative radial heat flux

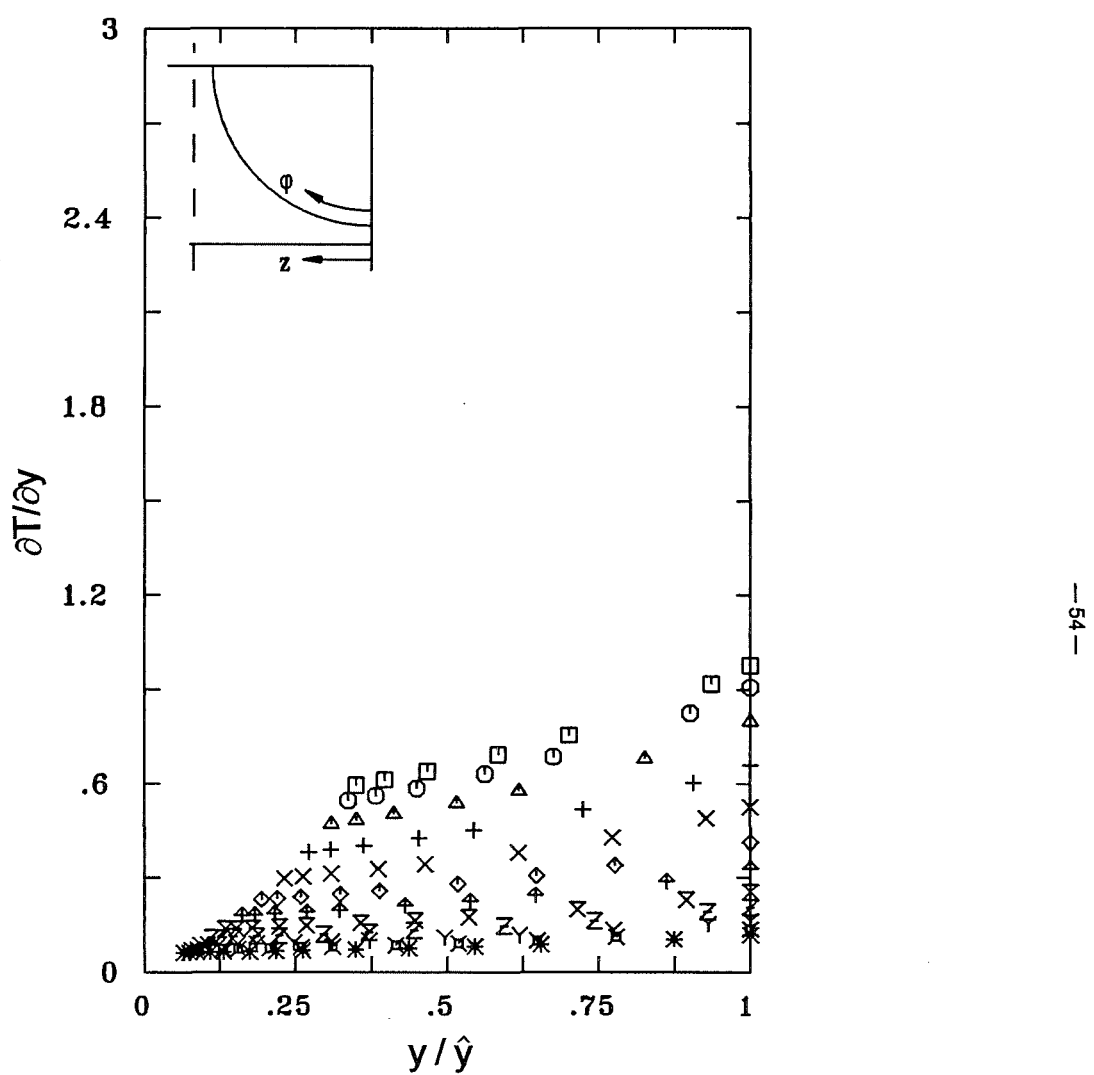
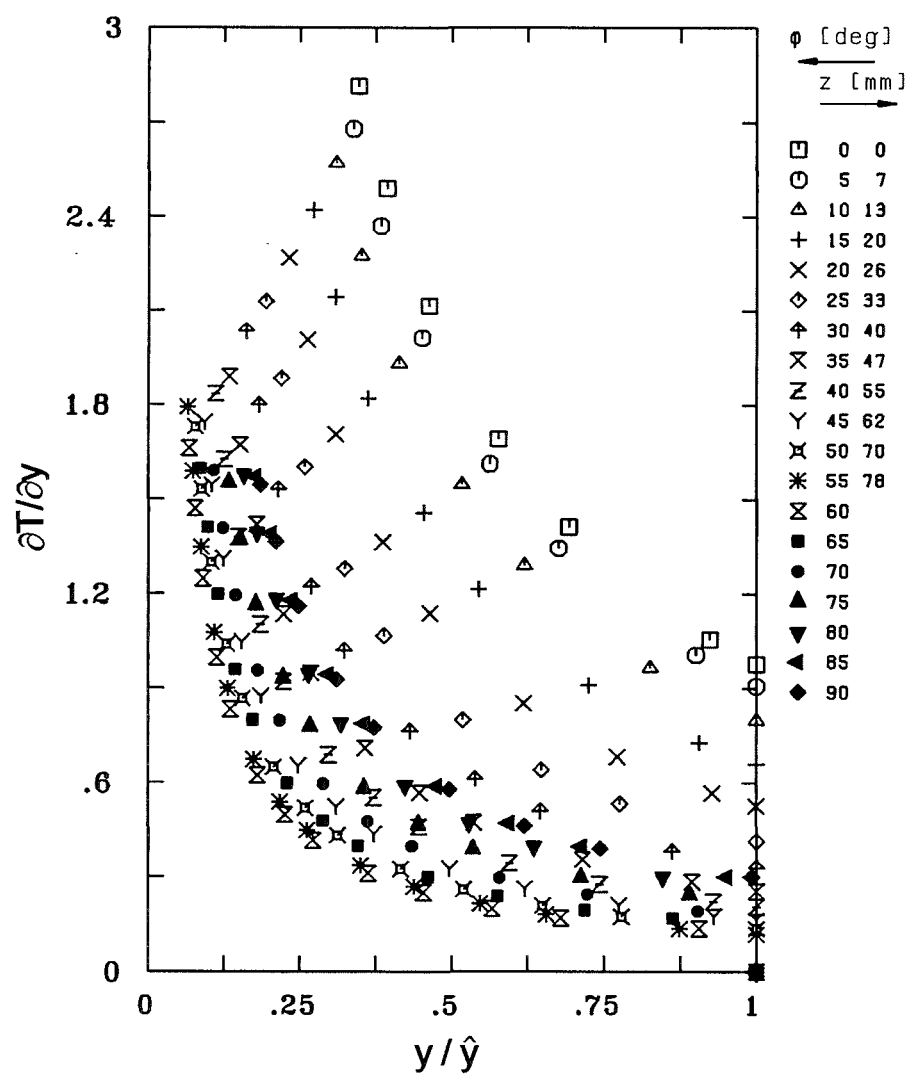


Fig. 39 Radial gradient of time mean temperature

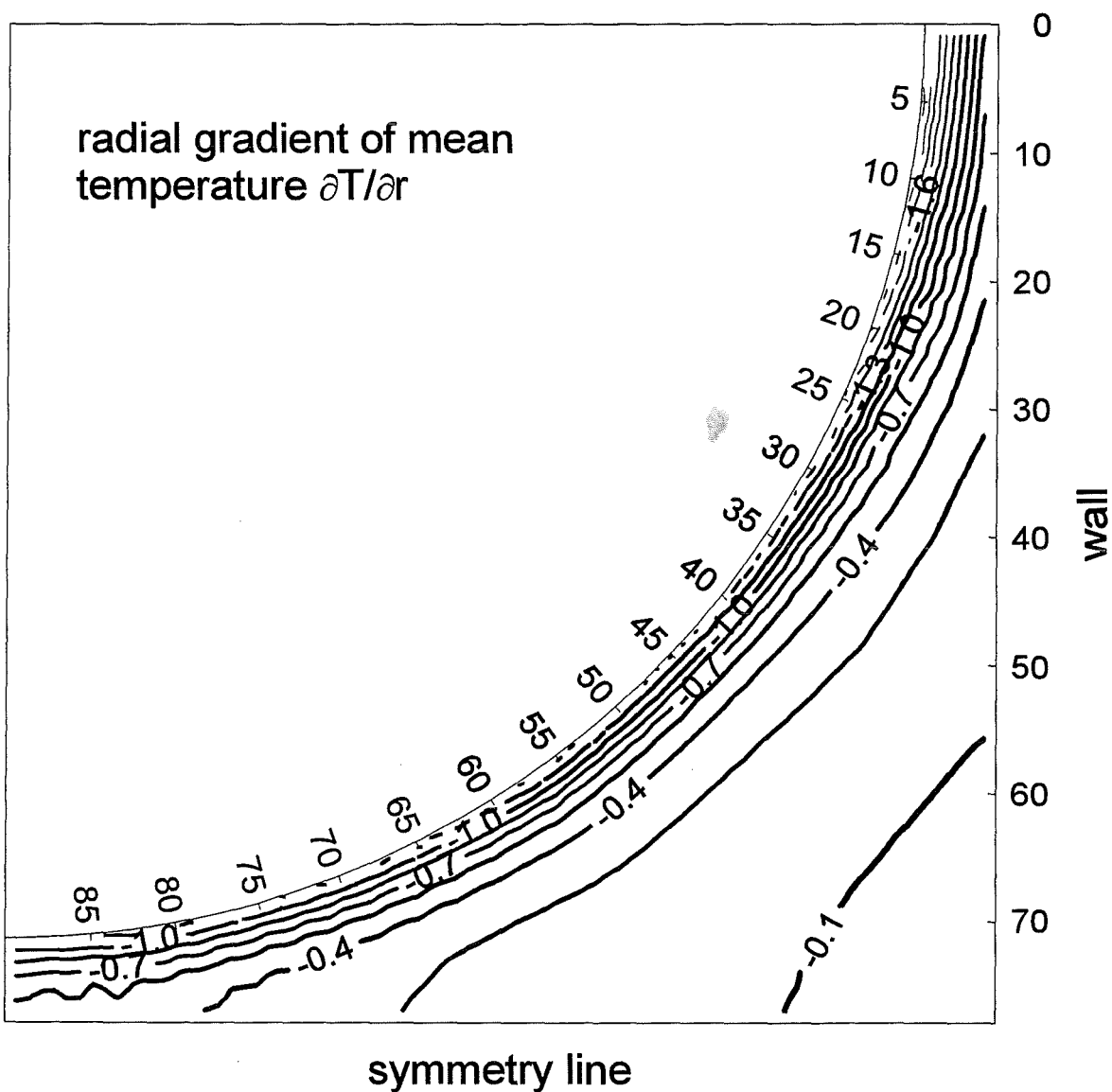


Fig. 40 Contour plot of the radial gradient of time mean temperature

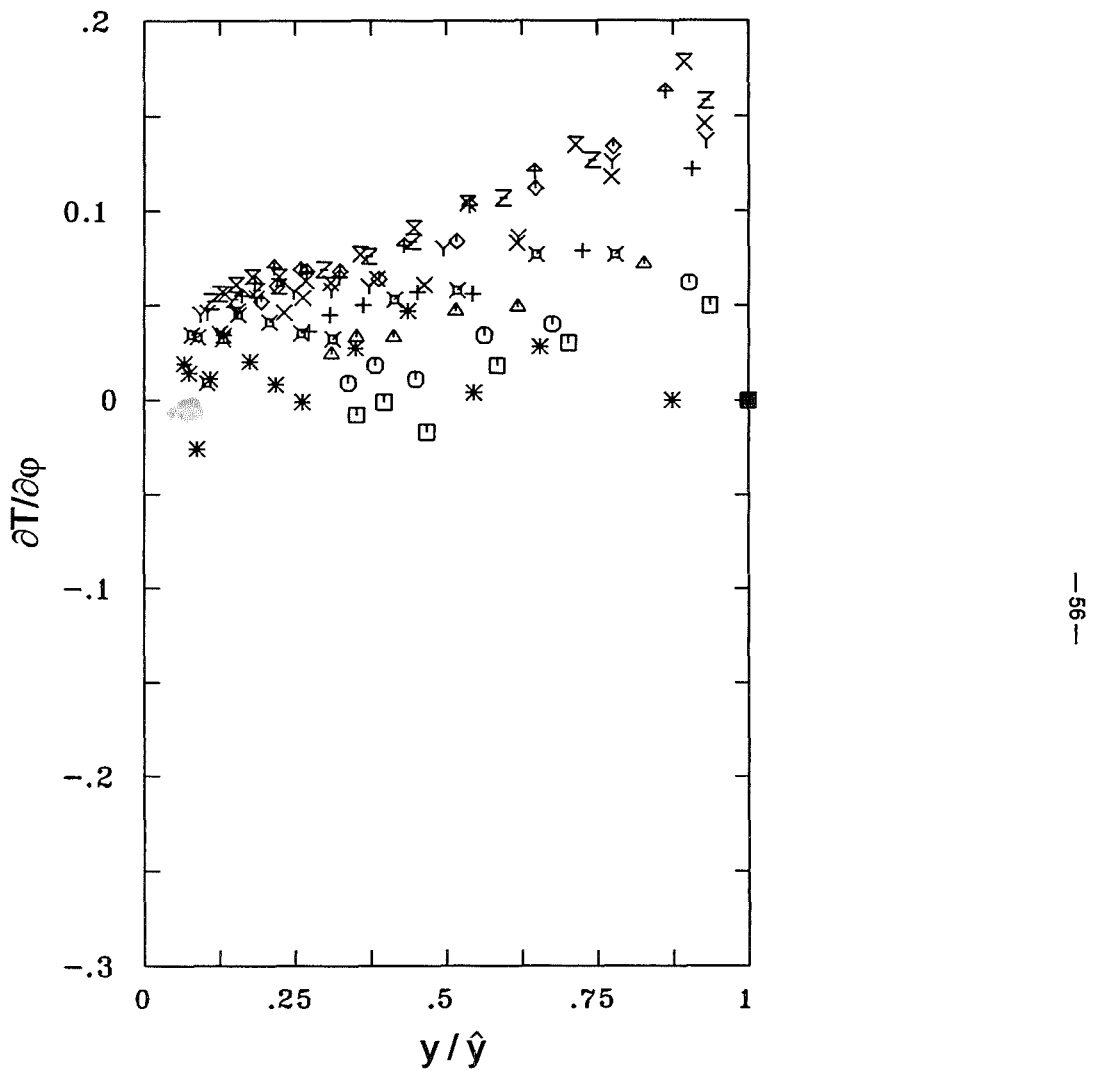
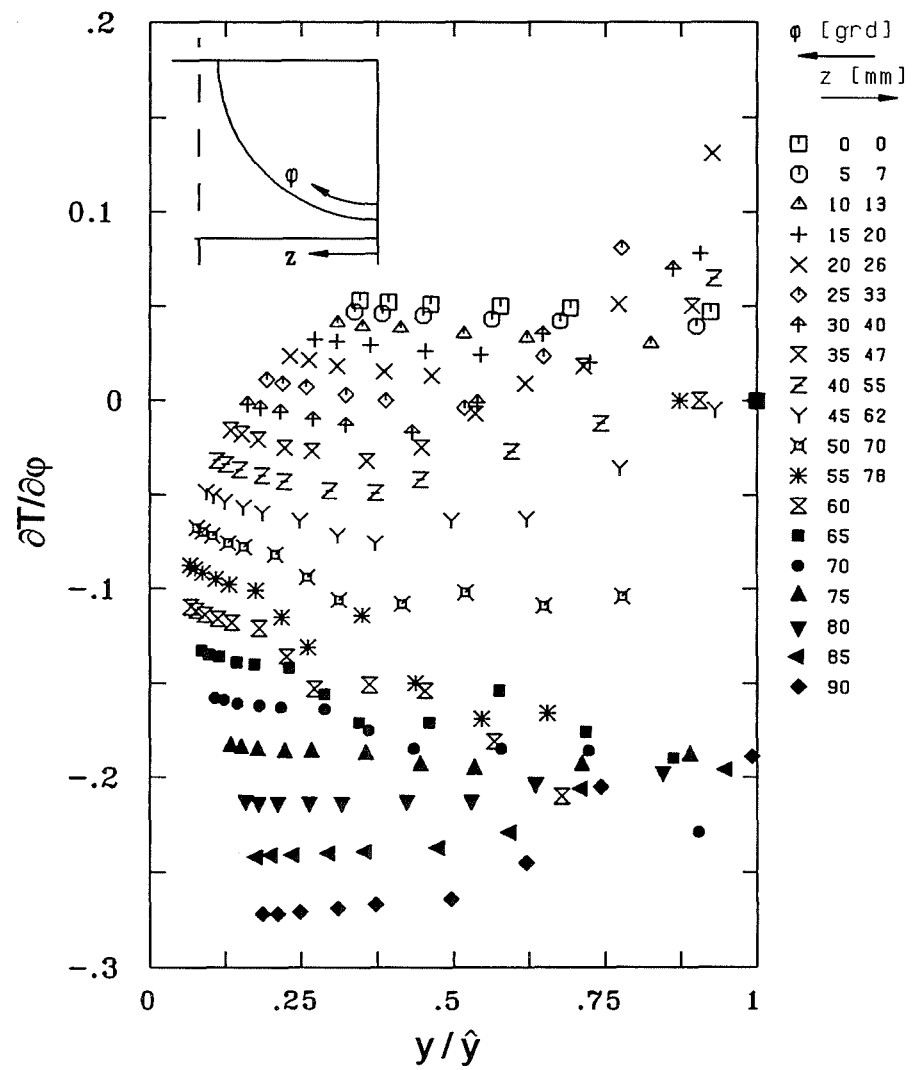


Fig. 41 Azimuthal gradient of time mean temperature

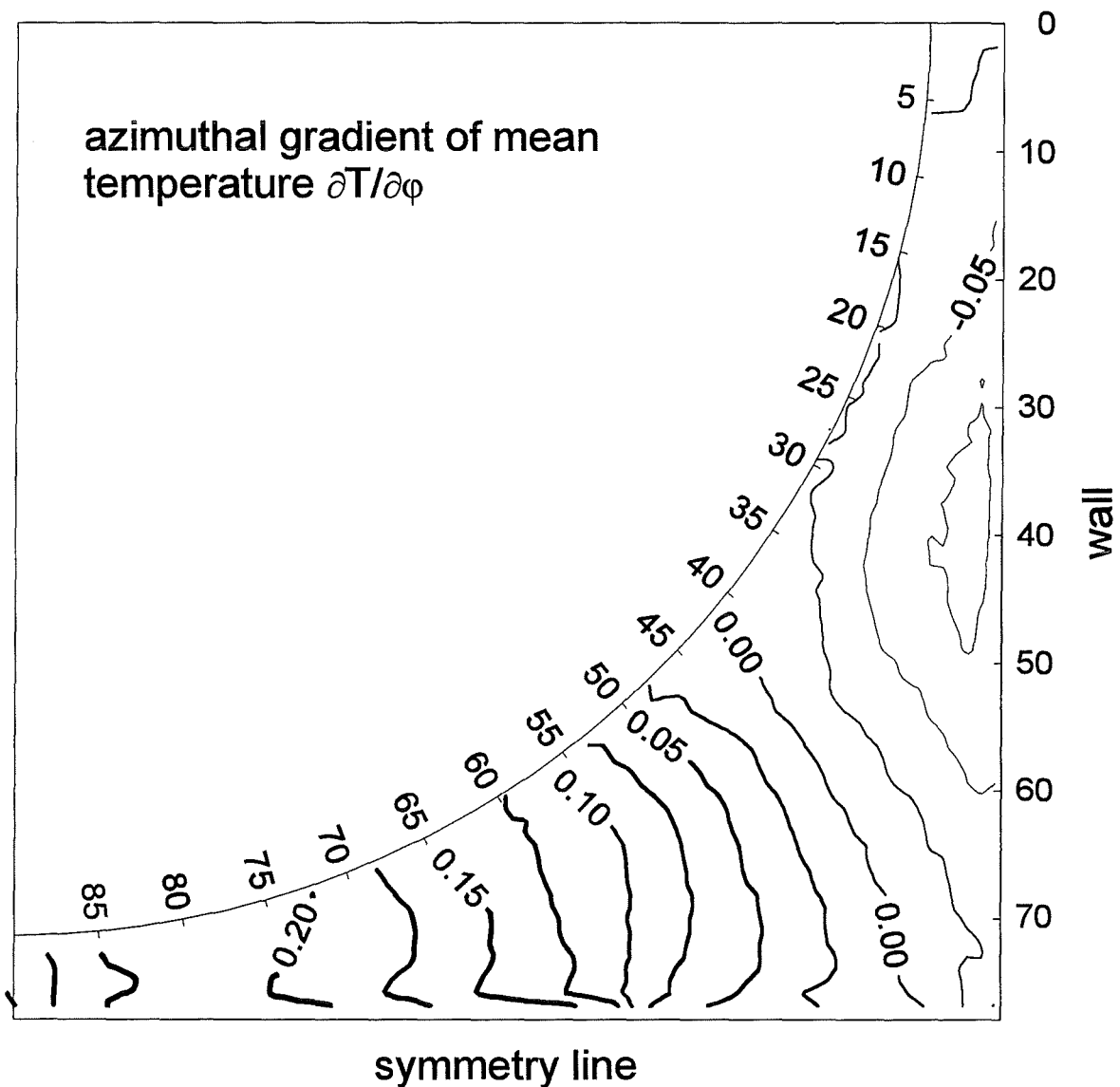


Fig. 42 Contour plot of the azimuthal gradient of time mean temperature

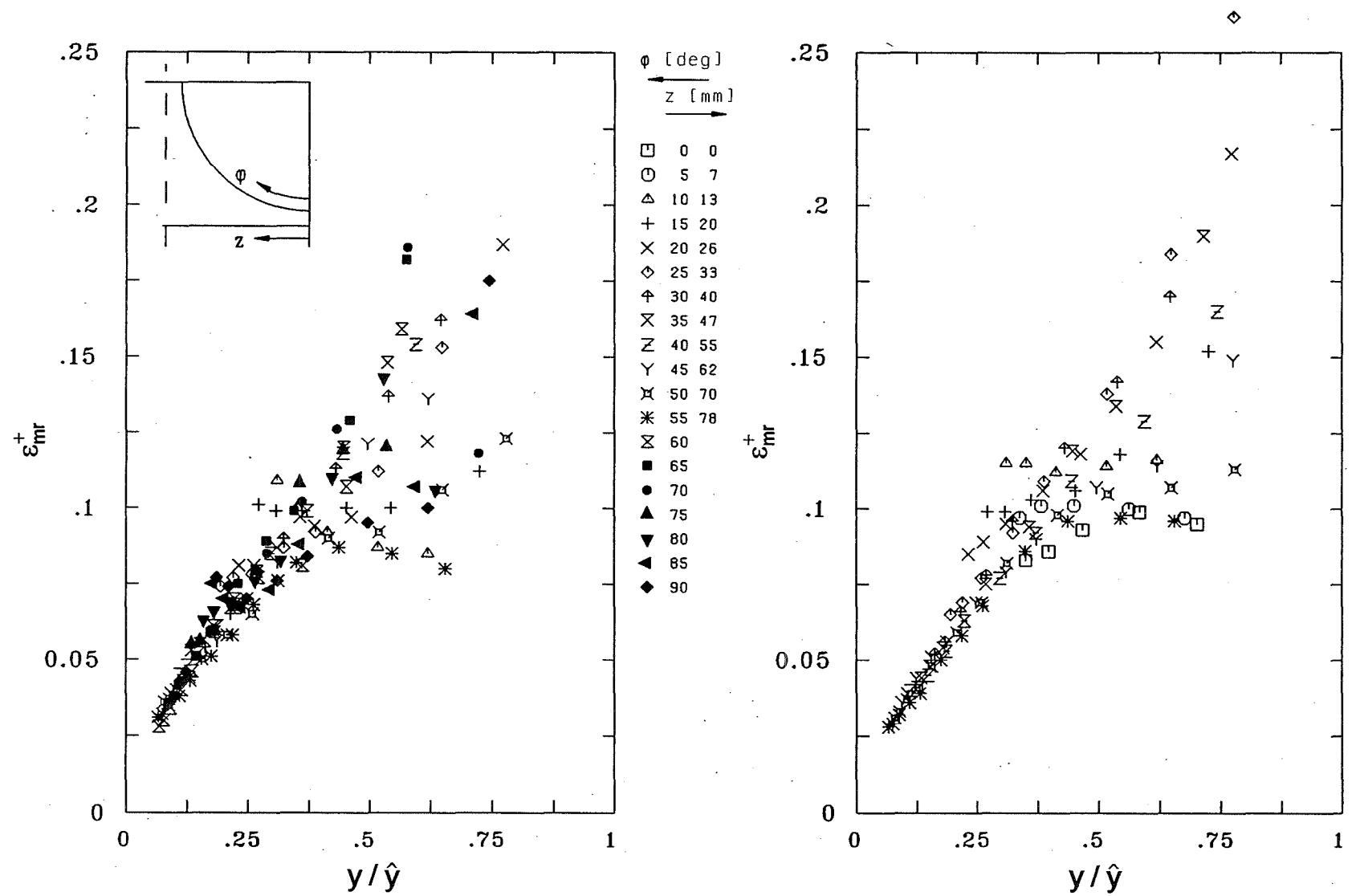


Fig. 43 Dimensionless eddy viscosity in radial direction

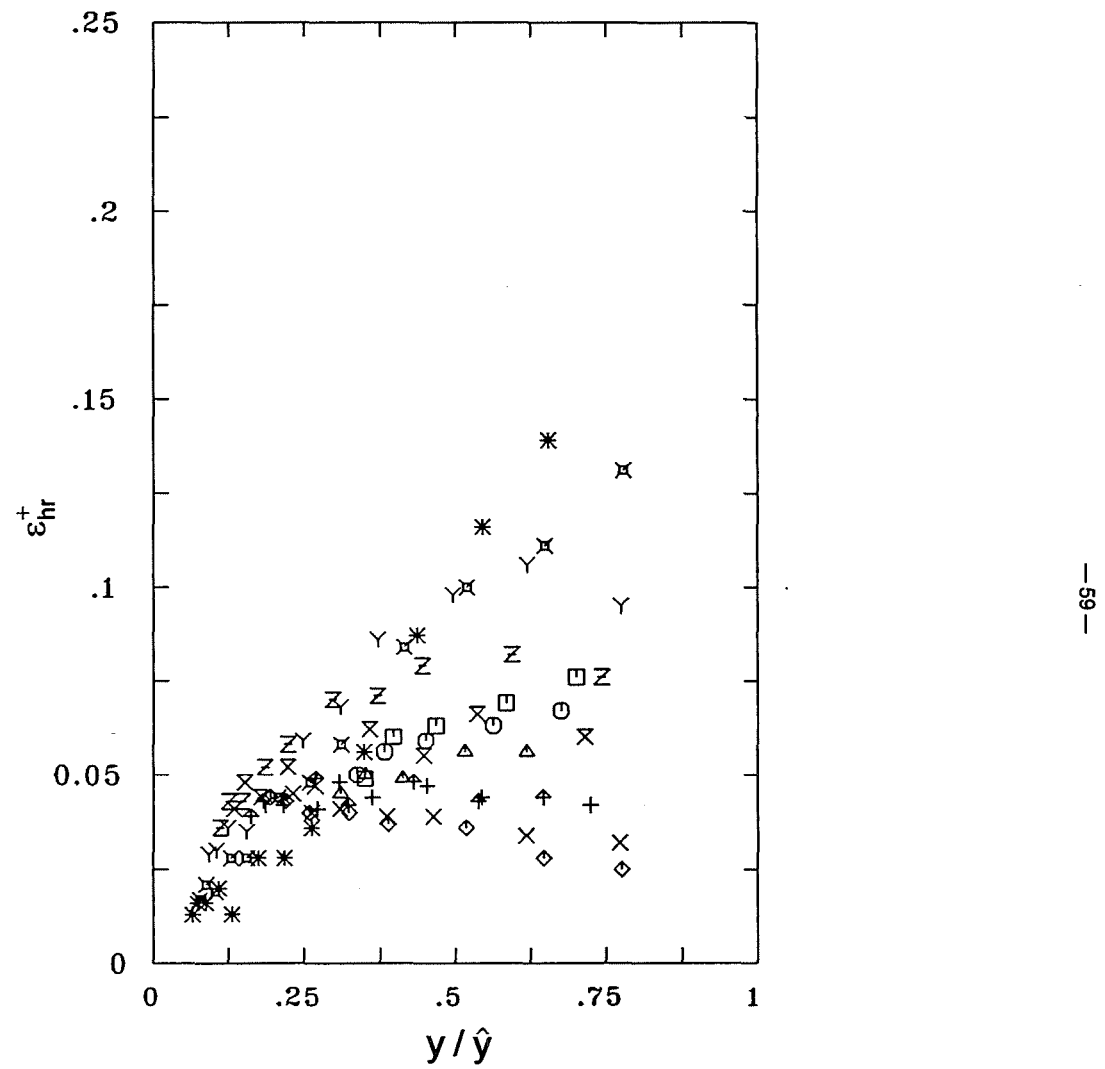
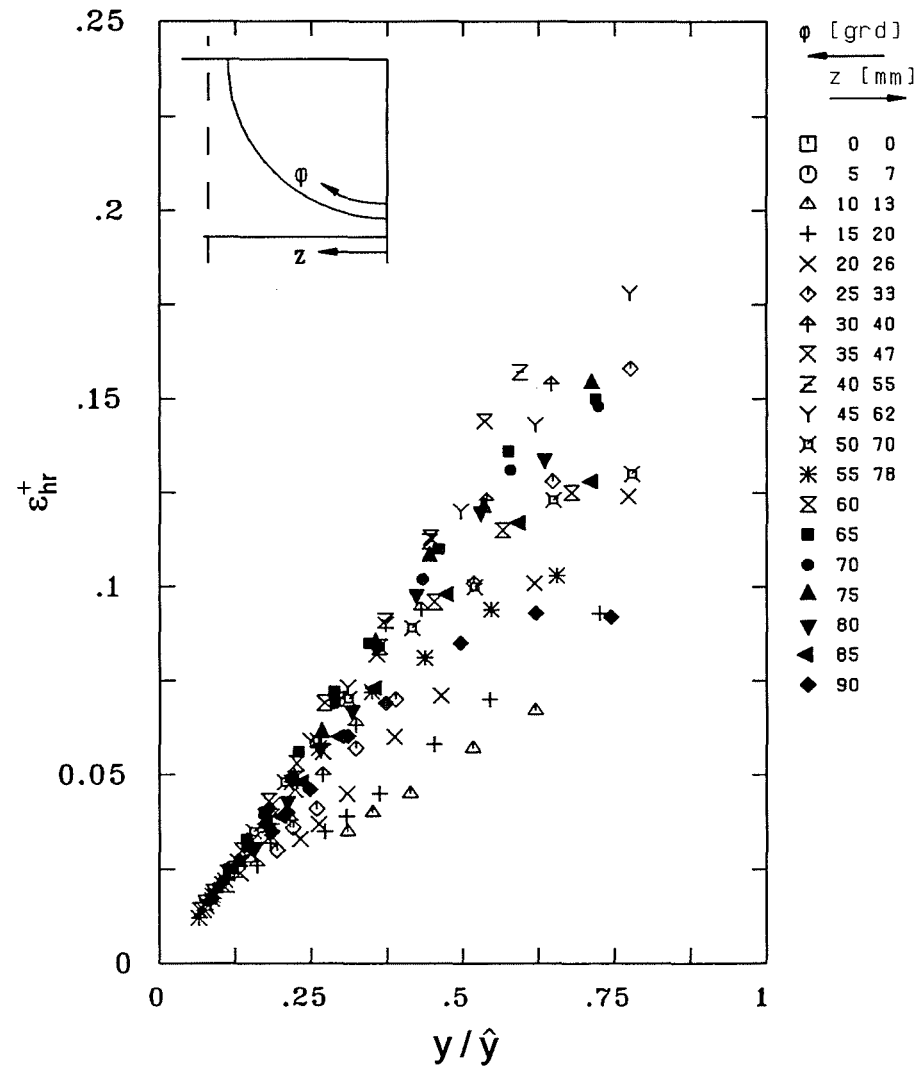


Fig. 44 Dimensionless eddy diffusivity of heat in radial direction

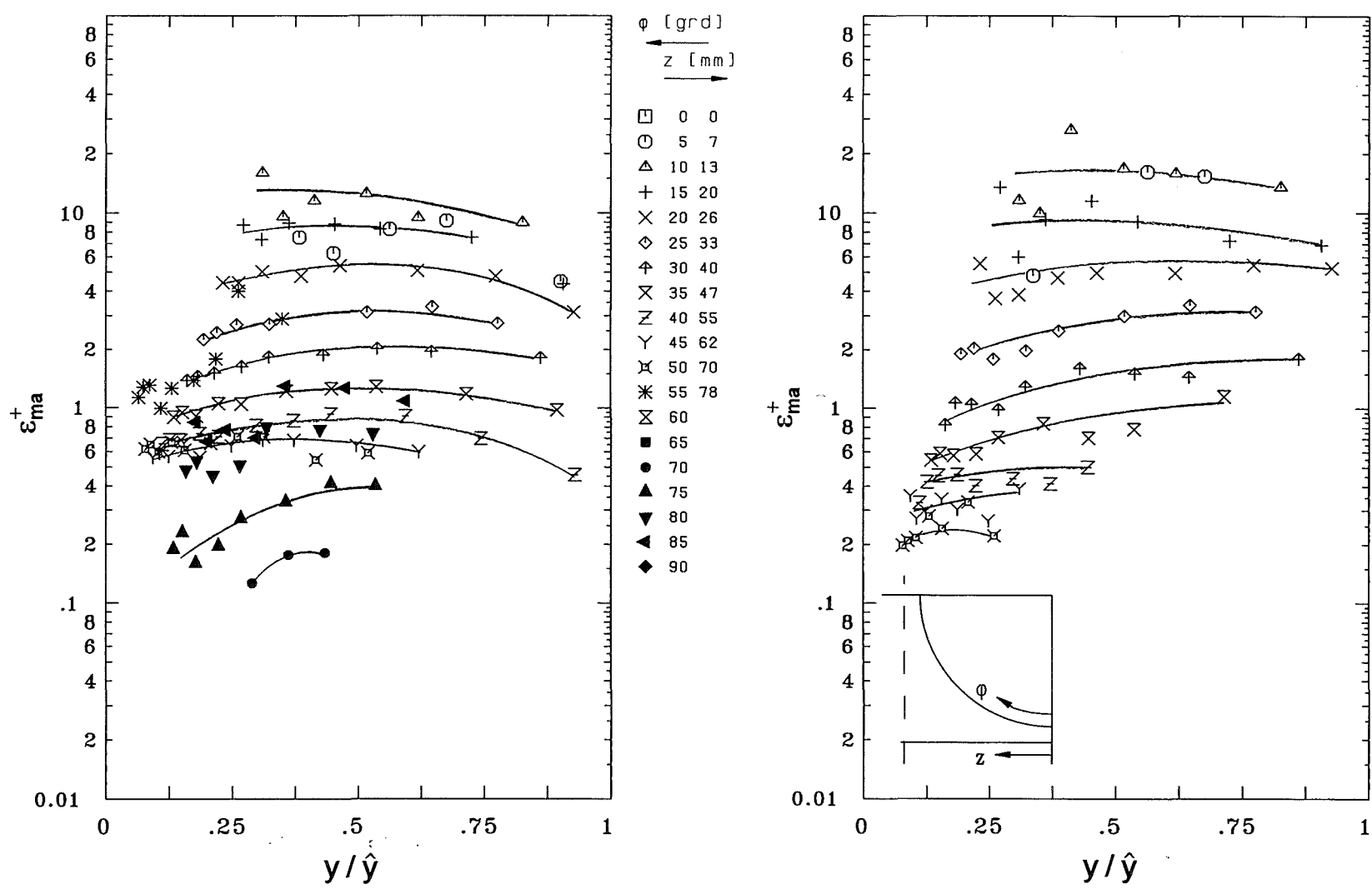


Fig. 45 Dimensionless eddy viscosity in azimuthal direction

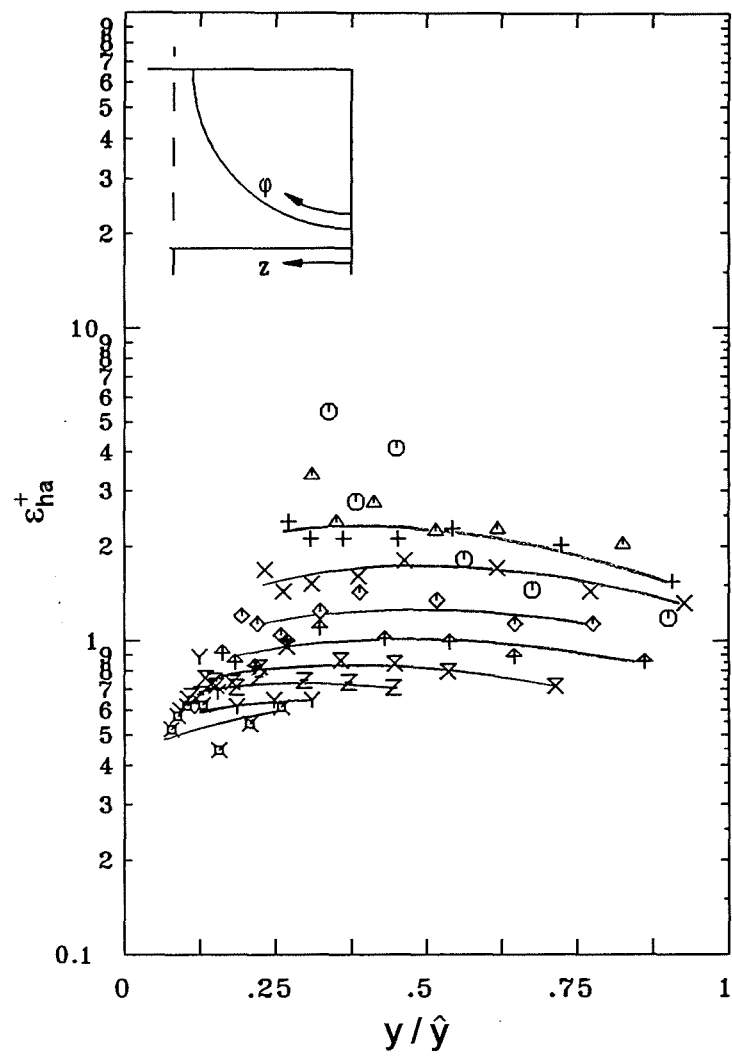
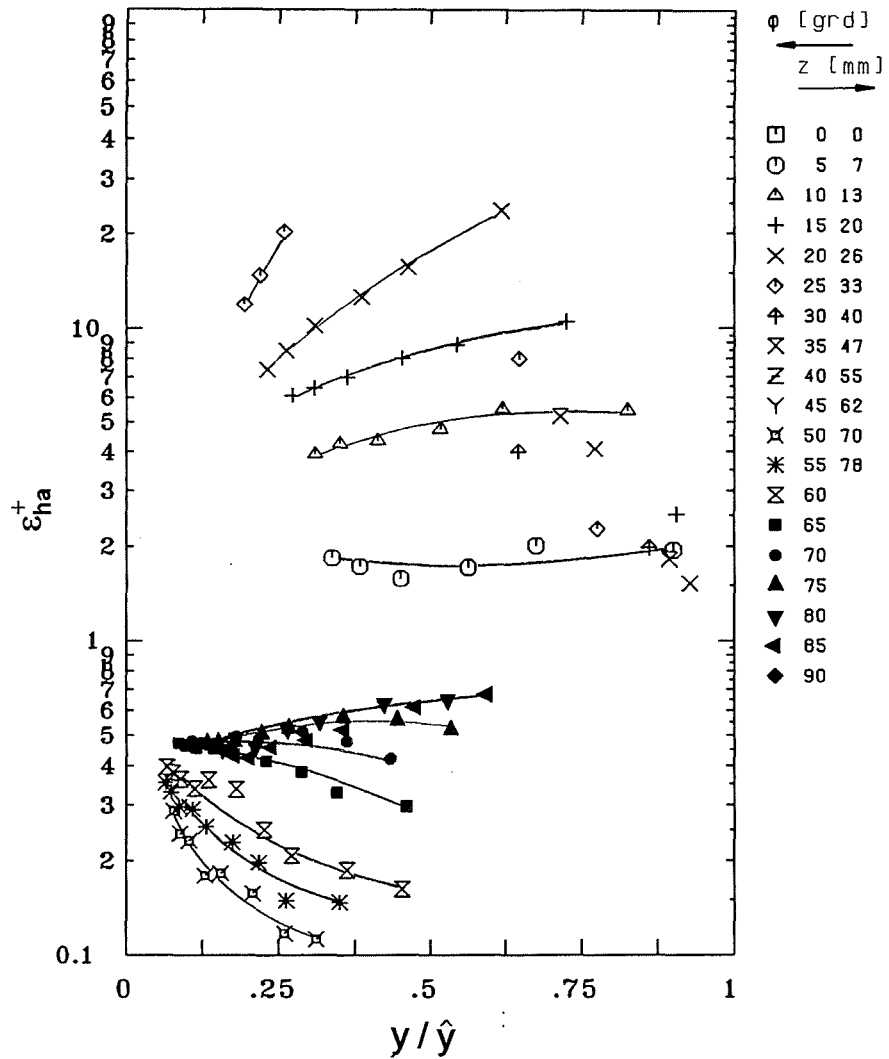


Fig. 46 Dimensionless eddy diffusivity of heat in azimuthal direction

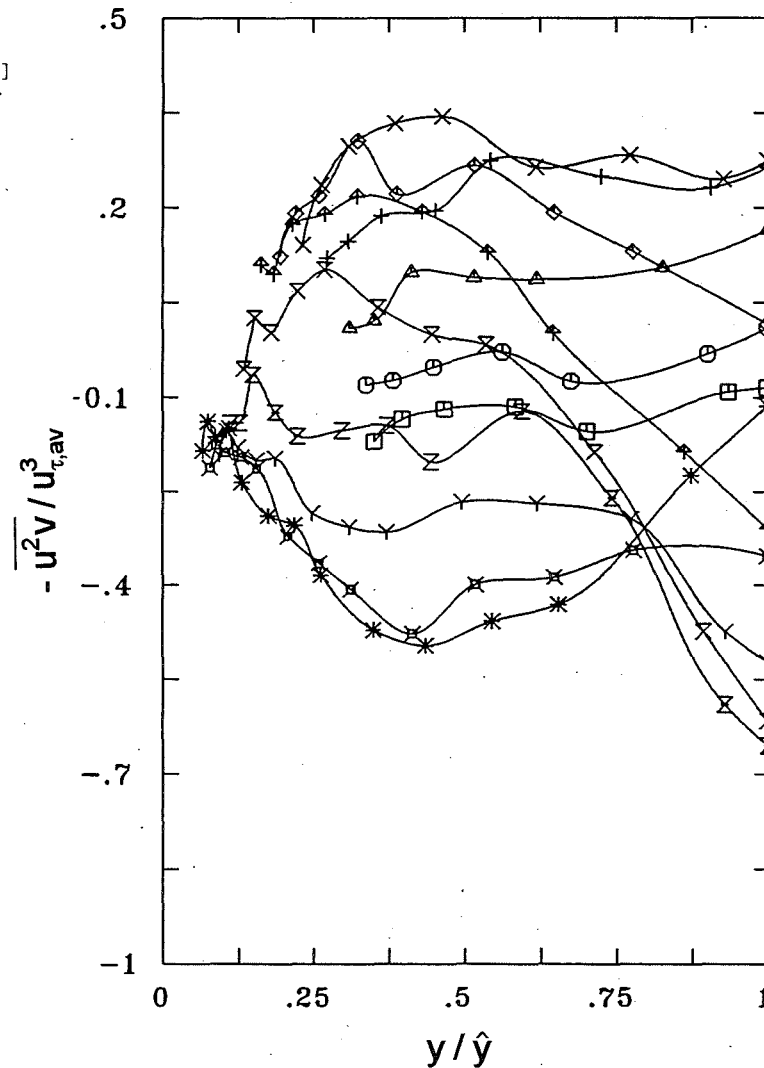
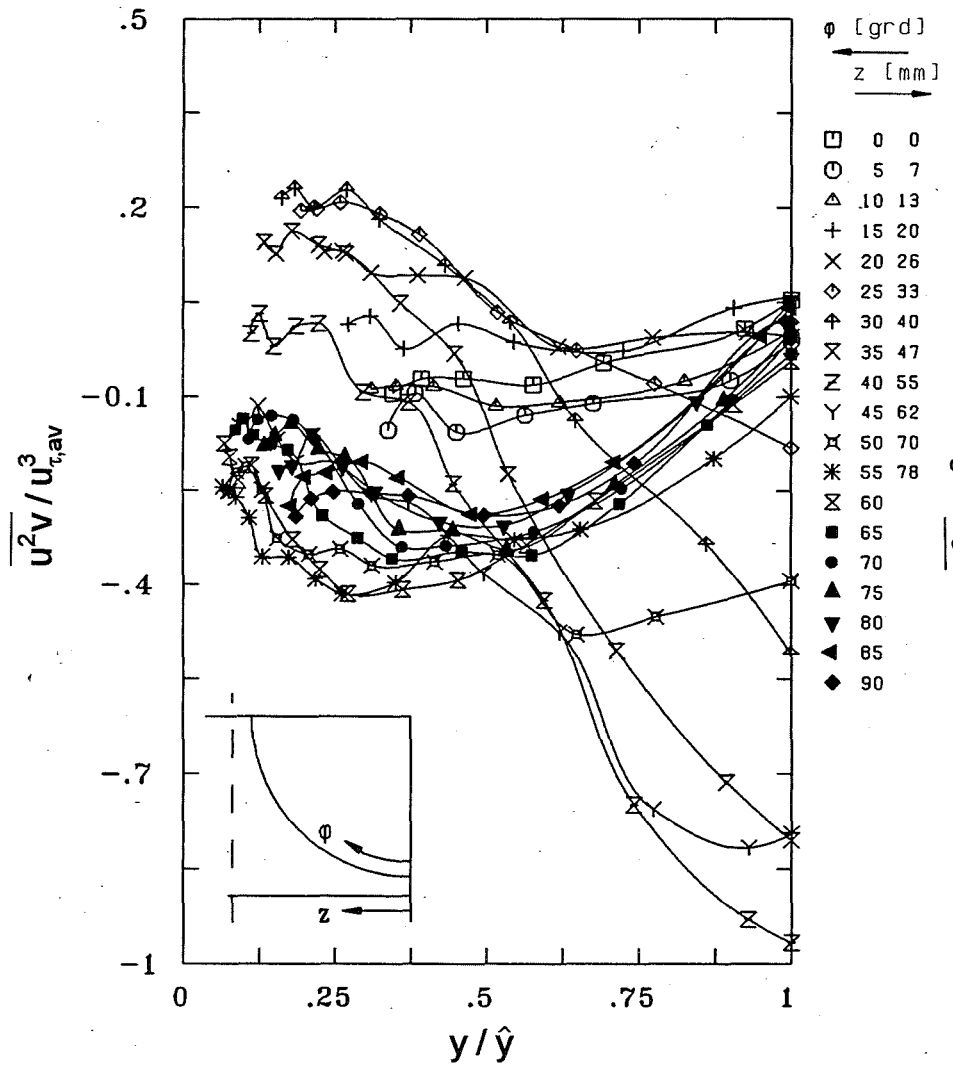


Fig. 47 Triple correlation of two axial components and the radial component

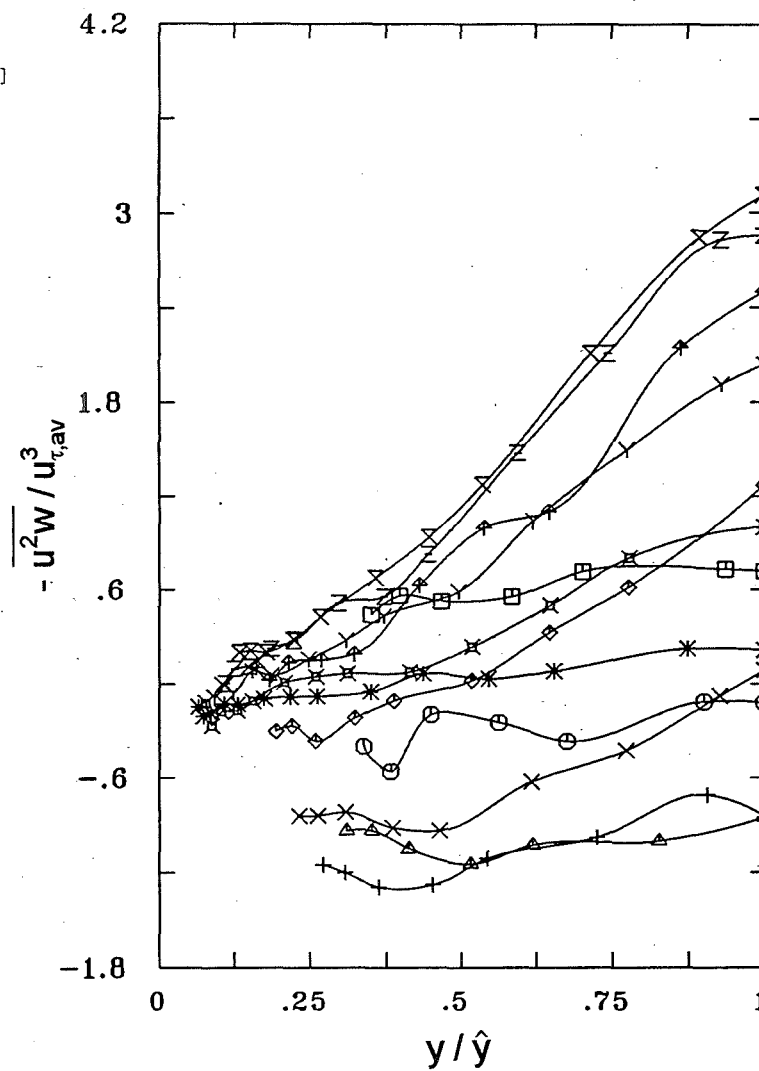
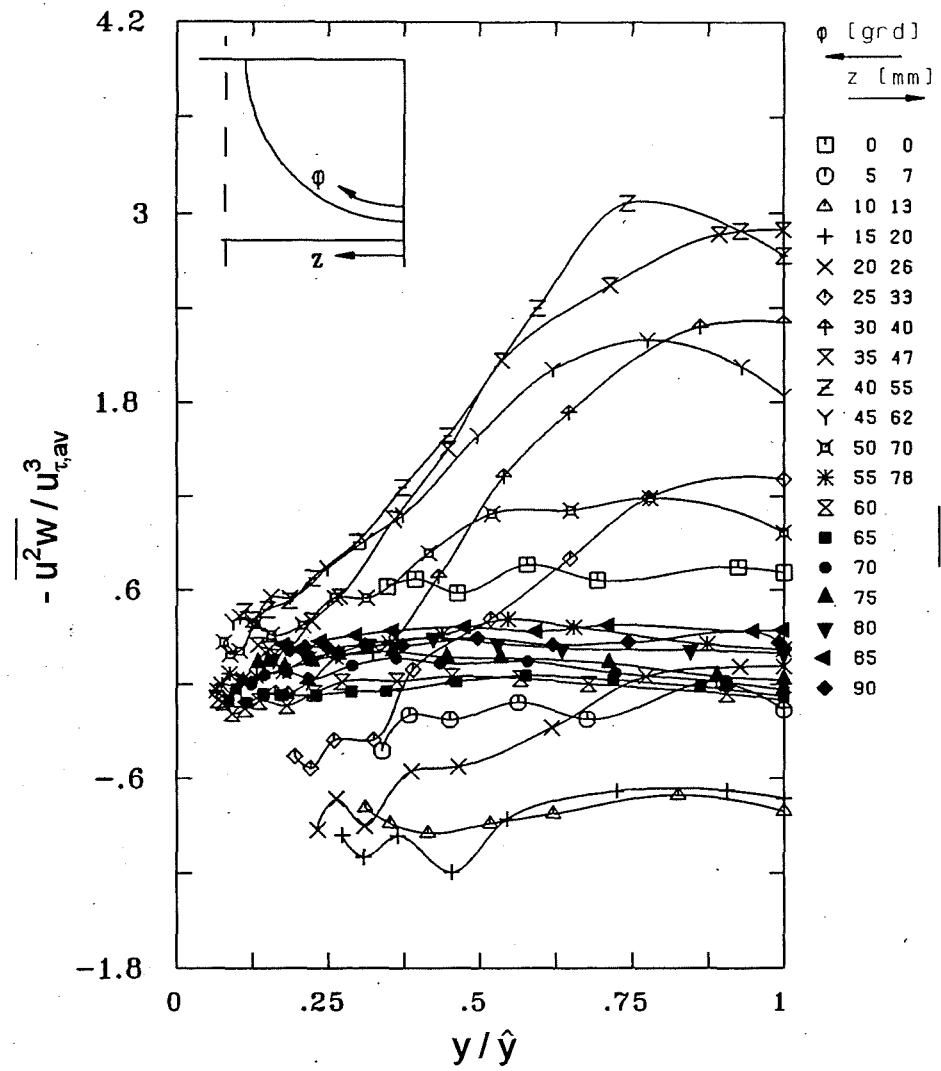


Fig. 48 Triple correlation of two axial components and the azimuthal component

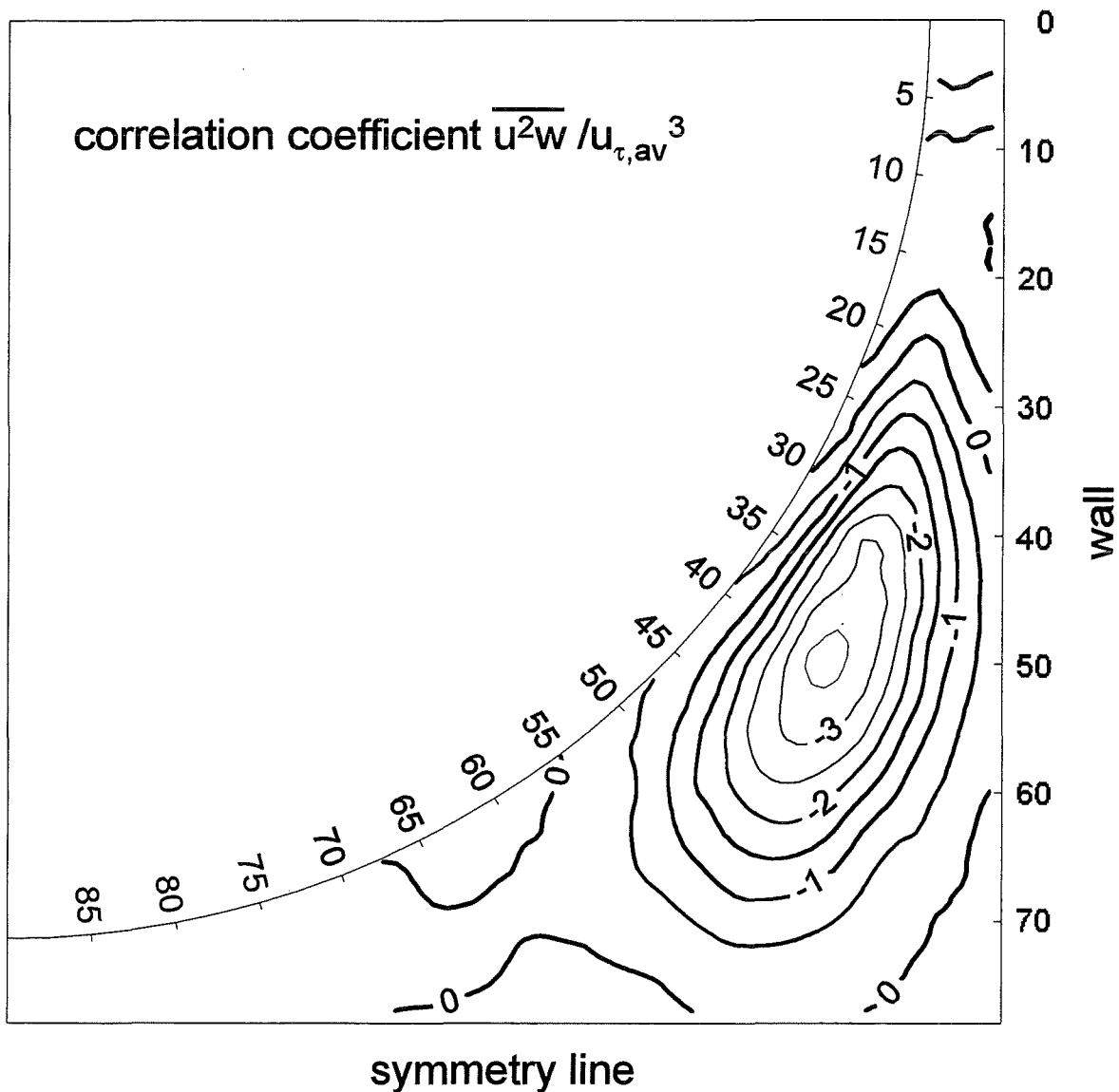


Fig. 49 Contour plot of the triple correlation of two axial components and the azimuthal component

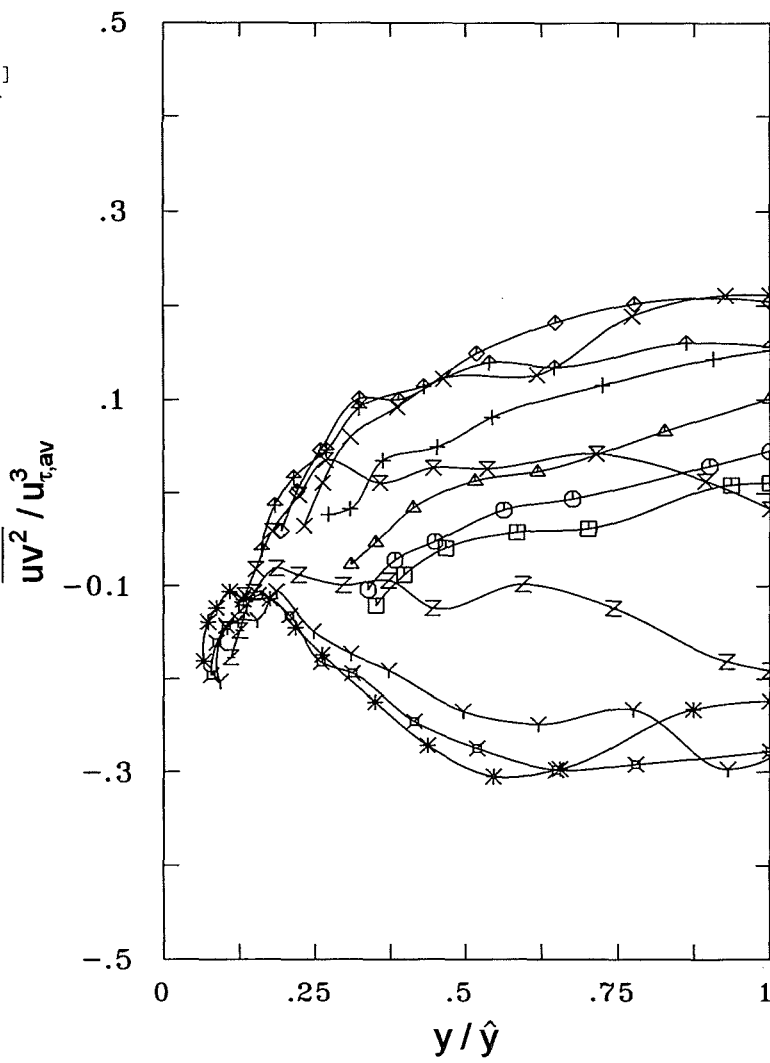
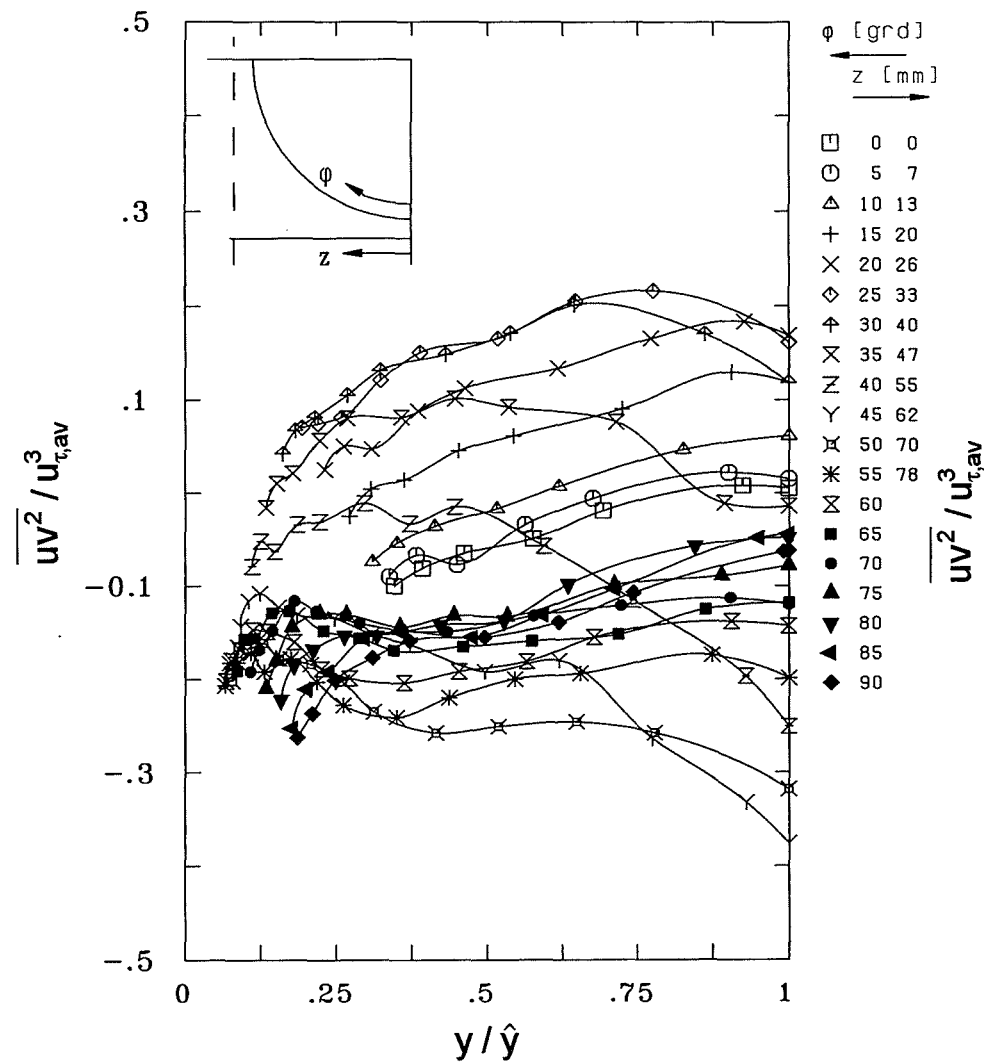


Fig. 50 Triple correlation of the axial component and two radial components

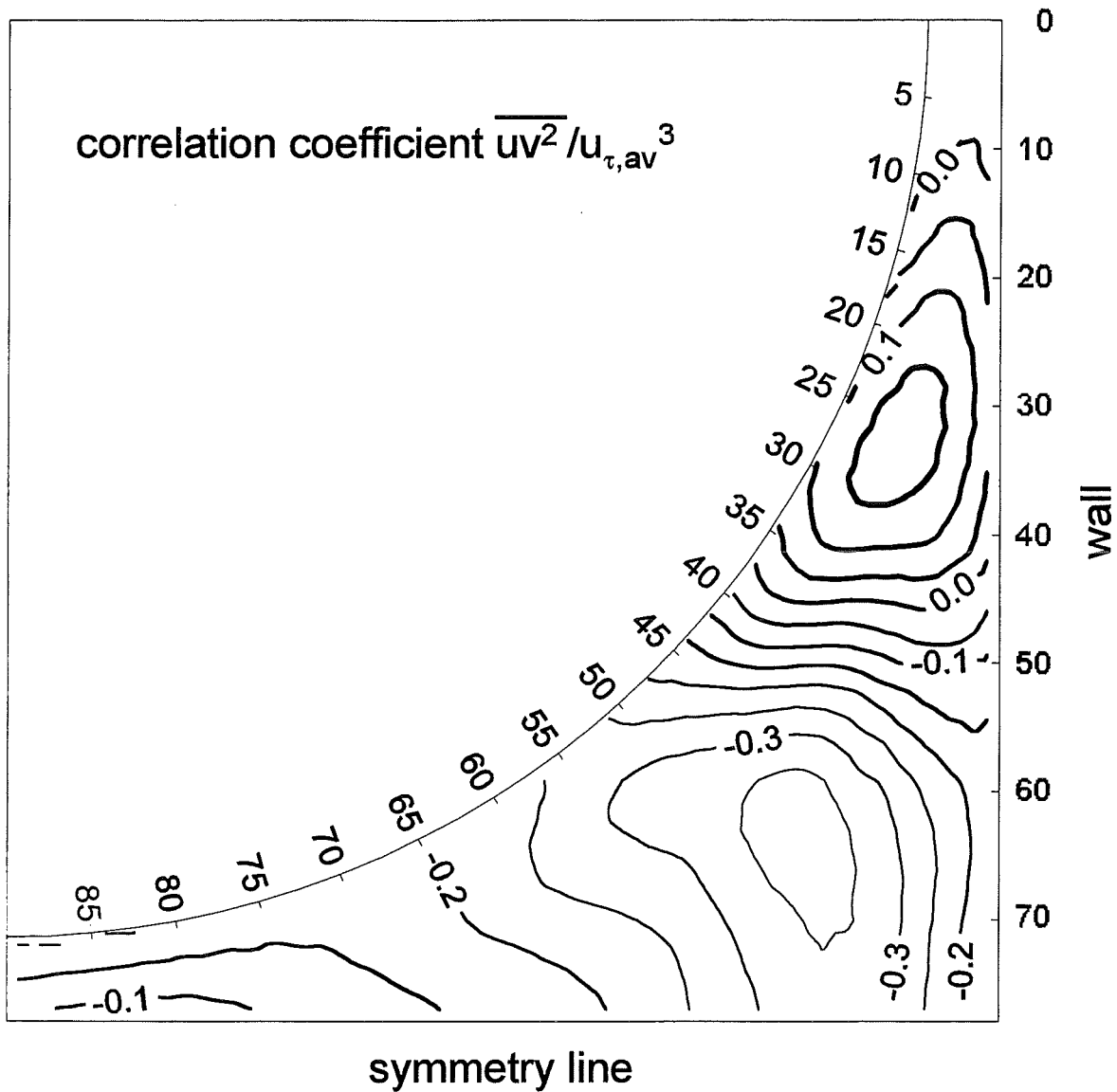


Fig. 51 Contour plot of the triple correlation of the axial component and two radial components

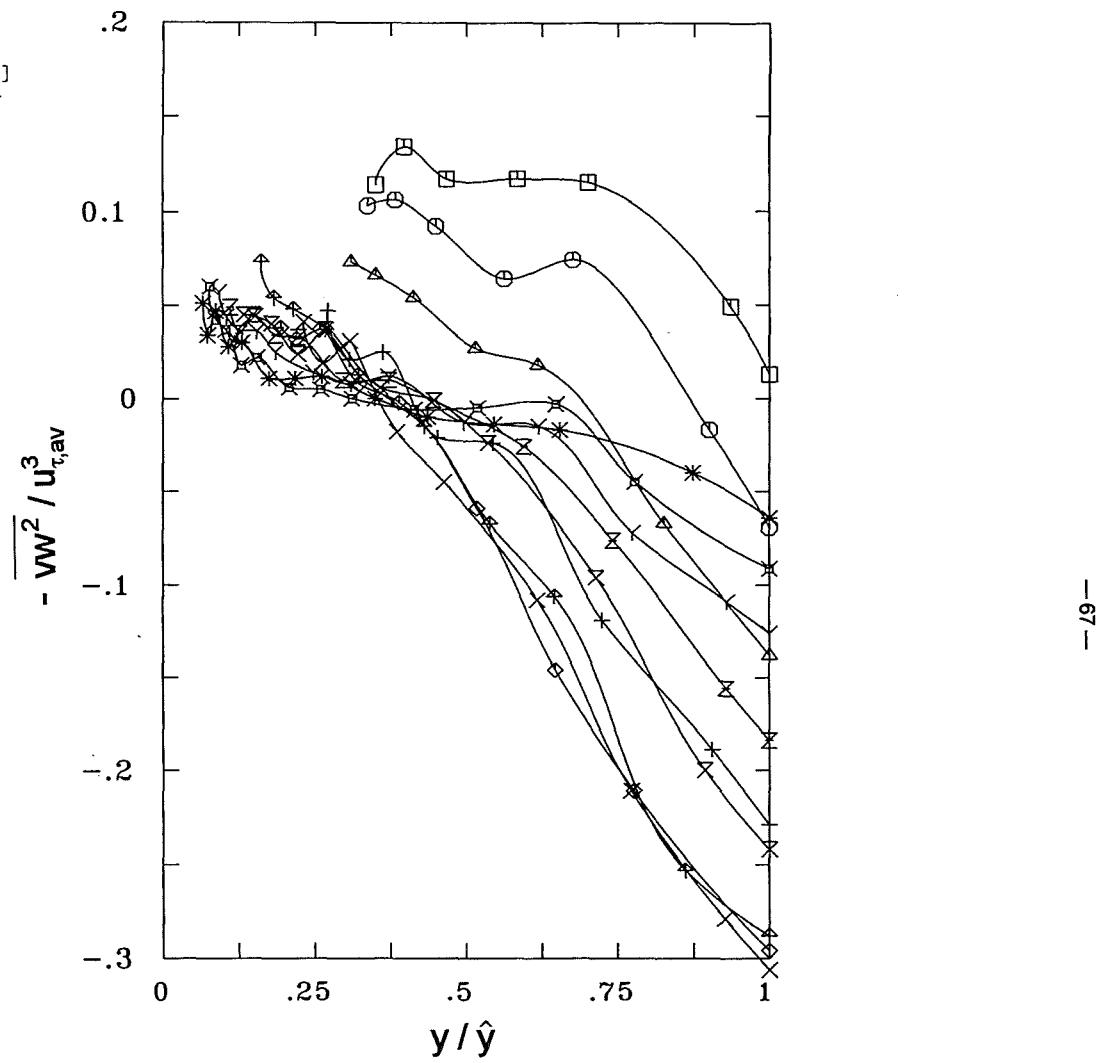
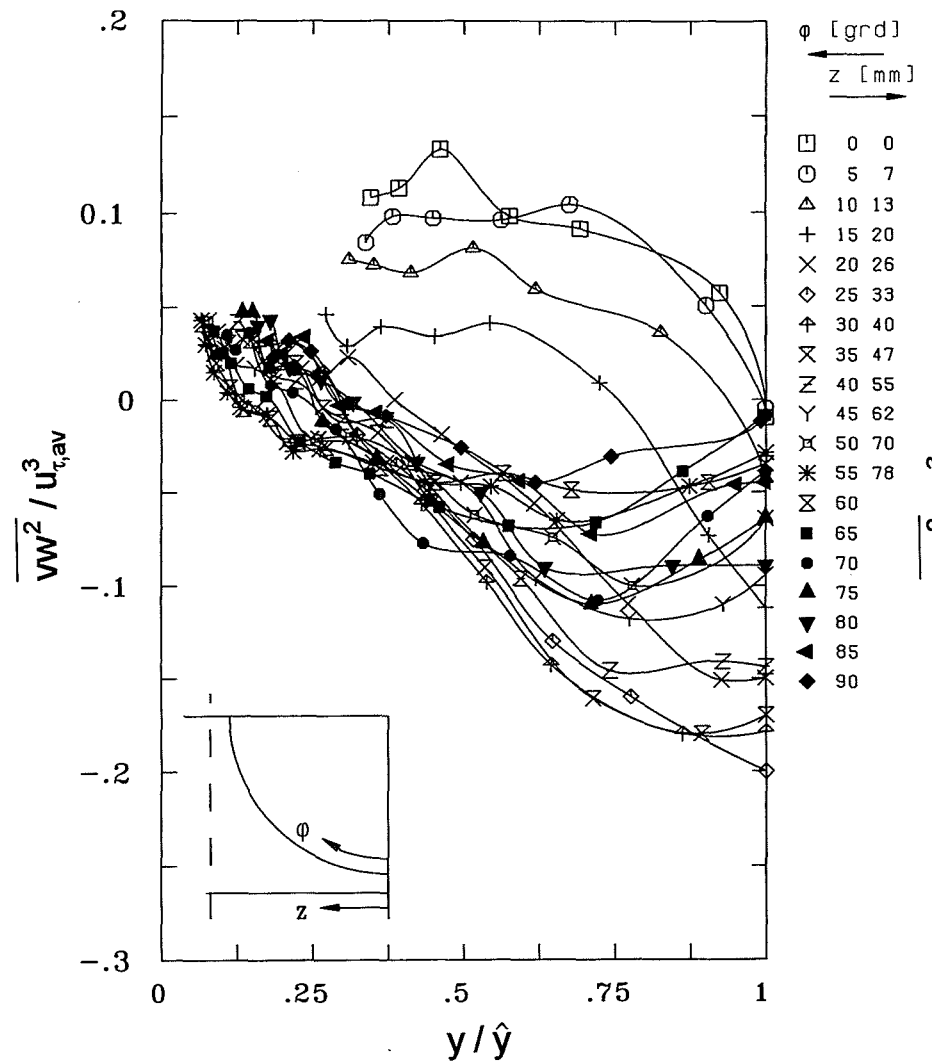


Fig. 52 Triple correlation of the radial component and two azimuthal components

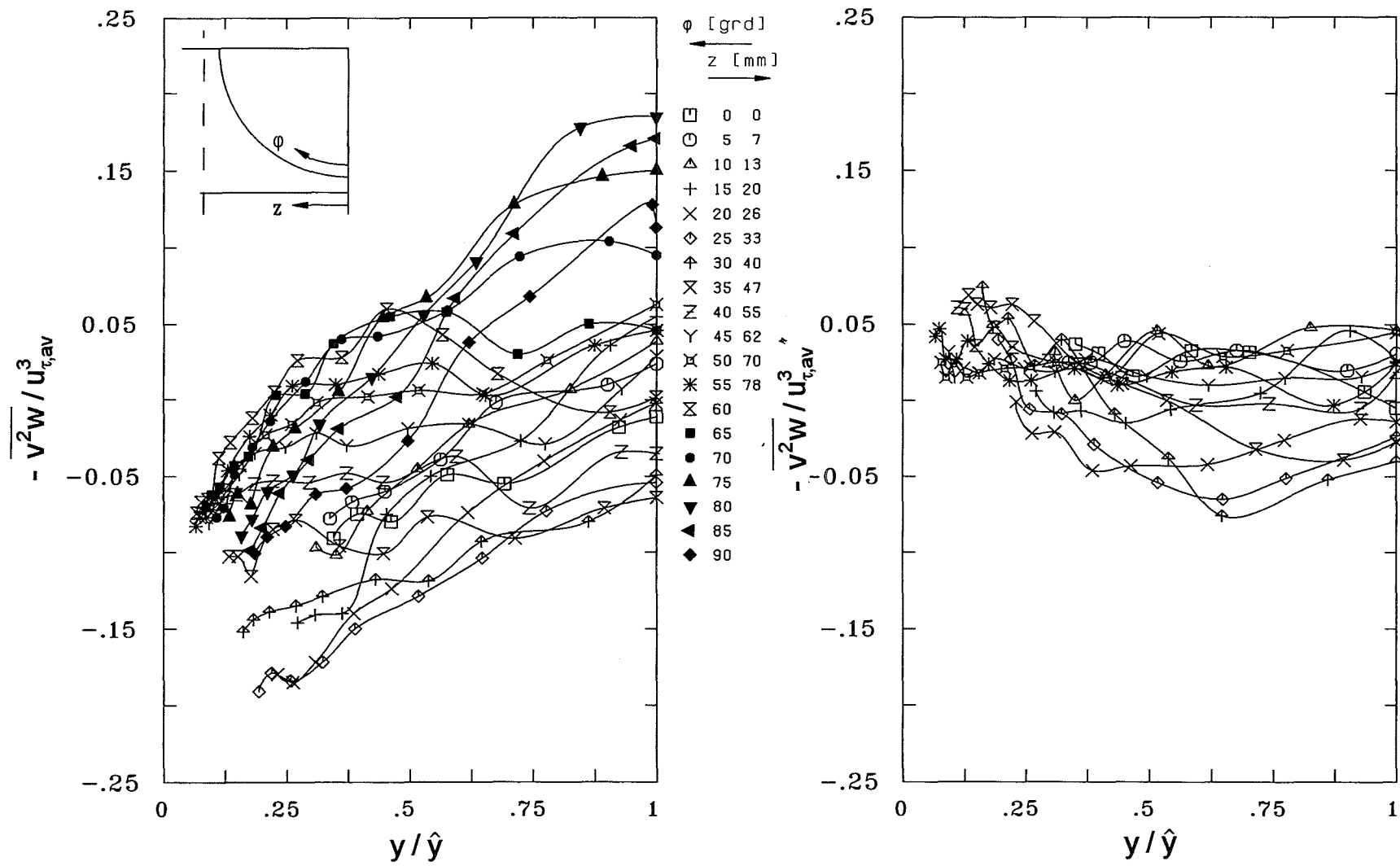


Fig. 53 Triple correlation of two radial components and the azimuthal component

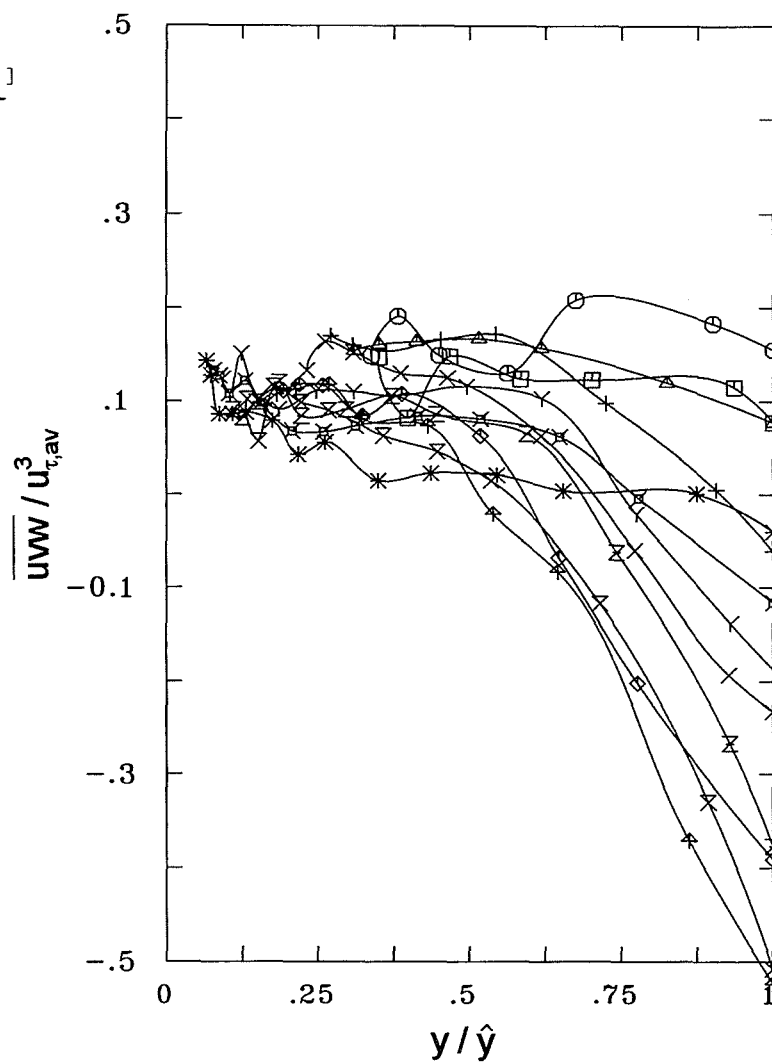
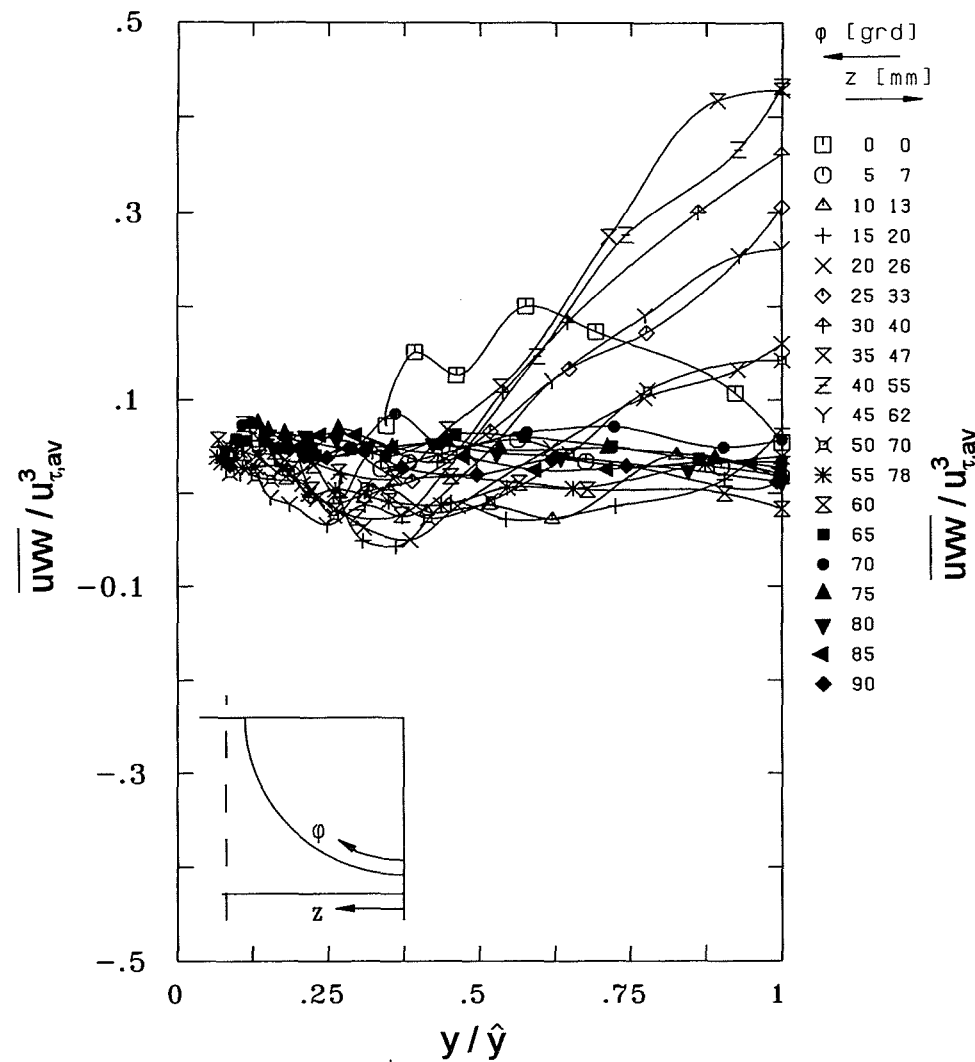


Fig. 54 Triple correlation of the axial, the radial and the azimuthal component

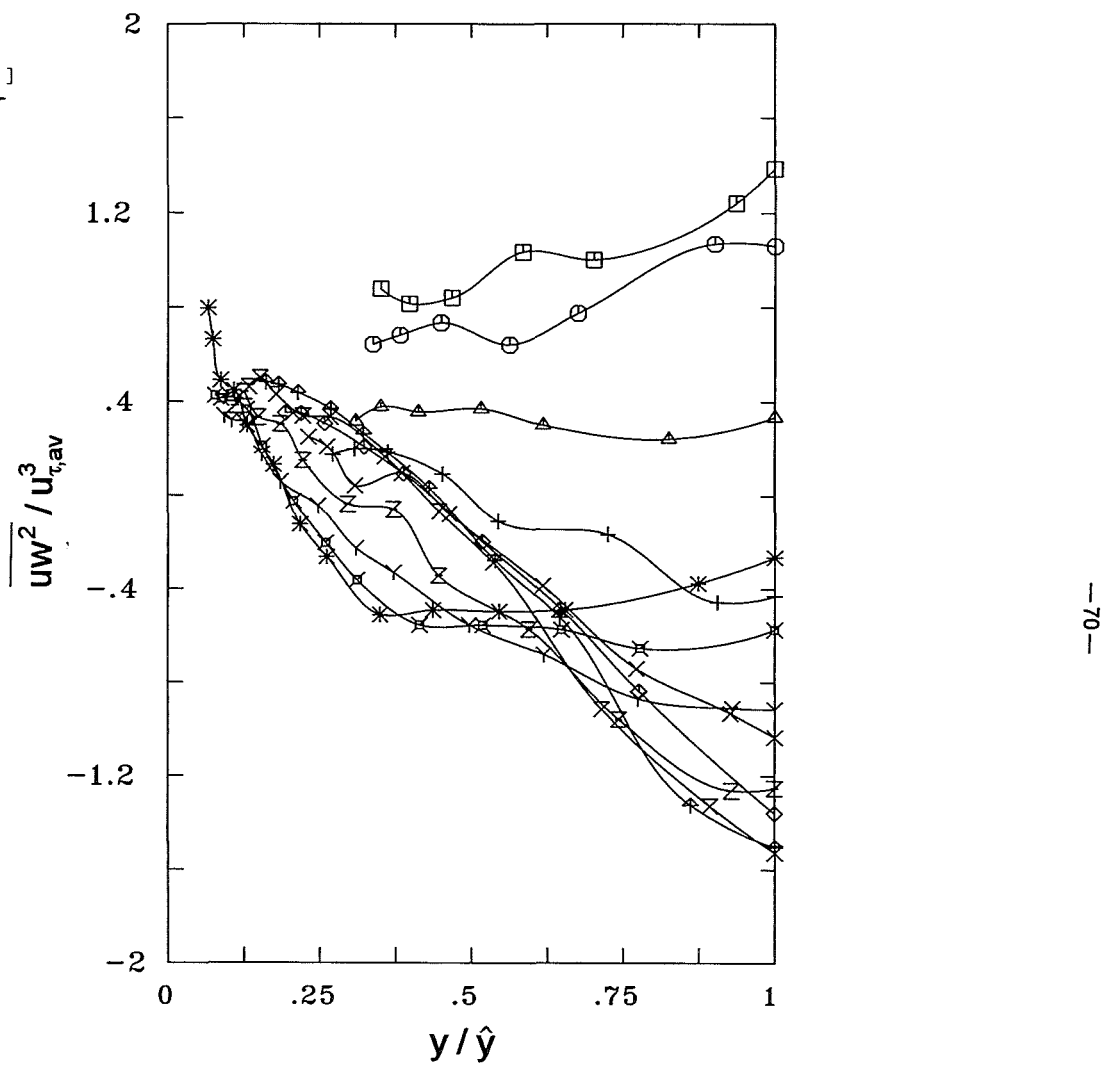
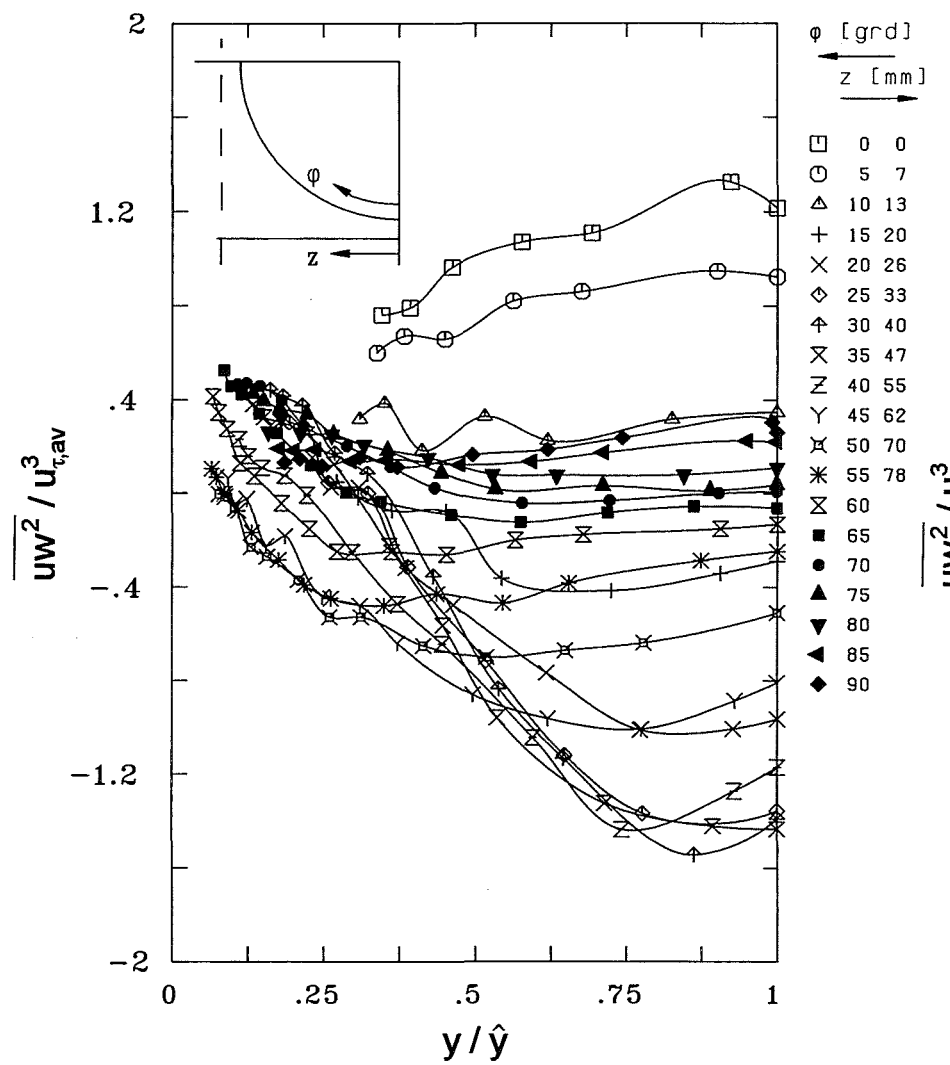


Fig. 55 Triple correlation of the axial and two azimuthal components

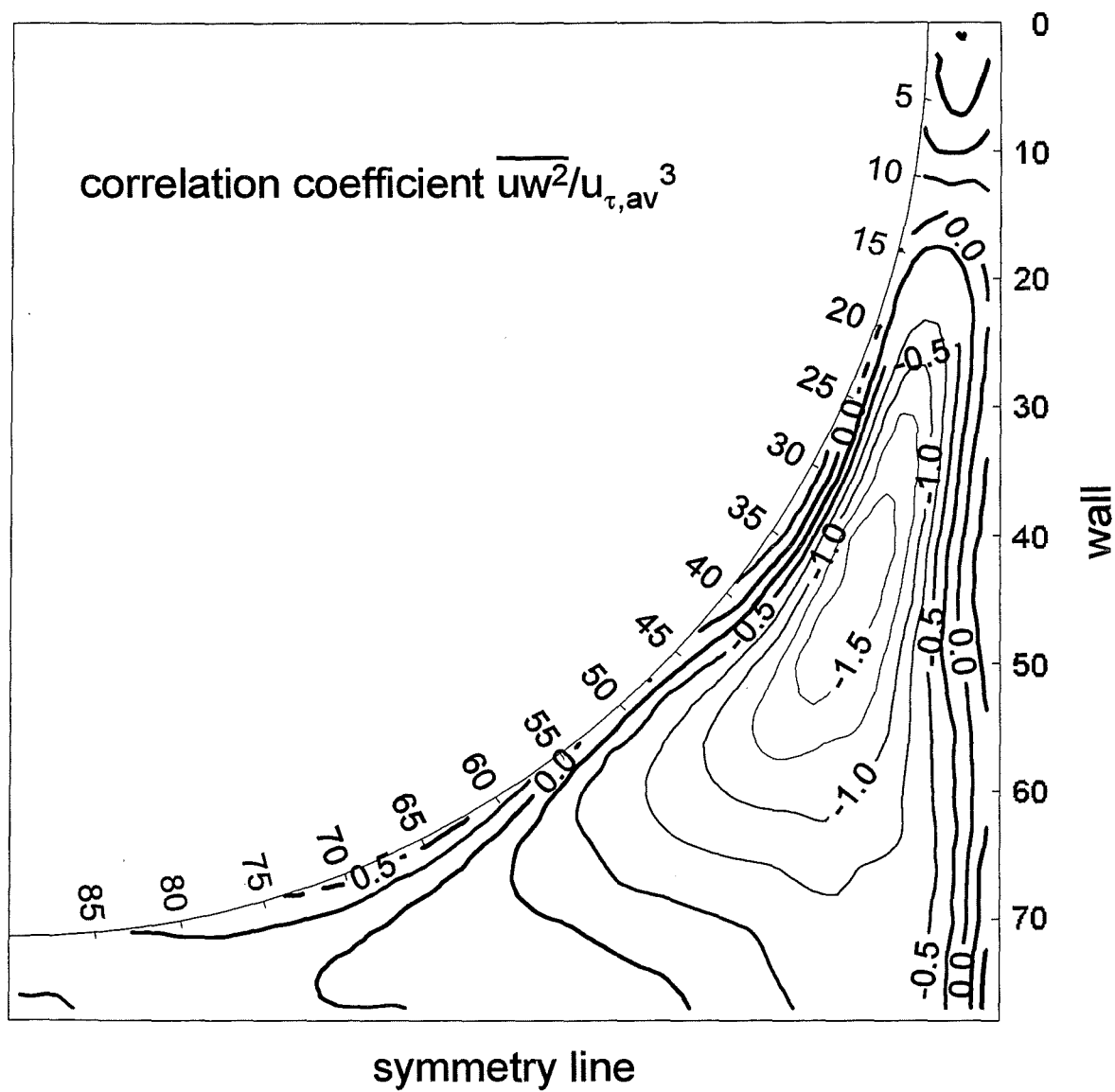


Fig. 56 Contour plot of the triple correlation of the axial component and two azimuthal components

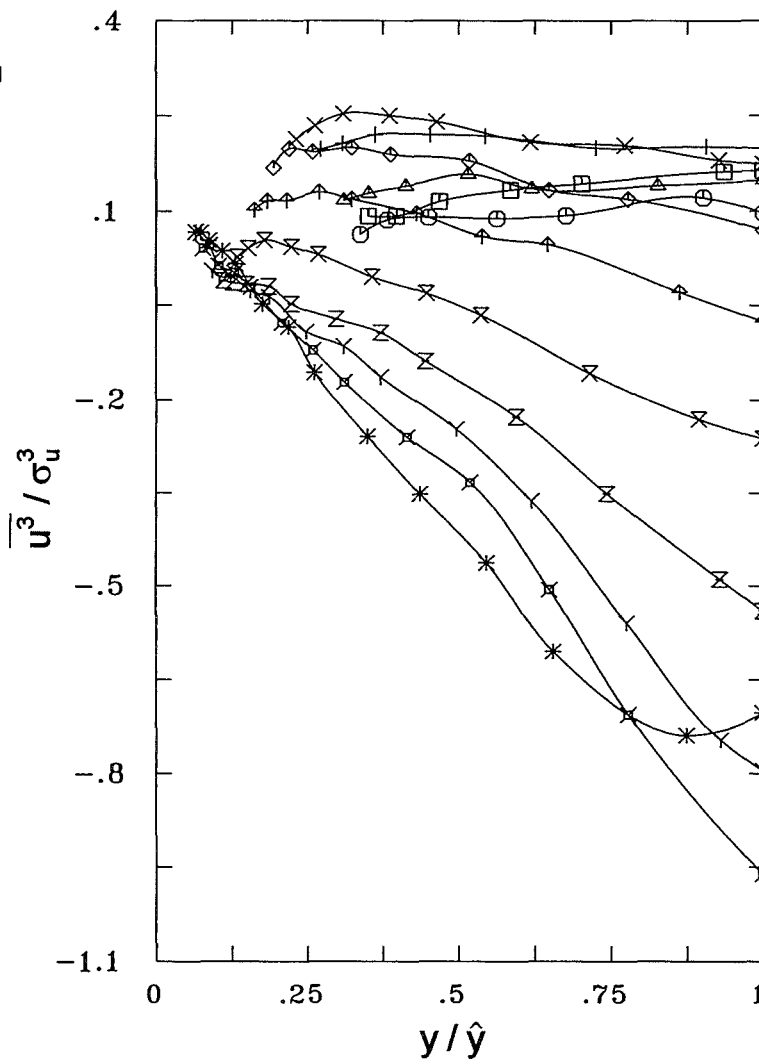
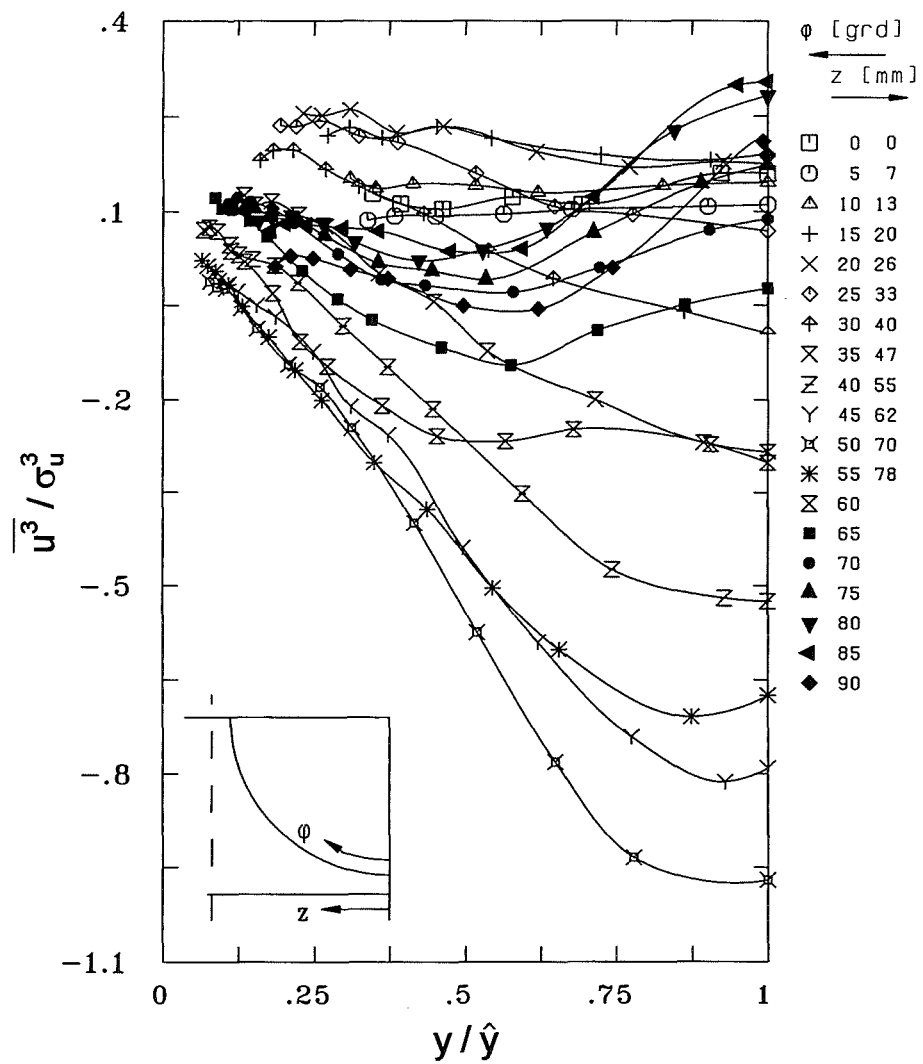


Fig. 57 Skewness of the axial velocity component

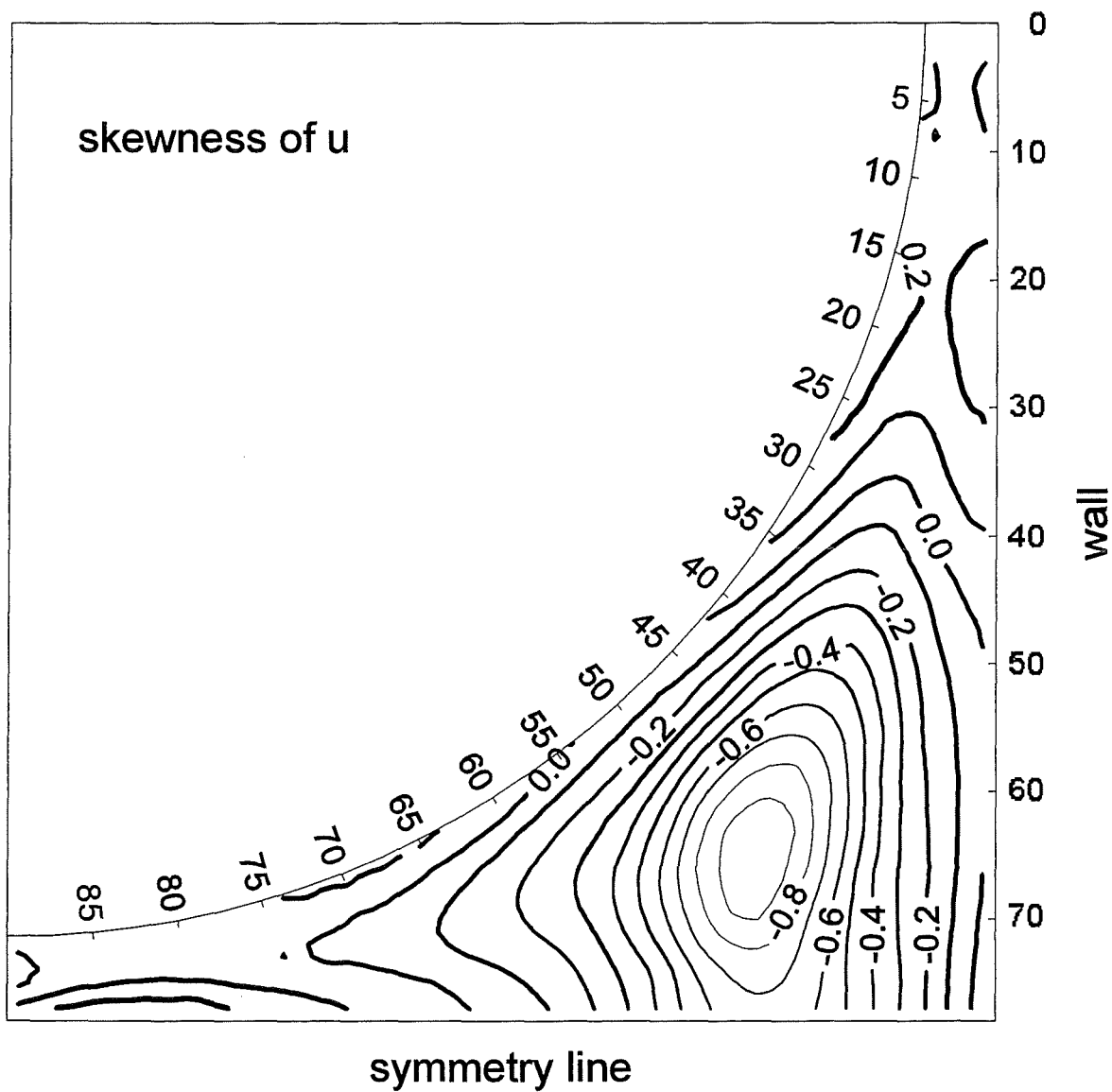


Fig. 58 Contour plot of the skewness of the axial velocity component

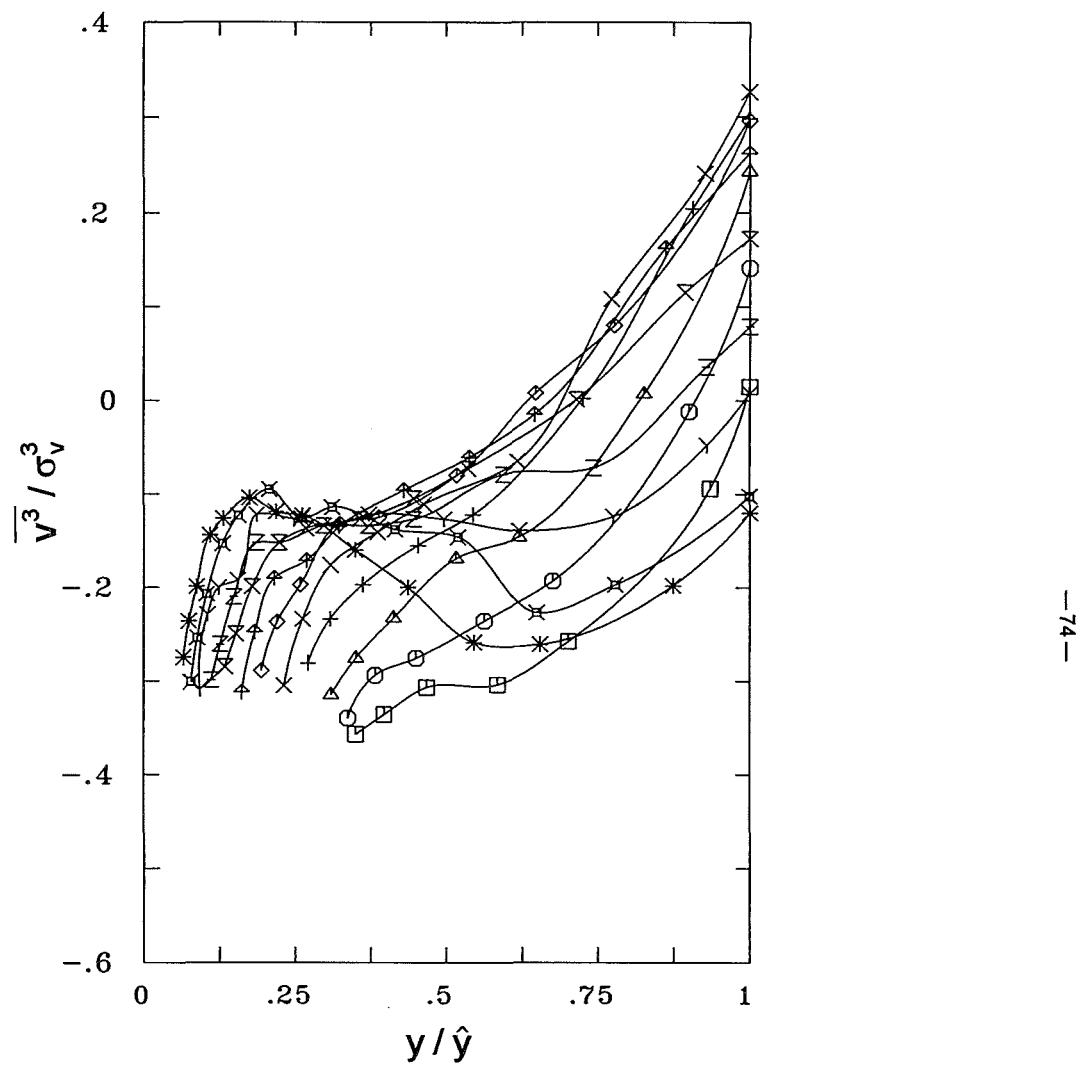
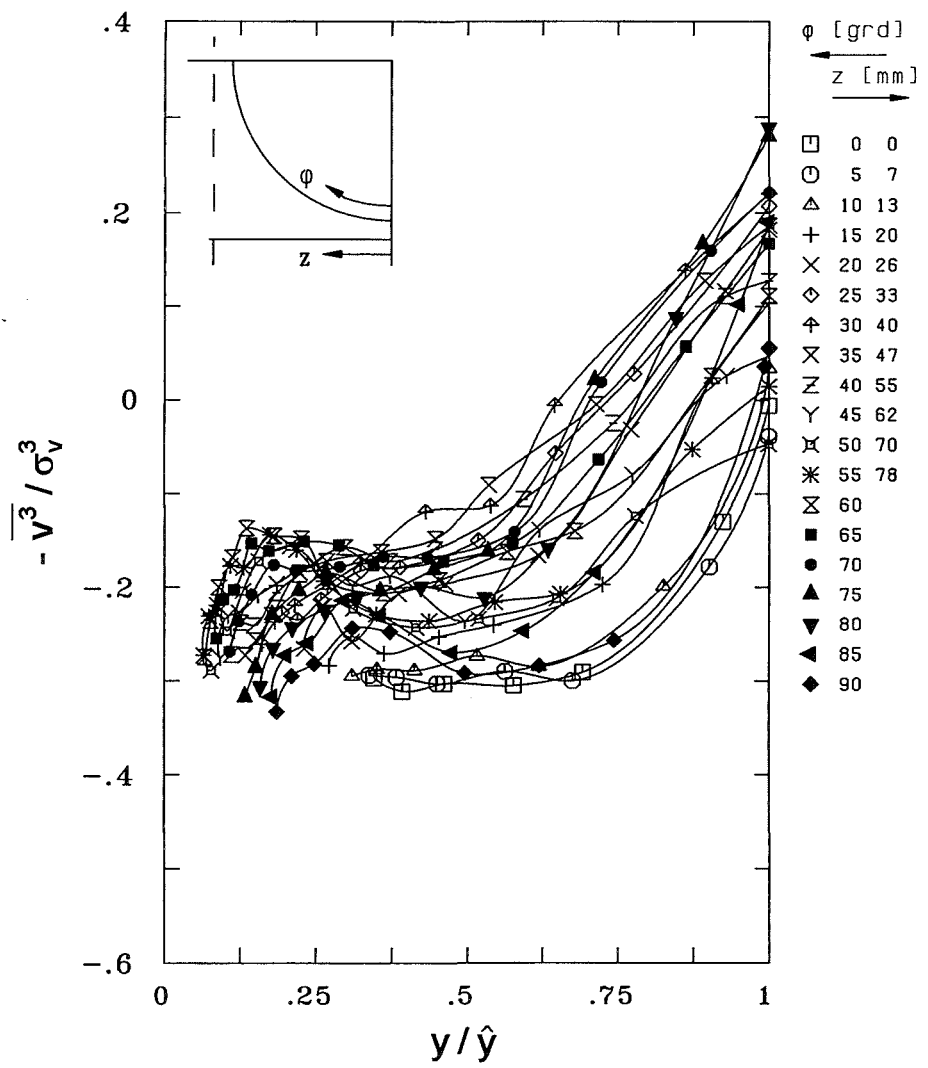


Fig. 59 Skewness of the radial velocity component

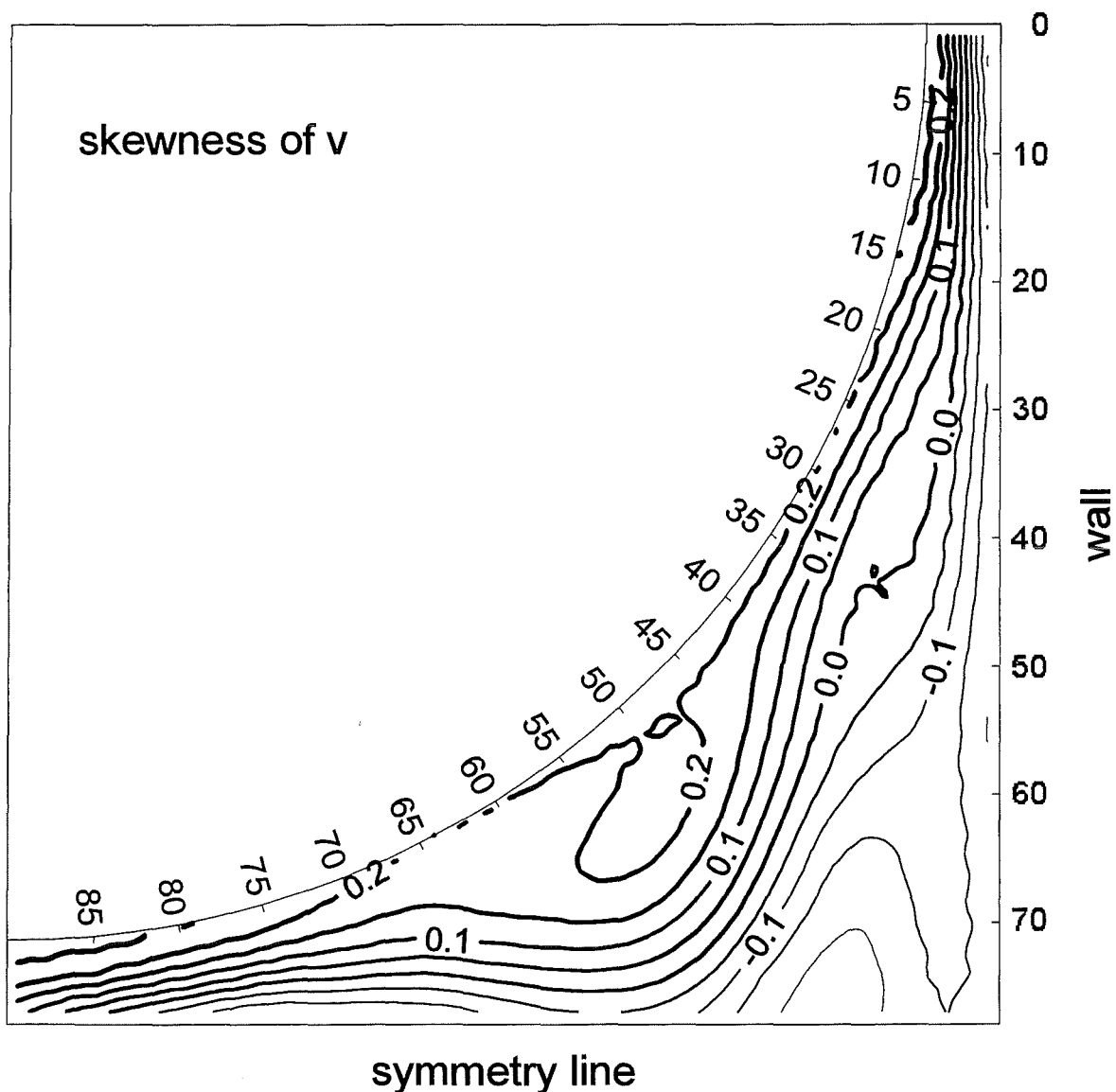


Fig. 60 Contour plot of the skewness of the radial velocity component

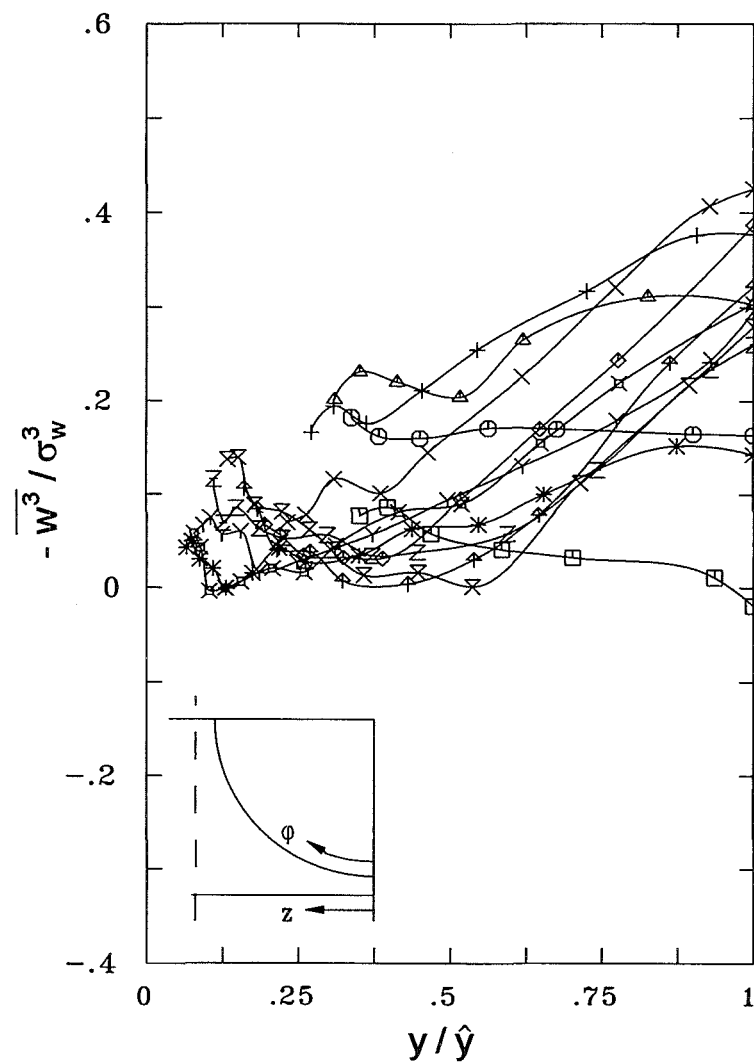
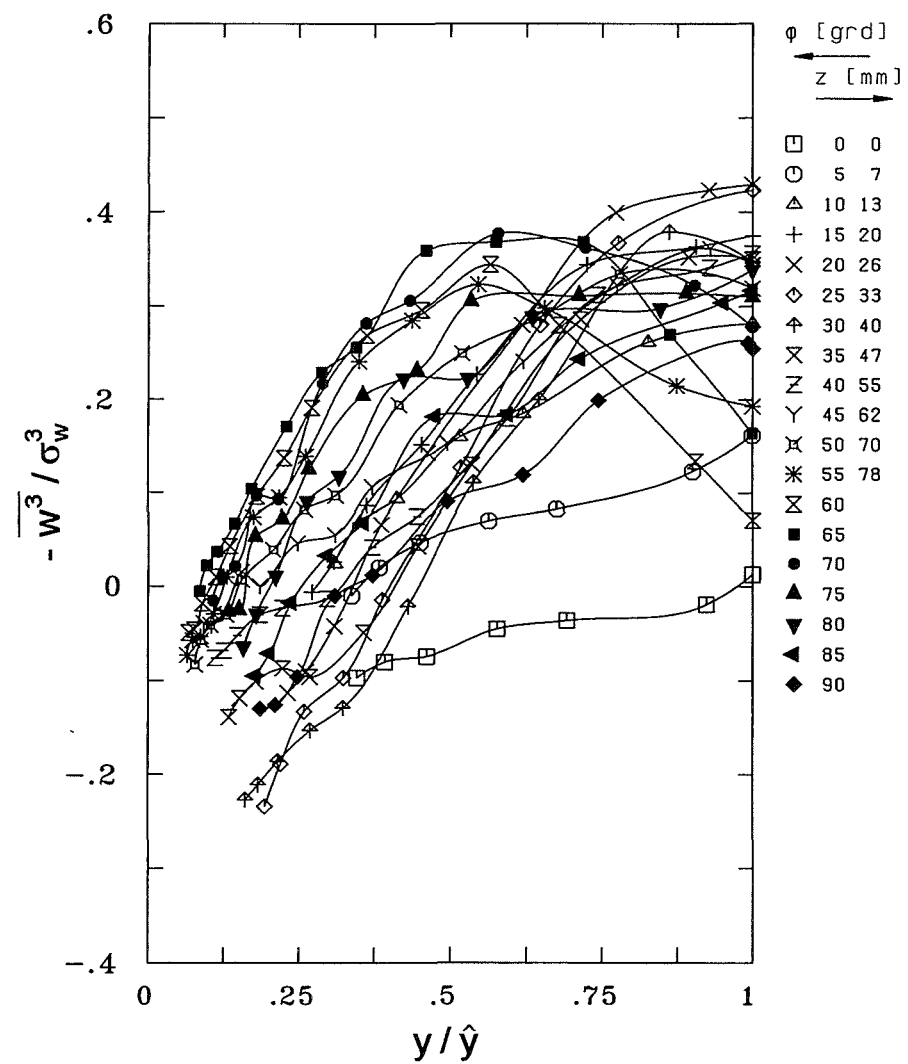


Fig. 61 Skewness of the azimuthal velocity component

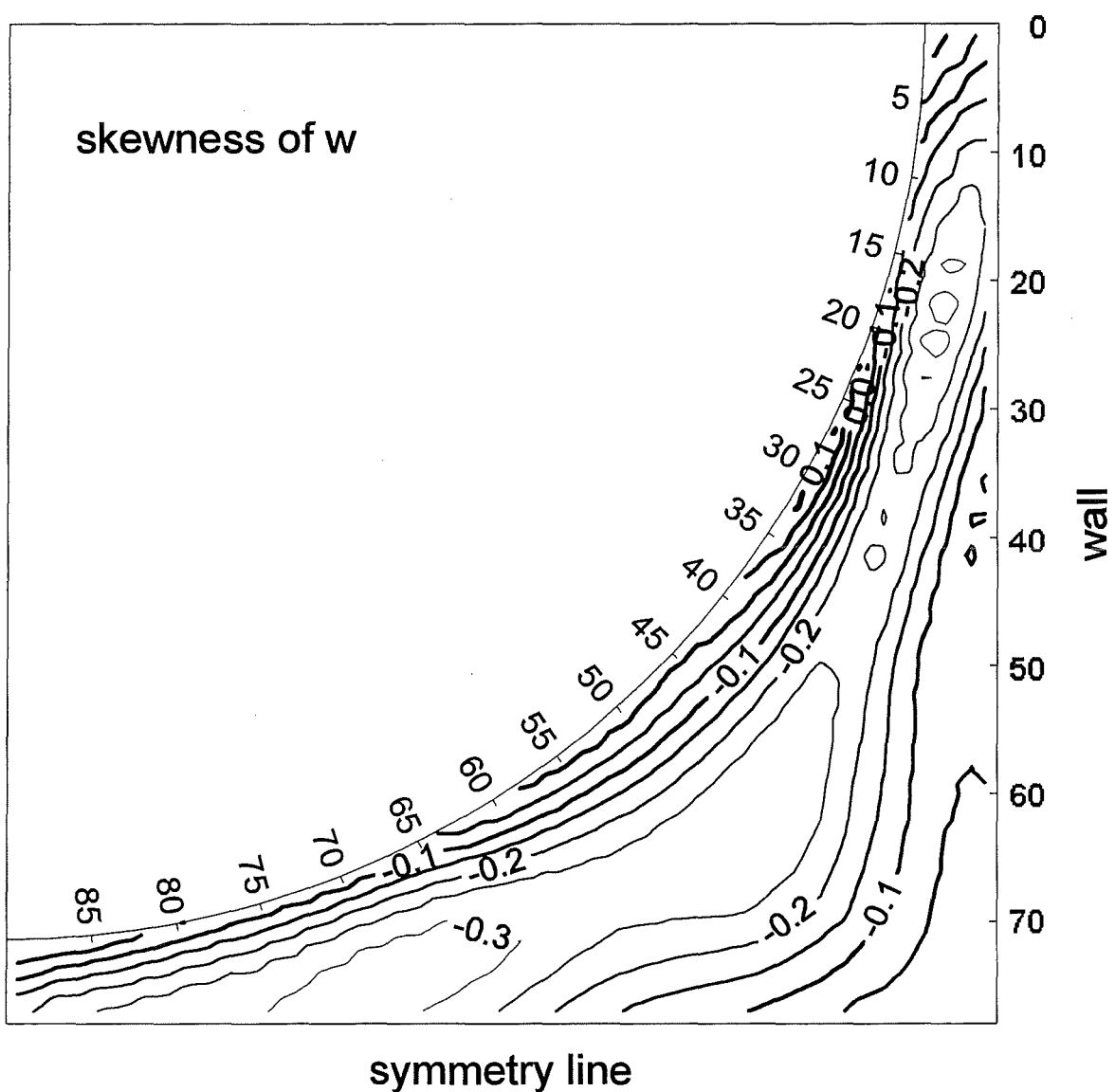


Fig. 62 Contour plot of the skewness of the azimuthal velocity component

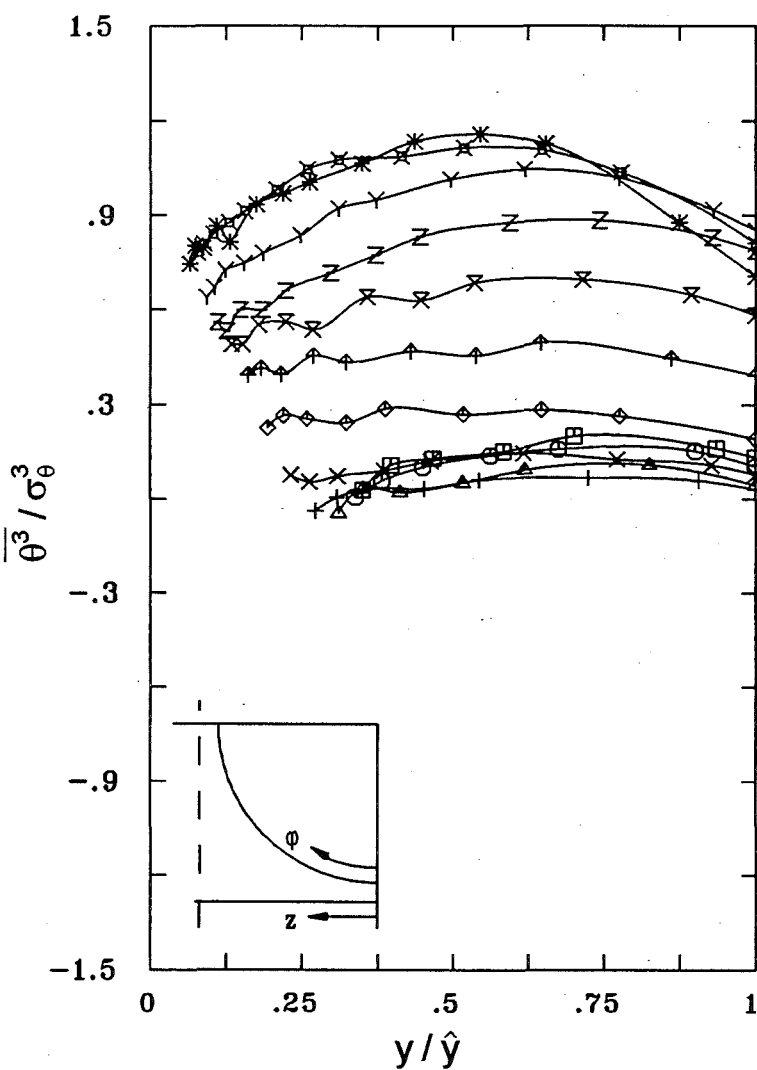
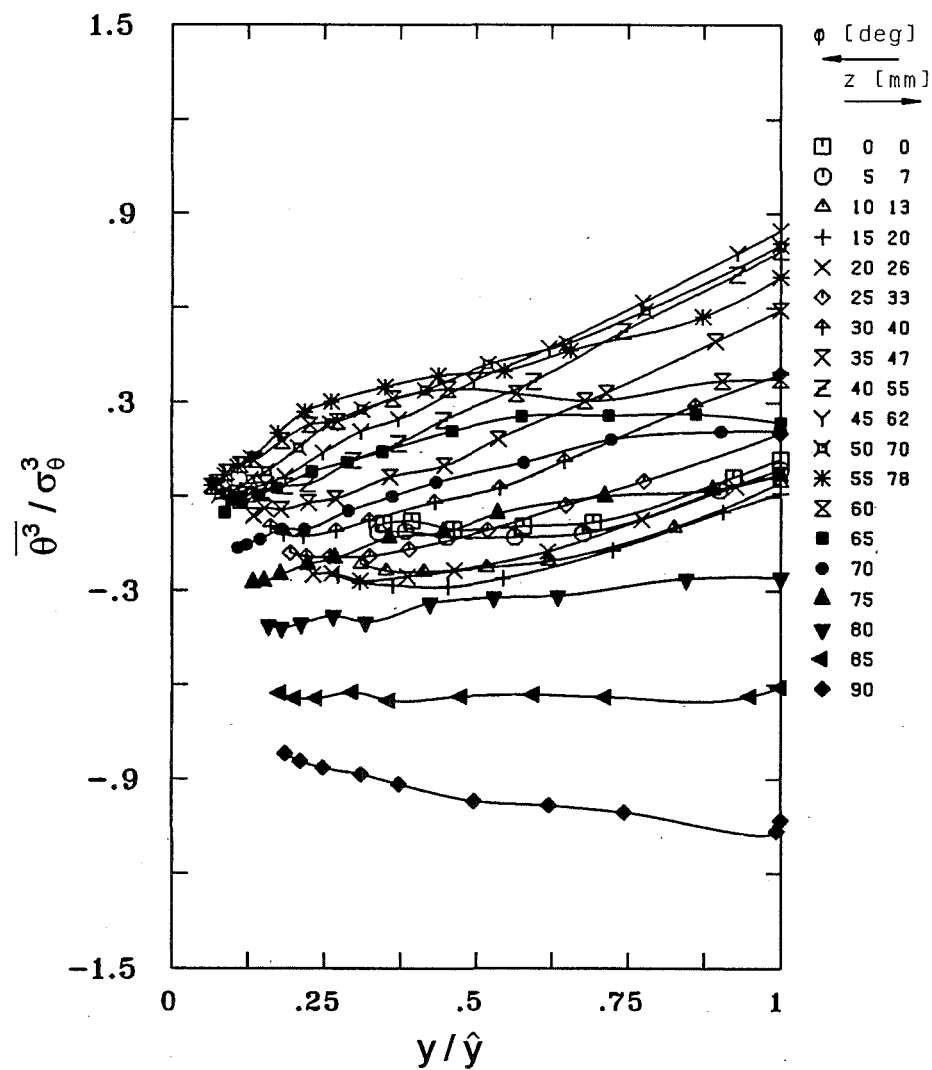


Fig. 63 Skewness of the temperature fluctuation

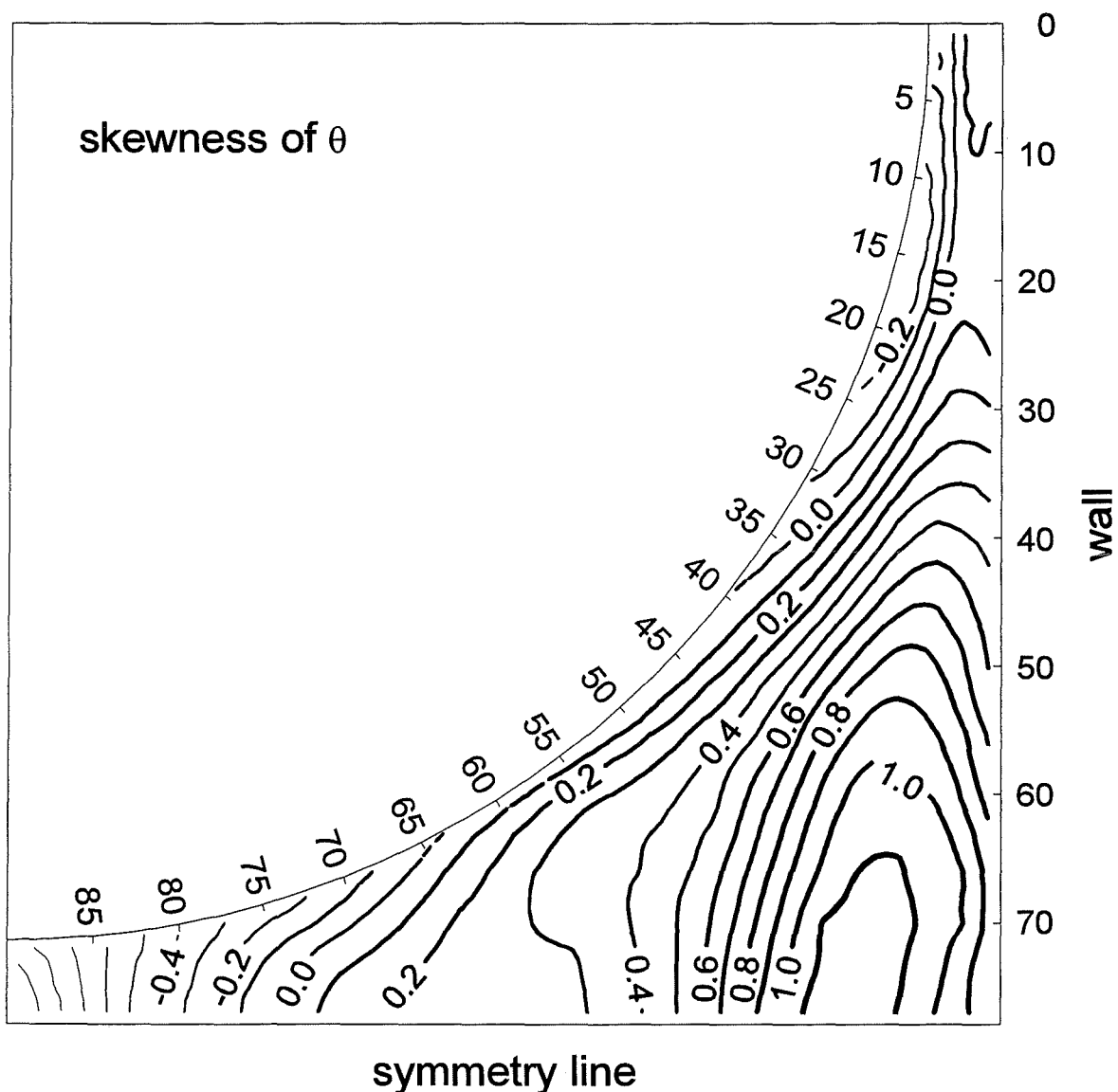


Fig. 64 Contour plot of the skewness of the temperature fluctuation

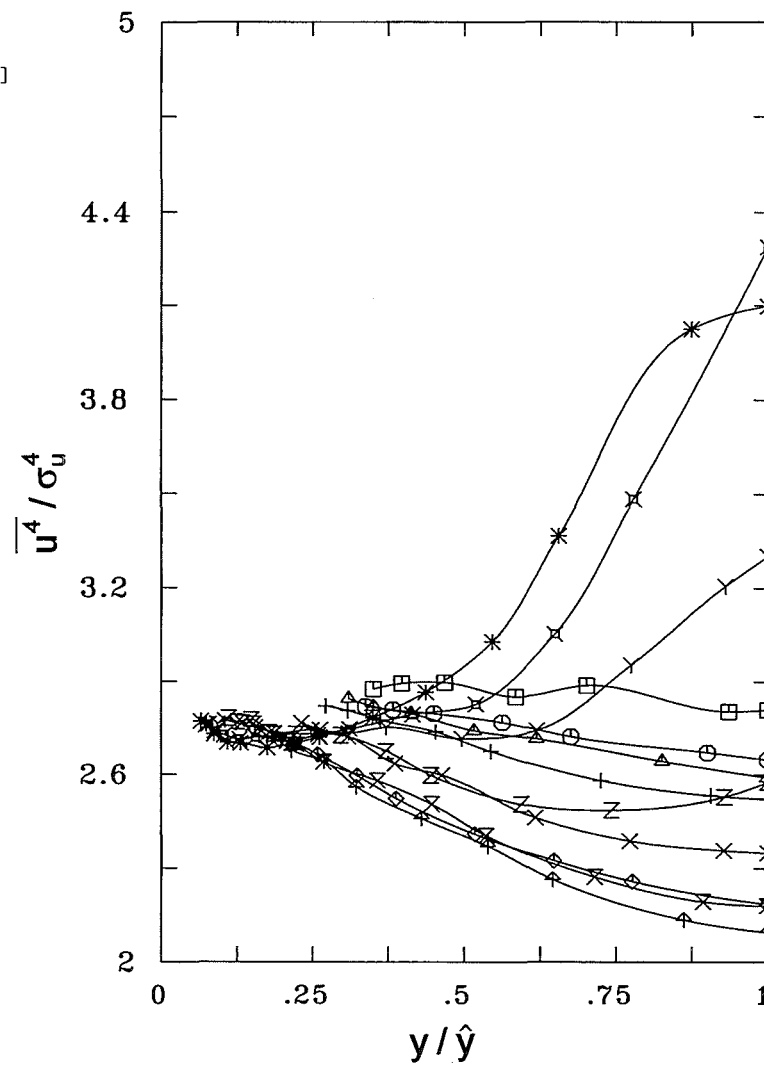
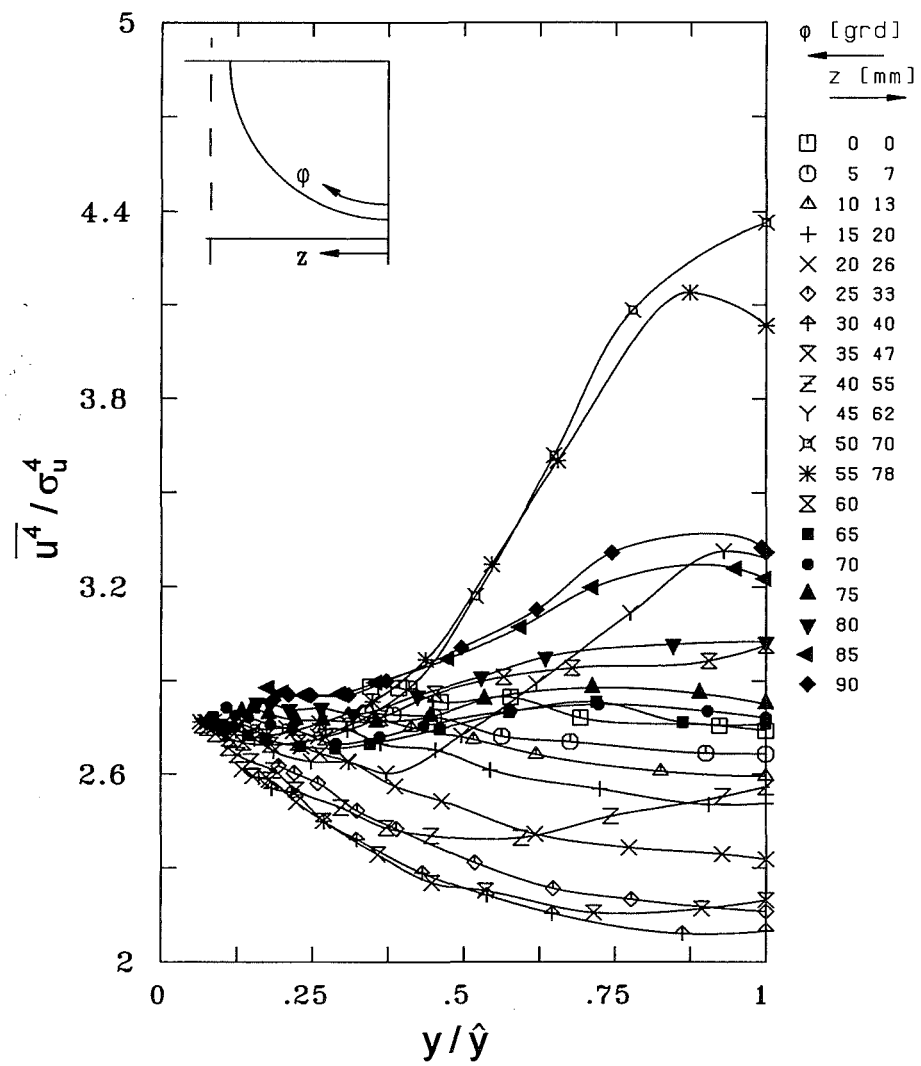


Fig. 65 Flatness of the axial velocity component

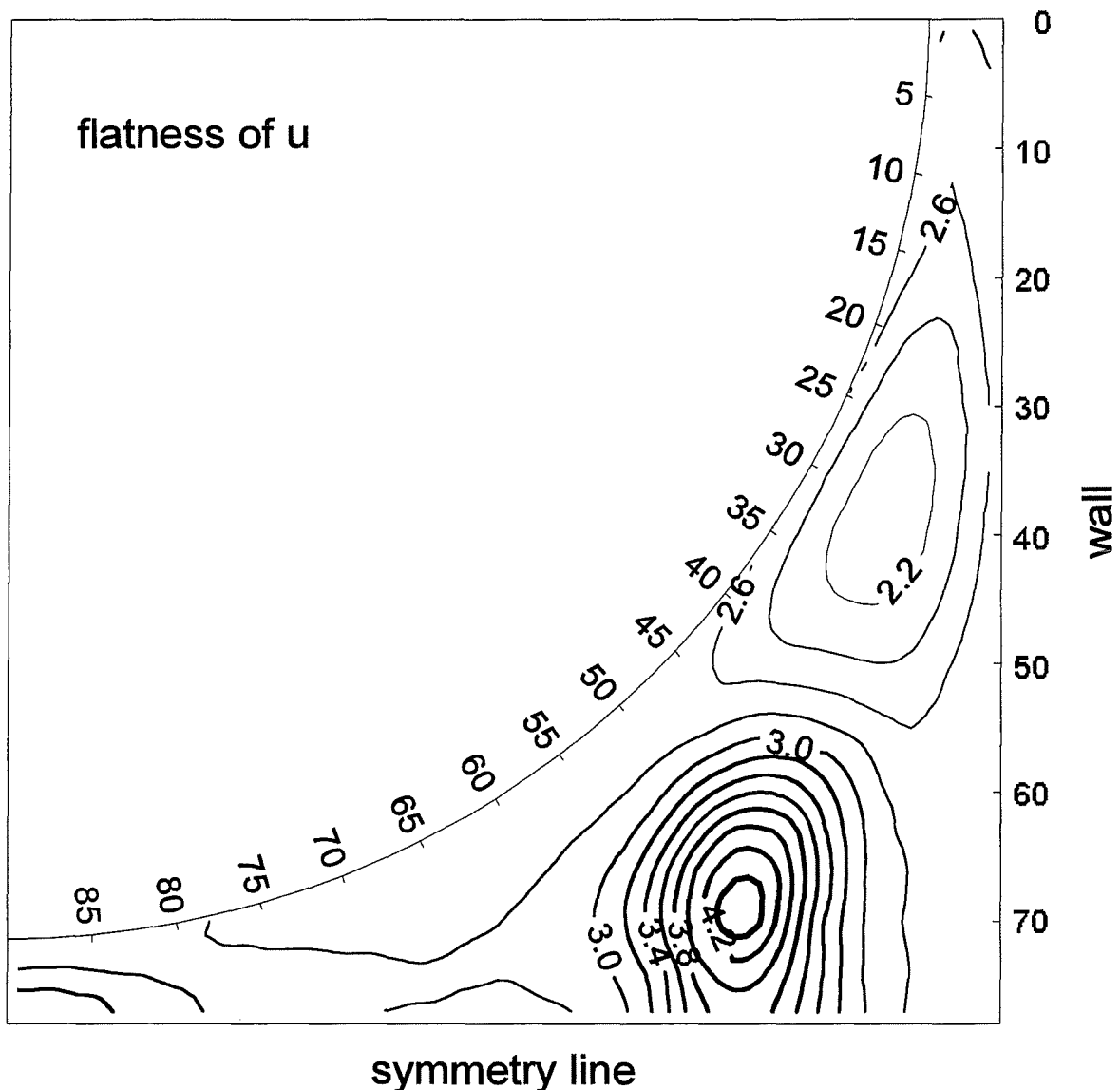


Fig. 66 Contour plot of the flatness of the axial velocity component

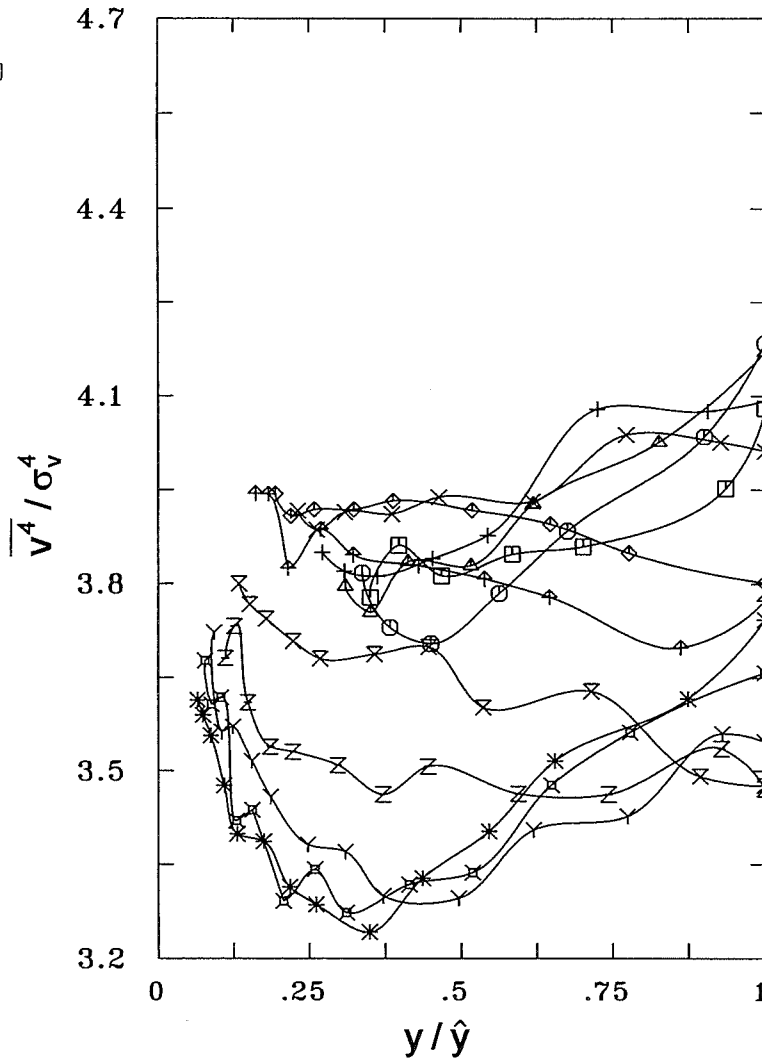
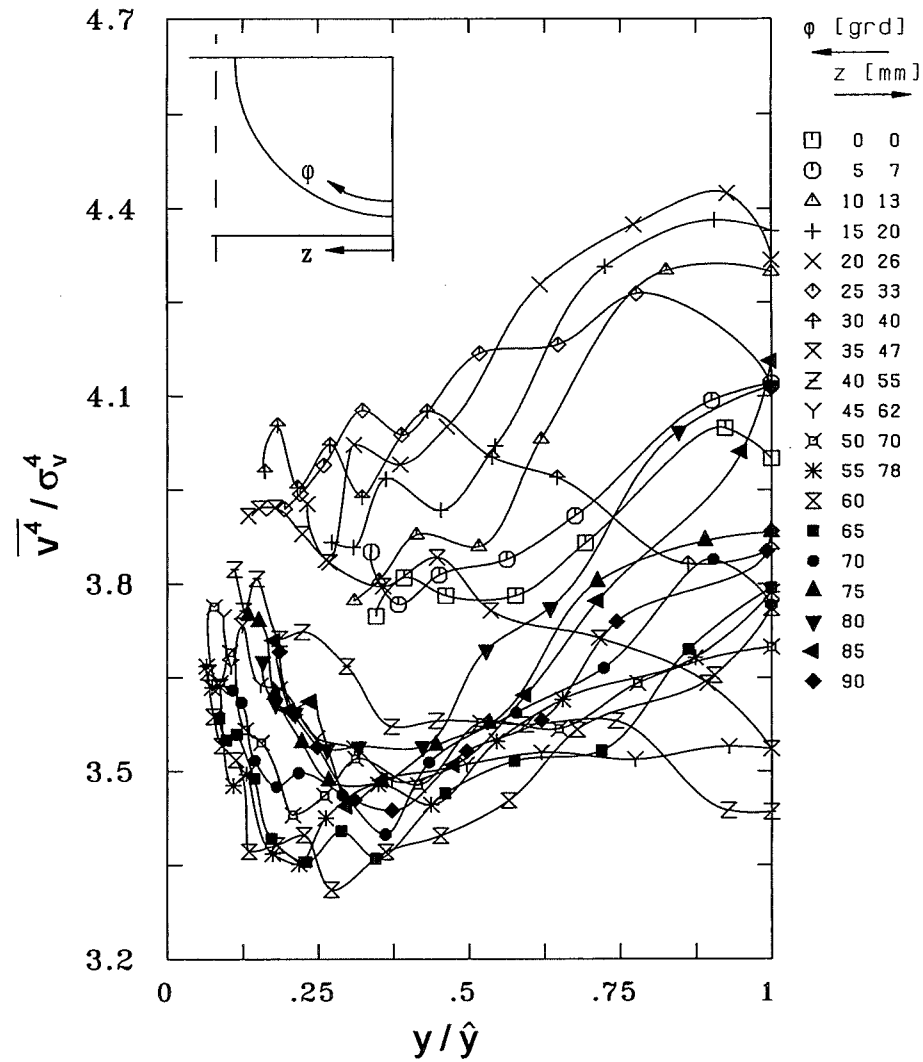


Fig. 67 Flatness of the radial velocity component

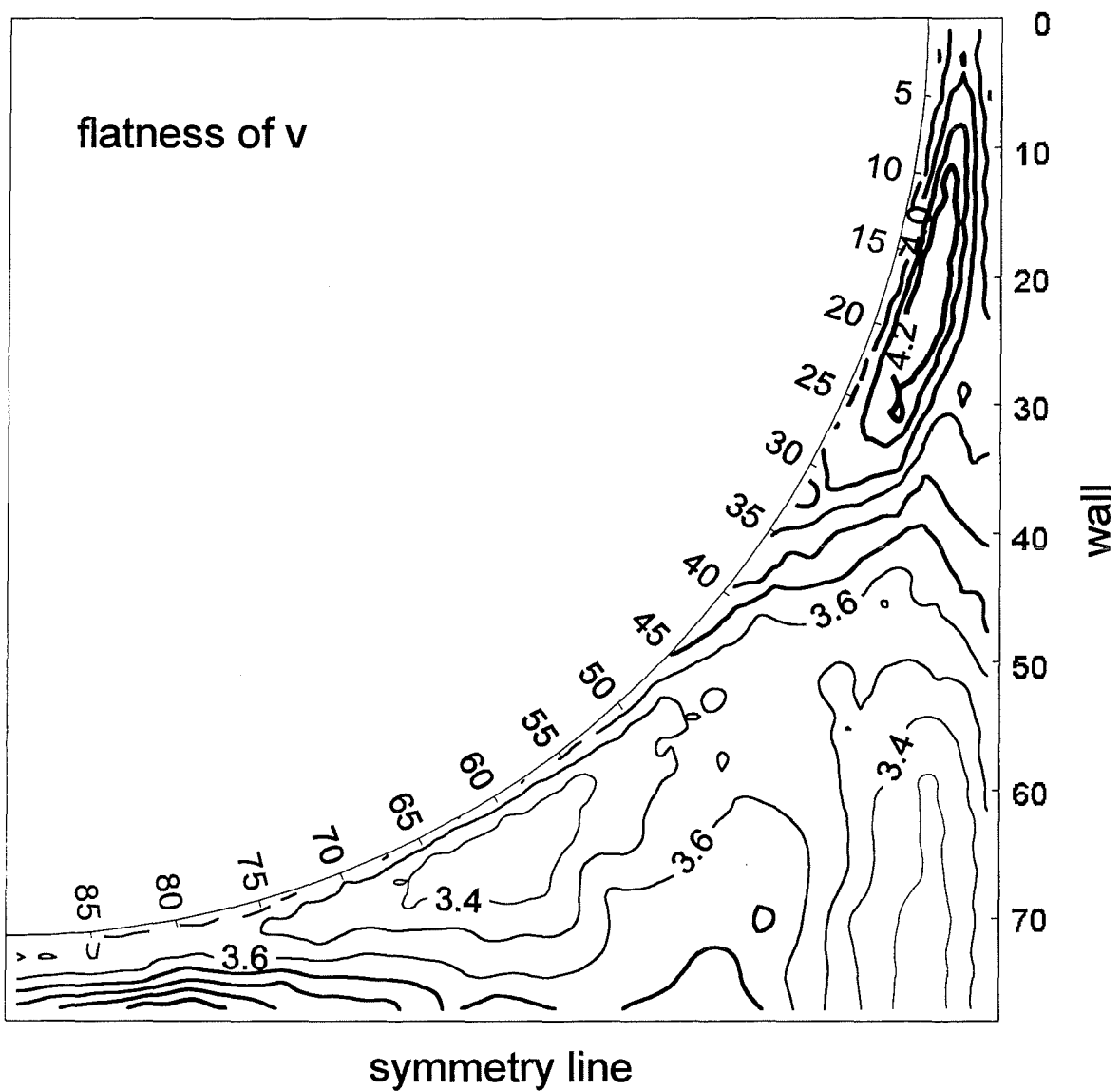


Fig. 68 Contour plot of the flatness of the radial velocity component

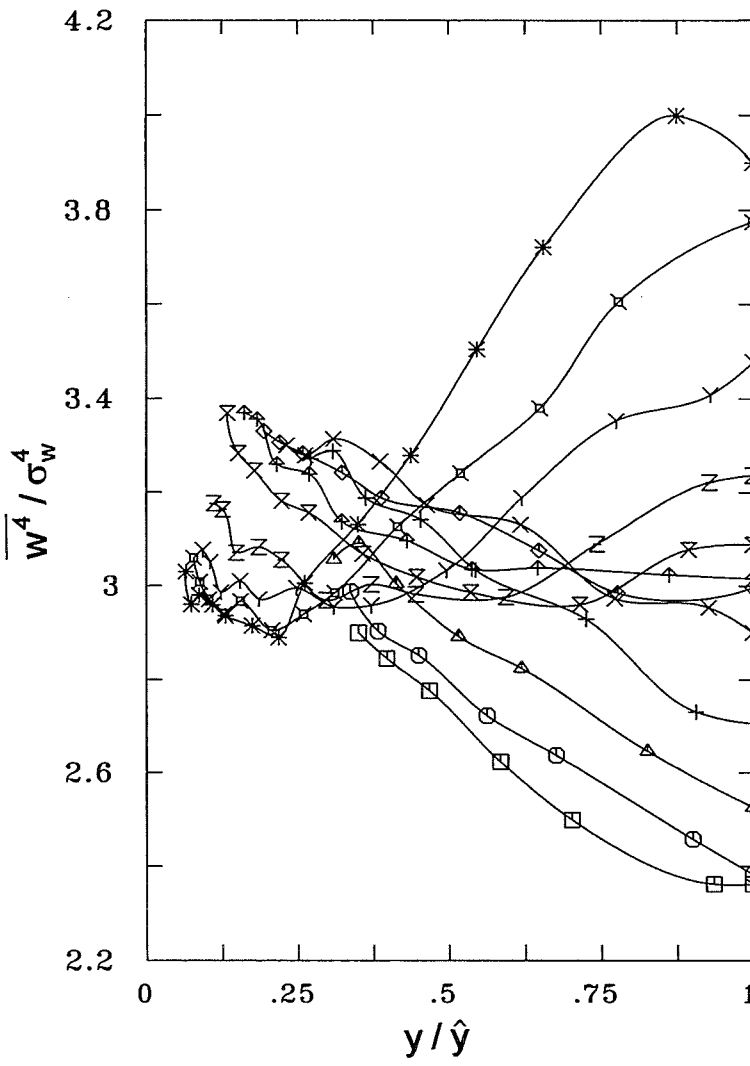
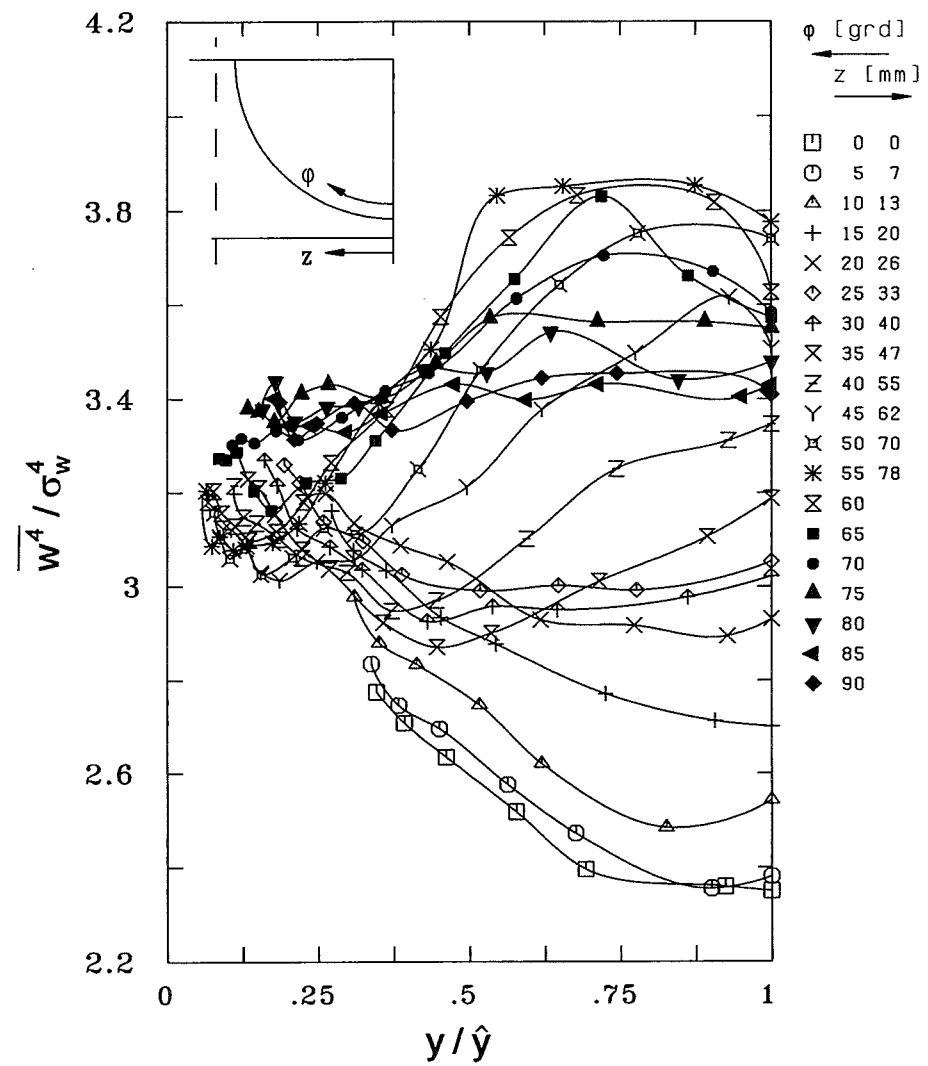


Fig. 69 Flatness of the azimuthal velocity component

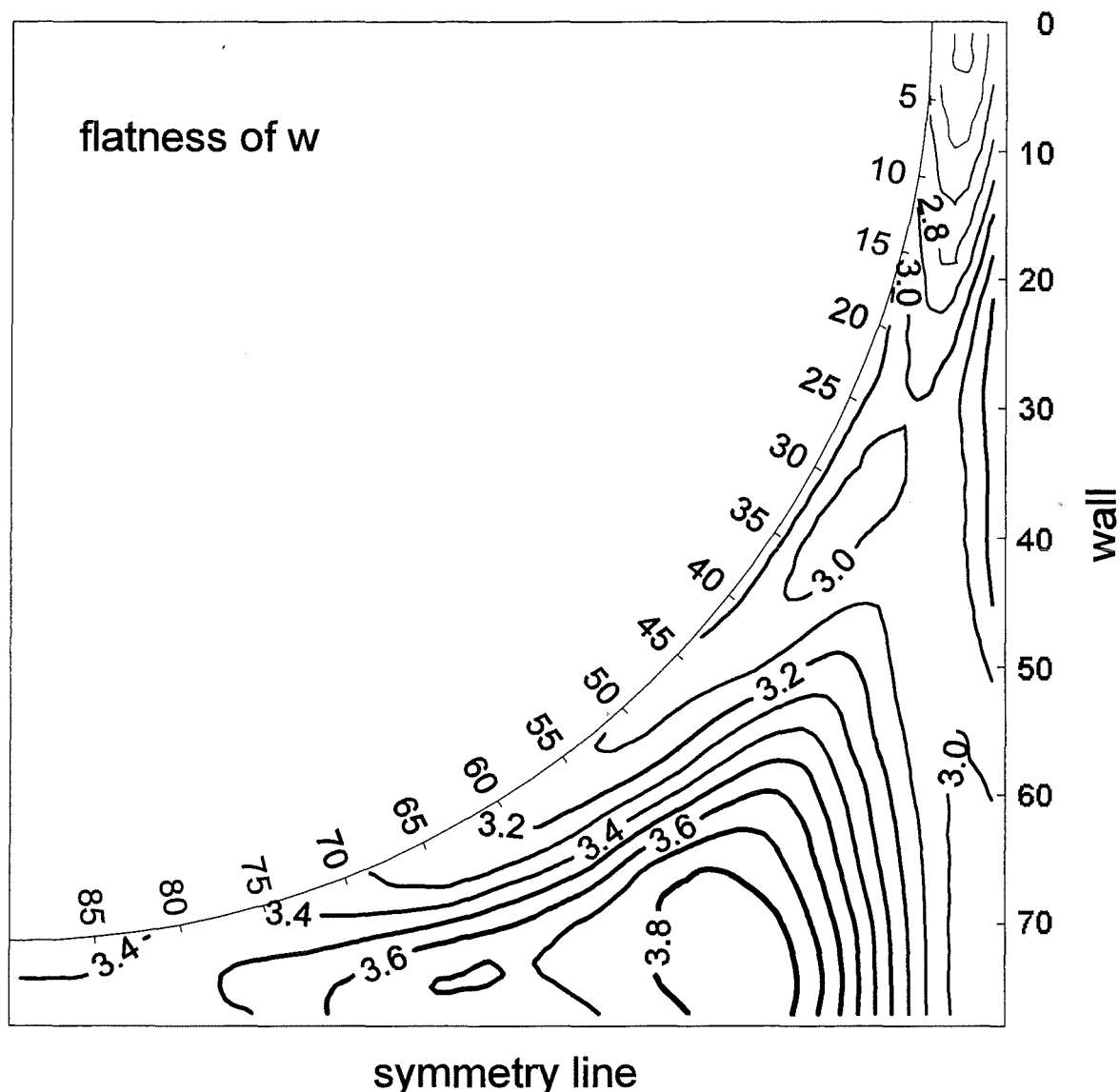


Fig. 70 Contour plot of the flatness of the azimuthal velocity component

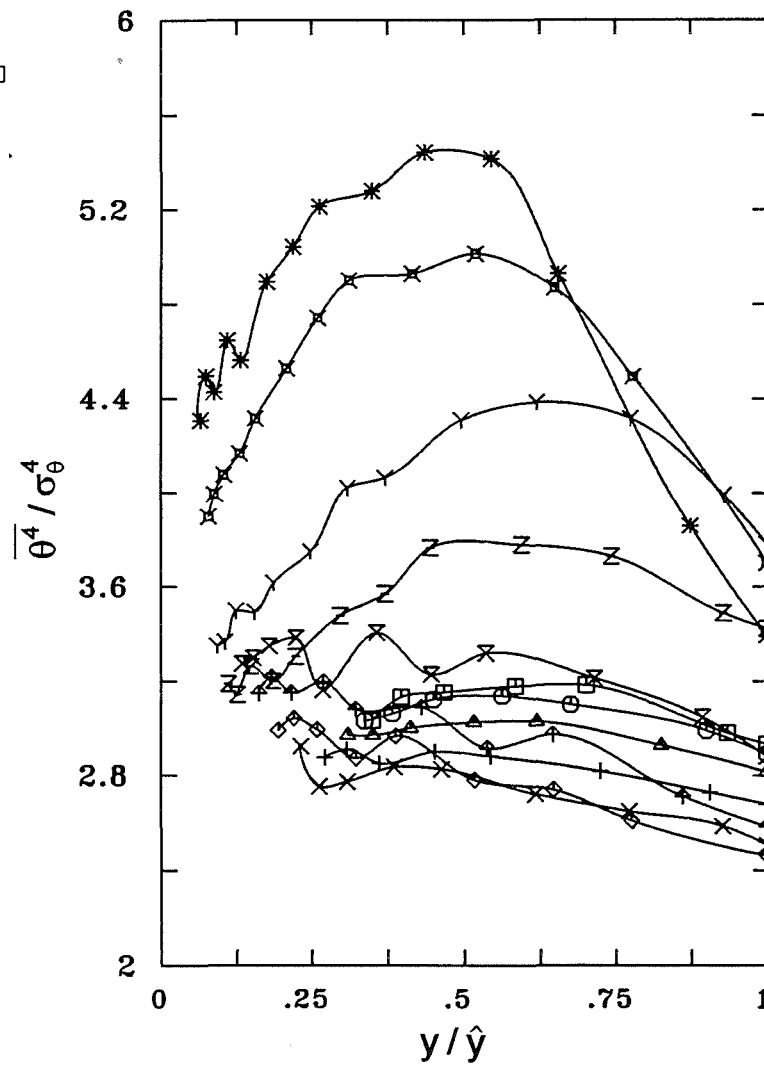
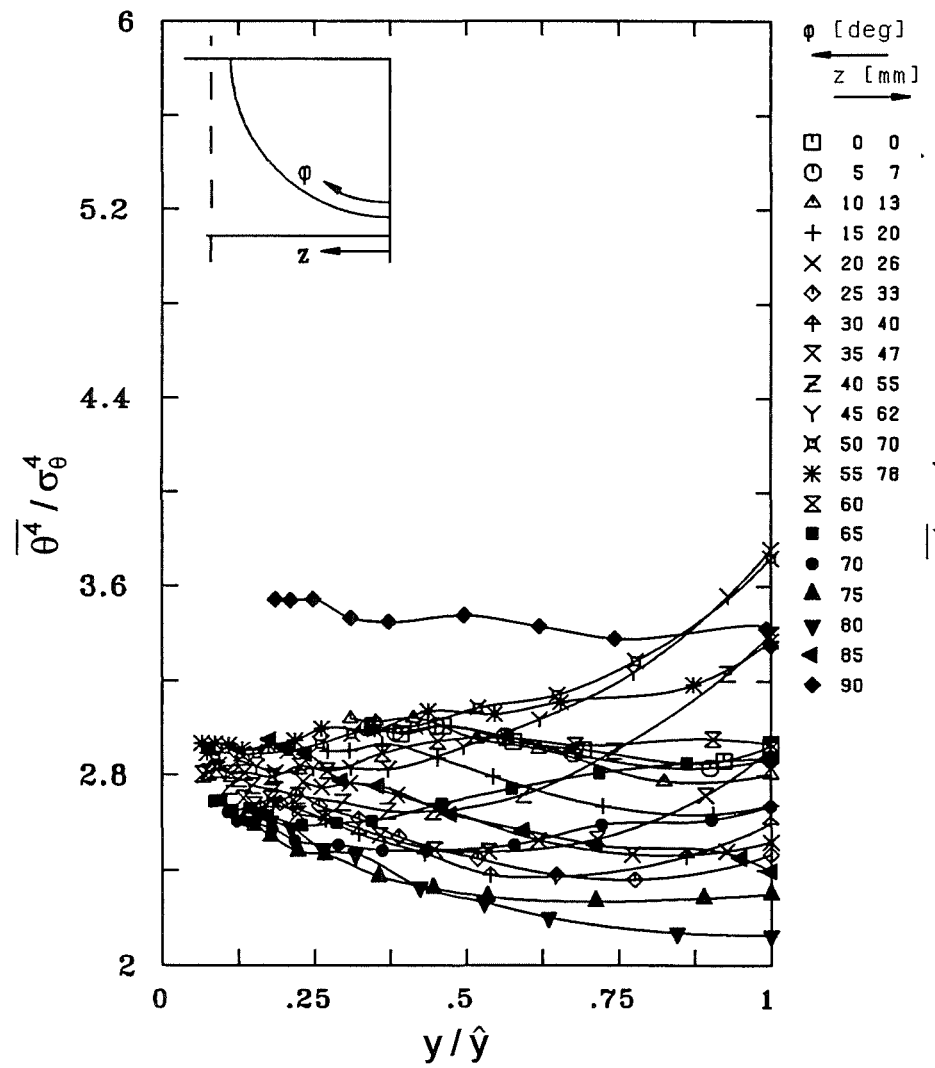


Fig. 71 Flatness of the temperature fluctuation

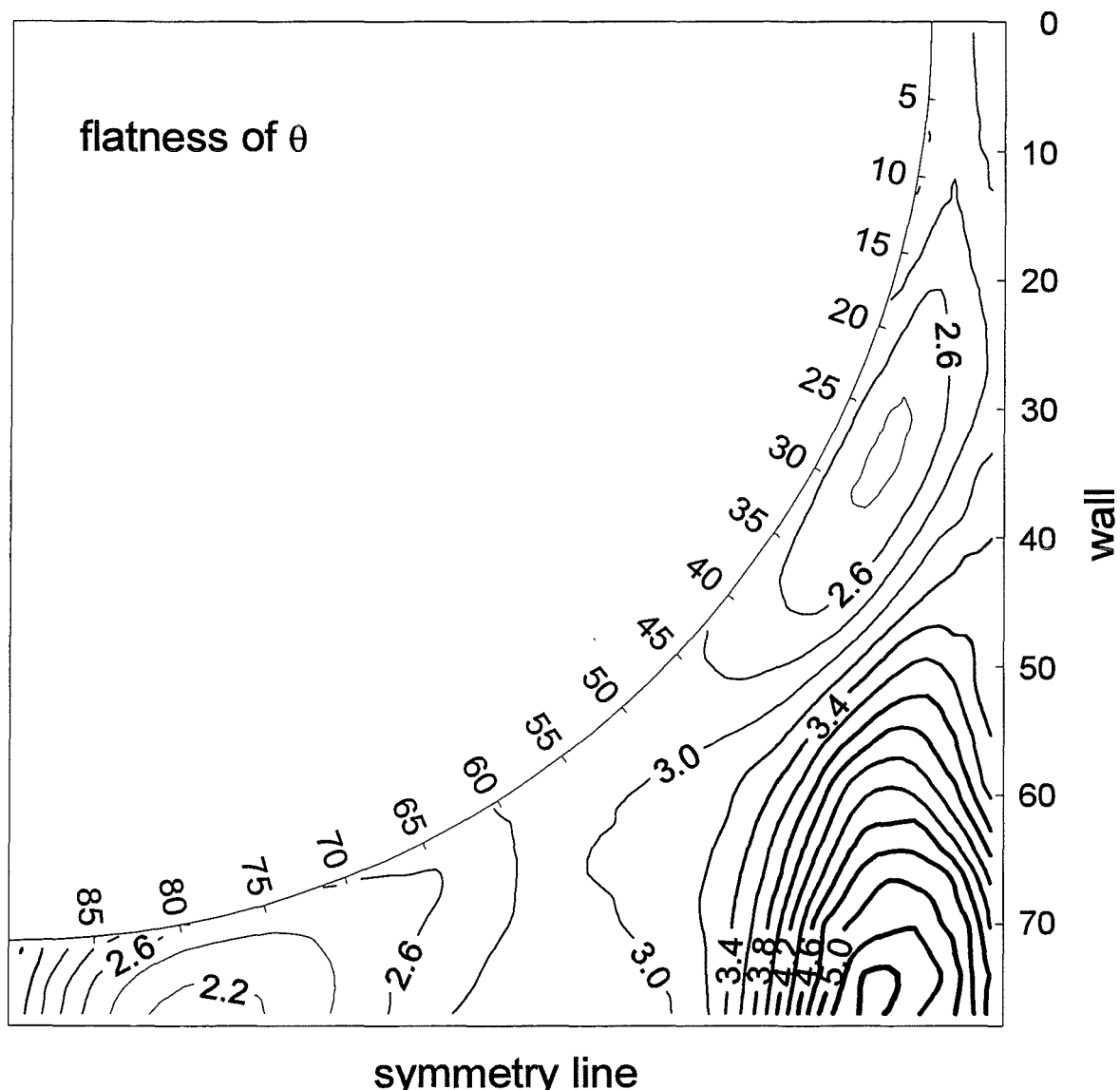


Fig. 72 Contour plot of the flatness of the temperature fluctuation

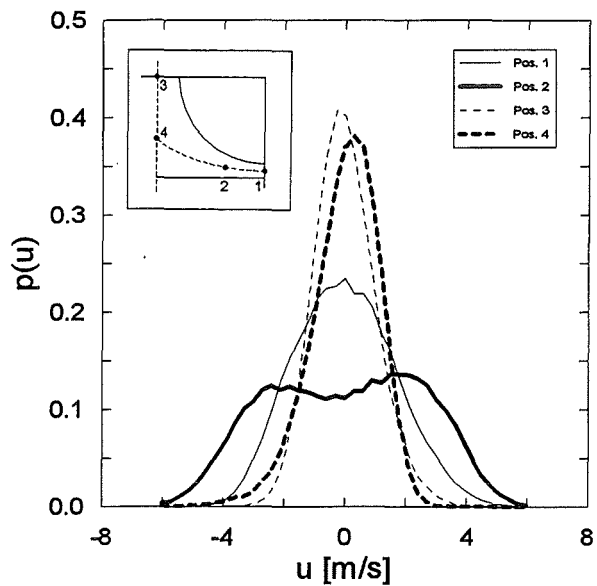


Fig. 73. Probability density function of the axial intensity.

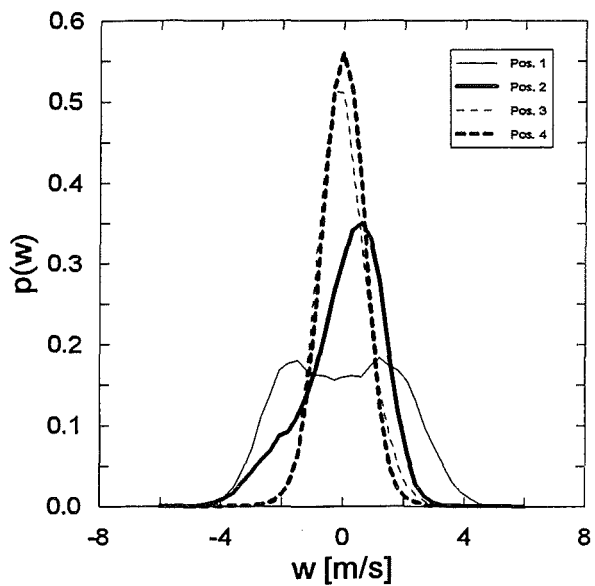


Fig. 74. Probability density function of the azimuthal intensity.

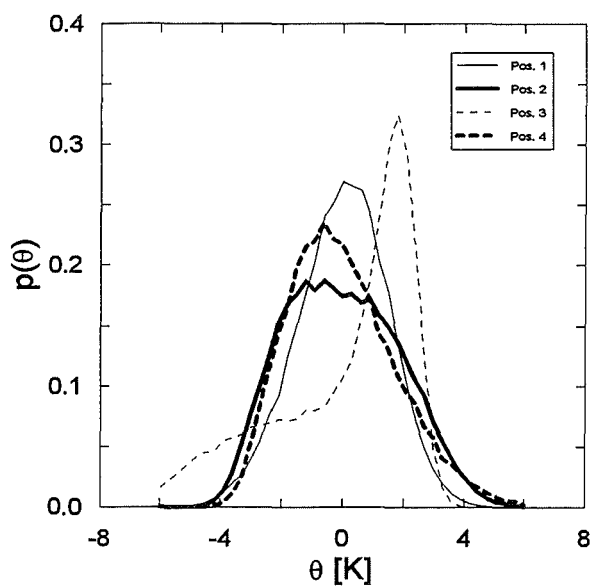


Fig. 75. Probability density function of the temperature fluctuation.

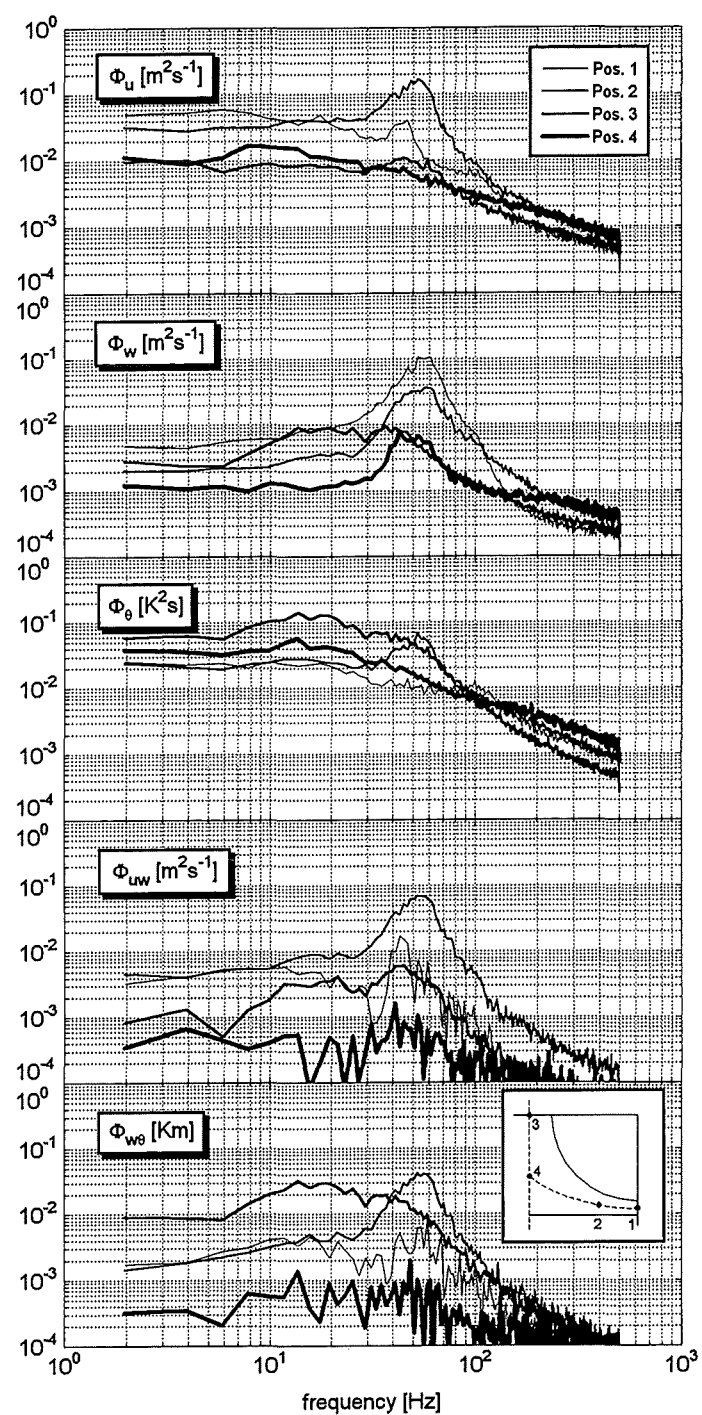


Fig. 76. Spectra of velocity and temperature fluctuations.

WALL SUBCHANNEL POSITION 0 mm
 Reference wall temperature $T_w = 48,65^\circ\text{C}$
 Local friction velocity $u^* = 0,933 \text{ m/s}$
 Average friction velocity $u^* = 1,019 \text{ m/s}$
 Average velocity in the wall cha $Ub = 19,4 \text{ m/s}$

REFERENCE: LOCAL REYNOLDS NUMBER = 65000
 Wall heat flux $q = 1,39 \text{ kW/m}^2$
 Local friction temperature $T^* = 1,298 \text{ K}$
 Average friction temperature $T^* = 1,193 \text{ K}$
 Average fluid temperature $T_b = 29,1^\circ\text{C}$

y/y _{max}	y +	U/Ub	U +	k +	u'/u*	v'/v*	w'/w*	u'v'/u ^{*2}	u'w'/u ^{*2}	-v'w'/u ^{*2}	S(u)	K(u)	S(v)	K(v)	S(w)	K(w)	eps _v	eps _w
0,351	91,000	0,755	15,490	3,620	1,950	0,747	1,697	0,476	-0,001	-0,132	0,092	2,875	-0,357	3,778	0,077	2,900	0,083	-
0,398	102,400	0,766	15,730	3,616	1,946	0,717	1,711	0,441	-0,031	-0,110	0,092	2,893	-0,336	3,861	0,086	2,845	0,086	-
0,468	119,600	0,782	16,040	3,583	1,933	0,694	1,717	0,408	-0,022	-0,158	0,115	2,896	-0,307	3,813	0,058	2,776	0,093	-
0,585	148,200	0,807	16,560	3,684	1,925	0,665	1,795	0,347	-0,042	-0,168	0,133	2,851	-0,304	3,847	0,041	2,623	0,099	-
0,702	176,800	0,821	16,850	3,669	1,901	0,639	1,820	0,271	-0,061	-0,198	0,143	2,887	-0,258	3,859	0,032	2,499	0,095	-
0,936	234,000	0,853	17,510	3,690	1,849	0,592	1,901	0,105	0,002	-0,233	0,162	2,804	-0,094	3,952	0,011	2,362	-	-
1,000	249,700	0,850	17,450	3,716	1,853	0,591	1,911	0,054	0,076	-0,228	0,164	2,810	0,015	4,080	-0,019	2,362	-	-

y/y _{max}	y +	(Tw-T)/(Tw-T _b)	T'/T*	-u'T'/u*T*	v'T'/u*T*	w'T'/u*T*	S(T)	K(T)	eptv	eptw	u'^2v'/u ^{*3}	u'^2w'/u ^{*3}	u'v'^2/u ^{*3}	v'^2w'/u ^{*3}	v'w'^2/u ^{*3}	u'v'w'/u ^{*3}	
0,351	91,000	1,092	0,812	0,511	0,056	-0,004	0,027	3,031	0,049	-	-0,171	0,440	-0,121	0,878	0,037	0,114	0,147
0,398	102,400	1,067	0,847	0,455	0,081	-0,049	0,115	3,131	0,060	-	-0,135	0,561	-0,088	0,815	0,031	0,134	0,082
0,468	119,600	1,063	0,894	0,468	0,093	-0,053	0,147	3,152	0,063	-	-0,119	0,526	-0,059	0,840	0,016	0,117	0,148
0,585	148,200	1,030	0,982	0,531	0,118	-0,039	0,189	3,178	0,069	-	-0,115	0,556	-0,042	1,035	0,033	0,117	0,124
0,702	176,800	1,009	1,061	0,584	0,150	-0,065	0,272	3,183	0,076	-	-0,154	0,715	-0,038	1,002	0,032	0,115	0,123
0,936	234,000	0,926	1,250	0,848	0,207	-0,092	0,259	2,979	-	-	-0,091	0,730	0,009	1,241	0,006	0,049	0,115
1,000	249,700	0,919	1,314	0,980	0,222	-0,064	0,224	2,931	-	-	-0,084	0,716	0,011	1,388	-0,005	0,013	0,077

TABLE I

WALL SUBCHANNEL POSITION 13 mm
 Reference wall temperature $T_w = 48,65^\circ\text{C}$
 Local friction velocity $u^* = 0,941 \text{ m/s}$
 Average friction velocity $u^* = 1,019 \text{ m/s}$
 Average velocity in the wall channel $Ub = 19,4 \text{ m/s}$

REFERENCE: LOCAL
 Wall heat flux
 Local friction temperature
 Average friction temperature
 Average fluid temperature

REYNOLDS NUMBER = 65000
 $q = 1,39 \text{ kW/m}^2$
 $T^* = 1,288 \text{ K}$
 $T^* = 1,193 \text{ K}$
 $T_b = 29,1^\circ\text{C}$

y/y _{max}	y +	U/Ub	U +	k +	u'/u*	v'/v*	w'/w*	u'v'/u ^{*2}	u'w'/u ^{*2}	-v'w'/u ^{*2}	S(u)	K(u)	S(v)	K(v)	S(w)	K(w)	eps _v	eps _w
0,310	91,700	0,761	15,500	3,561	2,042	0,760	1,542	0,540	0,883	-0,133	0,117	2,844	-0,315	3,796	0,201	3,057	0,115	11,594
0,351	103,200	0,769	15,650	3,604	2,053	0,752	1,558	0,532	0,860	-0,155	0,128	2,819	-0,276	3,754	0,231	3,092	0,115	9,969
0,413	120,500	0,787	16,020	3,607	2,044	0,727	1,583	0,504	0,937	-0,170	0,139	2,796	-0,233	3,835	0,220	3,005	0,112	26,367
0,516	149,300	0,805	16,390	3,633	2,045	0,701	1,611	0,478	1,112	-0,204	0,158	2,741	-0,169	3,829	0,204	2,892	0,114	16,847
0,620	178,200	0,827	16,840	3,656	2,041	0,678	1,639	0,436	1,211	-0,257	0,135	2,715	-0,146	3,927	0,265	2,824	0,116	15,901
0,826	235,800	0,856	17,430	3,711	2,010	0,643	1,723	0,321	1,443	-0,365	0,140	2,643	0,007	4,026	0,311	2,646	-	13,540
1,000	284,400	0,875	17,820	3,730	1,997	0,643	1,748	0,221	1,504	-0,415	0,149	2,591	0,243	4,170	0,303	2,526	-	-

y/y _{max}	y +	(Tw-T)/ (Tw-T _b)	T'/T*	-u'T'/ u*T*	v'T'/ u*T*	w'T'/ u*T*	S(T)	K(T)	ept _v	ept _w	u'v'/ u ^{*3}	u'w'/ u ^{*3}	u'v' ² / u ^{*3}	u'v' ² / u ^{*3}	v'w'/ u ^{*3}	v'w' ² / u ^{*3}	u'v'w'/ u ^{*3}
0,310	91,700	1,107	0,835	0,580	0,040	0,308	-0,051	2,970	0,045	3,365	0,009	-0,934	-0,077	0,316	0,032	0,073	0,154
0,351	103,200	1,082	0,870	0,583	0,051	0,300	0,034	2,968	0,050	2,383	0,020	-0,934	-0,053	0,377	0,000	0,066	0,161
0,413	120,500	1,065	0,912	0,624	0,053	0,345	0,022	2,999	0,049	2,741	0,098	-1,048	-0,016	0,356	0,017	0,054	0,164
0,516	149,300	1,051	0,981	0,677	0,073	0,401	0,062	3,023	0,056	2,236	0,090	-1,147	0,013	0,370	0,046	0,027	0,167
0,620	178,200	1,030	1,062	0,743	0,082	0,424	0,124	3,027	0,056	2,268	0,087	-1,025	0,023	0,301	0,023	0,018	0,157
0,826	235,800	0,992	1,231	0,952	0,113	0,557	0,169	2,926	-	2,029	0,106	-1,001	0,066	0,243	0,048	-0,067	0,120
1,000	284,400	0,922	1,411	1,300	0,133	0,619	0,076	2,815	-	-	0,165	-0,850	0,101	0,336	0,046	-0,138	0,077

TABLE I cont.

WALL SUBCHANNEL POSITION 26 mm
 Reference wall temperature $T_w = 48,65^\circ\text{C}$
 Local friction velocity $u^* = 0,943 \text{ m/s}$
 Average friction velocity $u^* = 1,019 \text{ m/s}$
 Average velocity in the wall cha $U_b = 19,4 \text{ m/s}$

REFERENCE: LOCAL
 Wall heat flux $q = 1,39 \text{ kW/m}^2$
 Local friction temperature $T^* = 1,285 \text{ K}$
 Average friction temperature $T^* = 1,193 \text{ K}$
 Average fluid temperature $T_b = 29,1^\circ\text{C}$

REYNOLDS NUMBER = 65000

y/y _{max}	y +	U/U _b	U +	k +	u'/u*	v'/v*	w'/w*	u'v'/u ^{*2}	u'w'/u ^{*2}	-v'w'/u ^{*2}	S(u)	K(u)	S(v)	K(v)	S(w)	K(w)	eps _v	eps _w
0,232	91,900	0,771	15,660	3,832	2,301	0,810	1,308	0,633	1,013	-0,089	0,213	2,766	-0,305	3,916	0,070	3,299	0,085	5,544
0,263	103,500	0,783	15,900	3,862	2,319	0,794	1,310	0,634	1,045	-0,107	0,234	2,744	-0,234	3,886	0,078	3,278	0,089	3,678
0,309	120,800	0,802	16,280	3,885	2,313	0,780	1,346	0,637	1,145	-0,124	0,253	2,722	-0,176	3,914	0,116	3,313	0,095	3,844
0,386	149,700	0,824	16,730	4,002	2,357	0,768	1,364	0,643	1,300	-0,140	0,250	2,634	-0,141	3,911	0,101	3,265	0,106	4,685
0,464	178,600	0,843	17,130	4,051	2,369	0,752	1,387	0,637	1,481	-0,180	0,240	2,598	-0,111	3,938	0,145	3,173	0,118	4,974
0,618	236,400	0,880	17,870	4,164	2,393	0,728	1,440	0,630	1,777	-0,252	0,208	2,462	-0,065	3,931	0,226	3,131	0,155	4,955
0,773	294,200	0,907	18,420	4,178	2,388	0,716	1,464	0,599	1,993	-0,327	0,203	2,388	0,108	4,038	0,321	2,973	0,217	5,454
0,927	352,000	0,924	18,760	4,195	2,359	0,718	1,521	0,540	2,209	-0,378	0,180	2,357	0,241	4,026	0,407	2,954	-	5,267
1,000	379,200	0,928	18,850	4,278	2,379	0,729	1,538	0,515	2,259	-0,471	0,174	2,350	0,326	4,012	0,425	2,901	-	-

y/y _{max}	y +	(T _w -T)/ (T _w -T _b)	T'/T*	-u'T'/ u*T*	v'T'/ u*T*	w'T'/ u*T*	S(T)	K(T)	eptv	eptw	u'v'/ u ^{*3}	u'w'/ u ^{*3}	u'v' ² / u ^{*3}	u'v' ² / u ^{*3}	v'w'/ u ^{*3}	v'w' ² / u ^{*3}	u'v'w'/ u ^{*3}
0,232	91,900	1,139	0,868	0,780	0,027	0,395	0,081	2,922	0,045	1,682	0,141	-0,841	-0,035	0,249	-0,001	0,041	0,133
0,263	103,500	1,138	0,883	0,802	0,021	0,396	0,059	2,753	0,040	1,436	0,236	-0,838	0,011	0,208	-0,022	0,019	0,164
0,309	120,800	1,127	0,922	0,821	0,025	0,481	0,083	2,774	0,041	1,519	0,297	-0,817	0,060	0,041	-0,021	0,031	0,152
0,386	149,700	1,118	0,987	0,939	0,024	0,524	0,111	2,835	0,039	1,603	0,333	-0,915	0,092	0,094	-0,046	-0,018	0,130
0,464	178,600	1,112	1,042	0,991	0,028	0,561	0,158	2,826	0,039	1,802	0,344	-0,934	0,122	-0,078	-0,043	-0,045	0,125
0,618	236,400	1,087	1,167	1,218	0,025	0,723	0,217	2,721	0,034	1,706	0,264	-0,625	0,126	-0,385	-0,042	-0,108	0,063
0,773	294,200	1,053	1,315	1,436	0,028	0,866	0,210	2,649	0,032	1,437	0,283	-0,427	0,189	-0,741	-0,026	-0,211	-0,060
0,927	352,000	0,999	1,453	1,658	0,042	0,983	0,199	2,587	-	1,318	0,246	-0,077	0,211	-0,933	-0,012	-0,279	-0,193
1,000	379,200	0,966	1,537	1,855	0,035	1,018	0,150	2,506	-	-	0,275	0,086	0,211	-1,034	-0,014	-0,306	-0,233

TABLE I cont.

WALL SUBCHANNEL POSITION 40 mm
 Reference wall temperature $T_w = 48,65^\circ\text{C}$
 Local friction velocity $u^* = 0,985 \text{ m/s}$
 Average friction velocity $u^* = 1,019 \text{ m/s}$
 Average velocity in the wall cha $Ub = 19,4 \text{ m/s}$

REFERENCE: LOCAL
 Wall heat flux
 Local friction temperature
 Average friction temperature
 Average fluid temperature

REYNOLDS NUMBER = 65000
 $q = 1,39 \text{ kW/m}^2$
 $T^* = 1,230 \text{ K}$
 $T^* = 1,193 \text{ K}$
 $T_b = 29,1^\circ\text{C}$

y/ymax	y +	U/Ub	U +	k +	u'/u*	v'/v*	w'/w*	u'v'/ u ^{*2}	u'w'/ u ^{*2}	-v'w'/ u ^{*2}	S(u)	K(u)	S(v)	K(v)	S(w)	K(w)	epsv	epsw
0,162	95,900	0,812	15,800	3,809	2,272	0,836	1,326	0,649	0,611	-0,062	0,102	2,724	-0,312	3,944	0,106	3,369	0,052	0,822
0,183	108,000	0,826	16,070	3,845	2,294	0,823	1,323	0,638	0,694	-0,063	0,116	2,720	-0,248	3,943	0,084	3,355	0,056	1,066
0,215	126,100	0,842	16,370	3,878	2,302	0,813	1,341	0,658	0,778	-0,064	0,117	2,677	-0,190	3,825	0,040	3,259	0,066	1,046
0,269	156,300	0,867	16,860	3,886	2,307	0,804	1,343	0,643	0,795	-0,073	0,130	2,642	-0,171	3,887	0,038	3,238	0,078	0,983
0,323	186,400	0,891	17,330	3,967	2,342	0,805	1,343	0,670	0,908	-0,063	0,119	2,560	-0,135	3,846	0,007	3,138	0,096	1,285
0,431	246,800	0,925	18,000	3,993	2,361	0,788	1,338	0,649	1,074	-0,069	0,096	2,459	-0,096	3,829	0,004	3,097	0,120	1,604
0,539	307,100	0,947	18,420	4,095	2,400	0,784	1,347	0,648	1,303	-0,114	0,060	2,371	-0,061	3,808	0,030	3,036	0,142	1,507
0,646	367,500	0,973	18,930	4,187	2,447	0,779	1,334	0,657	1,481	-0,157	0,047	2,265	-0,015	3,779	0,078	3,039	0,170	1,448
0,862	488,100	1,009	19,630	4,432	2,528	0,788	1,361	0,664	1,890	-0,280	-0,029	2,135	0,162	3,698	0,241	3,024	-	1,799
1,000	565,700	1,017	19,790	4,540	2,576	0,813	1,335	0,653	2,069	-0,354	-0,076	2,096	0,262	3,774	0,322	3,016	-	-
y/ymax	y +	(Tw-T)/ (Tw-Tb)	T'/T*	-u'T'/ u*T*	v'T'/ u*T*	w'T'/ u*T*	S(T)	K(T)	eptv	eptw	u'v'/ u ^{*3}	u'w'/ u ^{*3}	u'v' ² / u ^{*3}	u'v' ² / u ^{*3}	v'w'/ u ^{*3}	v'w'/ u ^{*3}	u'v'w'/ u ^{*3}	
0,162	95,900	1,197	0,872	0,742	0,012	0,385	0,416	3,149	0,039	0,915	0,110	0,104	-0,061	0,483	0,074	0,073	0,095	
0,183	108,000	1,197	0,904	0,779	0,018	0,405	0,455	3,216	0,043	0,855	0,096	0,025	-0,013	0,473	0,048	0,054	0,107	
0,215	126,100	1,205	0,927	0,816	0,018	0,443	0,444	3,151	0,042	0,828	0,174	0,138	0,017	0,438	0,054	0,048	0,113	
0,269	156,300	1,203	0,989	0,872	0,030	0,518	0,546	3,197	0,049	0,996	0,190	0,153	0,046	0,369	0,023	0,037	0,118	
0,323	186,400	1,186	1,036	0,966	0,022	0,548	0,546	3,080	0,042	1,103	0,218	0,191	0,091	0,263	0,040	0,013	0,081	
0,431	246,800	1,183	1,126	1,130	0,035	0,638	0,640	3,088	0,048	1,017	0,194	0,629	0,114	0,031	-0,009	-0,015	0,074	
0,539	307,100	1,170	1,241	1,384	0,034	0,782	0,687	2,914	0,043	0,993	0,130	0,997	0,139	-0,275	-0,038	-0,067	-0,021	
0,646	367,500	1,156	1,330	1,511	0,040	0,826	0,801	2,972	0,044	0,893	0,002	1,100	0,134	-0,520	-0,076	-0,106	-0,083	
0,862	488,100	1,101	1,543	1,974	0,032	1,071	0,838	2,712	-	0,859	-0,186	2,142	0,160	-1,323	-0,052	-0,253	-0,371	
1,000	565,700	1,067	1,686	2,366	0,015	1,154	0,802	2,585	-	-	-0,309	2,498	0,156	-1,504	-0,040	-0,288	-0,524	

TABLE I cont.

WALL SUBCHANNEL
 Reference wall temperature $T_w = 48,65^\circ\text{C}$
 Local friction velocity $u^* = 1,056 \text{ m/s}$
 Average friction velocity $u^* = 1,019 \text{ m/s}$
 Average velocity in the wall cha $U_b = 19,4 \text{ m/s}$

POSITION 55 mm
 Wall heat flux $q = 1,39 \text{ kW/m}^2$
 Local friction temperature $T^* = 1,148 \text{ K}$
 Average friction temperature $T^* = 1,193 \text{ K}$
 Average fluid temperature $T_b = 29,1^\circ\text{C}$

REFERENCE: LOCAL
REYNOLDS NUMBER = 65000

y/y_{max}	$y +$	U/U_b	$U +$	$k +$	u'/u^*	v'/v^*	w'/w^*	$u'v'/u^{*2}$	$u'w'/u^{*2}$	$-v'w'/u^{*2}$	$S(u)$	$K(u)$	$S(v)$	$K(v)$	$S(w)$	$K(w)$	ϵ_{psv}	ϵ_{psw}
0,112	101,700	0,869	15,940	3,707	2,089	0,848	1,527	0,681	0,334	-0,076	-0,011	2,782	-0,299	3,681	0,116	3,176	0,040	0,328
0,126	114,500	0,885	16,250	3,760	2,098	0,842	1,552	0,660	0,429	-0,053	-0,014	2,770	-0,261	3,732	0,069	3,163	0,041	0,422
0,149	133,700	0,899	16,500	3,729	2,077	0,843	1,560	0,660	0,433	-0,040	-0,016	2,777	-0,210	3,610	0,085	3,071	0,045	0,455
0,186	165,600	0,930	17,070	3,734	2,094	0,840	1,542	0,665	0,444	-0,023	-0,020	2,731	-0,152	3,539	0,063	3,083	0,053	0,460
0,223	197,600	0,950	17,450	3,716	2,086	0,846	1,538	0,674	0,414	-0,022	-0,048	2,730	-0,152	3,531	0,053	3,056	0,063	0,402
0,297	261,600	0,988	18,130	3,669	2,061	0,854	1,537	0,631	0,491	0,008	-0,072	2,726	-0,134	3,509	0,056	2,969	0,077	0,438
0,372	325,500	1,019	18,710	3,588	2,049	0,853	1,501	0,603	0,504	0,013	-0,094	2,675	-0,134	3,462	0,034	3,003	0,092	0,413
0,446	389,500	1,047	19,220	3,572	2,064	0,860	1,464	0,592	0,619	0,041	-0,139	2,597	-0,127	3,507	0,038	2,982	0,109	0,502
0,595	517,400	1,080	19,820	3,528	2,100	0,841	1,392	0,521	0,762	0,012	-0,227	2,505	-0,079	3,463	0,058	2,976	0,129	-
0,743	645,300	1,109	20,360	3,526	2,162	0,834	1,297	0,486	0,917	-0,042	-0,351	2,486	-0,072	3,462	0,126	3,090	0,165	-
0,929	805,200	1,132	20,780	3,654	2,255	0,835	1,235	0,478	1,170	-0,135	-0,489	2,529	0,036	3,536	0,234	3,221	-	-
1,000	866,200	1,139	20,910	3,619	2,258	0,840	1,196	0,451	1,190	-0,169	-0,540	2,576	0,079	3,471	0,261	3,236	-	-

y/y_{max}	$y +$	$(T_w-T)/(T_w-T_b)$	T'/T^*	$-u'T'/u^*T^*$	$v'T'/u^*T^*$	$w'T'/u^*T^*$	$S(T)$	$K(T)$	ϵ_{ptv}	ϵ_{ptw}	u'^2v'/u^{*3}	u'^2w'/u^{*3}	$u'v'^2/u^{*3}$	$u'v'^2/u^{*3}$	v'^2w'/u^{*3}	$v'w'^2/u^{*3}$	$u'v'w'/u^{*3}$
0,112	101,700	1,285	0,842	0,410	0,005	0,407	0,540	3,188	0,036	0,666	-0,142	0,004	-0,177	0,383	0,061	0,049	0,091
0,126	114,500	1,259	0,873	0,438	0,014	0,444	0,531	3,143	0,043	0,675	-0,141	0,098	-0,148	0,441	0,060	0,035	0,082
0,149	133,700	1,272	0,888	0,428	0,014	0,464	0,609	3,263	0,043	0,745	-0,064	0,112	-0,107	0,333	0,036	0,045	0,099
0,186	165,600	1,271	0,938	0,485	0,028	0,484	0,643	3,201	0,052	0,711	-0,124	0,226	-0,081	0,305	0,048	0,034	0,120
0,223	197,600	1,271	0,983	0,538	0,037	0,541	0,743	3,305	0,058	0,768	-0,162	0,275	-0,088	0,149	0,035	0,033	0,084
0,297	261,600	1,274	1,035	0,593	0,058	0,605	0,850	3,478	0,070	0,746	-0,153	0,516	-0,099	-0,037	0,026	0,010	0,091
0,372	325,500	1,255	1,120	0,775	0,064	0,658	0,995	3,570	0,071	0,737	-0,145	0,556	-0,094	-0,059	0,024	0,010	0,106
0,446	389,500	1,272	1,163	0,849	0,081	0,699	1,110	3,764	0,079	0,708	-0,203	0,829	-0,124	-0,342	0,015	-0,001	0,086
0,595	517,400	1,251	1,288	1,132	0,100	0,768	1,295	3,777	0,082	-	-0,122	1,476	-0,098	-0,572	-0,003	-0,026	0,065
0,743	645,300	1,239	1,427	1,406	0,104	0,799	1,446	3,728	0,076	-	-0,260	2,109	-0,124	-0,958	-0,002	-0,076	-0,062
0,929	805,200	1,193	1,610	1,760	0,116	0,895	1,531	3,490	-	-	-0,590	2,826	-0,181	-1,262	-0,005	-0,156	-0,267
1,000	866,200	1,189	1,672	1,889	0,125	0,857	1,512	3,425	-	-	-0,655	2,853	-0,191	-1,252	0,019	-0,184	-0,377

TABLE I cont.

WALL SUBCHANNEL
 Reference wall temperature $T_w = 48,65^\circ\text{C}$
 Local friction velocity $u^* = 1,085 \text{ m/s}$
 Average friction velocity $u^* = 1,019 \text{ m/s}$
 Average velocity in the wall channel $U_b = 19,4 \text{ m/s}$
POSITION 70 mm
 Wall heat flux $q = 1,39 \text{ kW/m}^2$
 Local friction temperature $T^* = 1,117 \text{ K}$
 Average friction temperature $T^* = 1,193 \text{ K}$
 Average fluid temperature $T_b = 29,1^\circ\text{C}$
REFERENCE: LOCAL
REYNOLDS NUMBER = 65000

y/y _{max}	y +	U/U _b	U +	k +	u'/u*	v'/v*	w'/w*	u'v'/u ^{*2}	u'w'/u ^{*2}	-v'w'/u ^{*2}	S(u)	K(u)	S(v)	K(v)	S(w)	K(w)	eps _v	eps _w
0,078	105,900	0,910	16,030	3,810	2,024	0,849	1,674	0,683	0,069	-0,119	0,041	2,762	-0,301	3,677	0,058	3,060	0,031	0,198
0,088	119,300	0,923	16,260	3,807	2,016	0,848	1,682	0,681	0,102	-0,116	0,046	2,740	-0,254	3,607	0,043	3,008	0,033	0,209
0,104	139,300	0,940	16,560	3,859	2,031	0,853	1,694	0,723	0,102	-0,091	0,013	2,727	-0,207	3,618	-0,004	2,971	0,037	0,217
0,130	172,600	0,968	17,050	3,835	2,013	0,854	1,700	0,712	0,137	-0,077	0,002	2,713	-0,153	3,420	-0,001	2,940	0,041	0,280
0,156	205,900	0,991	17,450	3,787	2,005	0,863	1,675	0,733	0,135	-0,062	-0,021	2,720	-0,123	3,437	0,006	2,967	0,048	0,242
0,208	272,500	1,032	18,180	3,701	1,975	0,870	1,656	0,731	0,174	-0,049	-0,078	2,706	-0,095	3,292	0,020	2,905	0,059	0,331
0,260	339,100	1,063	18,740	3,502	1,915	0,880	1,600	0,698	0,140	0,003	-0,122	2,727	-0,126	3,342	0,016	2,939	0,069	0,222
0,312	405,800	1,093	19,250	3,355	1,876	0,890	1,549	0,693	0,138	0,006	-0,172	2,746	-0,114	3,273	0,045	2,985	0,082	-
0,416	539,000	1,135	20,000	2,977	1,774	0,878	1,427	0,613	0,179	0,010	-0,260	2,793	-0,138	3,318	0,081	3,127	0,098	-
0,519	672,300	1,168	20,570	2,666	1,691	0,857	1,317	0,536	0,180	0,022	-0,333	2,826	-0,146	3,337	0,090	3,240	0,105	-
0,649	838,900	1,203	21,190	2,353	1,616	0,824	1,191	0,432	0,242	0,002	-0,506	3,053	-0,227	3,477	0,155	3,379	0,107	-
0,779	1005,400	1,224	21,570	2,133	1,569	0,788	1,087	0,332	0,317	-0,027	-0,706	3,483	-0,197	3,562	0,219	3,605	0,113	-
1,000	1289,000	1,254	22,080	1,869	1,502	0,754	0,957	0,201	0,370	-0,089	-0,961	4,290	-0,102	3,658	0,304	3,775	-	-

y/y _{max}	y +	(Tw-T)/(Tw-T _b)	T'/T*	-u'T'/u*T*	v'T'/u*T*	w'T'/u*T*	S(T)	K(T)	eptv	eptw	u'v'/u ^{*3}	u'w'/u ^{*3}	u'v' ² /u ^{*3}	u'v' ² /u ^{*3}	v'w'/u ^{*3}	v'w' ² /u ^{*3}	u'v'w'/u ^{*3}
0,078	105,900	1,299	0,725	0,098	-0,020	0,310	0,623	3,898	0,017	0,521	-0,213	-0,121	-0,196	0,425	0,025	0,060	0,133
0,088	119,300	1,334	0,739	0,078	-0,015	0,332	0,658	3,993	0,021	0,575	-0,176	-0,267	-0,161	0,413	0,015	0,042	0,127
0,104	139,300	1,322	0,752	0,069	-0,018	0,334	0,695	4,075	0,019	0,619	-0,189	-0,177	-0,143	0,418	0,024	0,037	0,108
0,130	172,600	1,338	0,782	0,075	-0,006	0,349	0,753	4,165	0,028	0,623	-0,196	-0,169	-0,125	0,366	0,015	0,018	0,122
0,156	205,900	1,336	0,820	0,092	-0,005	0,353	0,823	4,313	0,028	0,447	-0,214	-0,108	-0,110	0,211	0,018	0,022	0,098
0,208	272,500	1,334	0,863	0,095	0,017	0,391	0,929	4,527	0,044	0,544	-0,322	0,010	-0,132	-0,024	0,021	0,006	0,068
0,260	339,100	1,341	0,900	0,140	0,024	0,376	1,035	4,742	0,048	0,613	-0,365	0,047	-0,182	-0,200	0,022	0,005	0,067
0,312	405,800	1,335	0,930	0,147	0,040	0,384	1,101	4,900	0,058	-	-0,407	0,067	-0,194	-0,362	0,025	0,000	0,073
0,416	539,000	1,346	0,989	0,172	0,083	0,336	1,183	4,929	0,084	-	-0,478	0,076	-0,246	-0,555	0,015	-0,006	0,084
0,519	672,300	1,349	1,049	0,178	0,118	0,293	1,286	5,014	0,100	-	-0,399	0,236	-0,275	-0,555	0,044	-0,005	0,081
0,649	838,900	1,321	1,177	0,249	0,154	0,301	1,433	4,871	0,111	-	-0,387	0,500	-0,298	-0,574	0,029	-0,003	0,062
0,779	1005,400	1,319	1,323	0,317	0,214	0,290	1,506	4,493	0,131	-	-0,344	0,804	-0,292	-0,654	0,033	-0,045	-0,004
1,000	1289,000	1,252	1,595	0,531	0,289	0,207	1,421	3,701	-	-	-0,353	1,001	-0,278	-0,574	0,045	-0,091	-0,116

TABLE I cont.

WALL SUBCHANNEL
 Reference wall temperature
 $T_w = 48,65^\circ\text{C}$
 Local friction velocity
 $u^* = 0,951 \text{ m/s}$
 Average friction velocity
 $u^* = 1,019 \text{ m/s}$
 Average velocity in the wall chan
 $Ub = 19,4 \text{ m/s}$

ANGULAR POSITION 0°

REFERENCE: LOCAL
 Wall heat flux
 $q = 1,39 \text{ kW/m}^2$
 Local friction temperature
 $T^* = 1,274 \text{ K}$
 Average friction temperature
 $T^* = 1,193 \text{ K}$
 Average fluid temperature
 $T_b = 29,1^\circ\text{C}$

REYNOLDS NUMBER = 65000
 $Re = 65000$
 $Re = 65000$
 $Re = 65000$
 $Re = 65000$

y/y _{max}	y +	U/Ub	U +	k +	u'/u*	v'/v*	w'/w*	u'v'/ u ^{*2}	u'w'/ u ^{*2}	-v'w'/ u ^{*2}	S(u)	K(u)	S(v)	K(v)	S(w)	K(w)	eps _v	eps _w
0,346	92,700	0,777	15,640	3,782	1,960	0,761	1,773	0,476	0,020	-0,179	0,129	2,881	-0,297	3,748	-0,097	2,775	-	-
0,393	104,400	0,782	15,750	3,767	1,948	0,732	1,789	0,445	-0,018	-0,172	0,112	2,877	-0,311	3,810	-0,080	2,708	-	-
0,462	121,900	0,796	16,020	3,759	1,932	0,706	1,813	0,403	0,084	-0,202	0,104	2,832	-0,303	3,781	-0,074	2,635	-	-
0,577	151,100	0,818	16,470	3,691	1,902	0,658	1,826	0,303	0,015	-0,230	0,123	2,847	-0,305	3,781	-0,045	2,518	-	-
0,693	180,200	0,840	16,910	3,673	1,863	0,619	1,869	0,212	0,017	-0,239	0,111	2,781	-0,291	3,865	-0,036	2,396	-	-
0,924	238,600	0,846	17,020	3,527	1,801	0,573	1,866	0,028	0,035	-0,208	0,160	2,756	-0,130	4,049	-0,019	2,359	-	-
1,000	257,900	0,850	17,110	3,444	1,790	0,574	1,831	-0,027	0,081	-0,193	0,160	2,740	-0,006	4,000	0,013	2,350	-	-

y/y _{max}	y +	(Tw-T)/ (Tw-T _b)	T'/T*	-u'T'/ u*T*	v'T'/ u*T*	w'T'/ u*T*	S(T)	K(T)	eptv	eptw	u' ² v'/ u ^{*3}	u' ² w'/ u ^{*3}	u'v' ² / u ^{*3}	v'w' ² / u ^{*3}	u'v'w'/ u ^{*3}		
0,346	92,700	0,464	1,582	2,048	0,320	-0,149	-0,171	3,008	-	-	-0,095	0,622	-0,100	0,760	-0,091	0,108	0,072
0,393	104,400	0,518	1,562	1,984	0,320	-0,132	-0,155	2,973	-	-	-0,072	0,669	-0,081	0,791	-0,075	0,113	0,151
0,462	121,900	0,590	1,531	1,896	0,314	-0,110	-0,202	3,007	-	-	-0,071	0,579	-0,065	0,965	-0,080	0,133	0,126
0,577	151,100	0,677	1,503	1,755	0,294	-0,122	-0,180	2,939	-	-	-0,081	0,760	-0,049	1,071	-0,049	0,098	0,200
0,693	180,200	0,722	1,487	1,602	0,283	-0,116	-0,153	2,904	-	-	-0,046	0,662	-0,019	1,109	-0,055	0,091	0,173
0,924	238,600	0,858	1,390	1,173	0,244	-0,083	0,108	2,860	-	-	0,008	0,745	0,008	1,325	-0,018	0,057	0,107
1,000	257,900	0,891	1,343	1,004	0,224	-0,088	0,201	2,921	-	-	0,054	0,710	0,005	1,215	-0,011	-0,010	0,054

TABLE I cont.

WALL SUBCHANNEL
 Reference wall temperature $T_w = 48,65^\circ\text{C}$
 Local friction velocity $u^* = 0,960 \text{ m/s}$
 Average friction velocity $u^* = 1,019 \text{ m/s}$
 Average velocity in the wall cha $Ub = 19,4 \text{ m/s}$

ANGULAR POSITION 10°

REFERENCE: LOCAL
 Wall heat flux
 Local friction temperature
 Average friction temperature
 Average fluid temperature

REYNOLDS NUMBER = 65000
 $q = 1,39 \text{ kW/m}^2$
 $T^* = 1,263 \text{ K}$
 $T^* = 1,193 \text{ K}$
 $T_b = 29,1^\circ\text{C}$

y/y _{max}	y +	U/Ub	U +	k +	u'/u*	v'/v*	w'/w*	u'v'/ u ^{*2}	u'w'/ u ^{*2}	-v'w'/ u ^{*2}	S(u)	K(u)	S(v)	K(v)	S(w)	K(w)	eps _v	eps _w
0,310	93,600	0,784	15,630	3,838	2,083	0,780	1,652	0,511	1,115	-0,079	0,152	2,792	-0,295	3,773	0,024	2,978	0,109	16,021
0,351	105,400	0,790	15,750	3,782	2,064	0,750	1,656	0,473	1,139	-0,091	0,137	2,781	-0,288	3,806	0,068	2,880	0,100	9,543
0,413	123,000	0,812	16,190	3,717	2,033	0,724	1,666	0,426	1,152	-0,087	0,144	2,750	-0,289	3,878	0,094	2,834	0,092	11,587
0,516	152,400	0,830	16,550	3,735	2,034	0,683	1,693	0,358	1,250	-0,093	0,141	2,711	-0,274	3,859	0,160	2,747	0,087	12,566
0,620	181,900	0,847	16,900	3,696	2,010	0,644	1,714	0,276	1,369	-0,045	0,130	2,663	-0,285	4,031	0,185	2,621	0,085	9,492
0,826	240,700	0,871	17,380	3,599	1,945	0,594	1,750	0,119	1,474	-0,009	0,141	2,609	-0,199	4,301	0,262	2,485	-	8,984
1,000	290,300	0,876	17,470	3,504	1,942	0,579	1,704	-0,010	1,459	0,042	0,146	2,593	0,034	4,299	0,282	2,543	-	-

y/y _{max}	y +	(Tw-T)/ (Tw-T _b)	T'/T [*]	-u'T'/ u*T [*]	v'T'/ u*T [*]	w'T'/ u*T [*]	S(T)	K(T)	eptv	eptw	u'v'/ u ^{*3}	u'w'/ u ^{*3}	u'v' ² / u ^{*3}	u'v' ² / u ^{*3}	v'w' ² / u ^{*3}	v'w' ² / u ^{*3}	u'v'w'/ u ^{*3}
0,310	93,600	0,500	1,731	2,494	0,313	0,626	-0,464	3,038	0,035	3,924	-0,088	-0,787	-0,074	0,317	-0,097	0,075	-0,006
0,351	105,400	0,537	1,718	2,418	0,315	0,643	-0,506	3,026	0,040	4,237	-0,083	-0,885	-0,054	0,385	-0,102	0,072	0,004
0,413	123,000	0,596	1,670	2,269	0,295	0,641	-0,499	3,041	0,045	4,335	-0,084	-0,947	-0,036	0,183	-0,073	0,068	-0,020
0,516	152,400	0,660	1,646	2,192	0,301	0,644	-0,465	2,950	0,057	4,728	-0,115	-0,885	-0,017	0,329	-0,045	0,081	-0,013
0,620	181,900	0,733	1,618	2,046	0,294	0,703	-0,417	2,908	0,067	5,473	-0,109	-0,824	0,007	0,226	-0,016	0,059	-0,028
0,826	240,700	0,850	1,537	1,644	0,269	0,635	-0,188	2,773	-	5,436	-0,075	-0,706	0,046	0,318	0,007	0,036	0,041
1,000	290,300	0,929	1,430	1,309	0,235	0,567	0,081	2,803	-	-	0,006	-0,810	0,061	0,348	0,039	-0,043	0,014

TABLE I cont.

WALL SUBCHANNEL ANGULAR POSITION 20°
 Reference wall temperature Tw=48,65°C
 Local friction velocity 0,978 m/s
 Average friction velocity u* = 1,019 m/s
 Average velocity in the wall cha Ub = 19,4 m/s

REFERENCE: LOCAL
 Wall heat flux
 Local friction temperature
 Average friction temperature
 Average fluid temperature

REYNOLDS NUMBER = 65000
 q=1,39 kW/m²
 T* = 1,240 K
 T* = 1,193 K
 Tb = 29,1°C

y/y _{max}	y +	U/Ub	U +	k +	u'/u*	v'/v*	w'/w*	u'v'/ u ^{*2}	u'w'/ u ^{*2}	-v'w'/ u ^{*2}	S(u)	K(u)	S(v)	K(v)	S(w)	K(w)	eps _v	eps _w
0,232	95,300	0,798	15,620	4,008	2,318	0,809	1,410	0,581	1,384	-0,082	0,255	2,689	-0,266	3,927	-0,113	3,192	0,081	4,420
0,263	107,300	0,819	16,030	3,956	2,310	0,789	1,398	0,560	1,442	-0,055	0,252	2,666	-0,220	3,838	-0,090	3,198	0,081	4,421
0,309	125,300	0,829	16,230	3,954	2,304	0,772	1,416	0,554	1,512	-0,041	0,261	2,641	-0,258	4,022	-0,042	3,136	0,087	5,037
0,386	155,300	0,849	16,630	3,955	2,309	0,742	1,425	0,524	1,654	-0,018	0,224	2,561	-0,207	3,990	0,066	3,088	0,094	4,784
0,464	185,200	0,874	17,120	4,018	2,331	0,714	1,447	0,461	1,799	-0,010	0,234	2,514	-0,196	4,051	0,143	3,053	0,097	5,408
0,618	245,200	0,904	17,700	4,009	2,314	0,677	1,484	0,379	2,027	0,037	0,194	2,408	-0,166	4,278	0,280	2,929	0,122	5,094
0,773	305,100	0,920	18,010	3,957	2,294	0,656	1,490	0,283	2,118	0,088	0,170	2,365	-0,032	4,375	0,399	2,917	0,187	4,774
0,927	365,100	0,927	18,160	3,955	2,286	0,651	1,504	0,198	2,186	0,165	0,178	2,344	0,116	4,424	0,423	2,895	-	3,132
1,000	393,300	0,927	18,150	3,923	2,284	0,657	1,483	0,148	2,164	0,170	0,175	2,328	0,182	4,318	0,429	2,931	-	-

y/y _{max}	y +	(Tw-T)/ (Tw-T _b)	T'/T*	-u'T'/ u*T*	v'T'/ u*T*	w'T'/ u*T*	S(T)	K(T)	ept _v	ept _w	u'v'/ u ^{*3}	u'w'/ u ^{*3}	u'v' ² / u ^{*3}	u'v' ² / u ^{*3}	v'w'/ u ^{*3}	v'w'/ u ^{*3}	u'v'w'/ u ^{*3}
0,232	95,300	0,504	2,043	3,484	0,351	0,898	-0,623	2,770	0,033	7,375	0,130	-0,925	0,025	0,151	-0,180	0,017	-0,006
0,263	107,300	0,546	2,028	3,426	0,357	0,944	-0,610	2,748	0,037	8,486	0,131	-0,731	0,050	0,025	-0,185	0,012	-0,017
0,309	125,300	0,585	1,997	3,318	0,364	0,972	-0,655	2,765	0,045	10,194	0,097	-0,901	0,047	0,024	-0,172	0,023	-0,037
0,386	155,300	0,669	1,976	3,249	0,391	1,000	-0,615	2,716	0,060	12,588	0,093	-0,556	0,088	-0,316	-0,140	0,000	-0,050
0,464	185,200	0,724	1,939	3,147	0,385	1,078	-0,560	2,656	0,071	15,655	0,089	-0,527	0,112	-0,475	-0,124	-0,019	-0,014
0,618	245,200	0,822	1,881	2,857	0,413	1,127	-0,405	2,525	0,101	23,648	-0,021	-0,280	0,133	-0,767	-0,074	-0,056	0,048
0,773	305,100	0,906	1,793	2,519	0,408	1,103	-0,162	2,467	0,124	4,084	-0,006	0,050	0,165	-1,011	-0,040	-0,110	0,102
0,927	365,100	0,969	1,657	2,091	0,385	1,056	0,063	2,481	-	1,522	0,002	0,110	0,183	-1,006	-0,013	-0,151	0,132
1,000	393,300	0,999	1,580	1,864	0,360	0,968	0,138	2,519	-	-	-0,004	0,111	0,168	-0,965	-0,002	-0,150	0,160

TABLE I cont.

WALL SUBCHANNEL **ANGULAR POSITION 30°** **REFERENCE: LOCAL** **REYNOLDS NUMBER = 65000**
 Reference wall temperature $T_w = 48,65^\circ\text{C}$ Wall heat flux $q = 1,39 \text{ kW/m}^2$
 Local friction velocity $u^* = 1,018 \text{ m/s}$ Local friction temperature $T^* = 1,190 \text{ K}$
 Average friction velocity $u^* = 1,019 \text{ m/s}$ Average friction temperature $T^* = 1,193 \text{ K}$
 Average velocity in the wall cha $U_b = 19,4 \text{ m/s}$ Average fluid temperature $T_b = 29,1^\circ\text{C}$

y/ymax	y +	U/Ub	U +	k +	u'/u*	v'/v*	w'/w*	u'v'/ u ^{*2}	u'w'/ u ^{*2}	-v'w'/ u ^{*2}	S(u)	K(u)	S(v)	K(v)	S(w)	K(w)	epsv	epsw
0,162	99,200	0,847	15,940	4,016	2,351	0,834	1,345	0,631	1,118	-0,118	0,181	2,589	-0,261	3,979	-0,227	3,269	0,054	1,382
0,183	111,700	0,857	16,120	3,951	2,350	0,814	1,311	0,619	1,121	-0,109	0,196	2,554	-0,237	4,053	-0,211	3,215	0,058	1,450
0,215	130,400	0,870	16,360	3,948	2,345	0,805	1,324	0,614	1,208	-0,096	0,197	2,541	-0,219	3,953	-0,186	3,124	0,065	1,510
0,269	161,600	0,899	16,900	4,017	2,381	0,790	1,320	0,607	1,331	-0,072	0,167	2,449	-0,197	4,022	-0,153	3,085	0,079	1,627
0,323	192,800	0,919	17,280	4,053	2,400	0,774	1,322	0,581	1,462	-0,059	0,140	2,391	-0,174	3,938	-0,129	3,036	0,090	1,828
0,431	255,200	0,956	17,980	4,111	2,438	0,753	1,308	0,547	1,621	-0,023	0,097	2,284	-0,119	4,076	-0,021	2,926	0,113	1,877
0,539	317,700	0,975	18,340	4,261	2,487	0,744	1,335	0,518	1,891	0,047	0,038	2,213	-0,113	4,002	0,111	2,957	0,137	2,023
0,646	380,100	0,991	18,650	4,258	2,491	0,740	1,327	0,469	1,964	0,086	-0,007	2,155	-0,006	3,969	0,200	2,950	0,162	1,951
0,862	504,900	1,016	19,110	4,259	2,486	0,746	1,333	0,381	2,103	0,188	-0,060	2,091	0,138	3,832	0,379	2,977	-	1,813
1,000	585,100	1,018	19,150	4,202	2,478	0,768	1,294	0,322	1,980	0,264	-0,095	2,099	0,220	3,855	0,346	3,022	-	-

y/ymax	y +	(Tw-T)/ (Tw-Tb)	T'/T*	-u'T'/ u*T*	v'T'/ u*T*	w'T'/ u*T*	S(T)	K(T)	eptv	eptw	u'v'/ u ^{*3}	u'w'/ u ^{*3}	u'v ² / u ^{*3}	u'v ² / u ^{*3}	v'w'/ u ^{*3}	v'w ² / u ^{*3}	u'v'w'/ u ^{*3}
0,162	99,200	0,535	2,169	3,682	0,381	0,684	-0,247	2,663	0,026	-	0,215	-0,056	0,042	0,442	-0,152	0,029	0,037
0,183	111,700	0,560	2,173	3,675	0,412	0,713	-0,309	2,666	0,032	-	0,231	-0,061	0,067	0,415	-0,144	0,030	0,023
0,215	130,400	0,609	2,141	3,579	0,413	0,763	-0,319	2,660	0,038	-	0,200	0,004	0,081	0,375	-0,139	0,031	0,042
0,269	161,600	0,682	2,119	3,555	0,447	0,821	-0,274	2,611	0,050	-	0,228	0,182	0,105	0,171	-0,135	0,015	-0,005
0,323	192,800	0,720	2,127	3,585	0,470	0,923	-0,193	2,552	0,063	-	0,181	0,198	0,131	0,083	-0,129	-0,019	0,044
0,431	255,200	0,817	2,094	3,484	0,527	0,958	-0,048	2,471	0,094	-	0,109	0,684	0,148	-0,353	-0,118	-0,056	0,034
0,539	317,700	0,888	2,072	3,437	0,555	1,102	0,064	2,381	0,123	-	0,018	1,326	0,171	-0,835	-0,119	-0,098	0,108
0,646	380,100	0,939	2,004	3,194	0,580	1,107	0,267	2,373	0,154	3,999	-0,138	1,733	0,201	-1,132	-0,093	-0,143	0,183
0,862	504,900	1,056	1,858	2,677	0,583	1,096	0,635	2,459	-	1,979	-0,335	2,281	0,170	-1,543	-0,080	-0,180	0,300
1,000	585,100	1,107	1,722	2,306	0,550	0,985	0,788	2,597	-	-	-0,511	2,306	0,118	-1,389	-0,049	-0,179	0,361

TABLE I cont.

WALL SUBCHANNEL ANGULAR POSITION 40° REFERENCE: LOCAL
 Reference wall temperature $T_w = 48,65^\circ\text{C}$
 Local friction velocity $u^* = 1,072 \text{ m/s}$
 Average friction velocity $u^* = 1,019 \text{ m/s}$
 Average velocity in the wall cha $Ub = 19,4 \text{ m/s}$

REYNOLDS NUMBER = 65000
 $q = 1,39 \text{ kW/m}^2$
 $T^* = 1,130 \text{ K}$
 $T^* = 1,193 \text{ K}$
 $T_b = 29,1^\circ\text{C}$

y/y_{max}	$y+$	U/Ub	$U+$	$k+$	u'/u^*	v'/v^*	w'/w^*	$u'v'/u^{*2}$	$u'w'/u^{*2}$	$-v'w'/u^{*2}$	$S(u)$	$K(u)$	$S(v)$	$K(v)$	$S(w)$	$K(w)$	eps_v	eps_w
0,112	104,400	0,907	16,220	3,782	2,166	0,852	1,466	0,687	0,778	-0,160	0,047	2,684	-0,272	3,823	-0,076	3,214	0,045	0,655
0,126	117,600	0,922	16,480	3,703	2,153	0,838	1,439	0,681	0,780	-0,140	0,031	2,661	-0,238	3,757	-0,068	3,148	0,048	0,685
0,149	137,300	0,942	16,840	3,705	2,169	0,840	1,414	0,678	0,820	-0,169	0,024	2,640	-0,241	3,808	-0,052	3,135	0,052	0,683
0,186	170,100	0,965	17,250	3,693	2,169	0,839	1,407	0,683	0,858	-0,159	0,014	2,612	-0,206	3,712	-0,030	3,101	0,061	0,737
0,223	203,000	0,987	17,630	3,661	2,166	0,836	1,389	0,656	0,881	-0,131	-0,014	2,550	-0,186	3,723	-0,023	3,062	0,068	0,712
0,297	268,600	1,021	18,240	3,653	2,184	0,826	1,361	0,632	0,965	-0,104	-0,083	2,493	-0,157	3,668	-0,013	3,030	0,085	0,812
0,372	334,300	1,048	18,730	3,672	2,216	0,820	1,327	0,579	1,054	-0,059	-0,148	2,428	-0,172	3,572	0,042	2,948	0,099	0,860
0,446	400,000	1,069	19,110	3,711	2,250	0,818	1,301	0,562	1,105	-0,017	-0,215	2,403	-0,159	3,581	0,075	2,970	0,118	0,930
0,595	531,400	1,106	19,760	3,684	2,279	0,808	1,233	0,497	1,278	0,060	-0,352	2,397	-0,106	3,575	0,180	3,102	0,154	0,906
0,743	662,700	1,125	20,100	3,645	2,284	0,813	1,189	0,458	1,333	0,145	-0,474	2,465	-0,025	3,581	0,312	3,250	-	0,699
0,929	826,900	1,137	20,320	3,520	2,244	0,854	1,129	0,370	1,258	0,249	-0,520	2,528	0,111	3,437	0,341	3,311	-	0,458
1,000	889,700	1,133	20,260	3,442	2,207	0,879	1,115	0,322	1,217	0,294	-0,525	2,559	0,127	3,435	0,356	3,346	-	-

y/y_{max}	$y+$	$(T_w-T)/(T_w-T_b)$	T'/T^*	$-u'T'/u^*T^*$	$v'T'/u^*T^*$	$w'T'/u^*T^*$	$S(T)$	$K(T)$	$eptv$	$eptw$	u'^2v'/u^{*3}	u'^2w'/u^{*3}	$u'v'^2/u^{*3}$	$v'w'^2/u^{*3}$	$u'v'w'/u^{*3}$		
0,112	104,400	0,564	2,047	2,872	0,416	0,231	-0,034	2,753	0,021	-	0,000	0,462	-0,079	0,231	-0,068	0,031	0,074
0,126	117,600	0,608	2,048	2,844	0,443	0,242	0,008	2,781	0,025	-	0,032	0,412	-0,052	0,157	-0,064	0,042	0,064
0,149	137,300	0,635	2,030	2,845	0,441	0,285	0,041	2,754	0,029	-	-0,020	0,474	-0,063	0,106	-0,062	0,032	0,050
0,186	170,100	0,686	2,015	2,755	0,475	0,275	0,069	2,737	0,039	-	0,012	0,529	-0,034	0,074	-0,055	0,013	0,054
0,223	203,000	0,742	2,027	2,760	0,505	0,300	0,086	2,713	0,049	-	0,016	0,676	-0,031	-0,008	-0,053	0,010	0,004
0,297	268,600	0,818	2,010	2,726	0,538	0,366	0,256	2,685	0,070	-	-0,093	0,907	-0,011	-0,248	-0,054	-0,012	-0,026
0,372	334,300	0,870	2,016	2,766	0,566	0,452	0,377	2,649	0,091	-	-0,109	1,254	-0,033	-0,472	-0,048	-0,011	-0,023
0,446	400,000	0,931	2,004	2,762	0,578	0,463	0,543	2,647	0,112	-	-0,240	1,585	-0,015	-0,643	-0,054	-0,047	0,025
0,595	531,400	1,024	1,974	2,641	0,612	0,581	0,807	2,717	0,157	-	-0,425	2,401	-0,057	-1,043	-0,037	-0,096	0,146
0,743	662,700	1,108	1,907	2,391	0,622	0,582	1,118	2,899	-	-	-0,749	3,065	-0,115	-1,435	-0,071	-0,146	0,276
0,929	826,900	1,184	1,764	2,008	0,634	0,623	1,393	3,231	-	-	-0,930	2,889	-0,197	-1,272	-0,034	-0,141	0,366
1,000	889,700	1,203	1,689	1,828	0,619	0,628	1,475	3,399	-	-	-0,967	2,730	-0,251	-1,170	-0,035	-0,144	0,432

TABLE I cont.

WALL SUBCHANNEL
 Reference wall temperature $T_w = 48,65^\circ\text{C}$
 Local friction velocity $u^* = 1,112 \text{ m/s}$
 Average friction velocity $u^* = 1,019 \text{ m/s}$
 Average velocity in the wall cha $U_b = 19,4 \text{ m/s}$

ANGULAR POSITION 50°

REFERENCE: LOCAL
 Wall heat flux
 Local friction temperature
 Average friction temperature
 Average fluid temperature

REYNOLDS NUMBER = 65000
 $q = 1,39 \text{ kW/m}^2$
 $T^* = 1,090 \text{ K}$
 $T^* = 1,193 \text{ K}$
 $T_b = 29,1^\circ\text{C}$

y/y _{max}	y +	U/U _b	U +	k +	u'/u*	v'/v*	w'/w*	u'v'/ u ^{*2}	u'w'/ u ^{*2}	-v'w'/ u ^{*2}	S(u)	K(u)	S(v)	K(v)	S(w)	K(w)	eps _v	eps _w
0,078	108,300	0,959	16,540	3,482	1,944	0,858	1,565	0,716	0,518	-0,165	-0,012	2,767	-0,289	3,763	-0,083	3,158	0,036	0,618
0,088	121,900	0,973	16,770	3,449	1,944	0,850	1,548	0,713	0,534	-0,143	-0,021	2,770	-0,227	3,642	-0,057	3,102	0,037	0,651
0,104	142,300	0,993	17,120	3,395	1,927	0,852	1,533	0,722	0,522	-0,150	-0,023	2,764	-0,247	3,690	-0,041	3,060	0,040	0,599
0,130	176,400	1,012	17,450	3,356	1,921	0,852	1,514	0,701	0,561	-0,142	-0,054	2,763	-0,204	3,566	-0,030	3,081	0,044	0,670
0,156	210,400	1,036	17,870	3,300	1,900	0,850	1,505	0,698	0,551	-0,125	-0,087	2,745	-0,172	3,546	0,007	3,026	0,050	0,608
0,208	278,500	1,077	18,560	3,125	1,857	0,848	1,443	0,650	0,540	-0,099	-0,144	2,747	-0,156	3,430	0,039	3,062	0,058	0,659
0,260	346,600	1,105	19,050	3,001	1,827	0,850	1,394	0,587	0,511	-0,070	-0,180	2,722	-0,182	3,461	0,082	3,125	0,065	0,713
0,312	414,700	1,131	19,490	2,871	1,796	0,843	1,344	0,559	0,486	-0,059	-0,245	2,757	-0,223	3,520	0,097	3,112	0,076	0,712
0,416	550,900	1,166	20,100	2,615	1,742	0,827	1,229	0,475	0,474	0,005	-0,399	2,886	-0,243	3,478	0,194	3,249	0,090	0,544
0,519	687,100	1,198	20,650	2,384	1,694	0,794	1,126	0,376	0,473	0,026	-0,574	3,171	-0,234	3,578	0,250	3,461	0,092	0,589
0,649	857,300	1,220	21,040	2,163	1,637	0,773	1,025	0,318	0,435	0,072	-0,781	3,618	-0,212	3,568	0,289	3,642	0,106	-
0,779	1027,600	1,240	21,380	1,995	1,587	0,761	0,945	0,227	0,431	0,125	-0,934	4,083	-0,124	3,641	0,334	3,752	0,123	-
1,000	1317,400	1,252	21,590	1,833	1,491	0,804	0,893	0,109	0,414	0,172	-0,970	4,366	-0,047	3,699	0,319	3,741	-	-

y/y _{max}	y +	(Tw-T)/ (Tw-T _b)	T'/T*	-u'T/ u*T*	v'T/ u*T*	w'T/ u*T*	S(T)	K(T)	eptv	eptw	u'v'/ u ^{*3}	u'w'/ u ^{*3}	u'v' ² / u ^{*3}	u'v' ² / u ^{*3}	v'w' ² / u ^{*3}	v'w' ² / u ^{*3}	u'v'w'/ u ^{*3}
0,078	108,300	0,579	1,946	2,141	0,423	-0,349	0,003	2,918	0,015	0,287	-0,252	0,267	-0,202	-0,004	-0,076	0,043	0,043
0,088	121,900	0,619	1,943	2,110	0,439	-0,305	0,024	2,880	0,018	0,243	-0,222	0,188	-0,165	-0,015	-0,071	0,025	0,022
0,104	142,300	0,650	1,902	2,032	0,438	-0,298	0,038	2,907	0,021	0,231	-0,213	0,212	-0,167	-0,064	-0,065	0,026	0,046
0,130	176,400	0,697	1,907	1,999	0,466	-0,244	0,107	2,886	0,027	0,179	-0,250	0,381	-0,161	-0,229	-0,057	0,001	0,018
0,156	210,400	0,741	1,924	1,951	0,498	-0,254	0,162	2,887	0,035	0,182	-0,327	0,312	-0,178	-0,269	-0,043	-0,005	0,015
0,208	278,500	0,800	1,898	1,837	0,515	-0,230	0,314	2,899	0,048	0,157	-0,352	0,375	-0,184	-0,369	-0,023	-0,023	0,010
0,260	346,600	0,861	1,905	1,782	0,505	-0,196	0,474	2,929	0,059	0,117	-0,344	0,551	-0,203	-0,529	-0,016	-0,021	-0,024
0,312	414,700	0,904	1,894	1,696	0,504	-0,213	0,565	2,973	0,070	0,112	-0,370	0,548	-0,235	-0,529	-0,002	-0,020	0,007
0,416	550,900	0,979	1,846	1,531	0,478	-0,095	0,673	3,005	0,089	-	-0,364	0,836	-0,258	-0,651	0,002	-0,034	-0,027
0,519	687,100	1,046	1,829	1,362	0,423	-0,099	0,826	3,083	0,100	-	-0,353	1,088	-0,251	-0,700	0,006	-0,062	-0,008
0,649	857,300	1,118	1,805	1,183	0,416	-0,084	0,944	3,139	0,123	-	-0,480	1,110	-0,246	-0,671	0,004	-0,074	0,042
0,779	1027,600	1,165	1,735	0,936	0,362	-0,080	1,103	3,284	0,130	-	-0,452	1,188	-0,258	-0,638	0,026	-0,100	0,110
1,000	1317,400	1,262	1,601	0,535	0,316	-0,068	1,382	3,718	-	-	-0,394	0,966	-0,318	-0,510	0,063	-0,064	0,142

| 101 |

TABLE I cont.

WALL SUBCHANNEL
 Reference wall temperature Tw=48,65°C
 Local friction velocity u* = 1,109 m/s
 Average friction velocity u* = 1,019 m/s
 Average velocity in the wall cha Ub = 19,4 m/s

ANGULAR POSITION 60°

REFERENCE: LOCAL
 Wall heat flux q=1,39 kW/m²
 Local friction temperature T* = 1,093 K
 Average friction temperature T* = 1,193 K
 Average fluid temperature Tb = 29,1°C

REYNOLDS NUMBER = 65000
 S(u) K(u) S(v) K(v) S(w) K(w)
 -0,275 2,756 2,748 -0,236 3,588 -0,046 3,180 0,028
 -0,131 0,075 0,177 -0,121 0,069 2,729 -0,200 3,541 -0,018 3,157 0,034
 -0,092 0,037 0,216 0,092 0,069 2,714 -0,168 3,518 0,010 3,129 0,040
 -0,064 0,020 0,161 0,064 0,069 2,701 -0,137 3,372 0,043 3,099 0,046
 -0,029 0,031 0,155 0,029 0,069 2,694 -0,145 3,382 0,096 3,118 0,059
 -0,015 0,108 0,161 0,015 0,069 2,701 -0,148 3,398 0,137 3,180 0,067
 -0,017 0,147 0,151 0,017 0,069 2,719 -0,194 3,311 0,191 3,263 0,077
 -0,078 0,032 0,151 0,078 0,069 2,780 -0,206 3,371 0,269 3,378 0,081
 -0,025 0,044 0,151 0,025 0,069 2,858 -0,192 3,397 0,296 3,574 0,107
 -0,039 0,056 0,151 0,039 0,069 2,912 -0,162 3,453 0,344 3,743 0,159
 -0,088 0,066 0,151 0,088 0,069 2,941 -0,140 3,567 0,280 3,833 -
 -0,133 0,055 0,151 0,133 0,069 2,964 -0,026 3,654 0,134 3,818 -
 -0,136 0,050 0,151 0,136 0,069 3,014 -0,302 0,111 3,761 0,071 3,626 -

y/y _{max}	y +	U/Ub	U +	k +	u'/u*	v'/v*	w'/w*	u'v'/u ^{*2}	u'w'/u ^{*2}	-v'w'/u ^{*2}	S(u)	K(u)	S(v)	K(v)	S(w)	K(w)	eps _v	eps _w
0,068	108,000	0,964	16,660	3,323	1,904	0,853	1,514	0,727	0,173	-0,156	0,071	2,756	-0,275	3,658	-0,049	3,180	0,028	
0,077	121,600	0,977	16,890	3,285	1,900	0,850	1,496	0,738	0,177	-0,131	0,075	2,748	-0,236	3,588	-0,046	3,203	0,030	
0,091	141,900	0,994	17,180	3,297	1,903	0,845	1,503	0,740	0,219	-0,121	0,069	2,729	-0,200	3,541	-0,018	3,157	0,034	
0,113	175,900	1,023	17,680	3,192	1,877	0,841	1,467	0,734	0,216	-0,092	0,037	2,714	-0,168	3,518	0,010	3,129	0,040	
0,136	209,800	1,046	18,080	3,128	1,858	0,836	1,452	0,720	0,161	-0,064	0,020	2,701	-0,137	3,372	0,043	3,099	0,046	
0,181	277,700	1,078	18,630	2,993	1,812	0,832	1,417	0,689	0,155	-0,029	0,031	2,694	-0,145	3,382	0,096	3,118	0,059	
0,226	345,700	1,105	19,110	2,776	1,759	0,830	1,330	0,639	0,161	-0,015	0,108	2,701	-0,148	3,398	0,137	3,180	0,067	
0,272	413,600	1,130	19,540	2,633	1,711	0,828	1,285	0,638	0,151	0,017	-0,147	2,719	-0,194	3,311	0,191	3,263	0,077	
0,362	549,400	1,170	20,230	2,287	1,601	0,812	1,164	0,532	0,078	0,032	-0,210	2,780	-0,206	3,371	0,269	3,378	0,081	
0,453	685,200	1,196	20,670	1,989	1,490	0,792	1,063	0,439	0,025	0,044	-0,259	2,858	-0,192	3,397	0,296	3,574	0,107	
0,566	855,000	1,217	21,030	1,723	1,389	0,781	0,952	0,356	-0,039	0,056	-0,267	2,912	-0,162	3,453	0,344	3,743	0,159	
0,679	1024,800	1,236	21,370	1,533	1,309	0,767	0,874	0,269	-0,088	0,066	-0,248	2,941	-0,140	3,567	0,280	3,833	-	
0,906	1364,300	1,255	21,700	1,351	1,232	0,769	0,770	0,133	-0,143	0,055	-0,272	2,964	-0,026	3,654	0,134	3,818	-	
1,000	1505,500	1,262	21,820	1,308	1,210	0,774	0,743	0,082	-0,136	0,050	-0,302	3,014	0,111	3,761	0,071	3,626	-	

y/y _{max}	y +	(Tw-T)/(Tw-T _b)	T'/T*	-u'T'/u*T*	v'T'/u*T*	w'T'/u*T*	S(T)	K(T)	eptv	eptw	u'v'/u ^{*3}	u'w'/u ^{*3}	u'v ² /u ^{*3}	v'w'/u ^{*3}	v'w ² /u ^{*3}	u'v'w'/u ^{*3}	
0,068	108,000	0,492	2,132	2,444	0,418	-0,893	0,069	2,802	0,014	0,396	-0,176	-0,103	-0,202	0,414	-0,074	0,041	0,057
0,077	121,600	0,517	2,141	2,406	0,425	-0,872	0,099	2,809	0,016	0,380	-0,198	-0,117	-0,180	0,345	-0,067	0,033	0,043
0,091	141,900	0,554	2,131	2,394	0,444	-0,845	0,170	2,820	0,019	0,362	-0,235	-0,190	-0,168	0,275	-0,065	0,020	0,046
0,113	175,900	0,597	2,125	2,304	0,450	-0,802	0,227	2,804	0,024	0,338	-0,211	-0,159	-0,147	0,127	-0,038	0,007	0,044
0,136	209,800	0,637	2,147	2,313	0,476	-0,869	0,265	2,808	0,030	0,360	-0,259	-0,110	-0,149	0,072	-0,028	-0,005	0,038
0,181	277,700	0,683	2,153	2,215	0,504	-0,833	0,409	2,791	0,043	0,336	-0,328	-0,139	-0,160	-0,042	-0,012	-0,010	0,018
0,226	345,700	0,749	2,120	2,099	0,501	-0,695	0,521	2,835	0,053	0,250	-0,376	-0,058	-0,189	-0,150	0,005	-0,023	0,030
0,272	413,600	0,786	2,102	2,004	0,542	-0,649	0,543	2,816	0,069	0,207	-0,415	0,015	-0,199	-0,247	0,026	-0,026	0,048
0,362	549,400	0,843	2,077	1,826	0,495	-0,575	0,700	2,889	0,084	0,186	-0,408	0,019	-0,204	-0,249	0,028	-0,037	0,018
0,453	685,200	0,892	2,038	1,639	0,452	-0,512	0,752	2,942	0,096	0,162	-0,393	0,049	-0,192	-0,259	0,060	-0,045	0,018
0,566	855,000	0,942	2,023	1,499	0,427	-0,481	0,715	2,955	0,115	-	-0,337	0,037	-0,181	-0,198	0,043	-0,040	0,011
0,679	1024,800	0,977	2,018	1,394	0,390	-0,477	0,663	2,924	0,125	-	-0,267	0,001	-0,155	-0,174	0,017	-0,049	0,004
0,906	1364,300	1,044	2,032	1,285	0,340	-0,507	0,809	2,951	-	-	-0,113	-0,062	-0,138	-0,148	-0,008	-0,045	0,000
1,000	1505,500	1,062	2,001	1,186	0,303	-0,488	0,808	2,931	-	-	-0,043	-0,102	-0,143	-0,129	0,002	-0,035	-0,017

TABLE I cont.

WALL SUBCHANNEL
 Reference wall temperature $T_w = 48,65^\circ\text{C}$
 Local friction velocity $u^* = 1,078 \text{ m/s}$
 Average friction velocity $u^* = 1,019 \text{ m/s}$
 Average velocity in the wall cha $Ub = 19,4 \text{ m/s}$

ANGULAR POSITION 70°

REFERENCE: LOCAL
 Wall heat flux $q = 1,39 \text{ kW/m}^2$
 Local friction temperature $T^* = 1,124 \text{ K}$
 Average friction temperature $T^* = 1,193 \text{ K}$
 Average fluid temperature $T_b = 29,1^\circ\text{C}$

REYNOLDS NUMBER = 65000
 $Re = 65000$
 $Re = 65000$
 $Re = 65000$
 $Re = 65000$

y/y _{max}	y +	U/Ub	U +	k +	u'/u*	v'/v*	w'/w*	u'v'/ u ^{*2}	u'w'/ u ^{*2}	-v'w'/ u ^{*2}	S(u)	K(u)	S(v)	K(v)	S(w)	K(w)	eps _v	eps _w
0,108	105,000	0,933	16,590	3,071	1,908	0,849	1,334	0,725	-0,038	-0,110	0,113	2,813	-0,269	3,630	-0,015	3,301	0,042	
0,123	118,200	0,943	16,760	3,031	1,903	0,834	1,320	0,719	-0,022	-0,083	0,122	2,787	-0,237	3,610	0,010	3,315	0,046	
0,145	138,000	0,966	17,160	2,977	1,893	0,822	1,301	0,712	-0,036	-0,082	0,116	2,781	-0,208	3,517	0,021	3,305	0,051	
0,181	171,100	0,988	17,570	2,915	1,881	0,809	1,280	0,709	-0,062	-0,066	0,104	2,759	-0,176	3,475	0,097	3,332	0,060	
0,217	204,100	1,013	18,010	2,820	1,851	0,797	1,257	0,682	-0,065	-0,040	0,082	2,744	-0,182	3,497	0,093	3,312	0,068	
0,289	270,100	1,048	18,620	2,681	1,807	0,790	1,214	0,649	-0,094	0,003	0,033	2,697	-0,178	3,462	0,217	3,360	0,085	
0,361	336,200	1,074	19,090	2,537	1,753	0,786	1,176	0,608	-0,113	0,009	-0,009	2,718	-0,167	3,399	0,282	3,417	0,102	
0,434	402,200	1,097	19,500	2,344	1,687	0,780	1,110	0,570	-0,128	0,024	-0,018	2,755	-0,168	3,514	0,306	3,455	0,126	
0,578	534,300	1,124	19,970	2,039	1,569	0,784	1,001	0,479	-0,152	0,041	-0,029	2,803	-0,141	3,594	0,377	3,613	0,186	
0,723	666,400	1,145	20,350	1,826	1,471	0,799	0,922	0,370	-0,232	0,042	0,010	2,824	0,019	3,665	0,362	3,704	0,118	
0,904	831,500	1,160	20,610	1,652	1,390	0,812	0,844	0,223	-0,296	0,018	0,070	2,803	0,159	3,839	0,322	3,670	-	
1,000	919,500	1,162	20,650	1,634	1,382	0,833	0,816	0,135	-0,319	0,002	0,088	2,782	0,221	3,766	0,278	3,584	-	
y/y _{max}	y +	(T _w -T)/ (T _w -T _b)	T'/T*	-u'T'/ u*T*	v'T'/ u*T*	w'T'/ u*T*	S(T)	K(T)	eptv	eptw	u'v'/ u ^{*3}	u'w'/ u ^{*3}	u'v' ² / u ^{*3}	u'v' ² / u ^{*3}	v'w'/ u ^{*3}	v'w'/ u ^{*3}	u'v'w'/ u ^{*3}	
0,108	105,000	0,293	2,306	2,793	0,396	-0,943	-0,425	2,642	0,022	0,479	-0,169	0,025	-0,192	0,466	-0,077	0,035	0,073	
0,123	118,200	0,318	2,337	2,794	0,400	-0,936	-0,403	2,606	0,025	0,472	-0,138	-0,003	-0,168	0,470	-0,071	0,027	0,076	
0,145	138,000	0,348	2,316	2,776	0,417	-0,946	-0,355	2,600	0,031	0,471	-0,131	0,059	-0,148	0,459	-0,049	0,036	0,066	
0,181	171,100	0,400	2,340	2,771	0,448	-0,997	-0,276	2,574	0,041	0,494	-0,138	0,077	-0,116	0,397	-0,031	0,008	0,058	
0,217	204,100	0,429	2,354	2,727	0,445	-0,982	-0,276	2,524	0,049	0,483	-0,169	0,034	-0,127	0,291	-0,014	0,004	0,055	
0,289	270,100	0,498	2,384	2,661	0,469	-1,051	-0,125	2,506	0,069	0,514	-0,272	0,118	-0,140	0,201	0,012	-0,016	0,049	
0,361	336,200	0,538	2,390	2,540	0,456	-1,042	-0,002	2,483	0,084	0,477	-0,341	0,164	-0,148	0,111	0,040	-0,051	0,085	
0,434	402,200	0,580	2,346	2,375	0,464	-0,968	0,114	2,483	0,102	0,419	-0,339	0,132	-0,149	0,023	0,042	-0,077	0,052	
0,578	534,300	0,643	2,325	2,154	0,443	-0,850	0,279	2,506	0,131	-	-0,316	0,143	-0,132	-0,040	0,059	-0,084	0,065	
0,723	666,400	0,683	2,261	1,931	0,408	-0,810	0,456	2,591	0,148	-	-0,247	0,070	-0,121	-0,030	0,094	-0,108	0,071	
0,904	831,500	0,698	2,220	1,751	0,360	-0,768	0,511	2,612	-	-	-0,105	0,012	-0,113	0,002	0,104	-0,063	0,049	
1,000	919,500	0,720	2,189	1,713	0,318	-0,724	0,512	2,670	-	-	-0,008	-0,037	-0,120	0,009	0,095	-0,039	0,057	

TABLE I cont.

WALL SUBCHANNEL

ANGULAR POSITION 80°

REFERENCE: LOCAL

REYNOLDS NUMBER = 65000

Reference wall temperature

 $T_w = 48,65^\circ\text{C}$

Wall heat flux

 $q = 1,39 \text{ kW/m}^2$

Local friction velocity

 $u^* = 1,044 \text{ m/s}$

Local friction temperature

 $T^* = 1,161 \text{ K}$

Average friction velocity

 $u^* = 1,019 \text{ m/s}$

Average friction temperature

 $T^* = 1,193 \text{ K}$

Average velocity in the wall cha

 $Ub = 19,4 \text{ m/s}$

Average fluid temperature

 $T_b = 29,1^\circ\text{C}$

y/y_{max}	$y +$	U/Ub	$U +$	$k +$	u'/u^*	v'/v^*	w'/w^*	$u'v'/u^{*2}$	$u'w'/u^{*2}$	$-v'w'/u^{*2}$	$S(u)$	$K(u)$	$S(v)$	$K(v)$	$S(w)$	$K(w)$	ϵ_{psv}	ϵ_{psw}
0,159	101,800	0,906	16,630	2,806	1,871	0,842	1,184	0,688	-0,195	-0,102	0,086	2,828	-0,306	3,676	-0,064	3,379	0,063	0,485
0,180	114,600	0,917	16,830	2,748	1,853	0,826	1,176	0,685	-0,212	-0,088	0,092	2,826	-0,265	3,609	-0,029	3,438	0,066	0,540
0,212	133,700	0,937	17,200	2,655	1,831	0,803	1,146	0,667	-0,179	-0,077	0,094	2,808	-0,243	3,594	0,011	3,352	0,069	0,455
0,265	165,700	0,960	17,620	2,540	1,803	0,773	1,110	0,647	-0,234	-0,058	0,082	2,812	-0,224	3,536	0,091	3,383	0,076	0,514
0,317	197,700	0,986	18,080	2,434	1,763	0,754	1,091	0,612	-0,251	-0,049	0,052	2,793	-0,211	3,540	0,118	3,385	0,083	0,802
0,423	261,700	1,021	18,720	2,219	1,682	0,728	1,038	0,544	-0,306	-0,036	0,022	2,853	-0,199	3,540	0,223	3,463	0,110	0,780
0,529	325,700	1,043	19,140	2,027	1,600	0,711	0,994	0,473	-0,340	-0,037	0,039	2,913	-0,211	3,694	0,223	3,456	0,143	0,746
0,635	389,700	1,063	19,490	1,847	1,514	0,692	0,961	0,386	-0,379	-0,032	0,074	2,976	-0,158	3,762	0,289	3,542	0,106	-
0,846	517,700	1,082	19,850	1,598	1,381	0,692	0,900	0,224	-0,389	-0,066	0,227	3,017	0,088	4,044	0,298	3,441	-	-
1,000	610,700	1,088	19,960	1,523	1,343	0,704	0,864	0,117	-0,399	-0,088	0,283	3,026	0,289	4,116	0,339	3,480	-	-

 $| 10^{-4}$

TABLE I cont.

WALL SUBCHANNEL **ANGULAR POSITION 90°** **REFERENCE: LOCAL** **REYNOLDS NUMBER = 65000**
 Reference wall temperature $T_w = 48,65^\circ\text{C}$ Wall heat flux $q = 1,39 \text{ kW/m}^2$
 Local friction velocity $u^* = 1,029 \text{ m/s}$ Local friction temperature $T^* = 1,177 \text{ K}$
 Average friction velocity $u^* = 1,019 \text{ m/s}$ Average friction temperature $T^* = 1,193 \text{ K}$
 Average velocity in the wall cha $Ub = 19,4 \text{ m/s}$ Average fluid temperature $T_b = 29,1^\circ\text{C}$

y/y _{max}	y+	U/Ub	U+	k+	u'/u*	v'/v*	w'/w*	u'v'/ u ^{*2}	u'w'/ u ^{*2}	-v'w'/ u ^{*2}	S(u)	K(u)	S(v)	K(v)	S(w)	K(w)	eps _v	eps _w
0,186	100,300	0,871	16,210	2,464	1,710	0,849	1,133	0,676	-0,189	-0,098	0,012	2,839	-0,333	3,691	-0,130	3,393	0,077	
0,211	113,000	0,883	16,440	2,394	1,692	0,826	1,115	0,668	-0,167	-0,090	0,029	2,854	-0,295	3,591	-0,126	3,313	0,074	
0,248	131,900	0,903	16,790	2,288	1,665	0,797	1,081	0,630	-0,161	-0,077	0,025	2,852	-0,282	3,539	-0,096	3,347	0,070	
0,310	163,400	0,928	17,270	2,156	1,621	0,764	1,050	0,609	-0,189	-0,064	0,007	2,854	-0,244	3,454	-0,010	3,391	0,076	
0,372	195,000	0,956	17,790	1,999	1,567	0,733	1,003	0,551	-0,187	-0,059	-0,008	2,899	-0,248	3,437	0,012	3,333	0,084	
0,496	258,100	0,991	18,430	1,794	1,466	0,684	0,985	0,445	-0,215	-0,040	-0,051	3,005	-0,292	3,532	0,091	3,395	0,095	
0,620	321,200	1,019	18,950	1,582	1,361	0,648	0,945	0,349	-0,202	-0,046	-0,056	3,127	-0,284	3,582	0,119	3,444	0,100	
0,744	384,300	1,035	19,260	1,410	1,259	0,611	0,928	0,236	-0,217	-0,043	0,010	3,309	-0,257	3,739	0,199	3,454	0,175	
0,993	510,500	1,052	19,570	1,233	1,145	0,581	0,904	0,030	-0,197	-0,046	0,210	3,326	0,036	3,852	0,261	3,418	-	
1,000	514,300	1,050	19,530	1,210	1,135	0,578	0,892	0,024	-0,194	-0,057	0,189	3,310	0,056	3,884	0,255	3,409	-	

y/y _{max}	y+	(Tw-T)/ (Tw-T _b)	T'/T [*]	-u'T'/ u*T [*]	v'T'/ u*T [*]	w'T'/ u*T [*]	S(T)	K(T)	eptv	eptw	u'v'/ u ^{*3}	u'w'/ u ^{*3}	u'v' ² / u ^{*3}	u'v' ² / u ^{*3}	v'w'/ u ^{*3}	v'w'/ u ^{*3}	u'v'w'/ u ^{*3}
0,186	100,300	-0,165	1,983	2,054	0,333	-0,613	-1,885	3,543	0,035	-	-0,292	0,216	-0,263	0,129	-0,101	0,023	0,047
0,211	113,000	-0,136	2,010	2,030	0,339	-0,610	-1,966	3,540	0,040	-	-0,264	0,237	-0,237	0,145	-0,090	0,032	0,040
0,248	131,900	-0,102	2,010	2,003	0,331	-0,596	-2,015	3,544	0,046	-	-0,253	0,235	-0,201	0,114	-0,083	0,026	0,038
0,310	163,400	-0,056	2,057	1,975	0,342	-0,697	-2,114	3,466	0,060	-	-0,255	0,249	-0,177	0,151	-0,062	-0,002	0,046
0,372	195,000	-0,014	2,084	1,912	0,329	-0,704	-2,215	3,450	0,069	-	-0,259	0,246	-0,159	0,111	-0,058	-0,009	0,028
0,496	258,100	0,063	2,092	1,739	0,303	-0,861	-2,356	3,478	0,085	-	-0,290	0,295	-0,155	0,164	-0,027	-0,026	0,020
0,620	321,200	0,105	2,066	1,517	0,259	-0,858	-2,359	3,431	0,093	-	-0,274	0,250	-0,139	0,187	0,038	-0,045	0,036
0,744	384,300	0,143	2,090	1,365	0,208	-0,965	-2,440	3,379	0,092	-	-0,207	0,267	-0,107	0,238	0,068	-0,031	0,029
0,993	510,500	0,162	2,061	1,166	0,092	-1,026	-2,550	3,422	-	-	0,019	0,265	-0,063	0,306	0,128	-0,012	0,012
1,000	514,300	0,164	2,046	1,131	0,082	-0,956	-2,449	3,350	-	-	0,019	0,231	-0,062	0,261	0,113	-0,009	0,016

TABLE I cont.